MARTIN MARIETTA ENERGY SYSTEMS LIBRARIES

3 4456 0375937 8

ornl

ORNL/TM-12181

OAK RIDGE
NATIONAL
LABORATORY

MARTIN MARIETTA

Analysis and Design of Robust Decentralized Controllers for Nonlinear Systems

D. A. Schoenwald

OAK RIDGE NATIONAL LABORATORY
CENTRAL RESEARCH LIBRARY
CIRCULATION SECTION
4500N ROOM 175
LIBRARY LOAN COPY
DO NOT TRANSFER TO ANOTHER PERSON
If you wish someone else to see this report, send in name with report and this library will arrange a loan.

MANAGED BY
MARTIN MARIETTA ENERGY SYSTEMS, INC.
FOR THE UNITED STATES
DEPARTMENT OF ENERGY

This report has been reproduced directly from the best available copy.

Available to DOE and DOE contractors from the Office of Scientific and Technical Information, P.O. Box 62, Oak Ridge, TN 37831; prices available from (615) 576-8401, FTS 626-8401.

Available to the public from the National Technical Information Service, U.S. Department of Commerce, 5285 Port Royal Rd., Springfield, VA 22161.

This report was prepared as an account of work sponsored by an agency of the United States Government. Neither the United States Government nor any agency thereof, nor any of their employees, makes any warranty, express or implied, or assumes any legal liability or responsibility for the accuracy, completeness, or usefulness of any information, apparatus, product, or process disclosed, or represents that its use would not infringe privately owned rights. Reference herein to any specific commercial product, process, or service by trade name, trademark, manufacturer, or otherwise, does not necessarily constitute or imply its endorsement, recommendation, or favoring by the United States Government or any agency thereof. The views and opinions of authors expressed herein do not necessarily state or reflect those of the United States Government or any agency thereof.

ORNL/TM-12181

406
37

Instrumentation and Controls Division

ANALYSIS AND DESIGN OF ROBUST DECENTRALIZED CONTROLLERS FOR NONLINEAR SYSTEMS

D. A. Schoenwald

Date Published—July 1993

Prepared by
OAK RIDGE NATIONAL LABORATORY
Oak Ridge, Tennessee 37831-6285
managed by
MARTIN MARIETTA ENERGY SYSTEMS, INC.
for the
U.S. DEPARTMENT OF ENERGY
under contract DE-AC05-84OR21400

MARTIN MARIETTA ENERGY SYSTEMS LIBRARIES

3 4456 0375937 8

CONTENTS

LIST OF FIGURES vii

LIST OF TABLES ix

ABSTRACT xi

CHAPTER PAGE

1 INTRODUCTION 1

1.1 PROBLEM STATEMENT 1
1.2 SPACE STRUCTURES 2
1.3 FLEXIBLE ROBOTICS 5
1.4 ORGANIZATION OF REPORT 7

2 CONTROL THEORY TECHNIQUES 9

2.1 NONLINEAR CONTROL 9
2.1.1 Feedback Linearization 11
2.1.2 Nonlinear Observers 16
2.2 SINGULAR PERTURBATIONS 19
2.2.1 Multiple Time Scales Technique 20
2.2.2 Composite Control 23
2.3 SENSITIVITY ANALYSIS 26
2.4 DECENTRALIZED CONTROL 36
2.5 SUMMARY 40

3 FEEDBACK LINEARIZATION RESULTS 41

3.1 OPTIMIZATION OF FEEDBACK LINEARIZABLE SYSTEMS . 41
3.1.1 Problem Statement 42
3.1.2 Methods for Solving the NQR Problem 43
3.1.3 Derivation of the Method 44

3.1.4 Example 46
3.1.5 Conclusions 48
3.2 ROBUST FEEDBACK LINEARIZATION 49
3.2.1 Problem Statement 50
3.2.2 Modeling of the Parametric Uncertainty 51
3.2.3 Robust Stabilization 52
3.2.4 Zero Dynamics 57
3.2.5 Conclusions 61

4 CONTROL OF LARGE-SCALE SYSTEMS 62

4.1 DECENTRALIZED FEEDBACK LINEARIZATION 62
4.1.1 Problem Setup 63
4.1.2 Decentralized Nonlinear Observers 66
4.1.3 Decentralized Control of the Linearized System 69
4.1.4 Stabilization of Interconnected Subsystems 73
4.1.5 Weakly Coupled Systems 75
4.1.6 Relative Degree Enhancement of Multichannel Systems . . . 77
4.1.7 Concluding Remarks 83
4.2 SENSITIVITY MODELS FOR INTERCONNECTED SYSTEMS . 83
4.2.1 Decentralized Sensitivity Models 84
4.2.2 Decentralized Optimal Control via Sensitivity Functions . . 91
4.2.3 Example 94
4.2.4 Concluding Remarks 98

5 APPLICATIONS OF NONLINEAR CONTROL 100

5.1 FLEXIBLE MANIPULATOR CONTROL VIA SINGULAR PERTURBATIONS 100
5.1.1 Control via the Integral Manifold Approach 100
5.1.2 Distributed Actuator Control 105
5.1.3 Approximate Feedback Linearization 107
5.1.4 Simulation Results 109
5.1.5 Conclusions 111
5.2 APPLICATIONS OF SENSITIVITY MODELS TO THE SPACE STATION 116
5.2.1 Generation of Sensitivity Models 118
5.2.2 Optimal Control Design 121

6 SUMMARY AND FUTURE RESEARCH 124

REFERENCES 127

APPENDICES

A THE TWO-LINK FLEXIBLE STRUCTURE MODEL 139

A.1 DYNAMICAL EQUATIONS 143
A.2 CORRECTIVE CONTROL DESIGN 145
A.3 FINITE-DIMENSIONAL REPRESENTATION 146
A.4 REFERENCES 152

LIST OF FIGURES

FIGURE		PAGE
1	Spacecraft with rigid hub and attached flexible appendage.	4
2	Examples of common nonlinearities in physical systems.	10
3	Linearization via feedback.	15
4	Fast and slow manifolds of a singularly perturbed system.	25
5	Typical feedback control system with goal of driving $y(t) \longrightarrow r(t)$.	27
6	Mapping of parametric deviations into state deviations.	29
7	Closed loop control system with plant, G, and feedback H.	30
8	Model to simultaneously measure all p output sensitivity functions.	31
9	Method of sensitivity points.	32
10	Generation of trajectory sensitivity functions for a linear system.	33
11	Parameter identification using an adaptive model.	35
12	Optimal control using a sensitivity model.	35
13	Decentralized control architecture.	36
14	One-link manipulator with joint flexibility.	47
15	Decentralized strategy to observer design.	67
16	Multi-level approach to linearization and stabilization.	72
17	Illustration of the feedback method for linearization.	79
18	MIMO system with coupled linear subsystems.	85

19 Sensitivity model configurations for linear coupled subsystems. 89
20 Two-channel coupled nonlinear system. 90
21 Sensitivity models for coupled nonlinear systems. 91
22 Decentralized optimal control with sensitivity models. 94
23 Inverted penduli coupled by a spring. 95
24 Joint angle plots with PD feedback and O(1) linearizing control. . . . 112
25 Joint velocity plots with PD feedback and O(1) linearizing control. . . 112
26 Tip deflections of link 1 with and without distributed actuator. 113
27 Tip deflections of link 2 with and without distributed actuator. 113
28 Tip velocities of link 1 with and without distributed actuator. 114
29 Tip velocities of link 2 with and without distributed actuator. 114
30 Profiles of hub actuator energy. 115
31 Profiles of distributed actuator force. 115
32 Illustration of Space Station Freedom. 117
33 Dynamics of beta gimbal and solar array panel. 119
34 Block diagram for optimal control with sensitivity functions. 123
35 Geometry of two-link flexible manipulator. 142

LIST OF TABLES

TABLE		PAGE
1	Simulation results for flexible manipulator example	48
2	Closed loop poles with no uncertainty	97
3	Closed loop poles with 10% uncertainty	98
4	Closed loop poles with 20% uncertainty	99
5	Terms used in gimbal and array panel dynamics	120
6	Two-link dynamics terms	142

ABSTRACT

Decentralized control strategies for nonlinear systems are achieved via feedback linearization techniques. New results on optimization and parameter robustness of nonlinear systems are also developed. In addition, parametric uncertainty in large-scale systems is handled by sensitivity analysis and optimal control methods in a completely decentralized framework. This idea is applied to alleviate uncertainty in friction parameters for the gimbal joints on Space Station Freedom. As an example of decentralized nonlinear control, singular perturbation methods and distributed vibration damping are merged into a control strategy for a two-link flexible manipulator.

CHAPTER 1

INTRODUCTION

1.1 PROBLEM STATEMENT

"A purely linear world would be a sad place in which to live." [1]

Perhaps the above quote could be appended with the comment that it would be easier to control. But so many of today's high performance electronics, industrial equipment, appliances, transportation vehicles, and materials are successful precisely because they are nonlinear. These systems exploit their nonlinear characteristics to achieve better performance than previously available. However, linear systems are easier to control and understand. This motivates the subject of linearization which allows one to apply linear system theory to a nonlinear model.

Most theory of linearization has centered around the well-known Jacobian or operating point linearization in which the system is restricted to operate in a region small enough such that the system can be approximated as linear. But more recent theory has uncovered the fact that feedback can make a nonlinear system behave as a linear one *exactly*. That is, the system does not have to remain in some small region. This theory now allows one to employ the great abundance of linear control techniques without restricting the system to remain close to particular operating points. In this report, this method of linearization will be employed as a means of control for nonlinear systems that have more than one input-output channel. We will also focus on the issues of parametric uncertainty and optimal performance in nonlinear systems via feedback linearization.

A primary motivation for this work is the subject of control of large space structures. Indeed, one of the largest ever proposed of these structures, Space Station Freedom, is the topic of Chap. 5. These structures with their moving appendages, coupled rigid-body-flexible modes, and motorized joints are highly nonlinear and large in scale. Hence, decentralized control is a natural method of alleviating the computational burden that would accompany a highly centralized control scheme. Combining decentralized control and nonlinear systems was a major emphasis of this report.

Sensitivity analysis is a very useful tool designed to alleviate the effects of parameter uncertainty on control performance. We employ this tool to investigate the effects

of parameter variation in linear large-scale systems as well as an example of a motor with nonlinear friction utilized on the space station. Though sensitivity analysis is an old technique that has not garnered much recent attention, we show that there are fresh new avenues of research and applications for this theory.

Finally, the subject of singular perturbations is a well-known technique for the control of flexible structures. In addition to reviewing relevant theory of singular perturbations, we apply these techniques to a two-link flexible manipulator modeled after the one in use at The Ohio State University. This study combines the methods of singular perturbations with the rapidly developing area of distributed vibration control to achieve powerful new methods for controlling vibrations while conducting desired slewing maneuvers. This section (appearing in Chap. 5) is also a good example of decentralized nonlinear control since feedback linearization via the method of asymptotic expansions is achieved at each link using only locally measurable signals.

1.2 SPACE STRUCTURES

The subject of space travel has fascinated humans for thousands of years, but it was not until the launching of Sputnik in 1957 that it became a reality. Since then, vehicles designed for both manned and unmanned space travel have gone farther and explored more of the solar system than ever before. But, proposed new structures such as the space station, the national aerospace plane, and many experimental probes (e.g., space-based interferometers) will require higher performance and vibration suppression than previous structures.

Space structures must be designed to undergo large temperature changes, high speed motion, and quite varied orientations while maintaining a nearly vibration free environment for at least part of the structure. For instance, telescopes mounted on long arms must remain very steady in order to observe minute details of stars and other galactic features. Though materials may exist to provide such tolerance to vibrations, they are too heavy or expensive for a large space structure. Thus, active means of vibration damping must be pursued. Even if superior materials are developed, one can always achieve still better vibration suppression by employing active control.

Space structures have the following features: closely packed and lightly damped oscillatory modes, attached rotating appendages, and multiple actuators/sensors. The first of these features implies that active control is important in order to achieve acceptable damping ratios. The second of these features implies nonlinear dynamical behavior, and the third feature indicates that decentralized control may be desirable. Thus, this report is principally concerned with decentralized control of nonlinear systems especially as it relates to active vibration control of flexible structures.

Since most control techniques require the use of a mathematical model, the issue of modeling of space structures has been a subject of considerable interest. One of

the most common of these techniques is that of exact modeling or modeling from first principles. Since the structures themselves are distributed parameter systems (equations of motion depend on both time and position along the structure), the equations of motion will be partial differential equations. These equations are infinite dimensional in state space, thus discretization techniques such as assumed modes and finite differences are utilized to achieve finite-dimensional models. The methodology for generating these partial differential equations has been well known for centuries and includes such methods as Hamilton's Principle, Lagrange's equations, and the Newton-Euler formulation. More recent techniques include Kane's equations and Gibbs-Appel equations.

A classical example of a flexible structure is the Euler-Bernoulli beam in which a cantilevered beam vibrates in the transverse direction. The partial differential equation describing its behavior is written as

$$EI\frac{\partial^4 \alpha}{\partial x^4} + \rho\frac{\partial^2 \alpha}{\partial t^2} = 0 \tag{1.1}$$

which can be approximated as an ordinary differential equation via the assumed modes method. This technique is outlined in the appendix and is applied to the flexible robot example of Chap. 5.

Perhaps the most widely used modeling technique today for flexible structures is the finite-element method. This results in a finite-dimensional model from the start since the structure is divided into elements each of which is approximated as a second order mass-spring system. The resulting equations will have the general form

$$M(X)\ddot{X} + F(X,\dot{X}) + KX = BU \tag{1.2}$$

where M is the effective mass matrix, K is the effective stiffness matrix, and F is a possibly nonlinear term representing damping and other types of behavior.

Sometimes the process of modeling a structure is too difficult to be done analytically. Experimental results may be utilized directly to obtain a working model of the structure. This is known as system identification. It is also used to refine an analytically determined model and to reduce the order of an existing model. Indeed, system identification may be used to increase the confidence one has in a previously obtained model. Many methods exist (e.g., Eigensystem Realization Algorithm - ERA, Recursive Least Squares - RLS, Prony's Method, etc.) as well as combinations of these techniques.

Control of flexible structures (once a model is obtained) can be attacked by a variety of approaches. They run the scale from very simple to highly complex. The following list is by no means exhaustive but does give an indication as to the options available to control engineers of large space structures:

- Gain Scheduling (Proportional Integral Derivative - PID, output feedback)

- Dynamic Compensation (frequency shaping feedback)
- Optimal Control (Linear Quadratic Regulator/Linear Quadratic Gaussian - LQR/LQG)
- Singular Perturbation Control (slow and fast modes)
- Decentralized Control (multi-body dynamics)
- Nonlinear Control (adaptive, sliding mode, feedback linearization)
- Combinations of the above

The structures considered for application of the above techniques contain flexible components for which we wish to minimize vibrations. These structures also exhibit rotational and translating capabilities which result in nonlinear behavior. A simple example of such a structure is a rigid hub that can translate in two dimensions and rotate in one dimension. Attached to this hub is a flexible beam that exhibits planar vibrations. This structure represents a coupling of linear vibration characteristics with nonlinear slewing behavior and is illustrated in Fig. 1.

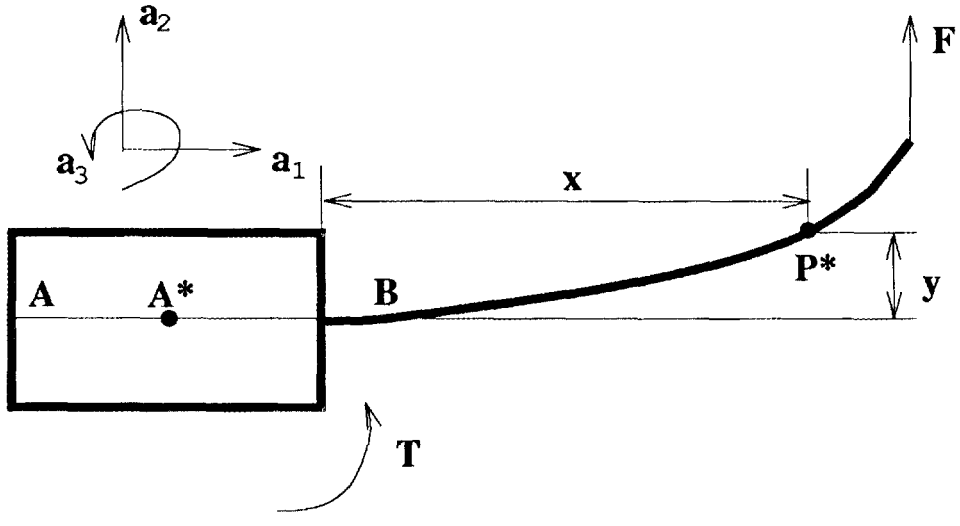

Fig. 1: Spacecraft with rigid hub and attached flexible appendage.

Equations of motion can be derived for this spacecraft by modeling the beam as clamped at the hub and free at the other end. Then using the assumed modes method we retain one mode in the model (more modes can be handled quite easily). We also ignore gravity in this model. Let u_1, u_2, u_3 be the velocity of A^* (center of mass of

hub A) in a_1, a_2, a_3 direction, respectively. Let u_4 and q_1 be the modal velocity and modal displacement, respectively, of the flexible beam B. The control variables are T and F which are the torque produced by the hub motor and the force produced by the jet at the beam's endpoint, respectively. All other parameters appearing in the model are constants representing masses, moments of inertia, stiffness constants, and various other physical quantities that will not be discussed further for the sake of brevity.

The equations of motion can then be written as

$$\begin{bmatrix} m_A + m_B & 0 & -E_1 q_1 & 0 & 0 \\ 0 & m_A + m_B & bm_B + e_B & E_1 & 0 \\ E_1 q_1 & -bm_B - e_B & -b^2 m_B - 2(e_B + I_B + J_3)) & -bE_1 + F_1 & 0 \\ 0 & E_1 & bE_1 + F_1 & G_{11} & 0 \\ 0 & 0 & 0 & 0 & 1 \end{bmatrix}$$

$$\cdot \begin{bmatrix} \dot{u}_1 \\ \dot{u}_2 \\ \dot{u}_3 \\ \dot{u}_4 \\ \dot{q}_1 \end{bmatrix} = \begin{bmatrix} (m_A + m_B)u_2 u_3 + 2E_1 u_3 u_4 + (bm_B + e_B)u_3^2 \\ -(m_A + m_B)u_1 u_3 + E_1 u_3^2 q_1 \\ E_1 u_2 u_3 q_1 + (bm_B + e_B)u_1 u_3 \\ -E_1 u_1 u_3 + G_{11} u_3^2 q_1 - H_{11} q_1 \\ u_4 \end{bmatrix}$$

$$+ \begin{bmatrix} 0 & 0 \\ 0 & 1 \\ -1 & -(b + L) \\ 0 & \phi_1(L) \\ 0 & 0 \end{bmatrix} \begin{bmatrix} T \\ F \end{bmatrix} \tag{1.3}$$

which is a fifth order nonlinear ordinary differential equation. The outputs can be chosen to be any of the five states, thus they will ordinarily be linear functions. By choosing two outputs (say, hub rotation, u_3, and tip displacement, q_1), we obtain a two-input, two-output nonlinear system. The first input/output port could be restricted to hub information only (u_1, u_2, u_3), and the second input/output port could be restricted to beam endpoint information only (u_4 and q_1). This decentralization constraint would be desirable for a real spacecraft of the type in Fig. 1 because of the difficulty in exchanging information between the two ports. Thus, this is the type of structure for which the theory developed in the following chapters would be most useful.

1.3 FLEXIBLE ROBOTICS

In some ways, robotics are a special case of the previous section. Many of the same modeling and control techniques applied to space structures will work well for robotics. However, because of their nature as smaller more dedicated structures, we devote

some discussion to their historical development. In particular, we concern ourselves with flexible robotics due to their light weight and utility in space applications. Further details on control and modeling of flexible robotics will appear in Chap. 5 and Appendix A.

In many applications that involve slewing of mechanical structures such as in spacecraft and robotics, performance is limited by the mass and rigidity of the moving appendages. The use of lightweight materials and slender appendages can enhance speed and mobility while reducing energy consumption but inevitably lead to flexibility. The principal drawback to flexibility in structures is the issue of control. This is due to the tremendous increase in complexity of the system dynamics as a result of the elasticity in the links. There is a wealth of literature on rigid robot control, but additional control strategies are needed to deal with the more complex dynamics of flexible links. Chapter 5 addresses the strategy of combining two methods for handling structural elasticity: perturbation techniques and distributed vibration damping.

Two works in particular, Spong et al. [2] and Siciliano and Book [3], apply perturbation techniques to flexible joint and flexible link robots, respectively. In Ref. [2], the integral manifold approach is employed to decompose the dynamics into a fast subsystem representing the elastic forces at the joints and a slow subsystem representing the rigid body motion. The control strategy is then an approximate feedback linearization which allows the use of rigid link control ideas. In Ref. [3], a singular perturbation approach is utilized to achieve a similar approximate linearization strategy for manipulators with elastic links.

In these perturbation methods, the system dynamics are a function of a small parameter ϵ which represents stiffness of the joints or links. As ϵ tends to zero the slow subsystem (integral manifold) tends to the rigid link manipulator model. The integral manifold is then expanded as a power series in ϵ about $\epsilon = 0$. The primary advantage of the integral manifold approach is that it enables one to linearize the system dynamics to an arbitrary order of ϵ via the torque controllers. Other approximate linearization strategies have been proposed for flexible-link manipulators such as pseudo-linearization [4] and input-output inversion [5]. But the integral manifold approach facilitates the incorporation of approximate linearization (for the slow subsystem) and distributed actuation (for the fast subsystem) as is done in this report.

The concept of exact feedback linearization which is extensively used throughout this report is not an option for flexible robotics. It has been shown in Ding et al. [6] and Khorrami and Zheng [7] among others that the necessary and sufficient conditions for exact feedback linearizability of flexible link robots are not satisfied. That is, torque control alone cannot exactly linearize the full-order dynamic system since there are not as many control inputs as output variables. The purpose of applying integral manifold theory to the above structure is to be able to reduce the

dynamics of the system to the rigid body motion. This reduced order system will account for the flexibility of the links. In addition, the effects of the rigid body motion on the flexure are given by a manifold condition.

The primary goal of distributed vibration damping is to add thin material (e.g., polymer films) to an elastic beam and apply control signals to effect a dampening of the modes of vibration. No particular distributed actuator is proposed here but instead analysis undertaken in Chap. 5 is applicable to a wide variety of thin film actuators whose characteristics are very similar in how they impact the equations but may differ in hardware implementation. The purpose of this analysis is to provide a description of how film actuators can reduce bending effects in flexible manipulators. The basic idea behind film actuators is that they produce a strain along the longitudinal axis of the links when applied with a voltage distributed along the link. It is shown here that feedback of various measured variables to this voltage can produce a strain which dampens the modes of vibration. Other actuators such as discrete actuators could have been employed, however, these actuators complicate the dynamics of the model and do not have the advantage of being able to control all the vibrational modes of a flexible beam as can a distributed actuator.

The effect of some film actuators on vibrating beams with various boundary conditions is described in Bailey and Hubbard [8], Burke and Hubbard [9, 10], and Crawley and de Luis [11]. In robotics, the action of the film is complicated by the rigid body motion, but it does not significantly alter the control of the slow subsystem (i.e., the slewing motion). A film actuator can also be used as a sensor as is done in Collins et al. [12] allowing one to measure link strain or tip deflection which can then be used for feedback control at the joints.

Our controller design is based upon a distributed parameter model of the two-link manipulator which is derived via the Hamiltonian formulation. Computer simulations are provided which show the results of the feedback linearizing torque control and the improvement in vibrational damping obtained with the distributed actuator. The computer simulation model is obtained from the distributed parameter model via the assumed modes method. Parametric data for the model are obtained from the OSU two-link flexible manipulator, and experimental identification results of this structure indicate that only one mode of vibration is apparent in the transverse motion (Yurkovich et al. [13]). Thus, a one-mode expansion was implemented in the simulations.

1.4 ORGANIZATION OF REPORT

The report starts in Chap. 2 with a survey of feedback linearization and nonlinear observer techniques based upon differential geometry. The chapter continues with a discussion of singular perturbation methods in control theory and sensitivity analysis for systems with uncertain parameters. This chapter finishes with a survey of

decentralized control theory. Chapter 3 covers two key issues in feedback linearization. One is that of optimal performance of a nonlinear system that has been feedback linearized. The second is that of robustness of feedback linearization to parametric uncertainty and additional control effort needed to rectify this situation.

Chapter 4 provides a quartet of results on decentralized control of nonlinear systems. The first of these is that of decentralized nonlinear observers. Next, the issue of controlling a linearized system in a decentralized manner is investigated. Third, stabilization of interconnected systems via decentralized feedback linearization and local linear-quadratic state feedback is studied. Fourth, the enhancement of linearizability properties of nonlinear systems is developed with the aid of partial feedback. The chapter concludes with a thorough investigation of decentralized control via sensitivity models for large-scale systems with parameter uncertainty.

Chapter 5 looks at two examples for applications of theoretical methods studied in this report. The first of these is a two-link flexible manipulator which is controlled by combining decentralized approximate linearization with distributed vibration control. The second example is the gimbal motors used for positioning the solar array panels on Space Station Freedom. Sensitivity analysis is applied to this motor by adding a term to a performance criterion that penalizes deviations of friction parameters from their nominal values. Chapter 6 provides concluding remarks and discussion of future avenues of research opened up by this report. Finally, Appendix A contains the modeling details of the two-link manipulator.

CHAPTER 2

CONTROL THEORY TECHNIQUES

2.1 NONLINEAR CONTROL

Control of linear systems is a highly developed subject area with many powerful analytical tools available and a long history of successful applications in physical problems. The study of nonlinear systems, though still extensive, is less developed due to the fewer analytical tools available and the significantly more complex dynamical behavior of these systems. One of the most common tools applied to linear, time-invariant systems is that of the transfer function. Due to the absence of linearity and superposition, the transfer function concept does not extend to nonlinear differential equations. It is this lack of linearity and superposition that makes much of linear system theory invalid in the study of nonlinear systems. In addition, such complex behavior as limit cycles (isolated closed curves in the state space), multiple equilibrium points, bifurcations (changes in stability behavior due to deviations in parameters), and chaos (extreme sensitivity to initial conditions) can occur in nonlinear systems.

This chapter analyzes some of the control techniques utilized in nonlinear systems. In particular, feedback linearization, observer theory, perturbation methods, and sensitivity analysis are discussed. All of these methods (except feedback linearization) are practiced in linear systems, and we make use of this fact. These analytical tools were chosen because they appear often in the research of this report. Other techniques such as phase plane analysis, describing functions, sliding modes, Lyapunov theory, and adaptive control (see the texts of Refs. [14, 15, 16, 17] for a treatment of these subjects) are quite common in nonlinear control theory but play only a minor role in this work.

We begin by discussing mathematical representations of nonlinear systems. In general, there are many nonlinearities that cannot be written as a differential or algebraic equation such as multi-valued functions, e.g. hysteresis (see Fig. 2). But these types of nonlinearities can still be incorporated into nonlinear control theory by defining specific regions of operation. Then each region will have its own control law with some kind of protocols establishing transitions between regions. This is a very common technique in industrial settings.

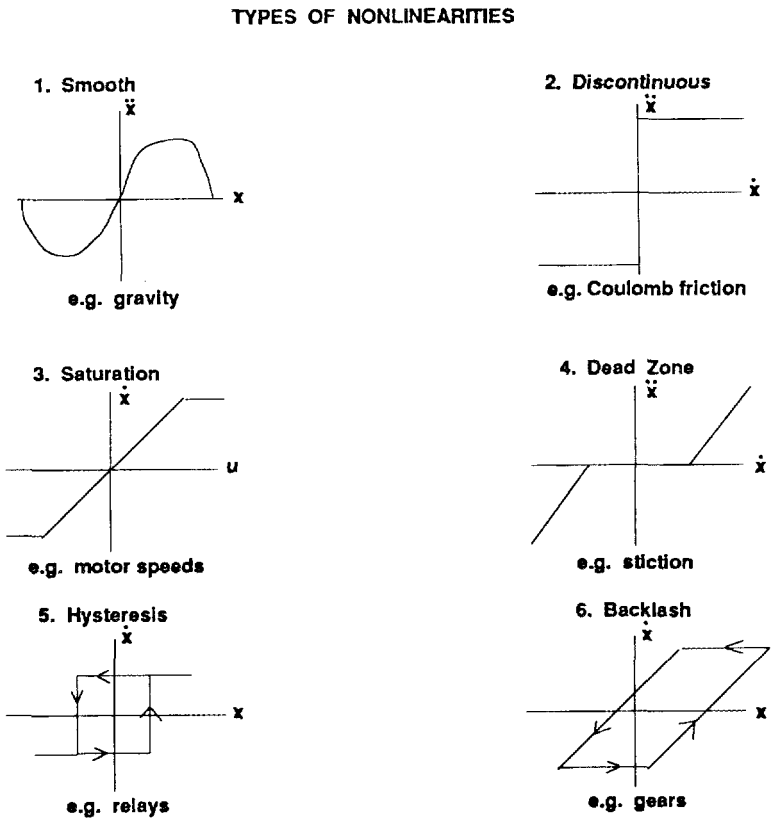

Fig. 2: Examples of common nonlinearities in physical systems.

Thus, we begin by looking at differential equations to describe nonlinear systems. Consider the following system

$$\dot{x} = f(x, u, t)\,, \quad y = h(x, u, t) \tag{2.1}$$

where $x \in R^n$ is the state vector of the system, $y \in R^p$ is the output vector, $u \in R^m$ is the input vector, and $t \in R$ is the independent variable. The function f is an R^n-valued mapping defined on the open sets U of R^n, V of R^m, and W of R. Likewise, h is an R^p-valued mapping defined on the same open sets as f. The functions f and h may be discontinuous in their arguments. In addition, distributed parameter systems (e.g. systems described by partial differential equations) could be characterized by (2.1) with the addition of another independent variable such as a spatial variable. Most of the differential equations dealt with in this report are time-invariant and are affine in the control. That is, an additional vector field $g(x)$ multiplies the control input. Furthermore, the outputs considered here rarely contain a throughput term

(i.e., h is not an explicit function of u). With these constraints, we obtain

$$\dot{x} = f(x) + g(x)u\,, \quad y = h(x) \tag{2.2}$$

which will become our standard nonlinear model. The vector fields, f and g, are smooth mappings of R^n into R^n defined on the open set U of R^n. By smooth, it is meant that f and g have continuous partial derivatives in x to any required order. The vector field h is a smooth mapping of R^n into R^p that is also defined on the set U. These domains and smoothness properties are to be assumed throughout the report except when otherwise noted. The above model has the additional feature that it is structurally similar to its linear counterpart

$$\dot{x} = Ax + Bu\,, \quad y = Cx\,, \tag{2.3}$$

which is useful in discussing linearizations of a nonlinear model.

This chapter starts by examining the concept of feedback linearization and the tools needed to accomplish this strategy. The chapter then proceeds to discuss the nonlinear observer problem. Since decentralized control is a primary focus of this report, it is necessary to examine methods for reconstructing the full state at particular input/output channels for synthesis of nonlinear control. Next, the issue of singular perturbations is dealt with which studies systems whose highest order derivatives are multiplied by a small parameter. This is a common situation in flexible structures in which rigid body and vibrational motion unfold at significantly different frequency ranges. Sensitivity analysis is the next topic surveyed due to its importance in the control of systems plagued by parametric uncertainty. Finally, this chapter culminates with an overview of decentralized control and the methods for its application.

2.1.1 Feedback Linearization

The concept of transforming a nonlinear system into a linear one via feedback has received a great deal of interest recently (see, for instance, Refs. [18, 19, 20, 21, 22]). The area of mathematics that has enabled this concept to come about is that of differential geometry. In particular, a key result utilized by most of the control techniques based upon differential geometry is the theorem of Frobenius [23]. To state this theorem, we first consider a set of m smooth vector fields $\{f_1(x), \ldots, f_m(x)\}$ defined on an open set U of R^n. The Frobenius theorem is principally concerned with the solution of the partial differential equation

$$\frac{\partial \lambda_i}{\partial x} f_1(x) + \cdots + \frac{\partial \lambda_i}{\partial x} f_m(x) = 0 \tag{2.4}$$

for $i = 1, \ldots, n-m$ where the smooth functions $\lambda_i(x)$ are what we wish to find. We have the following definitions.

Definition 2.1 A linearly independent set of vector fields $\{f_1(x), \ldots, f_m(x)\}$ defined on R^n is *completely integrable* if and only if there exist smooth scalar functions λ_i, $i = 1, \ldots, n-m$, satisfying (2.4) with the gradients $\frac{\partial \lambda_i}{\partial x}$, $i = 1, \ldots, n-m$ being linearly independent.

Definition 2.2 The iterated *Lie Derivative* of a vector field $h(x)$ with respect to the vector field $f(x)$ is defined as

$$L_f^k h(x) = \frac{\partial (L_f^{k-1} h(x))}{\partial x} f(x)\,, \quad L_f^0 h(x) = h(x) \tag{2.5}$$

where it is noted that the above (with $k = 1$) is simply a directional derivative with $f(x)$ serving as the trajectory along which the vector field h is differentiated.

Definition 2.3 We define the *Lie bracket* of a pair of vector fields $f_i(x), f_j(x)$ as

$$[f_i\,,\, f_j](x) \triangleq \frac{\partial f_j}{\partial x} f_i(x) - \frac{\partial f_i}{\partial x} f_j(x)\,. \tag{2.6}$$

Definition 2.4 A linearly independent set of vector fields $\{f_1(x), \ldots, f_m(x)\}$ is *involutive* if and only if there exist scalar functions $c_{ijk}(x)$ such that

$$[f_i\,,\, f_j](x) = \sum_{k=1}^{m} c_{ijk}(x) f_k(x) \quad \forall i, j \in \{1, \ldots, m\}\,. \tag{2.7}$$

Simply stated, involutivity means that the Lie bracket of all pairs of vector fields from the set $\{f_1, \ldots, f_m\}$ can be expressed as a linear combination of the original set of vector fields. The Frobenius theorem is now formally stated without proof.

Theorem 2.1 *The set of linearly independent vector fields $\{f_1, \ldots, f_m\}$ is completely integrable if and only if it is involutive.*

This theorem provides us with a necessary and sufficient condition for the solvability of the class of partial differential equations (2.4). Thus, the solvability of (2.4) can be determined by checking the involutivity of the vector fields which is considerably easier than trying to solve (2.4) without knowing if a solution exists. This class of partial differential equations arises often in nonlinear control theory particularly as related to feedback linearization and nonlinear observers. Hence, the Frobenius theorem has proven useful in finding conditions for the solvability of nonlinear control problems. Most of this report deals directly with the results of feedback linearization theorems without explicit reference to the Frobenius theorem. However, much of these theorems owe their existence to the Frobenius theorem.

The first paper to show that linearization was possible for single-input systems via feedback was Brockett [18]. Earlier work by Krener [24] had laid the groundwork

for such study. The more general methods of feedback linearization of multi-input systems was independently developed by Jakubczyk and Respondek [22], Hunt et al. [25, 20], and Su [26]. Linearization of systems with outputs was extensively discussed by Cheng et al. [19]. The notion of zero dynamics which describe a system's behavior when the outputs are constrained to be zero was introduced by Byrnes and Isidori [27].

Other more approximate methods such as extended linearization by Baumann and Rugh [28] and pseudo-linearization by Réboulet et al. [29] relax the exact linearizability conditions by performing it locally about a series of operating points. This method is reminiscent of gain scheduling whereby different sets of feedback laws are scheduled for different regions of operation. In some instances dynamic state feedback (i.e. the feedback law itself is described by a differential equation) can enhance the linearizability of a system as proposed by Charlet et al. [30]. Texts on nonlinear systems which have extensive sections devoted to feedback linearization include Isidori [21], Nijmeijer and Van der Schaft [31], and Slotine and Li [16].

There are several varieties of feedback linearization in the literature. Input-state linearization is exact state space linearization without regard to outputs. It is popular for systems which either have no outputs defined or have the freedom to use an arbitrary nonlinear function of the states as an output vector. Input-output linearization seeks to render the input-output response linear despite the presence of unobservable or zero dynamics that remain nonlinear but do not affect the input-output behavior. Finally, exact linearization or exact state-space linearization implies that not only the input-output response is linear but also the full state space response has been linearized. This type of linearization assumes that the output vector is given and does not seek any new output functions to enable the linearization process. Throughout most of this report, it is this latter form of linearization, state-space exact linearization that interests us. This is because for most systems only a few combinations of states represent physically meaningful outputs. This is not only the case due to interest in just a few variables, but also some of the states may not be easily measurable.

Multi-Input Multi-Output (MIMO) systems will interest us more than Single-Input Single-Output (SISO) systems due to the multivariable nature of large-scale systems, however both types of systems are analyzed here. The development of feedback linearization for MIMO systems parallels that of SISO systems with only minor differences in theory. The differences are more computational in nature than theoretical.

The process of state-space linearization requires the computation of the system's relative degree which is simply the number of times one must differentiate the output signal before the input term appears explicitly. Also needed is a coordinate transformation that converts the original system's dynamics into a normal form which makes apparent what the input term must be to cancel the nonlinearities. Thus, the system will be linear in only this new set of coordinates. Once linearized, the resulting system

will be linear and controllable lending itself easily to the wealth of linear control ideas.

We begin by examining MIMO nonlinear systems of the form

$$\dot{x} = f(x) + \sum_{i=1}^{m} g_i(x)u_i\,, \quad y_i = h_i(x)\,, \quad i = 1, \ldots, m\,, \tag{2.8}$$

where $x \in R^n$, $f(x)$ and $g_i(x)$ are smooth vector fields defined on an open set of R^n, $h_i(x)$ is a smooth scalar function of x, and the m u_i/y_i pairs are SISO channels. We also assume that each input/output pair has the full state x available for feedback. To begin the process of feedback linearization, we define the concept of relative degree.

Definition 2.5 The *vector relative degree* $\{r_1, r_2, \ldots, r_m\}$ of (2.8) at some point x^0 satisfies

$$L_{g_j} L_f^k h_i(x) = 0\,, \quad 1 \le i, j \le m \tag{2.9}$$

for all $k < r_i - 1$ in a neighborhood of x^0, and the mxm matrix

$$A(x) = \begin{bmatrix} L_{g_1} L_f^{r_1-1} h_1(x) & L_{g_2} L_f^{r_1-1} h_1(x) & \cdots & L_{g_m} L_f^{r_1-1} h_1(x) \\ L_{g_1} L_f^{r_2-1} h_2(x) & L_{g_2} L_f^{r_2-1} h_2(x) & \cdots & L_{g_m} L_f^{r_2-1} h_2(x) \\ \vdots & \vdots & \ddots & \vdots \\ L_{g_1} L_f^{r_m-1} h_m(x) & L_{g_2} L_f^{r_m-1} h_m(x) & \cdots & L_{g_m} L_f^{r_m-1} h_m(x) \end{bmatrix} \tag{2.10}$$

has full rank at $x = x^0$.

Note that the number r_i is associated with the ith output of (2.8) and is the number of times one has to differentiate y_i to have at least one component of the control vector u appear explicitly. With this definition of relative degree we present the following lemma due to [19] which provides the necessary and sufficient conditions for exact linearization of (2.8).

Lemma 2.1 *Assume that* rank $[g_1(x^0)\, g_2(x^0) \cdots g_m(x^0)] = m$. *Then (2.8) can be rendered linear via a state feedback and a coordinate transformation if and only if there exists a neighborhood of x^0 such that (2.8) has some vector relative degree $\{r_1, r_2, \ldots, r_m\}$ at x^0 and $r_1 + r_2 + \cdots + r_m = n$.*

The coordinate transformation sufficient for achieving this linearization is defined as

$$z = \Phi(x) = \left[\phi_1^1(x), \ldots, \phi_{r_1}^1(x), \ldots, \phi_1^m(x), \ldots, \phi_{r_m}^m(x)\right]^T \tag{2.11}$$

where

$$\phi_k^i(x) = L_f^{k-1} h_i(x)\,, \quad 1 \le r_i\,, \quad 1 \le m\,. \tag{2.12}$$

The linearizing feedback can be written as

$$u = \alpha(x) + \beta(x)v \tag{2.13}$$

with

$$\alpha(x) = -A^{-1}(x)\Gamma(x)\,, \quad \beta(x) = A^{-1}(x) \tag{2.14}$$

$$\Gamma(x) = \begin{bmatrix} L_f^{r_1} h_1(x) \\ L_f^{r_2} h_2(x) \\ \vdots \\ L_f^{r_m} h_m(x) \end{bmatrix} \tag{2.15}$$

and $v = [v_1, v_2, \ldots, v_m]^T$ is a vector of inputs to the linearized system. This results in a linear system of the form

$$\dot{z} = Az + Bv\,, \quad y = Cz \tag{2.16}$$

where (A, B, C) are in Brunovsky canonical form [32]. The linearizing feedback (2.13) is also the standard noninteracting control [33], i.e., the feedback that input-output decouples (2.8). Another important point is that the linearizing coordinates transformation and the linearizing feedback will be smooth vector fields if the original system vector fields in (2.8) are smooth [21]. Figure 3 demonstrates the concept of feedback linearization by clearly showing the composite linearized system.

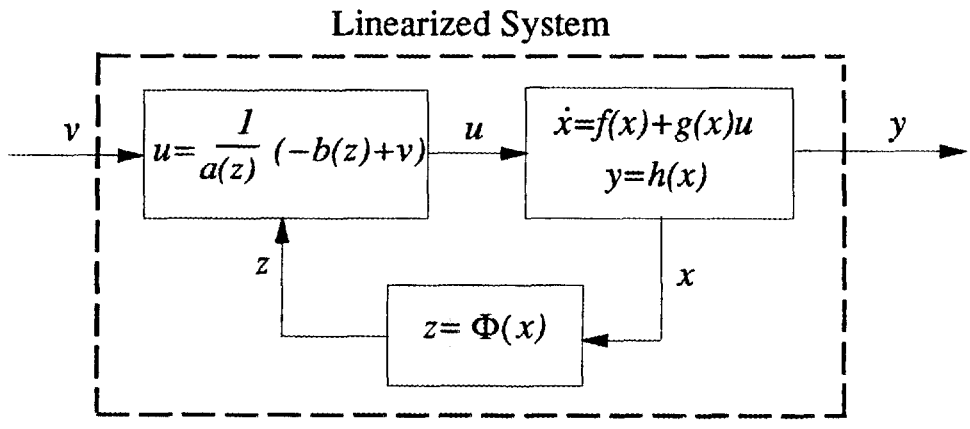

Fig. 3: Linearization via feedback.

The single-input single-output linearization problem is also examined here. Consider the following system

$$\dot{x} = f(x) + g(x)u\,, \quad y = h(x)\,, \tag{2.17}$$

where $x \in R^n$ and y and u are scalars. As in the MIMO case, we need the notion of relative degree.

Definition 2.6 The system (2.17) has *relative degree* r about a point x^0 if

$$L_g L_f^k h(x) = 0 \tag{2.18}$$

for all $k < r - 1$ and all x in a neighborhood of x^0 and

$$L_g L_f^{r-1} h(x^0) \neq 0 \,. \tag{2.19}$$

Lemma 2.2 *The SISO linearization problem is solvable in a neighborhood of x^0 if and only if (2.17) has relative degree $r = n$ at x^0.*

The linearizing coordinates in the SISO case are simply

$$z_i = \phi_i(x) = L_f^{i-1} h(x) \,, \quad 1 \leq i \leq n \,, \tag{2.20}$$

and the linearizing feedback is

$$u = \frac{1}{L_g L_f^{n-1} h(x)} \left(-L_f^n h(x) + v \right) \,. \tag{2.21}$$

This results in a linear system in normal form [27]

$$\begin{aligned} \dot{z}_1 &= z_2 \\ &\vdots \\ \dot{z}_{n-1} &= z_n \\ \dot{z}_n &= v \\ y &= z_1 \end{aligned} \tag{2.22}$$

which is simply a chain of n integrators.

As mentioned earlier, if one is not restricted to particular outputs, i.e., if one has freedom to choose new outputs, say $y = \lambda(x)$, then conditions involving $f(x)$ and $g(x)$ only (see Refs. [18, 20, 22]) can be formulated to provide the existence of these outputs such that the relative degree requirements are satisfied. These results rely heavily on the Frobenius theorem which enables one to find a solution to a particular differential equation yielding the new outputs.

2.1.2 Nonlinear Observers

Much of the feedback control methods available to engineers rely upon full state feedback. One can often achieve better closed loop performance with the full state than with just an output or a partial set of states. However, this may require expensive measuring devices and/or additional computing hardware. Thus, the issue of reconstructing the system state from available measurements has been a subject

of considerable study for decades. The theory for nonlinear systems is not as well developed as that for linear systems, but a number of results do exist. Observers based upon statistical linearization, Jacobian linearization, and sliding modes are well-known (see Ref. [34] for a survey).

In this section, we look at the nonlinear problem from a Lie-algebraic approach. The use of differential geometry for the single-output nonlinear observer problem was independently developed by Bestle and Zeitz [35] and Krener and Isidori [36]. The multi-output case was analyzed by Krener and Respondek [37] who also looked at the problem with inputs as well. Since these observers require a transformation to observer canonical form, some attempts to alleviate the solving of the partial differential equations that arise in this transformation have been attempted. One such effort is analogous to the extended Kalman filter for stochastic systems. It is based upon pseudo-linearization and is referred to as the extended Luenberger observer. This was introduced by Zeitz [38] and avoids the solution of partial differential equations.

To focus entirely on the observer problem let us restrict ourselves to the single output nonlinear system with no input and state of dimension n

$$\begin{aligned} \dot{x} &= f(x) \\ y &= h(x) \end{aligned} \tag{2.23}$$

where x^0 is the initial state vector. Most of this discussion follows that of Ref. [36]. Suppose there exists a coordinate transformation $z = \Phi(x)$ which transforms the vector field f and the output map h into

$$\left[\frac{\partial \Phi}{\partial x} f(x)\right]_{x=\Phi^{-1}(x)} = Az + k(Cz) \tag{2.24}$$

$$h(\Phi^{-1}(z)) = Cz \tag{2.25}$$

where (A, C) is an observable pair and k is an nx1 vector valued function. Then an observer of the form

$$\dot{\xi} = (A + GC)\xi - Gy + k(y), \tag{2.26}$$

where ξ is the estimate of the transformed state z, is obtained. The observer error $e = \xi - z = \xi - \Phi(x)$ has dynamics

$$\dot{e} = (A + GC)e \tag{2.27}$$

which is linear and controllable (through G). The following lemma states the necessary and sufficient conditions for constructing such an observer.

Lemma 2.3 *The observer linearization problem is solvable if and only if the following two conditions hold:*
(i) $dim(span\{dh(x^0), dL_f h(x^0), \ldots, dL_f^{n-1} h(x^0)\}\ ) = n$
(ii) the unique vector solution τ *of*

$$\begin{bmatrix} dh(x) \\ dL_f h(x) \\ \vdots \\ dL_f^{n-2} h(x) \\ dL_f^{n-1} h(x) \end{bmatrix} \tau(x) = \begin{bmatrix} 0 \\ 0 \\ \vdots \\ 0 \\ 1 \end{bmatrix} \tag{2.28}$$

is such that

$$\left[ad_f^i \tau, ad_f^j \tau\right] = 0 \tag{2.29}$$

for all $0 \leq i, j \leq n-1$.

To find an observer with linear and spectrally assignable error dynamics, we need both of the above conditions to hold. With condition (i) holding, we find the vector field τ by solving (2.28). With condition (ii) holding and our solution τ, we solve the partial differential equation

$$\frac{\partial F}{\partial z} = \begin{bmatrix} \tau(x) & -ad_f \tau(x) & \cdots & (-1)^{n-1} ad_f^{n-1} \tau(x) \end{bmatrix}_{x=F(z)} \tag{2.30}$$

to find the function F which is defined in a neighborhood V^0 of z_0 such that $F(z^0) = x^0$. Then setting $\Phi = F^{-1}$, we compute the mapping k as

$$k(z_n) = \begin{bmatrix} k_1(z_n) \\ k_2(z_n) \\ \cdots \\ k_n(z_n) \end{bmatrix} = \left[\frac{\partial \Phi}{\partial x} f(x)\right]_{x=\Phi^{-1}(z)} - \begin{bmatrix} 0 \\ z_1 \\ \cdots \\ z_{n-1} \end{bmatrix}, \tag{2.31}$$

which results in the observer in (2.26).

Condition (i) is the nonlinear analog of the observability rank condition for linear systems and condition (ii) is an involutivity condition. In some sense the nonlinear observer problem is the dual of the exact linearization problem where we needed a change in coordinates to more clearly solve the problem. The exact linearization and nonlinear observer problems are two key results utilized in this report to tackle nonlinear problems, in particular, decentralized control of nonlinear systems. Other results in the geometric theory of nonlinear systems not discussed here include disturbance decoupling and noninteracting control (see Refs. [21, 33]).

2.2 SINGULAR PERTURBATIONS

This section focuses on the methods of multiple scales and composite control for singularly perturbed systems. Singularly perturbed systems are ones in which their highest order derivatives are multiplied by a small parameter. This feature manifests itself as two-time-scale behavior. That is, a fast boundary layer system is coupled with a slow reduced-order system by a small parameter ϵ. Many examples of such behavior exist including flexible structures (fast vibrational behavior, slow slewing motion), fluid mechanics (fast boundary layer behavior, slow steady flow), and dc motors (fast armature current transients, slow armature angular speed). The idea behind singular perturbation techniques is to take these fast dynamics into account while only designing a control law explicitly for the reduced order or slow subsystem. This approximate technique can be carried out to as high an order in ϵ as one wishes but is generally only carried out to first order expansions in ϵ. Thus, ϵ should be small (i.e., its relative value to other constants in the system should be much less than one).

Singular perturbation methods are not as general as differential geometric methods because they are only useful in systems with multiple time scale behavior or boundary layer phenomenon. Differential geometric methods are applicable to more general nonlinear systems but conditions for implementation are more strict. In the next two subsections, the multiple time scale technique will be developed and applied to determine a composite control (one control for each time scale). Much of the theory of singular perturbations stems from the work of mathematicians such as Tikhonov [39], Vasil'eva [40], and Hoppensteadt [41] who analyzed the problem from a differential equations point of view. Much of this theory was utilized in fluid mechanics before it reached control theory (see texts of Cole [42] and Nayfeh [43]). Most of the applications of the singular perturbation literature to control systems was initiated by Kokotović and colleagues [44, 45, 46, 47, 48].

All singularly perturbed systems exhibit a small parameter ϵ which could represent many different physical properties such as stiffness in a vibratory system, Reynolds number in fluid flow, uncertainty in a system parameter such as stray capacitance in an electrical network, etc. When ϵ is zero the system has a lower dimension in state space than when ϵ is nonzero. Thus, the system is singularly perturbed. One of the primary methods in finding the solution to the set of equations describing a singularly perturbed system is the method of matched asymptotic expansions [43]. Solving singularly perturbed equations exactly is very difficult, often intractable. Thus, this method expands the solution variable as a power series in ϵ which is plugged into the original system equations. Then each term in the expansion is solved for separately by gathering the terms and obtaining a separate equation for each power of ϵ.

The equations are solved from the lowest order equation to as high as one wishes to go (the power series is infinite but ordinarily ϵ is small so only a few terms will

be needed) using the solution of the previous order. The matching comes about when one discovers that the approximate solution often does not satisfy the boundary conditions. This implies the existence of a small boundary layer (width of order ϵ) at the boundaries of the system. Then through a rather simple procedure (detailed in [43]) the asymptotic solution is matched to the boundary value by introducing an intermediate region of thickness $\delta > \epsilon$ (δ is the distinguished limit) in which the asymptotic solution is "smoothed" to converge to the boundary value at the end of the intermediate layer. The solution thus obtained will approximate the true solution to an error on the order of the power of ϵ to which one carried out the expansion.

However, the matched asymptotic expansion method does not always result in a good approximation to the true solution in a singularly perturbed system. For singularly perturbed systems which exhibit multiple time scale behavior the above method will result in secular terms (explode as $t \to \infty$). Thus a more general method is needed to analyze these systems. In fact, most singularly perturbed control systems will have multiple time scales, e.g., adaptive control systems with slow adaptation [49], vibratory systems [50, 51, 3, 2], etc. The method of multiple time scales which is explained in the following subsection converts an ordinary differential equation into a partial differential equation because there is more than one time variable, but the method results in solutions that do not contain secular terms.

2.2.1 Multiple Time Scales Technique

We examine the following example [43] to illustrate the method. Consider the linear damped oscillator

$$\ddot{x} + x = -2\epsilon\dot{x} \tag{2.32}$$

where ϵ is a small positive parameter. We will first attempt a straightforward asymptotic expansion of x in ϵ, i.e.,

$$x = x_0 + \epsilon x_1 + \epsilon^2 x_2 + \cdots \tag{2.33}$$

where each successive term in the expansion is of smaller order than the previous term. Now, (2.33) is substituted into (2.32) and equating terms of like powers of ϵ leads to

$$O(1): \quad \ddot{x}_0 + x_0 = 0 \tag{2.34}$$

$$O(\epsilon): \quad \ddot{x}_1 + x_1 = -2\dot{x}_0 \tag{2.35}$$

$$O(\epsilon^2): \quad \ddot{x}_2 + x_2 = -2\dot{x}_1. \tag{2.36}$$

The general solution of (2.34) is

$$x_0 = a\cos(t + \phi) \tag{2.37}$$

where a and ϕ are constants determined by the initial conditions. Substituting x_0 into (2.35) and solving we get

$$x_1 = -at\cos(t+\phi) \tag{2.38}$$

which when plugged into (2.36) results in

$$x_2 = \frac{1}{2}at^2\cos(t+\phi) + \frac{1}{2}at\sin(t+\phi). \tag{2.39}$$

Combining (2.37)-(2.39) we get the approximate solution

$$\begin{aligned} x &= a\cos(t+\phi) - \epsilon at\cos(t+\phi) \\ &+ \frac{1}{2}\epsilon^2 a[t^2\cos(t+\phi) + t\sin(t+\phi)] + O(\epsilon^3). \end{aligned} \tag{2.40}$$

Clearly there is a problem here. When $t > \frac{1}{\epsilon}$ the second and third terms are not small compared to the first term and thus we no longer have an asymptotic expansion. In fact x_1 and x_2 contain secular terms (terms that explode as $t \to \infty$). Thus, this expansion is not valid for $t > O(\epsilon^{-1})$.

To see why the expansion failed, we look at the exact solution of (2.32)

$$x = ae^{-\epsilon t}\cos[\sqrt{1-\epsilon^2}t + \phi]. \tag{2.41}$$

The exponential term in (2.41) yields the following Taylor series (about 0)

$$e^{-\epsilon t} = 1 - \epsilon t + \frac{1}{2}\epsilon^2 t^2 + \cdots. \tag{2.42}$$

The problem is that t can and will become very large which implies that a finite number of terms will result in a diverging value even though the infinite series converges to zero. When t is as large as ϵ^{-1}, the truncated expansion breaks down. All terms of the series are needed for the expansion to be valid for all time. Thus to find an expansion that is valid for times as large as $\frac{1}{\epsilon}$, the time scale ϵt should be kept as a separate variable $T_1 = O(1)$.

Likewise, the expansion of the cosine term

$$\cos(\sqrt{1-\epsilon^2}t + \phi) = \cos(t+\phi) + \frac{1}{2}\epsilon^2 t\sin(t+\phi) + \cdots \tag{2.43}$$

is not valid for t as large as $O(\epsilon^{-2})$. Then the time scale $\epsilon^2 t$ should be kept as a separate variable $T_2 = O(1)$. This procedure indicates that x depends not only on t but also on ϵt, $\epsilon^2 t$, $\cdots$, as well as on ϵ itself. To find a finite expansion that is valid for all times up to $O(\epsilon^{-M})$, we must find the dependence of x on the $M+1$ time scales T_0, T_1, $\cdots$, T_{M-1} where

$$T_i = \epsilon^i t, \tag{2.44}$$

and it should be noted that $T_0 = t$.

To apply these multiple time scales to our original problem (2.32), we need to use the chain rule to determine the new time derivatives, i.e.,

$$\frac{d}{dt} = \frac{\partial}{\partial T_0} + \epsilon\frac{\partial}{\partial T_1} + \epsilon^2\frac{\partial}{\partial T_2} + \cdots \tag{2.45}$$

where the time scale T_i is slower than T_{i-1}. We can rewrite (2.45) as

$$\frac{d}{dt} = \epsilon\frac{\partial}{\partial \xi} + (1 + \epsilon^2\omega_2 + \cdots + \epsilon^M\omega_M)\frac{\partial}{\partial \eta} \tag{2.46}$$

where $\xi = \epsilon t$ is the slow time scale and $\eta = (1 + \epsilon^2\omega_2 + \cdots + \epsilon^M\omega_M)t$ is the fast time scale. Then x can be expanded as

$$x(t;\epsilon) = x(\xi,\eta;\epsilon) = \sum_{i=0}^{M-1} \epsilon^i x_i(\xi,\eta) + O(\epsilon^M) \tag{2.47}$$

where ω_i is constant. Note now that the ordinary differential equation has been transformed into a partial differential equation.

Substituting (2.45) (and its second derivative which is obtained in a similar manner) into (2.32) and equating like coefficients of ϵ, one gets the following partial differential equations for x_0 and x_1 (assuming a two-term expansion)

$$\frac{\partial^2 x_0}{\partial T_0^2} + x_0 = 0 \tag{2.48}$$

$$\frac{\partial^2 x_1}{\partial T_0^2} + x_1 = -2\frac{\partial x_0}{\partial T_0} - 2\frac{\partial^2 x_0}{\partial T_0 \partial T_1}. \tag{2.49}$$

Using $i = \sqrt{-1}$ and overbar to denote complex conjugation, the general solution to (2.48) is

$$x_0 = a_0(T_1)e^{iT_0} + \bar{a}_0(T_1)e^{-iT_0} \tag{2.50}$$

where now the coefficients aren't constants but instead functions of the slow time scale T_1. Substituting (2.50) into (2.49), we get the general solution to x_1

$$\begin{aligned} x_1 &= a_1(T_1)e^{iT_0} + \bar{a}_1 T_1 e^{-iT_0} \\ &- \left(a_0 + \frac{\partial a_0}{\partial T_1}\right) T_0 e^{iT_0} - \left(\bar{a}_0 + \frac{\partial \bar{a}_0}{\partial T_1}\right) T_0 e^{-iT_0}. \end{aligned} \tag{2.51}$$

Examining (2.51), we see that x_1 will contain secular terms unless a_0 is chosen to eliminate the last two terms on the right hand side of (2.51). That is

$$a_0 + \frac{\partial a_0}{\partial T_1} = 0 \tag{2.52}$$

which implies

$$a_0 = c_0 e^{-T_1} \tag{2.53}$$

where c_0 is a constant depending on initial conditions.

We have the freedom to eliminate these secular terms because of the additional time scale. A condition on a_1 would be obtained by carrying out the expansion to $O(\epsilon^2)$. In general, to obtain the solution accurate to $n-1$ terms, one must carry out the expansion to n terms since its the next term that yields the nonsecularity condition for the previous term. Thus, we get the following one term expression for x

$$x = \left[c_0 e^{it} + \bar{c}_0 e^{-it}\right] e^{-\epsilon t} + O(\epsilon) \tag{2.54}$$

where initial conditions would determine c_0 and $\bar{c}_0$. The above expression is accurate to $O(\epsilon)$ for *all* t. To obtain an expression that is accurate to higher powers of ϵ, one needs to repeat the above process for more terms in the expansion of (2.32). The above method is referred to as the derivative expansion procedure [43] which is a variant of the method of multiple scales. If (2.46) had been used instead of (2.45) one obtains the two variable expansion procedure which would result in the same final expression for x. There is also a variant which uses nonlinear scales to handle more complicated problems.

2.2.2 Composite Control

Composite control is the application of the multiple time scales method to singularly perturbed control systems. These systems have the general form

$$\dot{x} = f(x, z, u), \quad x \in R^n, \quad u \in R^r \tag{2.55}$$

$$\epsilon \dot{z} = g(x, z, u), \quad z \in R^m \tag{2.56}$$

where u is the control variable and the smoothness assumptions and domain definitions are as in Sect. 2.1. The small parameter $\epsilon > 0$ represents the ratio of the speeds of the slow vs. the fast phenomena. The slow subsystem is represented by (2.55) and the fast subsystem is represented by (2.56). The control design is broken down into two stages. First a control u_s is designed for the slow subsystem then another control u_f is designed for the fast subsystem. The control applied to the full system is the composite control $u_c = u_s + u_f$. The method is detailed in Ref. [44]. To understand the method, the concepts of slow and fast manifolds must be explained.

Definition 2.7 A slow manifold M_ϵ is defined as

$$M_\epsilon = \{x, z \mid z = h(x, u, \epsilon)\}. \tag{2.57}$$

The differentiable function h exists if the Jacobian $\frac{\partial g}{\partial z}$ is nonsingular and h satisfies

$$\epsilon \frac{dh}{dx} f(x, h, u) = g(x, h, u) \tag{2.58}$$

for ϵ sufficiently small. The derivative in (2.58) is defined as

$$\frac{dh}{dx} \triangleq \frac{\partial h}{\partial x} + \frac{\partial h}{\partial u}\frac{du}{dx}. \tag{2.59}$$

This definition can be thought of as the nonlinear analog of a linear subspace. Note that (2.58) is an existence condition for the slow manifold M_ϵ. Now we introduce the fast variable

$$\eta = z - h(x, u, \epsilon), \tag{2.60}$$

which represents deviations of the fast subsystem from the slow manifold, i.e., it represents the transient response in converging to the slow manifold.

The graph in Fig. 4 illustrates slow and fast manifolds for the case of $n = m = 1$. The family of fast manifolds is represented by lines parallel to the z axis, i.e., the slow variable x is restricted to some fixed function (in this case a constant). The slow manifolds are represented by S_1 and S_2. The "descent" to S_1 and S_2 along the fast manifolds is much faster than the "slide" along the slow manifolds themselves. In this figure, S_1 is an unstable manifold (i.e., repulsive) while S_2 is an attractive manifold. Another important property of the slow manifolds is that they are invariant, that is, if the system trajectories have converged to the slow manifold they remain there for all time. This means that a separate control can be designed to get the system to the slow manifold, i.e. fast control, and another control can be designed for the system once it is on the slow manifold, i.e., slow control. To exploit this decomposition, the slow control is expanded as a power series in ϵ

$$u = u_0(x) + \epsilon u_1(x) + u_f(\eta), \quad u_f(0) = 0 \tag{2.61}$$

where only a two term expansion is taken in the slow control and no expansion is needed for the fast control.

The slow control is designed by letting $\eta = 0$ and approximating the slow manifold function h by $h_0 + \epsilon h_1$ to obtain the slow model

$$\dot{x} = f(x, h_0 + \epsilon h_1, u_0 + \epsilon u_1). \tag{2.62}$$

But the choice of u_0 and u_1 is constrained by (2.58), i.e.,

$$\epsilon \left(\frac{dh_0}{dx} + \frac{dh_1}{dx} \right) f(x, h_0 + \epsilon h_1, u_0 + \epsilon u_1) = g(x, h_0 + \epsilon h_1, u_0 + \epsilon u_1). \tag{2.63}$$

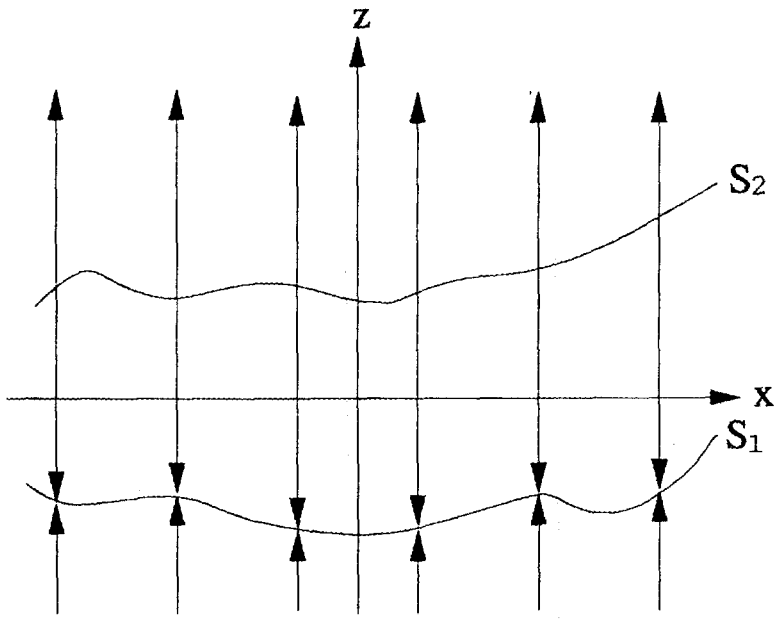

Fig. 4: Fast and slow manifolds of a singularly perturbed system.

When the terms of like powers of ϵ are equated, these constraints reduce to

$$0 = g(x, h_0, u_0) \tag{2.64}$$

$$\frac{dh_0}{dx} f(x, h_0, u_0) = \frac{\partial g}{\partial z} h_1 + \frac{\partial g}{\partial u} u_1 \tag{2.65}$$

where again it is noted that (2.65) is a partial differential equation.

The design procedure is as follows: solve (2.64) for $h_0(x, u_0)$ and plug it into (2.62). Then (2.62) can be used to design $u_0(x)$, the $\epsilon = 0$ slow control term. The u_0 term is then chosen to meet a design objective for $\epsilon = 0$ (e.g., linearization, PID control, etc.). Next, we use $u_0(x)$ and $h_0(x, u_0(x))$ and substitute them into (2.65) to find h_1 as function of x and u. Then h_1 is substituted into (2.62) which becomes our model for the design of the u_1 term. This term, which represents a nonzero ϵ correction term to u_0, will normally be chosen to achieve the same design objective as for u_0. The fast design model is

$$\epsilon\dot{\eta} = g(x, h(x, u, \epsilon) + \eta, u) - g(x, h(x, u, \epsilon), u) \tag{2.66}$$

with (2.61) and x, u_0, and u_1 fixed. Thus, the only variables in (2.66) are η and $u_f(\eta)$. The purpose of the fast control $u_f(\eta)$ is to drive η to 0. This may not be necessary

if the fast subsystem is already asymptotically stable (which it often is), but the fast control can be used to speed up convergence of the system trajectories to the slow manifold where the slow control takes over. The physics of the control problem will determine the type of fast control employed.

It should be noted that the above composite control design procedure is an example of hierarchical control. In Ref. [52] it is pointed out that the slow subsystem is a higher level authority which sets the overall control goals of the whole system. Suppose there are M fast subsystems each operating on a faster time scale than the one preceding it. Then there is a hierarchy where information needed for control filters down from the slower subsystems to the faster subsystems. This hierarchy can be dynamic as it is in Ref. [52] because each level could be implementing optimal control. The slow subsystem can be thought of as a decision-making authority which determines the overall control objectives and sends the necessary information to the lower level fast subsystems to control the system. This control can be dynamic (i.e., optimal) and takes place in real time.

2.3 SENSITIVITY ANALYSIS

The primary purpose to feedback in the control of physical systems is to overcome uncertainty. Whether this be uncertainty in the model of the plant that the control design is based upon, uncertainty in external signals corrupting the plant, uncertainty in numerical and computational aspects of the processing of information, or uncertainty in communications with the outside world, feedback can be employed to overcome these difficulties. Figure 5 illustrates the typical feedback control system that is assigned the goal of tracking a given reference trajectory. If there is no uncertainty in this system and its environment whatsoever, feedback would not be necessary to accomplish this goal. It is precisely because of this uncertainty that so much effort has been expended in designing control systems that are robust to modeling errors, disturbances, and numerical issues.

The uncertainty that is most commonly addressed in control theory is that of plant uncertainty. This refers to errors in modeling the physical processes of a system. It is difficult to write down differential equations that exactly model a system for all regions of operation taking into account all the system's dynamics. The two basic types of plant uncertainty are structured and unstructured uncertainty. Structured uncertainty refers to errors in the coefficients multiplying the derivatives in the system differential equations. More precisely, structured uncertainty manifests itself as errors in the parameters of the system. These parameters can be physical constants (e.g., g, the acceleration due to gravity) or physical dimensions (e.g., mass, length, material properties, etc.). Unstructured uncertainty implies that entire terms are missing or ignored in the mathematical model of the system. That is, there may be higher order dynamics (e.g., stray capacitances in an electrical network, vibrational modes

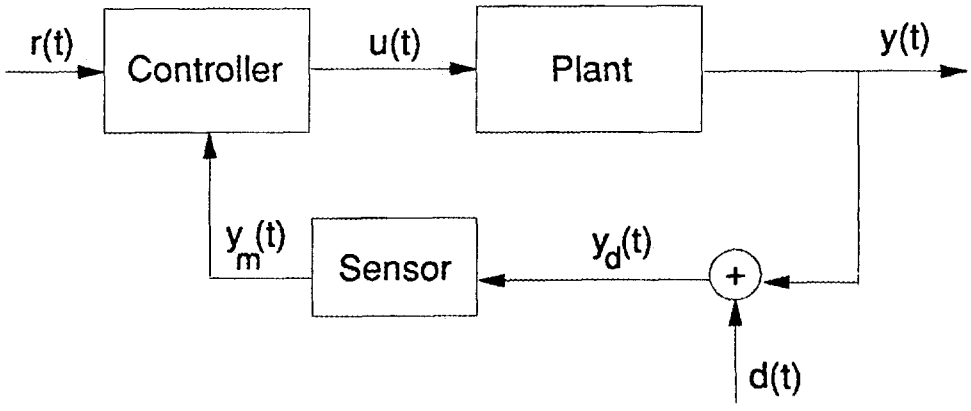

Fig. 5: Typical feedback control system with goal of driving $y(t) \longrightarrow r(t)$.

in an elastic structure, etc.) that are being ignored or cannot be easily modeled. Furthermore, control system designers are often forced to work with lower order models due to the computational complexity of designing control systems for high order systems.

Sensitivity analysis concerns itself primarily with structured or parametric uncertainty. Singular perturbation analysis, the subject of the previous section, is primarily concerned with unstructured uncertainty. Parametric uncertainty is important to consider because it is very common in engineering systems, and it can significantly alter the performance of the closed loop plant if it is not addressed. Parameters of interest besides coefficients of differential equations include initial conditions, natural frequencies, sampling times, and time delays. They can be caused by manufacturing tolerances, measurement errors, model approximations, component degradation, and changes in operating conditions.

Most feedback control systems are designed based on some kind of model for the plant. If the model parameters differ from the plant parameters, the system state and outputs may deviate significantly from desired behavior. Repeating the controller design for a more accurate model is not only time-consuming but impractical for time-varying parameters. Sensitivity analysis allows one to take into account parameter errors without repeating the controller design.

Since a sensitivity function is essentially a gradient (i.e., it shows how the system state or output changes with respect to the parameters), its most basic uses are in optimization and identification. Examples would be parameter identification, adaptive control, optimizing input signals for system identification, and optimal control. However, sensitivity analysis is not a panacea for all instances of parametric uncertainty. One needs nominal values of parameters as a starting point in analysis then considers

perturbations from these nominal values. If one doesn't know the nominal values of the parameters then some adaptive identification might be useful to get these values before embarking on a sensitivity analysis design.

Sensitivity studies usually focus on parameter deviations small enough to require the use of only first-order sensitivity functions (to be defined shortly). If parameter deviations are large, more than 25% deviation from the nominal values for instance, then the theory of Kharitonov polynomials or second order sensitivity functions might be more fruitful. Both of these techniques are considerably more complex than first order sensitivity functions. Also a problem in sensitivity studies is the appearance of external disturbances. Though sensitivity analysis can still handle this situation, other techniques such as dynamic disturbance decoupling or sliding mode control would be more productive. But, sensitivity analysis can still be used effectively in nonlinear and time-varying systems.

Historically, mathematicians have studied the effects of changes in coefficients of a differential equation on its solution. This analysis was motivated primarily by the desire to obtain solutions to differential equations when a coefficient was varied. Bode was the first to study sensitivity effects in the design of control systems by introducing his frequency domain sensitivity function in the 1940s [53]. Horowitz defined a more practical sensitivity function for transfer functions, but this was shown to be equivalent to Bode's sensitivity function in the early 1960s [54]. Perkins and Cruz extended this function to include MIMO, time-varying, and even nonlinear systems via the comparison sensitivity operator in 1964 [55].

Kokotović developed the method of sensitivity points to simultaneously determine all output sensitivity functions from a single model in the frequency domain in 1964 [56]. Wilkie and Perkins extended this idea to state space in 1969 [57, 58] via the total symmetry property and the complete simultaneity property. Whitaker and colleagues were the first to utilize the sensitivity function in adaptive control systems with the MIT rule in 1961 [59]. Dorato introduced the problem of parametric sensitivity of the performance criterion in optimal control systems during the early 1960s [60]. Recent work by Bingulac, Chow, and Winkelman demonstrates a simpler method than Wilkie and Perkins for generating the sensitivity functions of a linear MIMO system (1988) without requiring a transformation of the system to phase canonical form [61]. Extensions to nonlinear systems have been developed by Šiljak [62]. Texts on sensitivity analysis have been authored by Cruz [63, 64], Frank [65], and Tomović [66].

Consider a general nonlinear system model

$$\dot{x} = f(x, \alpha, u, t), \quad x(t_0) = x_0 \tag{2.67}$$

where x is the state, α is the parameter vector, and u is the control. The *actual* parameters α differ from the *nominal* parameters α^0 (the parameters used in the

model) in the following way:

$$\alpha = \alpha^0 + \Delta\alpha\,. \tag{2.68}$$

The sensitivity function S relates the error in parameters $\Delta\alpha$ to the parameter-induced errors of the state Δx as follows:

$$\Delta x \approx S(\alpha^0)\Delta\alpha \tag{2.69}$$

where the sensitivity function S depends on the nominal parameters α^0 which are known.

The sensitivity function S can be seen as a mapping from parameter space into state space. In particular, S maps the subspace of parameter variations $\Delta\alpha$ about α^0 into the subspace of parameter-induced errors in the state Δx. Figure 6 illustrates this concept. This mapping is in general nonlinear, but if deviations are small enough we can make a first-order approximation.

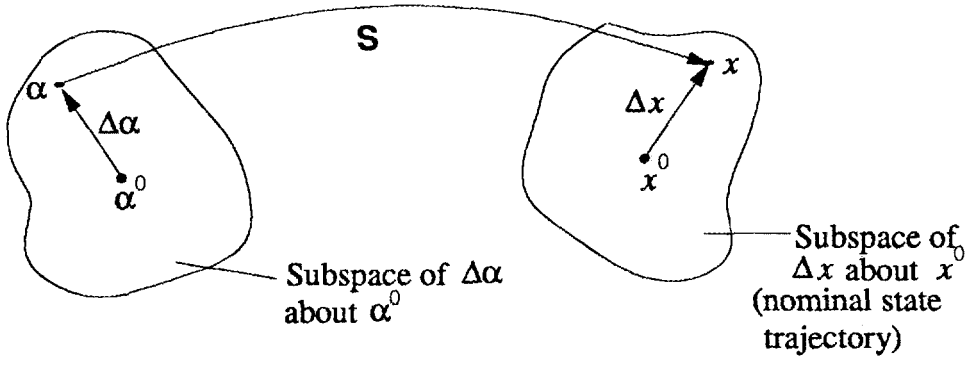

Fig. 6: Mapping of parametric deviations into state deviations.

Briefly, we introduce the concept of frequency domain sensitivity functions. Let $G = G(s,\alpha)$ and $G^0 = G(s,\alpha^0)$ be the actual and nominal transfer functions. Bode's sensitivity function with respect to the jth parameter of the parameter vector α is [53]

$$S^G_{\alpha_j}(s) \triangleq \frac{\partial \ln G}{\partial \ln \alpha_j}\,|_{\alpha=\alpha^0} = \frac{\partial G}{\partial \alpha_j}\,|_{\alpha=\alpha^0}\,\frac{\alpha_j^0}{G^0}\,. \tag{2.70}$$

We can also consider the sensitivity of a transfer function with respect to a subsystem transfer function. For example, consider the simple closed loop control system depicted in Fig. 7.

The sensitivity of the closed loop transfer function, T, to changes in the plant G is

$$S^T_G = \frac{\partial \ln T}{\partial \ln G}\,|_{G^0} = \frac{1}{1 + G(s,\alpha^0)H(s,\alpha^0)} \tag{2.71}$$

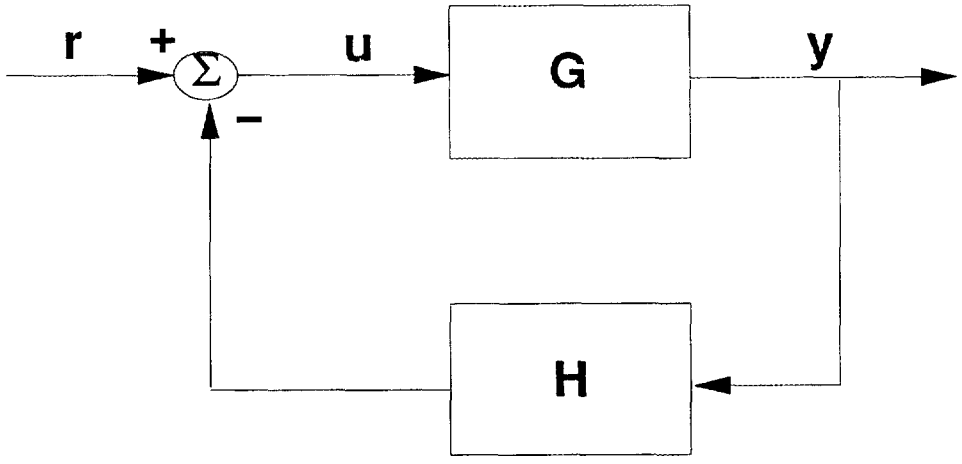

Fig. 7: Closed loop control system with plant, G, and feedback H.

where $T = \frac{G}{1+GH}$. This result shows that increasing the loop gain GH will reduce the sensitivity of the closed loop system to the plant which is the basis for amplifier design.

Frequency domain sensitivity functions are useful for linear systems but not helpful for nonlinear systems. Consider again the general nonlinear system

$$\dot{x} = f(x, \alpha, u, t), \quad x(t_0) = x_0 \tag{2.72}$$

with an output vector

$$y = h(x, \alpha, u, t)\,. \tag{2.73}$$

The output of the system $y(t, \alpha^0 + \Delta\alpha)$ can be expanded as a Taylor series about α^0

$$y(t, \alpha) = y(t, \alpha^0) + \frac{\partial y}{\partial \alpha}\,|_{\alpha^0}\,\Delta\alpha + \frac{1}{2}\frac{\partial^2 y}{\partial \alpha^2}\,|_{\alpha^0}\,\Delta\alpha^2 + \cdots\,. \tag{2.74}$$

If $\Delta\alpha << \alpha^0$ ($\alpha^0 \neq 0$), then the series can be truncated beyond the first order term with little loss in accuracy.

If there are p parameters and m outputs, the *output sensitivity matrix* is defined as

$$\sigma(t, \alpha^0) \triangleq \frac{\partial y}{\partial \alpha}\,|_{\alpha^0} = \left[\frac{\partial y_k}{\partial \alpha_j}\right], \tag{2.75}$$

$k = 1, \ldots, m$, $j = 1, \ldots, p$. Thus, to first order, the output error due to parameter deviations can be written as

$$\Delta y(t, \alpha) \approx \sigma(t, \alpha^0)\Delta\alpha\,. \tag{2.76}$$

Likewise, if there are n states, we define the *trajectory sensitivity matrix* as

$$\lambda(t,\alpha^0) \triangleq \frac{\partial x}{\partial \alpha}\,|_{\alpha^0} = \left[\frac{\partial x_i}{\partial \alpha_j}\right], \tag{2.77}$$

$i = 1,\ldots,n$, $j = 1,\ldots,p$. Where again the parameter-induced errors in the state trajectory for small $\Delta\alpha_j$'s are

$$\Delta x(t,\alpha) \approx \lambda(t,\alpha^0)\Delta\alpha\,. \tag{2.78}$$

One can solve for the sensitivity functions by solving the equations explicitly. Another way is to use a structural approach in which the nominal model of the system is combined with a *sensitivity model* to generate the sensitivity functions. Figure 8 shows the general scheme for generating sensitivity functions via a sensitivity model. The signals coming out of the nominal system model going into the sensitivity models will vary with the method used. The initial conditions for the sensitivity models are always zero. The sensitivity models are always linear even if the plant is nonlinear. If the plant is nonlinear or time-varying then the sensitivity model will be a linear time-varying system.

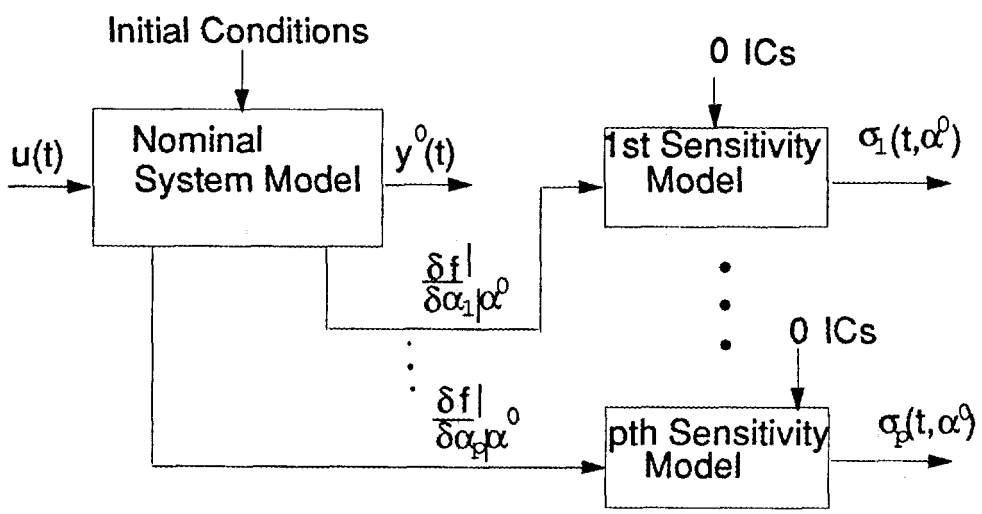

Fig. 8: Model to simultaneously measure all p output sensitivity functions.

There are different methods to compute sensitivity functions via sensitivity models. In the frequency domain, the two primary techniques are the variable component method [67] and the method of sensitivity points [56]. The variable component method is concerned with subsystems that depend on the unknown parameters. Each subsystem gets its own sensitivity model which is just a copy of the original subsystem. In the method of sensitivity points, it is shown that just one sensitivity model

is needed to generate all p output sensitivity functions, but it is restricted to linear systems. The key point is that the sensitivity model is just a copy of the nominal system model (see Fig. 9). This method was extended to state space by Wilkie and Perkins [57, 58].

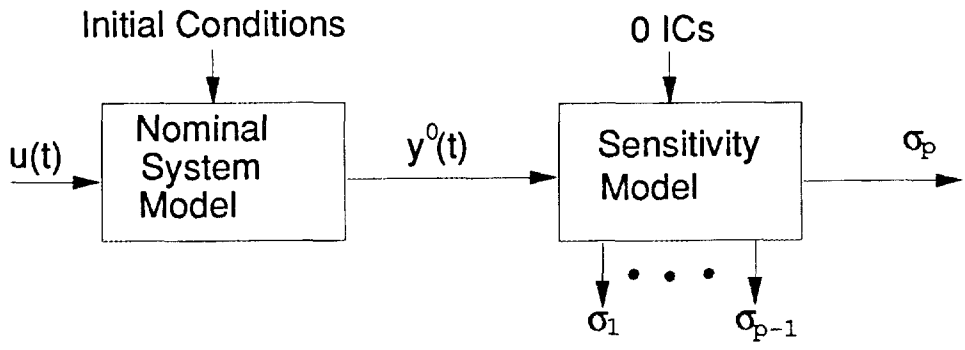

Fig. 9: Method of sensitivity points.

To consider time-domain generation of sensitivity functions, we start with a linear system

$$\dot{x} = Ax + Bu, \quad x(t_0) = x_0 \tag{2.79}$$

and an output vector

$$y = Cx + Du \tag{2.80}$$

where A, B, C, D depend on the unknown parameters α. The trajectory sensitivity model can be formed by writing the differential equations

$$\begin{aligned} \frac{\partial \dot{x}}{\partial \alpha} &= A\frac{\partial x}{\partial \alpha} + \frac{\partial A}{\partial \alpha}x + \frac{\partial B}{\partial \alpha}u \\ \frac{\partial y}{\partial \alpha} &= C\frac{\partial x}{\partial \alpha} + \frac{\partial C}{\partial \alpha}x + \frac{\partial D}{\partial \alpha}u\,. \end{aligned} \tag{2.81}$$

Noting the definitions from before, we get the system

$$\begin{aligned} \dot{\lambda} &= A^0\lambda + \frac{\partial A}{\partial \alpha}\,|_{\alpha^0}\, x^0 + \frac{\partial B}{\partial \alpha}\,|_{\alpha^0}\, u\,, \ \lambda(t_0) = 0 \\ \sigma &= C^0\lambda + \frac{\partial C}{\partial \alpha}\,|_{\alpha^0}\, x^0 + \frac{\partial D}{\partial \alpha}\,|_{\alpha^0}\, u \end{aligned} \tag{2.82}$$

which is a linear system! Not only that, it has the same A matrix as the nominal linear system, and it's time-invariant if the original system is time-invariant. The only difference are some additional input terms. Figure 10 illustrates this relationship.

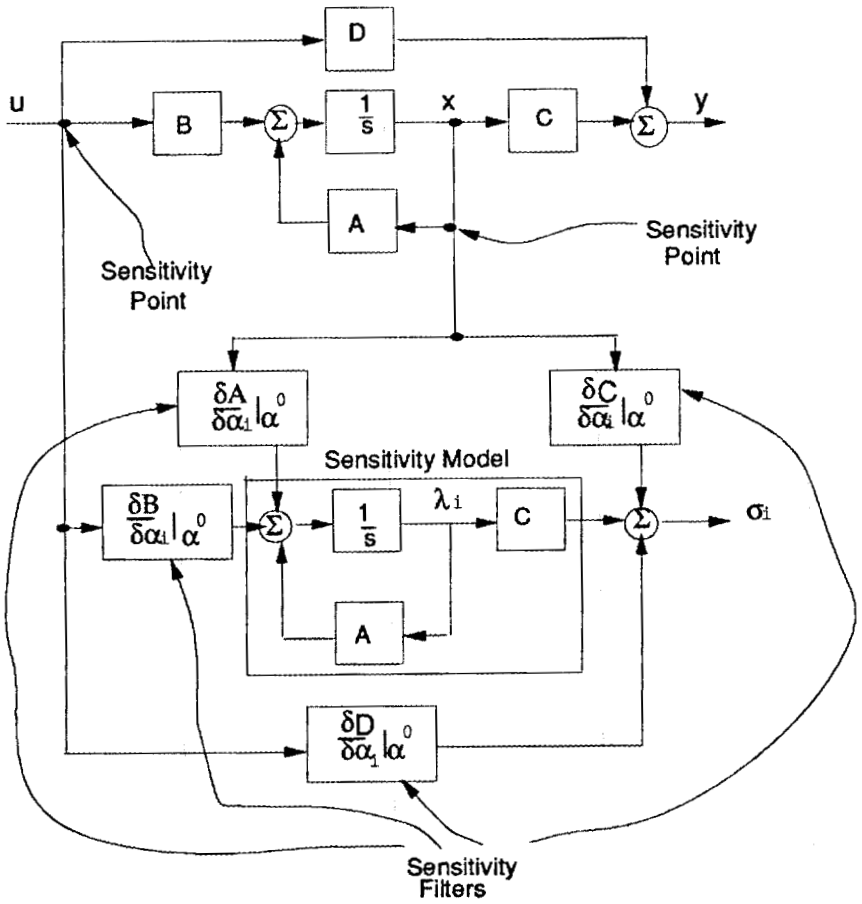

Fig. 10: Generation of trajectory sensitivity functions for a linear system.

This concept can easily be generalized to nonlinear systems (2.72)-(2.73). In this case we get the linear but time-varying sensitivity model

$$\dot{\lambda} = \frac{\partial f}{\partial x}\,|_{\alpha^0}\,\lambda + \frac{\partial f}{\partial \alpha}\,|_{\alpha^0}\,,\ \lambda(t_0) = 0 \tag{2.83}$$

$$\sigma = \frac{\partial h}{\partial x}\,|_{\alpha^0}\,\lambda + \frac{\partial g}{\partial \alpha}\,|_{\alpha^0}$$

where the external input, u, is assumed independent of α. For both the linear time-varying and nonlinear cases we need p sensitivity models using the above equations. This is not necessarily true for linear time-invariant systems due to the results of Wilkie and Perkins shown next.

Two fundamental properties of sensitivity models for linear time-invariant systems were exploited by Wilkie and Perkins. These properties lead to the fundamental theorem which follows below.
Total Symmetry Property: The antidiagonals of the sensitivity matrix are equal. That is,

$$\lambda = \begin{bmatrix} \lambda_{11} & \lambda_{12} & \lambda_{13} \\ \lambda_{12} & \lambda_{13} & \lambda_{14} \\ \lambda_{13} & \lambda_{14} & \lambda_{15} \end{bmatrix}. \tag{2.84}$$

This means that there are only $2n-1$ independent trajectory sensitivity functions.
Complete Simultaneity Property: If the original (linear) system model is put into phase canonical form (companion form) then all sensitivity functions can be obtained as linear combinations of state variables of a single sensitivity model along with the nominal linear system.

Theorem 2.2 *For a linear time-invariant SISO system, all trajectory sensitivity functions with respect to all p parameters can be generated by the nominal system model and just one sensitivity model in companion form.*

This result has not been extended to nonlinear or time-varying systems, but Bingulac, Chow and Winkelman [61] have shown that it is not necessary to put the system in companion form if transfer matrices are utilized which may require less computation for most systems.

The utility of sensitivity functions is witnessed by their successful application in such areas as system identification, adaptive control, optimal control, and sampled-data systems as well as their basic purpose of reducing a closed-loop plant's sensitivity to variations in its parameters from modeled values. One such example is illustrated in Fig. 11 which shows that sensitivity functions can be used to estimate the unknown parameters of a plant. This is done by using the sensitivity functions to update a model until convergence is achieved.

Another example is optimal control. Figure 12 shows how the addition of a sensitivity model in the feedback loop can reduce the system's sensitivity to parameter deviations while minimizing a cost functional. To decrease the parameter sensitivity of an optimal feedback system, the sensitivity functions can be included in the cost criterion as follows

$$J = \int_{t_0}^{t_f} \left[x^T Q x + u^T R u + \sum_{i=1}^{p} \left(\lambda_i^T S \lambda_i \right) \right] dt. \tag{2.85}$$

The control law then has the form

$$u = -K_x x - K_{\lambda_i} \lambda_i \tag{2.86}$$

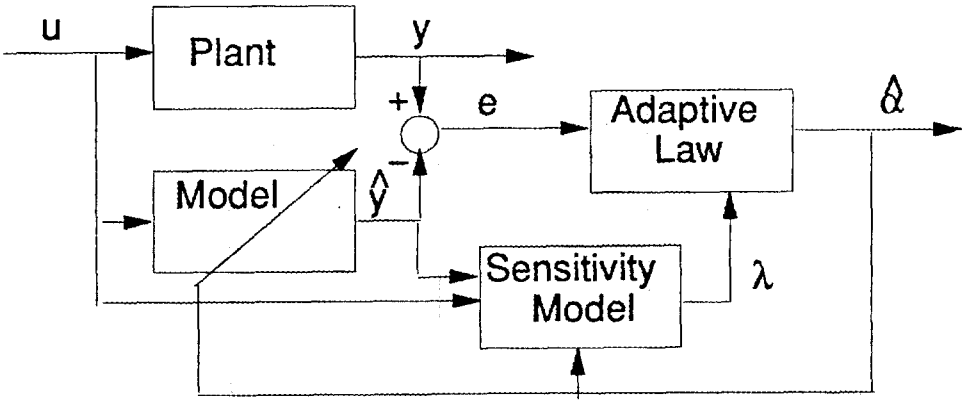

Fig. 11: Parameter identification using an adaptive model.

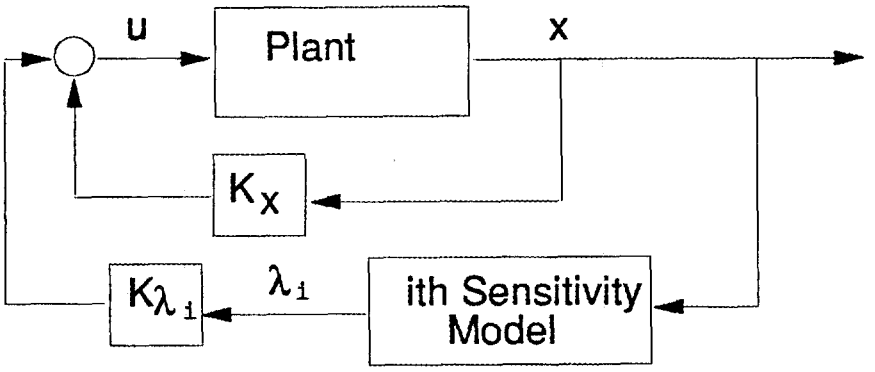

Fig. 12: Optimal control using a sensitivity model.

where the gains, K, are determined via Riccati equations.

The purpose of this section besides surveying methods of sensitivity theory was to establish a mathematical framework for some of the results that follow in this report. These results employ sensitivity models in decentralized control schemes as well as optimal feedback loops to reduce a system's sensitivity to parameter errors. Much recent control theory effort has looked at sophisticated techniques for handling uncertainty such as H^∞ methods and Kharitonov polynomials. Though these results are quite useful for many applications, the relatively old ideas of sensitivity analysis should not be forgotten since they do not require as much mathematical sophistication. These ideas have also been very successful in industry and can still be applied to challenging problems in control theory as this report demonstrates.

2.4 DECENTRALIZED CONTROL

In many large-scale systems it would be impractical to send information from one controller to another due to hardware and communication constraints. Thus, decentralized control is a necessary strategy to controlling these large systems. Decentralization implies that each controller will use only input/output and state information available at its own channel to generate its input signal. Decentralized control may be necessary to achieve a degree of redundancy in a system since if one controller fails or malfunctions there are still other controllers that could accomplish the desired objectives. In addition, decentralized control provides relief from the extreme computational burden that would be inherent in a centralized control approach to a large-scale system. Figure 13 shows the general decentralized structure where each controller has access only to the output (and possibly the associated state) present at the local channel where the input signal will be applied.

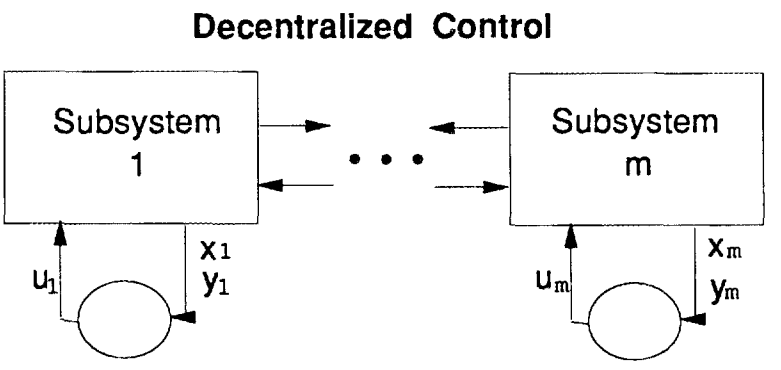

Fig. 13: Decentralized control architecture.

Historically, decentralized control has its origins in hierarchical control which was developed by Lefkowitz, Mesarović, and colleagues in the 1950s and 1960s. Hierarchical control is primarily an open loop strategy though it can be done in a closed loop setting. Early work in decentralized control can be credited to Wang and Davison [68] who introduced the concept of decentralized fixed modes, Šiljak and Vukčević [69] who developed decentralized stabilization schemes, and Davison [70, 71, 72] for introducing the concept of the decentralized servocompensator. Geromel and Bernussou [73, 74] contributed to decentralized optimal control schemes and Sundareshan [75] developed decentralized state estimators among others. Other mathematical techniques such as game-theoretic methods (Mageriou and Ho [76]) and graph-theoretic methods (Sezer and Šiljak [77]) have been employed to develop decentralized stabilization strategies. Surveys and texts on decentralized control by Sandell et al. [78], Jamshidi [79], and Šiljak [80] among others explain these and other topics in detail.

Mahmoud [81] defined a system as "large" if it required more than one controller. This definition certainly includes many of today's large power, space, and industrial systems. Decentralized control has become common in these systems, but little has been done in the arena of nonlinear large systems. This motivates much of the work of this report. Indeed, Chap. 4 looks at optimal and robust control of nonlinear systems via decentralized control.

The primary disadvantage to decentralized control is that one cannot achieve any better performance and often not even as good a performance as with a centralized control strategy. This is apparent in pole placement involving state feedback. In a centralized control strategy one has access to the full state and thus can achieve the limits of performance allowed by the controllability properties of the system. But in a decentralized setting, there may be open-loop poles called fixed modes[82, 83, 68] that cannot be placed where one desires even though they may be controllable in a centralized sense. Thus, one must be careful in designing decentralized controllers. The concept of fixed modes was introduced by Wang and Davison [68] and are defined simply as the modes of a linear system that are invariant under decentralized static output feedback. If any of these modes are unstable then even dynamic decentralized output feedback will be unable to stabilize the system. Algebraic conditions for the existence of such modes were formulated by Anderson and Clements [82] as well as Davison and Özgüner [83].

For each input/output channel a control framework must be decided upon. That is, the structure of the feedback law must be determined *a priori*. Currently, the most popular approaches to decentralized controllers are optimal control, adaptive control, and variable structure control. The optimal control approach utilized in this report is the decentralized servocompensator of Davison [70, 71, 72] further refined by Geromel and Bernussou [73, 74] which is outlined shortly. This technique attempts to minimize a quadratic cost criterion with penalties on the input signal and a composite state which consists of the output error (from a specified setpoint) and the derivative of the state for each channel independently. The resulting controller is a proportional integral (PI) controller, i.e., the input signal of the ith channel will be proportional to the state available at the ith channel and the integral of the output error at the ith channel. The feedback gains are obtained by solving two coupled Lyapunov equations [84]. One of the primary uses for this compensator is that of disturbance attenuation for large-scale systems under decentralization constraints [85].

The most common applications for decentralized control are large-scale systems in which the processing of information would be impractical on a centralized basis. Such systems include large space structures, e.g., the proposed space station, large power systems, transportation and wide area communication networks, and manufacturing systems. Even smaller systems such as multi-arm robotic manipulators and multiple mirror optical tracking systems are more conveniently designed with decentralized control laws.

Consider the basic *decentralized quadratic regulator problem*:

$$\dot{x} = Ax + \sum_{i=1}^{N} B_i u_i\,, \quad x(0) = x_0 \tag{2.87}$$

$$y_i = C_i x\,, \quad i = 1, \ldots, N. \tag{2.88}$$

where N is the number of input/output channels, m_i is the dimension of u_i, and p_i is the dimension of y_i . We wish to minimize the cost criterion

$$J = \int_0^\infty (x^T Q x + \sum_{i=1}^{N} u_i^T R_i u_i)\, dt \tag{2.89}$$

with the following feedback structure constraint

$$u_i = K_i\, y_i\,, \quad i = 1, \ldots, N. \tag{2.90}$$

It can be shown that [73, 74, 50, 84, 86] the necessary conditions for minimizing J given by (2.89) with the controller structure (2.90) imply the solution of the following system of nonlinear algebraic equations:

$$\begin{aligned} A_c^T P + P A_c + \bar{Q} &= 0 \\ A_c L + L A_c^T + X_0 &= 0 \end{aligned} \tag{2.91}$$

and

$$\nabla_{K_i} J = B_i^T P L C_i^T + R_i K_i C_i L C_i^T = 0 \tag{2.92}$$

where

$$\begin{aligned} A_c &= A + \sum_{i=1}^{N} B_i K_i C_i \\ \bar{Q} &= Q + \sum_{i=1}^{N} C_i^T K_i^T R_i K_i C_i \\ X_0 &= x_0\, x_0^T. \end{aligned} \tag{2.93}$$

The incorporation of set–points into the standard quadratic regulator problem is considered next. Consider the system

$$\begin{aligned} \dot{x} &= Ax + Bu \\ y_r &= Cx\,, \end{aligned} \tag{2.94}$$

under the cost criterion

$$J = \int_0^\infty (z^T Q z + \dot{u}^T R \dot{u}) dt\,, \tag{2.95}$$

where $z(t)$ is defined as

$$z(t) \triangleq \begin{bmatrix} \dot{x} \\ \Delta y \end{bmatrix} \tag{2.96}$$

$$\Delta y(t) \triangleq y_r(t) - y^d, \tag{2.97}$$

and y^d, a constant set point, has been specified.

The state equations for the system with $\dot{u}$ as input and z as state vector can now be written. If Q =block-diag$\{Q_1, Q_2\}$ then the solution of the above problem takes the form

$$u = K^1 x + K^2 \int_0^t (y_r(\tau) - y^d) d\tau \tag{2.98}$$

where the $\{K^1, K^2\}$ pairs are calculated from the associated Riccati equations.

Let the matrix solution to the Riccati equation be partitioned as

$$P = \begin{bmatrix} P_1 & P_3 \\ P_3^T & P_2 \end{bmatrix}$$

and let

$$S = BR^{-1}B^T.$$

Then the Riccati equation decouples into three equations:

$$-P_3^T S P_3 + Q_2 = 0$$

$$P_3^T A + P_2 C - P_3^T S P_1 = 0$$

$$A^T P_1 + C^T P_3^T + P_1 A + P_3 C - P_1 S P_1 + Q_1 = 0.$$

As can be seen, P_3 can be calculated from the first equation. Then

$$P_2 = P_3^T (A - SP_1) C^T (CC^T)^{-1}, \tag{2.99}$$

and P_1 can be calculated from the Riccati equation

$$A^T P_1 + P_1 A - P_1 S P_1 + (Q + C^T P_3^T + P_3 C) = 0. \tag{2.100}$$

The optimal cost is given by

$$J^* = z^T(0) P z(0). \tag{2.101}$$

2.5 SUMMARY

This chapter has surveyed some common control system design methods that will be utilized in later chapters. It is by no means meant to be an exhaustive reference for most control design techniques in use today. The chapter highlighted nonlinear control theory with emphasis on feedback linearization and nonlinear observers. The techniques of singular perturbations and sensitivity analysis, which have proven useful for both linear and nonlinear systems, were reviewed as methods for the robust control of nonlinear systems. The subject of decentralized control was also analyzed and is well-suited to the control of large-scale systems.

Many other control techniques have proven useful in nonlinear and large-scale systems but are not included here due to the scope of this report. For instance, the theory of sliding modes has been applied to the control of nonlinear systems since it was introduced in the West by Utkin [87]. This theory has been effective in dealing with modeling uncertainty and external disturbances for both linear and nonlinear systems. The idea is to utilize a switching control law to drive the system to a sliding mode on which the system is immune to external disturbances. The primary disadvantage to this approach is a discontinuous control law that can lead to chattering in the system response.

The theory of adaptive control is also applied to the robust control of nonlinear systems. Here, the uncertain parameters are updated on-line until convergence to their true values is achieved. The drawback is a nonlinear time-varying feedback loop whose dynamical behavior is not always well-behaved. Describing functions are yet another approach to nonlinear control. These functions are an analytical tool used to predict the existence of limit cycles. The idea is to approximate the nonlinearities in question as linear gains with a sinusoidal input signal. This is essentially a nonlinear Fourier analysis. It is most useful when input signals are sinusoidal or nearly so. It is not as useful in the case of modeling uncertainty. The theory of H^∞ control is dedicated to a broad range of uncertainty in systems but is primarily geared toward linear systems. Some recent results utilizing game theory have been aimed at addressing uncertainty in nonlinear systems [88], but this is still in the early stages.

Besides decentralized control, the techniques of hierarchical control and supervisory control have been applied to large-scale systems. Though not strictly decentralized, these methods take advantage of the interconnected nature of large-scale systems by applying multi-level strategies to control design. In this report, decentralized control was chosen due to the lessening of computational burdens in local control laws. However, combinations of decentralized and multi-level control strategies would be useful in dealing with large space structures especially when it comes to determining control objectives at the subsystem level.

CHAPTER 3

FEEDBACK LINEARIZATION RESULTS

3.1 OPTIMIZATION OF FEEDBACK LINEARIZABLE SYSTEMS

The principal idea behind feedback linearization is to be able to cancel system nonlinearities in some new coordinate system such that the transformed system behaves as a linear one. Much research has focused on techniques for achieving this linearization as well as methods for handling uncertainty in the plant model (see Refs. [89, 90, 91, 92]). But very little attention has been paid to performance issues in feedback linearizable systems. In particular, the problem of finding a control which minimizes a quadratic cost function for a feedback linearizable system has not been addressed in a systematic manner.

The problem of optimizing cost functionals for nonlinear systems has been studied extensively for many decades (see the texts of Refs. [93, 94] for details), but for a standard quadratic cost criterion the problem is virtually intractable for all but the simplest nonlinear systems. However, it should be possible to take advantage of the linearizability of some nonlinear systems and solve such a problem. In this section, we propose a method which combines feedback linearization with the linear quadratic regulator (LQR) problem. On the surface, such a problem would seem fairly simple. But when one applies the linearizing coordinates transformation, the cost function changes from a quadratic one to a non-quadratic index in general. This new problem consisting of a linear system with a non-quadratic cost index can be just as difficult to solve as a nonlinear system with a quadratic index.

There are two simplifying approaches one might attempt in this situation. The first is to use operating-point linearization (i.e., Taylor series linearization) to linearize the nonlinear system about some point of interest and then use the original quadratic cost index to solve the LQR problem. Though this approach is mathematically tractable, it has the disadvantage of only being applicable in a small region of the chosen operating point. This will either necessitate restrictions on the operating region or require successive linearization about a series of operating points and a schedule for assigning LQR gains. This may be too restrictive for most applications. The other approach is to feedback linearize the system and continue using the same

Q and R matrices for the new coordinates and control inputs. This approach implies the minimization of an altogether different performance index which will very likely yield physically meaningless solutions.

Our approach is to feedback linearize the system followed by an approximation on the transformed cost index to yield a quadratic criterion with a cross-term. The result is an easy problem to solve via LQR theory. These new Q, R, and S matrices (the S matrix multiplies the cross-term) represent a good approximation to the original quadratic cost index in the linearizing coordinates and new input term. In addition, the cost of the feedback linearization itself is being accounted for in this cost functional. We begin by defining the problem followed by our solution. We end by looking at a robotics problem in which it is desired to minimize a quadratic cost functional while slewing a payload-carrying link through a given angle. Comparisons will be drawn between our approach and the other aforementioned approaches to this problem.

3.1.1 Problem Statement

Consider the following nonlinear system with outputs

$$\begin{aligned} \dot{x} &= f(x) + \sum_{i=1}^{m} g_i(x) u_i \\ y_i &= h_i(x) \end{aligned} \tag{3.1}$$

where $i = 1, \ldots, m$, $x \in R^n$, and f,g_i,h_i are smooth vector functions defined on R^n. We want to find the control vector $u = [u_1\,,\, u_2\,,\, \ldots\,,\, u_m]$ such that the quadratic cost index

$$J = \int_0^\infty (x^T Q x + u^T R u) dt \tag{3.2}$$

is minimized. The matrices Q and R are of appropriate dimensions and time-invariant. We shall refer to this as the Nonlinear Quadratic Regulator (NQR) problem. We assume that the cost index (3.2) is a physically relevant quantity (such as energy), and its minimization is of practical significance. We concern ourselves with nonlinear systems (3.1) that are state space feedback linearizable. That is, we need the following assumption.

Assumption 3.1 The vector relative degree $\{r_1, r_2, \ldots, r_m\}$ (see Sect. 2.1.1 for a definition) satisfies $r_1 + r_2 + \cdots + r_m = n$ about some point x_0.

Assumption 3.1 guarantees the existence of a diffeomorphism $z = \Phi(x)$ and smooth state feedback $u = a(z) + b(z)v$ such that in the linearizing coordinates, z, we obtain the linear system

$$\dot{z} = Az + Bv\,, \quad y = Cz \tag{3.3}$$

where (A,B,C) are in Brunovsky canonical form and $v = [v_1, v_2, \ldots, v_m]$ is a vector of external inputs.

3.1.2 Methods for Solving the NQR Problem

We wish to elaborate on several possible solutions to the NQR problem that one might attempt. These methods will serve as a basis for our method.

Method 1. Taylor series linearize the system about some operating point (i.e., throw out the higher order terms) and solve the subsequent LQR problem. This could be done about a series of operating points with a gain scheduling approach.

Method 2. Feedback linearize the system and set $J = \int_0^\infty (z^T Q z + v^T R v) dt$. Then solve the LQR problem in the z coordinates (i.e., the same Q and R as in (3.2) are utilized).

Method 3. Solve the Euler-Lagrange equations to obtain an exact solution.

Method 1 implies that the system (3.1) behaves linearly near an operating point. If such operating points exist and are of interest then this is a valid method. However, restricting the system to operate in a region near these operating points may be impractical. Furthermore, higher order nonlinearities are being ignored which implies that the closed-loop system will still be nonlinear. Method 2 is a naive approach that, though simple, will yield meaningless results except when z is nearly equal to x. Method 2 has actually changed the problem into a different one since minimizing this cost criterion will not solve the original problem. Thus, the results will have little physical meaning. Finally, Method 3 is a mathematically rigorous means of solving the NQR problem. However, for most systems of dimension $n > 2$ the solution will be exceedingly difficult to obtain. With this motivation, we propose the following method.

Method 4. We proceed as in Method 2 by feedback linearizing the system with $z = \Phi(x)$ and $u = a(z) + b(z)v$. But in order to retain the physically meaningful performance index (3.2), we substitute $x = \Phi^{-1}(z)$ and u into J to get

$$\begin{aligned} J &= \int_0^\infty [\Phi^{-T}(z) Q \Phi^{-1}(z) + a^T(z) R a(z) \\ &+ a^T(z) R b(z) v + v^T b^T(z) R a(z) + v^T b^T(z) R b(z) v] dt \,. \end{aligned} \tag{3.4}$$

We then approximate the above by

$$J = \int_0^\infty (z^T Q^* z + v^T R^* v + 2 z^T S^* v) dt \tag{3.5}$$

where Q^*, R^*, S^* are constant matrices. These matrices are obtained by expanding $\Phi^{-1}(z)$, $a(z)$, and $b(z)$ about an operating point and truncating to first order. These

matrices are as follows

$$Q^* = \left(\frac{\partial \Phi}{\partial x}\,|_{x=x_0}\right)^{-T} Q \left(\frac{\partial \Phi}{\partial x}\,|_{x=x_0}\right)^{-1} + \left(\frac{\partial a}{\partial z}\,|_{z=z_0}\right)^{T} R \left(\frac{\partial a}{\partial z}\,|_{z=z_0}\right) \tag{3.6}$$

$$R^* = b^T(z_0) R b(z_0) \tag{3.7}$$

$$S^* = \left(\frac{\partial a}{\partial z}\,|_{z=z_0}\right)^{T} R b(z_0) \tag{3.8}$$

where x_0 ($z_0 = \Phi(x_0)$) is the vector of operating points. With the linearized system $\dot{z} = Az + Bv$, the LQR solution will be

$$v = -R^{*-1}\left[B^T P + S^{*T}\right] z \tag{3.9}$$

where P is the positive definite solution to the Algebraic Riccati Equation

$$\begin{aligned} 0 &= P(A - BR^{*-1}S^{*T}) + (A^T - S^* R^{*-1} B^T)P \\ &- PBR^{*-1}B^T P + Q^* - S^* R^{*-1} S^{*T} \end{aligned} \tag{3.10}$$

The optimal cost is $J^* = z^T(0)Pz(0)$. We also need the following assumption for the LQR problem with cross-term to exhibit a nonnegative definite solution to (3.10) and an asymptotically stable closed-loop system [95].

Assumption 3.2 (a.) $R^* > 0$ (this will be satisfied if $R > 0$ since $b(z_0) \neq 0$ due to Assumption 3.1).
(b.) $Q^* - S^* R^{*-1} S^* \geq 0$.
(c.) The pair (A, B) is stabilizable.
(d.) The pair (A, D) is detectable where $DD^T = Q^* - S^* R^{*-1} S^{*T}$.

3.1.3 Derivation of the Method

The purpose of this method is to provide us with a means of choosing a cost index for the linearized system that is in some sense close to the original cost index. The matrices from above are derived by considering the cost criterion (3.2) with $u = a(z) + b(z)v$ and $z = \Phi(x)$. This results in Equation (3.4). The next step is to expand the vector fields $\Phi(x)$, $a(z)$, and $b(z)$ about the operating point $z_0 = \Phi(x_0)$. That is,

$$\Phi(x) = \Phi(x_0) + \frac{\partial \Phi}{\partial x}\,|_{x=x_0}\,(x - x_0) + \text{H.O.T.} \tag{3.11}$$

$$a(z) = a(z_0) + \frac{\partial a}{\partial z}\,|_{z=z_0}\,(z - z_0) + \text{H.O.T.} \tag{3.12}$$

$$b(z) = b(z_0) + \frac{\partial b}{\partial z}\,|_{z=z_0}\,(z - z_0) + \text{H.O.T.} \tag{3.13}$$

where it is assumed that the above vector fields are analytic about x_0 and z_0 respectively. From (3.11), x can be approximated as

$$x = \Phi^{-1}(z) \approx \left[\frac{\partial \Phi}{\partial x}\,|_{x=x_0}\right]^{-1} [z - \Phi(x_0)] + x_0 \tag{3.14}$$

for x near x_0. Now, (3.11)-(3.14) are substituted into (3.4) resulting in the following performance criterion

$$\begin{aligned}
J \;=\; & \int_0^\infty [z^T\{\left(\frac{\partial \Phi}{\partial x}\,|_{x=x_0}\right)^{-T} Q \left(\frac{\partial \Phi}{\partial x}\,|_{x=x_0}\right)^{-1} \\
+ \; & \left(\frac{\partial a}{\partial z}\,|_{z=z_0}\right)^T R \left(\frac{\partial a}{\partial z}\,|_{z=z_0}\right)\}z \\
+ \; & v^T\{b^T(z_0)Rb(z_0)\}v + 2z^T\left\{\left(\frac{\partial a}{\partial z}\,|_{z=z_0}\right)^T Rb(z_0)\right\}v \\
+ \; & z^T\{2\left(\frac{\partial \Phi}{\partial x}\,|_{x=x_0}\right)^{-T} Qx_0 - 2\left(\frac{\partial \Phi}{\partial x}\,|_{x=x_0}\right)^{-T} Q\Phi(x_0) \\
+ \; & 2\left(\frac{\partial a}{\partial z}\,|_{z=z_0}\right)^T Ra(z_0) - 2\left(\frac{\partial a}{\partial z}\,|_{z=z_0}\right)^T Rz_0\} \\
+ \; & v^T\{2b^T(z_0)Ra(z_0) - 2b^T(z_0)R\left(\frac{\partial a}{\partial z}\,|_{z=z_0}\right)z_0\} \\
+ \; & \Phi^T(x_0)\left(\frac{\partial \Phi}{\partial x}\,|_{x=x_0}\right)^{-T} Q\left(\frac{\partial \Phi}{\partial x}\right)^{-1}\Phi(x_0) + x_0^T Qx_0 \\
- \; & 2\Phi^T(x_0)\left(\frac{\partial \Phi}{\partial x}\,|_{x=x_0}\right)^{-1} Qx_0 + a^T(z_0)Ra(z_0) \\
+ \; & z_0^T\left(\frac{\partial a}{\partial z}\,|_{z=z_0}\right)^T R\left(\frac{\partial a}{\partial z}\,|_{z=z_0}\right)z_0 \\
- \; & 2a^T(z_0)R\left(\frac{\partial a}{\partial z}\,|_{z=z_0}\right)z_0 + \text{H.O.T.}]dt\,.
\end{aligned} \tag{3.15}$$

Remark 3.1 The formulas for Q^*, R^*, and S^* can be obtained from the first four lines of (3.15) which yields (3.6)-(3.8). The remaining terms from above will not affect the minimizing control law since they are either first or zeroeth order in z or v. The higher order terms are neglected. Note that the inverse of the Jacobian of $\Phi(x)$ will exist since $\Phi(x)$ is a diffeomorphism. The operating point x_0 can be chosen as the equilibrium point of the plant or as a series of operating points. But this is still preferable to Method 1 because the system remains linear. Also note that all

matrices A,B,C,Q^*,R^*, and S^* are time-invariant since $f(x)$,$g(x)$,$h(x)$,Q, and R are time-invariant. Finally, the true solution to the NQR problem is in general a nonlinear controller. Thus, our method is a means of finding a linear optimal controller for a quadratic cost index that closely approximates the original NQR problem. The control law is optimal insofar as the quadratic cost index approximates the original performance criterion.

3.1.4 Example

Consider the one-link flexible joint robot depicted in Fig. 14 [96]. The system is described by

$$\begin{aligned} I\ddot{q}_1 + MgL\sin q_1 + k(q_1 - q_2) &= 0 \\ J\ddot{q}_2 - k(q_1 - q_2) &= u \end{aligned} \tag{3.16}$$

which is a fourth-order nonlinear system. The nonlinearity is due to gravity. The system is placed into state space form by letting $x_1 = q_1$, $x_2 = \dot{q}_1$, $x_3 = q_2$, $x_4 = \dot{q}_2$, $y = q_1$ which gives us

$$\dot{x} = \begin{bmatrix} x_2 \\ -\frac{MgL}{I}\sin x_1 - \frac{k}{I}(x_1 - x_2) \\ x_4 \\ \frac{k}{J}(x_1 - x_3) \end{bmatrix} + \begin{bmatrix} 0 \\ 0 \\ 0 \\ \frac{1}{J} \end{bmatrix} u \tag{3.17}$$

where the control u is a scalar representing torque output from the joint motor and the output y is a scalar representing the angular displacement of the link with respect to the base coordinate frame at the motor.

We wish to minimize the performance index $J = \int_0^\infty (x^T Q x + u^T R u)dt$ where $Q = I$ and $R = 1$. A check of the system's relative degree reveals $r = n = 4$ $\forall x \in R^4$. Computing the coordinate transformation $z = \Phi(x)$ and the linearizing feedback $u = a(z) + b(z)v$ results in a linear controllable system of fourth order in the Brunovsky canonical form (A,B,C). To simplify notation, let the physical parameters I,J,k,L,Mg be set to one. This yields

$$z = \Phi(x) = \begin{bmatrix} x_1 \\ x_2 \\ -\sin x_1 - (x_1 - x_3) \\ -x_2 \cos x_1 - (x_2 - x_4) \end{bmatrix} \tag{3.18}$$

$$u = a(z) + b(z)v = -\left[z_2^2 \sin z_1 - (\cos z_1 + 1)z_3 - (z_3 + \sin z_1)\right] + v\,. \tag{3.19}$$

We choose the operating point for the expansions (3.11)-(3.13) to be the same as the intended final state, $x_0 = [0\ 0\ 0\ 0]^T$ which is an equilibrium point. That is, we wish to

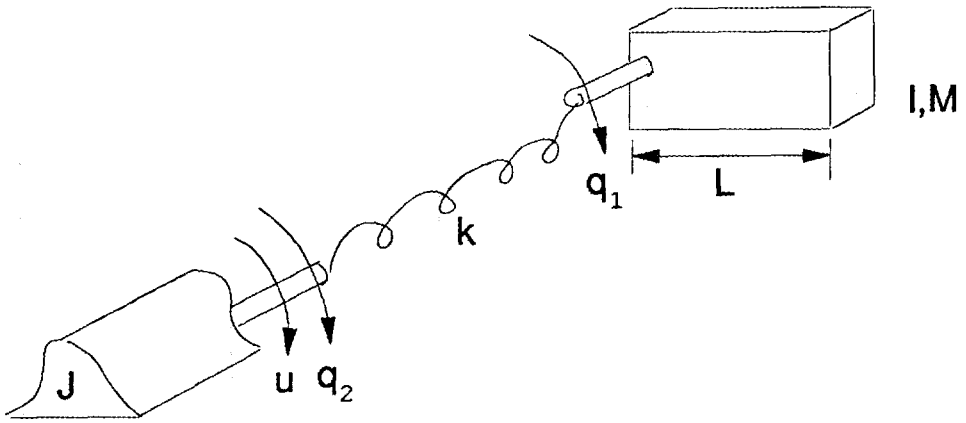

Fig. 14: One-link manipulator with joint flexibility.

drive the system from various initial conditions to a state at which there is no torsion on the spring joint and all states are at rest.

The Q^*,R^*,S^* matrices are now computed via the formulas (3.6)-(3.8) utilizing the above information

$$Q^* = \begin{bmatrix} 6 & 0 & 5 & 0 \\ 0 & 5 & 0 & 2 \\ 5 & 0 & 10 & 0 \\ 0 & 2 & 0 & 1 \end{bmatrix}, \quad R^* = 1, \quad S^* = \begin{bmatrix} 1 \\ 0 \\ 3 \\ 0 \end{bmatrix}. \tag{3.20}$$

Clearly, the strategy of Method 2 results in quite different matrices than Q^* and S^* above. It is easily shown that the conditions of Assumption 3.2 are satisfied. Indeed, for (c.) and (d.) complete controllability and complete observability hold which implies that the solution of the algebraic Riccati equation will be unique and positive definite.

Three different LQR designs were carried out representing Methods 1,2, and 4. Method 1 was implemented about the operating point $x_0 = [0\,0\,0\,0]^T$. For Method 2, $Q = I$, $R = 1$, and $S = 0$. Method 4 is outlined above. An initial condition of $x(0) = [45°\ 0\ 35°\ 0]$ representing a 10° initial twist on the spring was simulated with the desired final state at zero. The simulations were carried out on MATLAB (trade name of The MathWorks, Inc.), and the results are tabulated in Table 1.

Remark 3.2 In Table 1, the approximate cost for Methods 2 and 4 refers to J^* with the higher order terms neglected. Thus, the true cost includes these terms. The approximate cost for Method 1 yields J^* for the linearized system. The true cost for Method 1 refers to J^* with the obtained optimal control law applied to the true nonlinear system. As can be seen, Method 2 yielded much higher costs

Table 1: Simulation results for flexible manipulator example

	Approximate cost	True cost	Closed-loop poles	
Method 1	2.6704	2.6058	-0.6726±j0.7042,	-0.2517±j1.5874
Method 2	5.3772	4.6435	-0.9511±j0.309,	-0.5878±j0.809
Method 4	2.6755	2.6286	-0.6726±j0.7042,	-0.2517±j1.5874

and closed-loop poles in locations quite different from the other two methods. The operating-point linearization method and our method yielded the same closed-loop poles. These poles more accurately represent the desired performance implied by the original cost function than is the case for Method 2. But it must be pointed out for Method 1 that the true closed-loop system is *nonlinear*, whereas it is exactly linear (in z) for Method 4. The costs of these two methods are nearly equal. Note also that the true cost for Method 4 is only 1.8% less than the approximate cost indicating that the quadratic approximation of (3.15) was justified for this example. Finally, Method 3 was attempted, but as mentioned earlier, it proved intractable for a fourth-order nonlinear system.

3.1.5 Conclusions

We have presented a method for optimal control of feedback linearizable systems. This method exactly linearizes the system (in the state space sense) and solves the resultant LQR problem by approximating the performance index in the linearizing coordinates as a quadratic index. The optimal control law for this method is considerably easier to compute than would be the case for exact optimal solutions via Euler-Lagrange equations. This allows one to compute optimal controllers for much higher order systems than otherwise possible. In addition, the method has the advantage of producing a closed-loop linear system that is globally linear instead of locally linear around an operating point (provided that the feedback linearization is globally defined).

It is this last point that provides the principal advantage over Taylor series linearization. In the case of Taylor series linearization, the closed-loop system remains nonlinear which implies that concepts such as closed-loop poles are no longer valid. In our method, even though the performance index is approximated, the closed-loop system will still be linear making concepts such as pole placement more appropriate. A fourth-order robotics example was presented that illustrates the method and its performance as compared to more simplistic approaches.

3.2 ROBUST FEEDBACK LINEARIZATION

In this section, we consider the robust control of nonlinear systems that exhibit parametric uncertainty via feedback linearization. The principal difficulty with feedback linearization is that the system dynamics must be known exactly for the nonlinearities to be successfully cancelled. Uncertainty in the system will result in residual nonlinear terms which will make the stabilization of the system more difficult. Uncertainty in nonlinear systems can arise from many sources: parametric uncertainty, unmodeled dynamics, computational errors, implementation details (e.g. sampling), etc. We consider the first of these sources.

Parametric uncertainty can arise from inexact knowledge of system quantities such as lengths, masses, material constants, etc. This is a common situation in engineering applications. But the elegance and utility of feedback linearization methods make it desirable to try to combine a linearizing control law with a stabilizing controller. Much work has been done in this area from two primary viewpoints. First, there is the adaptive control approach. Work done by Nam and Arapostathis [97] and Sastry and Isidori [98] assume that the family of systems characterized by the uncertainty is feedback linearizable. That is, that the range of uncertainty does not alter the linearizability of the true plant. The works of Akhrif and Blankenship [89], Kanellakopoulos et al. [99], and Taylor et al. [92] only require the linearizability of the nominal plant but additionally assume the satisfaction of a matching condition.

In parallel with this approach are the Lyapunov based stabilization methods of Spong et al. [91, 96]. This method assumes an available (or computable) model that is feedback linearizable and further assumes that the uncertainty satisfies a structure matching condition. The drawback to this approach is that the linearizing coordinate transformation depends on the uncertainty, thus it is unknown. This makes the stabilization difficult to implement without an observer (see Sect. 2.1.2 for theory on construction of observers for nonlinear systems). But, the method has the advantage of not requiring the additional nonlinear dynamics of an adaptive control law. The stabilizing control law is based on the idea that the Lyapunov function for the nominal linearized system remains a Lyapunov function for the perturbed system provided that the matching condition holds and the residual nonlinearities can be bounded from above.

Here, we follow the Lyapunov based approach, but we employ a different parameterization of the system which avoids some of the liabilities of the methodology in [91, 96]. Earlier work based on this approach appears in Ref. [90]. One of the key differences between this work and that in [91, 96] is that we show exponential stability is possible instead of just uniform boundedness. We start by expanding the state space equation of the uncertain system about the nominal parameter vector. Next, we linearize the nominal system (which is assumed to be linearizable) which results in a linear subsystem with higher order nonlinear terms. The linearizing coordinates are

completely known (assuming the original state is measurable). Furthermore, the upper bound on the uncertain residual terms is much easier to obtain in this framework since this bound can be expressed directly in terms of parameter variations.

This is intuitively appealing for sensitivity analysis studies in which one is interested in examining the stability of a system under specific relative parameter variations. We also require a matching condition, but only the nominal system need be linearizable. Finally, we analyze the case of nonlinear systems with zero dynamics. The result with full relative degree is extended when there is a deficiency in relative degree. It is shown that exponential stability is still possible, and all bounds can be computed *a priori* or easily measured on-line. Two examples are presented to illustrate the methods of this section.

3.2.1 Problem Statement

Consider the single-input, single-output (SISO) nonlinear model

$$\begin{aligned} \dot{x} &= f(x,\alpha) + g(x,\alpha)u \\ y &= h(x) \end{aligned} \tag{3.21}$$

where it is assumed that $f(x,\alpha)$, and $g(x,\alpha)$ are C^∞ vector fields defined on a dense submanifold $M \subset R^n$. It is also assumed that $h(x)$ is C^∞ on M. In addition, x is defined on an open set U of R^n. The vector α is the unknown parameter vector. It is assumed that f and g are smooth vector fields for every $\alpha \in B_\alpha \subset R^p$ where B_α is an admissible set of unknown parameter vectors. Without loss of generality, we also assume that $f(0,\alpha) = 0$ and $h(0) = 0$. The nominal parameter vector α_n is assumed known and the perturbations about α_n are represented as

$$\alpha = \alpha_n + \delta\alpha\,. \tag{3.22}$$

Furthermore, the vector fields f and g are analytic in α about $\alpha = \alpha_n$.

Our goal is to find a diffeomorphism $\Phi(x)$ on M and nonlinear functions $a(x)$ and $b(x)$ such that the nominal system is rendered linear in the coordinates $z = \Phi(x)$. That is,

$$\frac{\partial\Phi(x)}{\partial x}[f(x,\alpha_n) + g(x,\alpha_n)a(x)]_{x=\Phi^{-1}(z)} = Az \tag{3.23}$$

$$\frac{\partial\Phi(x)}{\partial x}[g(x,\alpha_n)b(x)]_{x=\Phi^{-1}(z)} = B \tag{3.24}$$

with the nonlinear feedback

$$u = a(x) + b(x)v\,. \tag{3.25}$$

This results in the linear plant

$$\begin{aligned} \dot{z} &= Az + Bv \\ y &= Cz \end{aligned} \tag{3.26}$$

where (A,B,C) are in the Brunovsky canonical form [32].

The input v will not only be utilized to stabilize the nominal linear system (which has all its poles at the origin), but it will be used to exponentially stabilize the system once the parametric uncertainty is introduced. In the following sections, we define the Taylor series expansion about α_n and the control approach to stabilizing the uncertain system. In this section, all vector norms are assumed to be the usual Euclidean norm, and all matrix norms are consistent with this vector norm.

3.2.2 Modeling of the Parametric Uncertainty

We begin by expanding $\dot{x}$ as a Taylor series in α about $\alpha = \alpha_n$

$$\begin{aligned} \dot{x} &= f(x,\alpha_n) + g(x,\alpha_n)u + \left(\frac{\partial f}{\partial \alpha} + \frac{\partial g}{\partial \alpha}u\right)|_{\alpha=\alpha_n}\,\delta\alpha \\ &+ \frac{1}{2}\delta\alpha^T\left(\frac{\partial^2 f}{\partial \alpha^2} + \frac{\partial^2 g}{\partial \alpha^2}u\right)|_{\alpha=\alpha_n}\,\delta\alpha + O(\|\,\delta\alpha\,\|^3) \end{aligned} \tag{3.27}$$

where it is noted that we have made no assumption regarding the linearity (or nonlinearity) of the uncertain parameters. We do, however, need the following assumption.

Assumption 3.3 The relative degree (see Sect. 2.1.1 for a definition) of the nominal system

$$\begin{aligned} \dot{x} &= f(x,\alpha_n) + g(x,\alpha_n)u \\ y &= h(x) \end{aligned} \tag{3.28}$$

is $r = n$.

Assumption 3.3 implies that the diffeomorphic state transformation

$$z = \Phi(x,\alpha_n) = \begin{bmatrix} h(x) \\ L_{f(x,\alpha_n)}h(x) \\ \vdots \\ L^{r-1}_{f(x,\alpha_n)}h(x) \end{bmatrix} \tag{3.29}$$

and the standard linearizing feedback

$$\begin{aligned} u &= a(x,\alpha_n) + b(x,\alpha_n)v \\ &= \frac{-L^r_{f(x,\alpha_n)}h(x)}{L_{g(x,\alpha_n)}L^{r-1}_{f(x,\alpha_n)}h(x)} + \frac{1}{L_{g(x,\alpha_n)}L^{r-1}_{f(x,\alpha_n)}h(x)}v \end{aligned} \tag{3.30}$$

result in the perturbed system

$$\begin{aligned}\dot{z} &= Az + Bv + \frac{\partial \Phi(x,\alpha_n)}{\partial x}(\frac{\partial f}{\partial \alpha} + \frac{\partial g}{\partial \alpha}a(x,\alpha_n) \\ &+ \frac{\partial g}{\partial \alpha}b(x,\alpha_n)v) \mid_{\substack{\alpha=\alpha_n \\ x=\Phi^{-1}(z)}} \delta\alpha + \mathrm{O}(\| \delta\alpha \|^2) \qquad (3.31) \\ y &= Cz\end{aligned}$$

where $L_f h(x) = \frac{\partial h}{\partial x} f$ denotes the Lie derivative of $h(x)$ along $f(x)$. With the exception of $\delta\alpha$ (which can easily be bounded once relative parameter deviation is considered), all terms in (3.31) are known since they are evaluated about $\alpha = \alpha_n$. If the system is linear in the uncertainty α then the expansion (3.31) will be exact to first order in $\delta\alpha$. We now make the following assumption.

Assumption 3.4 The parameter vector α appears linearly in (3.21).

Assumption 3.4 is reasonable since in most sensitivity studies one will normally consider maximal parametric deviations of no more than 15 or 20% which will make the second order term quite small. For most of the literature on nonlinear systems with parametric uncertainty, the unknown parameters are assumed to appear linearly in the system dynamics. However, the work of this section can easily be extended to higher order terms in $\delta\alpha$ as suggested by the expansion in (3.27). We shall note this throughout the section by denoting $\mathrm{O}(\| \delta\alpha \|^2)$ where higher order terms can be inserted.

3.2.3 Robust Stabilization

The first step in the stabilization of the true nonlinear model is to place the poles of the nominal linear system (A,B,C) into the left-half plane. This can be done via linear quadratic regulator theory or pole placement methods and will not be further discussed here. Instead, we assume the existence of a constant $1 \times n$ matrix K (which is easy to find since the pair (A,B) is completely controllable) such that $A_c = A + BK$ is stable. Thus, we let $v = Kz + \Delta v$ which results in the new model

$$\begin{aligned}\dot{z} &= A_c z + B\Delta v \\ &+ \frac{\partial \Phi}{\partial x}\left(\frac{\partial f}{\partial \alpha} + \frac{\partial g}{\partial \alpha}a(x,\alpha_n) + \frac{\partial g}{\partial \alpha}b(x,\alpha_n)Kz\right) \mid_{\substack{\alpha=\alpha_n \\ x=\Phi^{-1}(z)}} \delta\alpha \\ &+ \frac{\partial \Phi}{\partial x}\frac{\partial g}{\partial \alpha}b(x,\alpha_n) \mid_{\substack{\alpha=\alpha_n \\ x=\Phi^{-1}(z)}} \Delta v\delta\alpha + \mathrm{O}(\| \delta\alpha \|^2)\,, \qquad (3.32)\end{aligned}$$

where Δv is an additional control term to stabilize the residual nonlinearities. To be able to control the above model, we need a matching condition that guarantees that the uncertain nonlinear terms lie in the range space of the input. More formally, we need the following assumption.

Assumption 3.5 $\forall x \in M$, $\forall \alpha \in B_\alpha$, we require that $\frac{\partial g}{\partial \alpha} \mid_{\alpha=\alpha_n} \delta\alpha \in \text{Span}\{g(x,\alpha_n)\}$ and $\frac{\partial f}{\partial \alpha} \mid_{\alpha=\alpha_n} \delta\alpha \in \text{Span}\{g(x,\alpha_n)\}$.

The above assumption simply means that the uncertainty in (3.21) is mapped to a reachable part of the input space when transformed by the nominal linearizing coordinates. This assumption is less restrictive than some in the literature due to the fact that the $\text{Span}\{g(x,\alpha_n)\}$ depends only on the nominal value of the parameters whereas in some works (e.g. Ref. [91]) it will depend on the uncertainty. It is also easier to satisfy than the feedback linearizability of (3.21) $\forall \alpha \in B_\alpha$ (as is required in Ref. [98]) because the relative degree of a system can be sensitive to small changes in parameters. Furthermore, the second part of Assumption 3.5 can be relaxed by replacing it with a condition involving Lie brackets as outlined in Ref. [89]. It is shown there that this condition involving Lie brackets is less restrictive than the above. We now rewrite (3.32) as

$$\dot{z} = A_c z + B\Delta v + \eta(z, \Delta v) \tag{3.33}$$

where higher order terms in $\delta\alpha$ have been ignored and

$$\begin{aligned} \eta(z,\Delta v) &= \frac{\partial \Phi}{\partial x}\left(\frac{\partial f}{\partial \alpha} + \frac{\partial g}{\partial \alpha} a(x,\alpha_n) + \frac{\partial g}{\partial \alpha} b(x,\alpha_n) K z\right) \mid_{\substack{\alpha=\alpha_n \\ x=\Phi^{-1}(z)}} \delta\alpha \\ &+ \frac{\partial \Phi}{\partial x}\frac{\partial g}{\partial \alpha} b(x,\alpha_n) \mid_{\substack{\alpha=\alpha_n \\ x=\Phi^{-1}(z)}} \delta\alpha \Delta v \,. \end{aligned} \tag{3.34}$$

Our next assumption concerns the bounds on the uncertainty term $\eta(z, \Delta v)$.

Assumption 3.6 We assume the existence of a function $\rho(z,t)$ such that $\| \eta \| \leq \rho(z,t)$ and $\| \Delta v \| \leq \rho(z,t)$.

The second part of this assumption will automatically be satisfied once the control law is chosen. The function $\rho(z,t)$ is written explicitly as a function of time because it depends on the state z. Utilizing the above and the triangle inequality, we get

$$\begin{aligned} \rho(z,t) &= \left[1 - \| \frac{\partial \Phi}{\partial x}\frac{\partial g}{\partial \alpha} b(x,\alpha_n) \|_{\substack{\alpha=\alpha_n \\ x=\Phi^{-1}(z)}} \overset{\sup}{\alpha} \| \delta\alpha \|\right]^{-1} \| \frac{\partial \Phi}{\partial x}(\frac{\partial f}{\partial \alpha} \\ &+ \frac{\partial g}{\partial \alpha} a(x,\alpha_n) + \frac{\partial g}{\partial \alpha} b(x,\alpha_n) K z) \|_{\substack{\alpha=\alpha_n \\ x=\Phi^{-1}(z)}} \overset{\sup}{\alpha} \| \delta\alpha \| \,. \end{aligned} \tag{3.35}$$

It is important to note in (3.35) that everything on the right hand side is known *a priori* except for $\overset{\sup}{\alpha} \| \delta\alpha \|$ which is easily determined once one decides on a relative parameter deviation to consider. That is, we have expressed the uncertainty directly in terms of the parameter deviations which is physically more meaningful than if the parametric uncertainty were embedded within a complicated expression. For instance,

if one wishes to determine the effects of 15% relative uncertainty for a scalar nonzero α then $\overset{\sup}{\alpha}\| \delta\alpha \| = 0.15\alpha_n$. Our next assumption concerns the measurability of the state.

Assumption 3.7 The state x (hence z) is available by direct measurement or via an observer.

The key idea is that since the transformed state z is defined about the nominal parameters α_n, it will be measurable if x is measurable. The exponential stability proven in this section is local due to the term in brackets in (3.35) possibly becoming unbounded. This determines the set S of admissible initial conditions. From (3.35), the term in brackets must be bounded away from zero for all time to avoid a singularity. Since exponential stability will be proven in Theorems 3.1 and 3.2, we only require this inequality to hold at time $t = t_0$. Under the conditions of the theorems, the inequality will then hold for all time. This is an advantage over Refs. [91, 96] which can only claim uniform boundedness.

Assumption 3.8 The inequality

$$\left\| \frac{\partial \Phi}{\partial x} \frac{\partial g}{\partial \alpha} b(x, \alpha_n) \right\|_{\substack{\alpha=\alpha_n \\ x=\Phi^{-1}(z)}} \overset{\sup}{\alpha}\| \delta\alpha \| < 1 \tag{3.36}$$

must hold at the initial conditions $z^0 = \Phi(x^0)$ and $t = t_0$.

Additional assumptions made on the structure of $\rho(z, t)$ in [91, 96] are not needed here which leads to a simpler control law to implement. The set of admissible initial conditions S is then defined as

$$S = \left\{ z^0 \in R^n \mid \left\| \frac{\partial \Phi}{\partial x} \frac{\partial g}{\partial \alpha} b(x, \alpha_n) \right\|_{\substack{\alpha=\alpha_n \\ x^0=\Phi^{-1}(z^0)}} \overset{\sup}{\alpha}\| \delta\alpha \| < 1 \right\} . \tag{3.37}$$

The theorem that follows gives us the control law for Δv and the stability result for the full system.

Theorem 3.1 *Under Assumptions 3.3-3.8, the equilibrium $z = 0$ of the system (3.33) is exponentially stable with respect to initial conditions lying in S (defined in (3.37)) if Δv satisfies*

$$\Delta v = \begin{cases} -\frac{\rho(z,t)}{\|B\|}, & z^T PB \geq 0 \\ \frac{\rho(z,t)}{\|B\|}, & z^T PB < 0 \end{cases} \tag{3.38}$$

where $\| B \| = 1$ for the SISO case, and P is the unique symmetric positive definite solution to the Lyapunov equation

$$PA_c + A_c^T P + Q = 0 \tag{3.39}$$

with Q a given symmetric positive definite matrix.

Proof: We first note that all terms in the above control law are completely known except for $\overset{\sup}{\alpha}\| \delta\alpha \|$ which was discussed earlier. Further, the second part of Assumption 3.6 ($\| \Delta v \| \leq \rho(z,t)$) is satisfied by the above choice of control law. The proof follows some of the steps in the proof of Theorem 1 in Ref. [100], but we show exponential stability due to the different assumptions in this section.

We start with the Lyapunov function for the nominal linearized system, $V(z) = z^T P z$. We proceed by showing that $V(z)$ is also a Lyapunov function for the system (3.33) with respect to the set S in (3.37). Differentiating along solutions of (3.33) and utilizing (3.39), we obtain

$$\begin{aligned} \dot{V} &= 2z^T P A_c z + 2z^T P B \Delta v + 2z^T P \eta(z, \Delta v) \\ &= -z^T Q z + 2z^T P B \Delta v + 2z^T P \eta(z, \Delta v) \\ &= -z^T Q z + 2z^T P B(\Delta v + \tilde{\eta}(z, \Delta v)) , \end{aligned} \tag{3.40}$$

where the last line is obtained from Assumption 3.5 (matching condition). This condition implies the existence of a function $\tilde{\eta}(z, \Delta v)$ such that

$$\eta(z, \Delta v) = B\tilde{\eta}(z, \Delta v) . \tag{3.41}$$

A bound is obtained on $\tilde{\eta}$ as follows.

$$\| \eta \| = \| B\tilde{\eta} \| = | \tilde{\eta} | \| B \| \leq \rho(z,t) \tag{3.42}$$

since $\tilde{\eta}$ is a scalar (SISO). From this we get

$$-\frac{\rho(z,t)}{\| B \|} \leq \tilde{\eta} \leq \frac{\rho(z,t)}{\| B \|} \tag{3.43}$$

which leads to

$$\dot{V} \leq \begin{cases} -z^T Q z + 2z^T P B \left(\Delta v + \frac{\rho(z,t)}{\|B\|}\right) , & z^T P B \geq 0 \\ -z^T Q z - 2 \mid z^T P B \mid \left(\Delta v - \frac{\rho(z,t)}{\|B\|}\right) , & z^T P B < 0 \end{cases} . \tag{3.44}$$

With the choice of control law in (3.38), we have

$$\dot{V} \leq -z^T Q z \Longrightarrow \dot{V} \leq -\lambda_{\min}(Q) \| z \|^2 . \tag{3.45}$$

Since Q is positive definite, all of its eigenvalues are positive. Thus, with reference to standard stability texts (e.g. Ref. [101], pp. 210-211), the equilibrium $z = 0$ of (3.33) is exponentially stable subject to initial conditions lying in the set S in (3.37). This completes the proof. □

It should be noted that the control law in (3.38) is easier to implement than the control laws in Refs. [100, 91, 96]. This is because the bound $\rho(z,t)$ is simpler to

compute, since it can depend nonlinearly on z instead of forcing one to find constants that make it a linear function of z as in Refs. [100, 91, 96]. Uniform boundedness of all solutions of (3.33) can be shown utilizing the same Lyapunov function. This might be useful in the event of more than one equilibrium point contained in the set S. A linear high gain control law is also possible to design. That is, there exists a large enough constant $\gamma > 0$ such that $\Delta v = -\gamma B^T P z$ will make solutions of (3.33) uniformly ultimately bounded with respect to a different set S. The details of this approach are to be found in Refs. [102, 103]. Assumption 3.7 can be relaxed (i.e. measurement noise) with only minor modifications by implementing some of the theory in Refs. [102, 100]. Finally, the multi-input multi-output (MIMO) case requires some additional matrix manipulations, but the above result can still be extended to MIMO systems.

Example 3.1 We analyze the following second-order system

$$\begin{bmatrix} \dot{x}_1 \\ \dot{x}_2 \end{bmatrix} = \begin{bmatrix} -x_2 \\ x_2 e^{-x_1} \end{bmatrix} + \begin{bmatrix} 0 \\ \alpha \end{bmatrix} u\,, \quad y = x_1\,, \tag{3.46}$$

which exhibits linear parametric uncertainty and has the origin as its equilibrium point. The nominal value of α is $\alpha_n = 1$. The matching condition (Assumption 3.5) is also satisfied. We now consider the relative degree of the system

$$\begin{aligned} L_g h &= 0 \\ L_g L_f h &= -\alpha \neq 0\,. \end{aligned}$$

From above we see that for $\alpha = \alpha_n = 1$, $r = n = 2$ as required in Assumption 3.3. This holds for a dense submanifold $M = R^2$ and the ball $B_\alpha = \{\alpha \in R \mid \alpha \neq 0\}$.

Continuing, we find that the linearizing coordinates and linearizing feedback in the nominal parameter is

$$\begin{aligned} z_1 &= x_1 \\ z_2 &= -x_2 \\ u &= -x_2 e^{-x_1} - v\,. \end{aligned}$$

The Taylor series expansion of (3.46) about $\alpha = 1$ in the new coordinates yields

$$\begin{aligned} \dot{z}_1 &= z_2 \\ \dot{z}_2 &= v + (-z_2 e^{-z_1} + v)(\alpha - 1) \\ y &= z_1 \end{aligned} \tag{3.47}$$

which is in the form of (3.31). To determine the control law, we compute the bound $\rho(z,t)$. Substituting the above information and $\alpha = 1$ into (3.35), the bound

$$\rho(z,t) = \left[1 - \sup_{\alpha} |\, \alpha - 1 \,|\right]^{-1} \cdot |\, z_2 e^{-z_1} + z_1 + z_2 \,|^2 \cdot \sup_{\alpha} |\, \alpha - 1 \,| \tag{3.48}$$

is obtained. In producing this bound, the gain vector $K = [-1 \; -1]$ was chosen to place the poles of the nominal linearized plant in the open left-half plane. Since $\| B \| = 1$, the control law is

$$\Delta v = \begin{cases} -\rho(z,t), & (0.5z_1 + z_2) \geq 0 \\ \rho(z,t), & (0.5z_1 + z_2) < 0 \end{cases} \tag{3.49}$$

resulting in exponential stability of the origin. This was computed from (3.38) utilizing P in (3.39) with Q being the identity matrix.

Finally, the set of allowable initial conditions S_z was calculated utilizing Assumption 3.8 and (3.48). It can be seen that $S = R^2$ provided that $\overset{\text{sup}}{\alpha} | \alpha - 1 | < 1 \; \forall \alpha \in B_\alpha$. That is, the equilibrium $x = 0$ of (3.46) is globally exponentially stable with the control law (3.49) for nearly 100% relative uncertainty in α (i.e., $0 < \alpha < 2$).

3.2.4 Zero Dynamics

The relative degree condition of Assumption 3.3 is restrictive, and it is of interest to investigate the stabilization of uncertain nonlinear systems which do not satisfy this condition. We start with the system (3.21) and allow $r < n$. The same linearizing feedback as in (3.30) will be employed, but this will not result in the linearization of the full state space. Therefore, we must handle zero dynamics of dimension $n - r$ (for a complete definition of zero dynamics, see Ref. [21]). We begin by partitioning the state space as follows

$$\zeta = \begin{bmatrix} z_1 \\ \vdots \\ z_r \end{bmatrix}, \; \psi = \begin{bmatrix} z_{r+1} \\ \vdots \\ z_n \end{bmatrix}, \; z = \begin{bmatrix} \zeta \\ \psi \end{bmatrix}, \; \Phi(x) = \begin{bmatrix} \Phi_\zeta(x) \\ \Phi_\psi(x) \end{bmatrix} \tag{3.50}$$

where $\Phi_\zeta(x, \alpha_n)$ is as in (3.29) and $\Phi_\psi(x, \alpha_n)$ is chosen such that $L_{g(x,\alpha_n)}\Phi_\psi(x, \alpha_n) = 0$. This last condition is not a strict requirement. It is always possible to satisfy this condition, but it can be relaxed without significantly altering the control strategy in this section. The full system is now rewritten as

$$\begin{aligned} \dot{\zeta} &= A\zeta + Bv + \frac{\partial \Phi_\zeta}{\partial x}\left(\frac{\partial f}{\partial \alpha} + \frac{\partial g}{\partial \alpha} a(x, \alpha_n)\right. \\ &+ \left.\frac{\partial g}{\partial \alpha} b(x, \alpha_n) v\right) \Big|_{\substack{\alpha=\alpha_n \\ x=\Phi^{-1}(z)}} \delta\alpha + O(\| \delta\alpha \|^2) \\ \dot{\psi} &= [L_f \Phi_\psi + \frac{\partial \Phi_\psi}{\partial x}\left(\frac{\partial f}{\partial \alpha} + \frac{\partial g}{\partial \alpha} a(x, \alpha_n)\right. \\ &+ \left.\frac{\partial g}{\partial \alpha} b(x, \alpha_n) v\right)] \Big|_{\substack{\alpha=\alpha_n \\ x=\Phi^{-1}(z)}} \delta\alpha + O(\| \delta\alpha \|^2) \end{aligned} \tag{3.51}$$

where it is noted that Assumption 3.4 is still enforced.

It is desired to stabilize the nominal linearized system, however the full nominal system is of order n. This implies that we must extract a linear part from the zero dynamics because the full $n \times n$ A matrix cannot be stabilized with static state feedback. This is true since the bottom $n-r$ rows of this matrix are all zeros until the linear part is extracted. Hence, we rewrite (3.51) as

$$\begin{aligned}
\begin{bmatrix} \dot{\zeta} \\ \dot{\psi} \end{bmatrix} &= \begin{bmatrix} A & 0 \\ A_1 & A_2 \end{bmatrix} \begin{bmatrix} \zeta \\ \psi \end{bmatrix} + \begin{bmatrix} B \\ 0 \end{bmatrix} v \\
&+ \begin{bmatrix} \frac{\partial \Phi_\zeta}{\partial x} \left(\frac{\partial f}{\partial \alpha} + \frac{\partial g}{\partial \alpha} a(x, \alpha_n) + \frac{\partial g}{\partial \alpha} b(x, \alpha_n) v \right) \Big|_{\substack{\alpha=\alpha_n \\ x=\Phi^{-1}(z)}} \delta\alpha \\ \frac{\partial \Phi_\psi}{\partial x} \left(\frac{\partial f}{\partial \alpha} + \frac{\partial g}{\partial \alpha} a(x, \alpha_n) + \frac{\partial g}{\partial \alpha} b(x, \alpha_n) v \right) \Big|_{\substack{\alpha=\alpha_n \\ x=\Phi^{-1}(z)}} \delta\alpha \end{bmatrix} \\
&+ \begin{bmatrix} \mathrm{O}(\| \delta\alpha \|^2) \\ (L_f \Phi_\psi - A_1 \zeta - A_2 \psi) \Big|_{\substack{\alpha=\alpha_n \\ x=\Phi^{-1}(z)}} + \mathrm{O}(\| \delta\alpha \|^2) \end{bmatrix} \qquad (3.52) \\
y &= \begin{bmatrix} C & 0 \end{bmatrix} \begin{bmatrix} \zeta \\ \psi \end{bmatrix}
\end{aligned}$$

where (A,B,C) are in the Brunovsky form, and A_1 and A_2 are of compatible dimensions. We have complete freedom to choose A_1 and A_2 such that the pair

$$\bar{A} = \begin{bmatrix} A & 0 \\ A_1 & A_2 \end{bmatrix}, \; B_c = \begin{bmatrix} B \\ 0 \end{bmatrix} \qquad (3.53)$$

is completely controllable. Then we can choose $v = Kz + \Delta v$ such that

$$A_c = \begin{bmatrix} A & 0 \\ A_1 & A_2 \end{bmatrix} + \begin{bmatrix} B \\ 0 \end{bmatrix} \begin{bmatrix} K_1 & K_2 \end{bmatrix} \qquad (3.54)$$

is stable.

The system is now written in the more compact form

$$\dot{z} = A_c z + B_c \Delta v + \beta_0 + \beta_1 \delta\alpha + \beta_2 \delta\alpha \Delta v + \mathrm{O}(\| \delta\alpha \|^2) \qquad (3.55)$$

where

$$\beta_0 = \begin{bmatrix} 0 \\ L_f \Phi_\psi - A_1 \zeta - A_2 \psi \end{bmatrix} \qquad (3.56)$$

$$\beta_1 = \begin{bmatrix} \frac{\partial \Phi_\zeta}{\partial x} \left(\frac{\partial f}{\partial \alpha} + \frac{\partial g}{\partial \alpha} a(x, \alpha_n) + \frac{\partial g}{\partial \alpha} b(x, \alpha_n) K z \right) \Big|_{\substack{\alpha=\alpha_n \\ x=\Phi^{-1}(z)}} \\ \frac{\partial \Phi_\psi}{\partial x} \left(\frac{\partial f}{\partial \alpha} + \frac{\partial g}{\partial \alpha} a(x, \alpha_n) + \frac{\partial g}{\partial \alpha} b(x, \alpha_n) K z \right) \Big|_{\substack{\alpha=\alpha_n \\ x=\Phi^{-1}(z)}} \end{bmatrix} \qquad (3.57)$$

$$\beta_2 = \begin{bmatrix} \frac{\partial \Phi_\zeta}{\partial x} \frac{\partial g}{\partial \alpha} b(x, \alpha_n) \Big|_{\substack{\alpha=\alpha_n \\ x=\Phi^{-1}(z)}} \\ \frac{\partial \Phi_\psi}{\partial x} \frac{\partial g}{\partial \alpha} b(x, \alpha_n) \Big|_{\substack{\alpha=\alpha_n \\ x=\Phi^{-1}(z)}} \end{bmatrix}. \qquad (3.58)$$

With the above terms, we define our new nonlinear system as

$$\dot{z} = A_c z + B_c \Delta v + \tilde{\beta}(z, \Delta v) \tag{3.59}$$

where higher order terms in $\delta\alpha$ have been ignored and $\tilde{\beta}(z, \Delta v) = \beta_0 + \beta_1 \delta\alpha + \beta_2 \delta\alpha \Delta v$. Assumption 3.6 is again required to hold with η replaced by $\tilde{\beta}$. In the case of zero dynamics, the bound is denoted as ρ_z and satisfies the following equality

$$\rho_z(z,t) = [1 - \| \beta_2 \|^{\sup}_{\alpha} \| \delta\alpha \|]^{-1} [\| \beta_0 \| + \| \beta_1 \|^{\sup}_{\alpha} \| \delta\alpha \|] \tag{3.60}$$

where again it is noted that everything on the right hand side is known except for $^{\sup}_{\alpha} \| \delta\alpha \|$ which will be determined once a relative parameter uncertainty is decided upon. Assumption 3.8 must be modified slightly to take zero dynamics into account and appears as Assumption 3.9 below.

Assumption 3.9 In a very similar manner to Assumption 3.8, it is assumed that $\| \beta_2 \|^{\sup}_{\alpha} \| \delta\alpha \| \leq 1$ holds for the initial condition $z^0 = \Phi(x^0)$ and $t = t_0$.

With Assumption 3.9, the set of allowable initial conditions is now

$$S_z = \left\{ z^0 \in R^n \mid \| \beta_2 \|^{\sup}_{\alpha} \| \delta\alpha \| < 1 \right\} . \tag{3.61}$$

The matching condition must be strengthened due to the uncontrollability of the zero dynamics.

Assumption 3.10 We require $\forall x \in M$, $\forall \alpha \in B_\alpha$ that

$$\frac{\partial g}{\partial \alpha} |_{\alpha=\alpha_n} \delta\alpha \in \text{Span}\{g(x, \alpha_n)\} \bigcap \aleph \left(\frac{\partial \Phi_\psi}{\partial x} \right) \tag{3.62}$$

and

$$\frac{\partial f}{\partial \alpha} |_{\alpha=\alpha_n} \delta\alpha \in \text{Span}\{g(x, \alpha_n)\} \bigcap \aleph \left(\frac{\partial \Phi_\psi}{\partial x} \right) \tag{3.63}$$

where $\aleph \left(\frac{\partial \Phi_\psi}{\partial x} \right)$ represents the null space of $\frac{\partial \Phi_\psi}{\partial x}$. Further, it is assumed that $L_f \Phi_\psi$ is linear in z.

In words, Assumption 3.10 requires the uncertainty not only to lie in the range space of the input but also in the null space of the coordinates transformation for the zero dynamics. That is, the uncertainty must not be contained in the zero dynamics. Further, the zero dynamics must be linear in the z coordinates. Though this is restrictive, it does represent a class of systems with insufficient relative degree and uncertain parameters that can still be exponentially stabilized. The zero dynamics counterpart to Theorem 3.1 follows.

Theorem 3.2 *Under Assumptions 3.4,3.6,3.7,3.9, and 3.10, the equilibrium $z = 0$ of the system (3.59) is exponentially stable for all initial conditions in S_z (defined in (3.61)) if Δv satisfies*

$$\Delta v = \begin{cases} -\frac{\rho_z(z,t)}{\|B_c\|}, & z^T P B_c \geq 0 \\ \frac{\rho_z(z,t)}{\|B_c\|}, & z^T P B_c < 0 \end{cases} \tag{3.64}$$

where $\| B_c \| = 1$ for the SISO case.

Proof: The proof proceeds exactly as in Theorem 3.1. Assumption 3.10 implies the existence of a scalar function $\tilde{\beta}_c$ such that $\tilde{\beta} = B_c \tilde{\beta}_c$. Then from Assumption 3.6, we have that $\tilde{\beta}_c \leq \frac{\rho_z(z,t)}{\|B_c\|}$. With the Lyapunov function $V(z) = z^T P z$, we obtain

$$\dot{V} \leq \begin{cases} -z^T Q z + 2 z^T P B_c \left(\Delta v + \frac{\rho_z(z,t)}{\|B_c\|}\right), & z^T P B_c \geq 0 \\ -z^T Q z - 2 \mid z^T P B_c \mid \left(\Delta v - \frac{\rho_z(z,t)}{\|B_c\|}\right), & z^T P B_c < 0 \end{cases} . \tag{3.65}$$

where P and Q are defined with respect to A_c in (3.54). From this, the control law in (3.64) is obtained, and the exponential stability result follows. □

Example 3.2 Consider the third-order system

$$\begin{bmatrix} \dot{x}_1 \\ \dot{x}_2 \\ \dot{x}_3 \end{bmatrix} = \begin{bmatrix} -x_3 \\ x_1 x_3 \\ x_2 \end{bmatrix} + \begin{bmatrix} 0 \\ \alpha \\ 0 \end{bmatrix} u, \quad y = x_3 \tag{3.66}$$

where α is a scalar parameter with nominal value $\alpha_n = 1$. This system also exhibits linear parametric uncertainty, and it does satisfy Assumption 3.10. A check of the system's relative degree reveals $r = n - 1 = 2$ which holds for the entire state space and $B_\alpha = \{\alpha \in R \mid \alpha \neq 0\}$. The linearizing coordinates and feedback evaluated about the nominal parameter are

$$\begin{aligned} z_1 &= x_3 \\ z_2 &= x_2 \\ z_3 &= x_1 \\ u &= -x_1 x_3 + v \end{aligned} \tag{3.67}$$

where $z_3 = \Phi_\psi(x)$ was chosen such that $L_g \Phi_\psi = 0$ and $\Phi_\psi(0) = 0$. Continuing with the analysis, we put the system in the form of (3.52) which results in

$$\begin{bmatrix} \dot{z}_1 \\ \dot{z}_2 \\ \dot{z}_3 \end{bmatrix} = \begin{bmatrix} 0 & 1 & 0 \\ 0 & 0 & 0 \\ -1 & 0 & 0 \end{bmatrix} \begin{bmatrix} z_1 \\ z_2 \\ z_3 \end{bmatrix} + \begin{bmatrix} 0 \\ 1 \\ 0 \end{bmatrix} v + \begin{bmatrix} 0 \\ (-z_1 z_3 + v)(\alpha - 1) \\ 0 \end{bmatrix}, \tag{3.68}$$

where $A_1 = [-1 \;\; 0]$ and $A_2 = 0$ were chosen to make the pair $(\bar{A}, B_c)$ completely controllable. Then $K = [-3 \;\; -3 \;\; -1]$ was chosen to make A_c stable.

Next, the bound $\rho_z(z,t)$ was computed, yielding

$$\rho_z(z,t) = \left[1 - \overset{\sup}{\alpha} \mid \alpha - 1 \mid\right]^{-1} \left[(z_1 z_3 + 3z_1 + 3z_2 + z_3) \overset{\sup}{\alpha} \mid \alpha - 1 \mid\right] . \tag{3.69}$$

This results in the control law

$$\Delta v = \begin{cases} -\rho_z(z,t), & (-0.35z_1 + 0.05z_2 + 0.5z_3) \geq 0 \\ \rho_z(z,t), & (-0.35z_1 + 0.05z_2 + 0.5z_3) < 0 \end{cases} \tag{3.70}$$

noting that $\| B_c \| = 1$. The matrix P was again solved for by using $Q = I$ in (3.39). Finally, the set of allowable initial conditions S_z was calculated utilizing Assumption 3.9 and (3.69). It can be seen that $S_z = R^3$ provided that $\overset{\sup}{\alpha} \mid \alpha - 1 \mid < 1 \; \forall \alpha \in B_\alpha$. That is, the equilibrium $x = 0$ of (3.66) is globally exponentially stable $\forall \alpha \in (0,2)$ with the control law (3.70).

3.2.5 Conclusions

We have shown that linearization and stabilization of nonlinear systems exhibiting parametric uncertainty is possible via a Lyapunov based approach if certain assumptions (principally a structure matching condition) are satisfied. The principal advantages of the approach in this section are that exponential stability instead of just uniform boundedness can be achieved and a control law that is easier to compute. In addition, the linearizing coordinates are known because they are defined about the nominal parameters, and systems without full relative degree can also be exponentially stabilized in this framework. Further, the bounds are expressed directly in terms of parametric uncertainty which makes them simple to compute once maximum parameter deviations are decided upon.

The method avoids the feedback linearizability assumption of the whole family of uncertain plants as well as the additional dynamics imposed by an adaptive controller (as in Refs. [97, 98, 92]). The approach also works well with the ideas of sensitivity theory due to fact that the uncertainty is expressed directly in terms of the parameter deviations. Though many assumptions are made in this section to achieve exponential stability results, these assumptions are no more difficult to satisfy than in the works cited herein. In fact, many are easier to satisfy. The relative degree assumption was relaxed to include zero dynamics. The matching condition represents the most difficult requirement to satisfy. There has been some effort made to relax the matching condition for linear systems with parametric uncertainty. For nonlinear systems, different forms of this condition exist but all amount to a restriction on the range space of the uncertainty. A possible control technique to alleviate the matching condition is that of high gain linear feedback. Of course, problems associated with high gains would be the tradeoff.

CHAPTER 4

CONTROL OF LARGE-SCALE SYSTEMS

4.1 DECENTRALIZED FEEDBACK LINEARIZATION

Much attention has been focused on nonlinear systems in recent years due to their prominence in such fields as robotics, aircraft, and space structures. With this attention have come many techniques for dealing with the additional complexities associated with nonlinear systems. In particular, the idea of transforming a nonlinear system into a linear one through feedback has received a great deal of interest. In this section, we consider multi-input multi-output (MIMO) nonlinear systems with restrictions on the feedback information available to the controller. The restrictions considered here require the use of locally available signals at each input-output channel due to communication and/or structural restrictions. This decentralization constraint implies that each input has available for feedback a local input or in the case of composite systems, a local state only.

Most of the decentralized control literature has concentrated on linear systems. Decentralized control of nonlinear systems has received some interest by Refs. [104, 105, 106] from the variable structure control point of view. But decentralized feedback linearization has received little prior attention. In the MIMO feedback linearization approach (Refs. [18, 30, 19, 21, 22]), each input is assumed to have the full system state available for feedback. Restricting each input to use a transformation of the full state vector generally makes the problem more difficult. In the case of composite systems, this is due to interactions between subsystems not being canceled. Thus, decentralized feedback linearization must focus on the observer problem as well as looking at specific classes of systems for which the problem may be solvable.

In this section, we concern ourselves with several methods for decentralized control of nonlinear systems which make use of the concept of feedback linearization. Our approach begins by considering the nonlinear observer problem (Refs. [35, 107, 36, 37, 34, 108, 38]) for a decentralized system. If just one input-output pair is successfully able to observe the full state then this channel could be used for linearization. The first approach we shall introduce is to close a subset of the input-output ports with output feedback and choose these output feedback functions such that the conditions

for solving the observer problem at one of the remaining open input-output channels are met.

Related to this problem is the decentralized controllability of the linearized system obtained upon successful feedback linearization. It is of interest to show that the linearized system, which is in Brunovsky canonical form [32], can be asymptotically stabilized via decentralized dynamic output feedback. That is, it is desired to show that this particular canonical form contains no decentralized fixed modes [82, 83, 68]. Thus, if the decentralized feedback linearization problem can be solved by one controller then the task of controlling the linearized system can be relegated to another controller.

The second approach we introduce, addresses the linearization and stabilization of coupled subsystems, each of which is nonlinear as well as the coupling terms. Each subsystem has its local state available for feedback. If the nonlinear subsystem can be linearized except for the coupling terms, then a suitably chosen local linear state feedback can exponentially stabilize not only the linearized subsystem but the composite system with the nonlinear interconnections as well. This assumes that the nonlinear interconnection terms satisfy some norm bounding assumptions.

Finally, we examine the issue of state space linearization of MIMO systems when the conditions for exact linearization are not satisfied. The approach followed is to utilize the same idea as in the observer problem of applying feedback at a subset of the input-output channels to enhance the linearizability of the remaining input-output pairs. These feedback functions are chosen such that the vector relative degree condition for single-input single-output (SISO) linearization is satisfied at the open input-output pair. Several examples are presented to demonstrate the method.

4.1.1 Problem Setup

We start by looking at nth order nonlinear systems with m inputs and m outputs both of the general

$$\dot{x} = f(x) + \sum_{i=1}^{m} g_i(x)u_i\,, \quad y_i = h_i(x)\,, \quad i = 1, \ldots, m \tag{4.1}$$

and interconnected subsystems variety

$$\dot{x}_i = \sum_{j=1}^{m} f_{ij}(x_j) + g_i(x_i)u_i\,, \quad y_i = h_i(x_i)\,, \quad i = 1, \ldots, m \tag{4.2}$$

where it is assumed that $f(x)$, $f_{ij}(x_j)$, and $g_i(x)$ are smooth vector fields and $h_i(x)$ are smooth functions defined on an open set of R^n. We seek control laws of the form $u_i = K_i(y_i, v_i)$, $i = 1, \ldots, m$ which will render the systems (4.1), (4.2) linear with a nonlinear change of coordinates. The v_i are external inputs available to control the

linearized system. In general, the output feedback functions K_i will be nonlinear, and we assume they are smooth. In the interconnected system case, we also allow for the possibility of local state feedback, i.e., $u_i = K_i(x_i, v_i)$, $i = 1, \ldots, m$. It is also assumed in this section that the individual input-output pairs (u_i, y_i) are SISO, though this is easily generalized to multivariable input-output channels.

The MIMO exact linearization problem has been solved in [19], and a key concept in the proof of this result is that of a vector relative degree. For a SISO nonlinear system the relative degree is the number of times one must differentiate the output until the input appears explicitly. For a MIMO nonlinear system the relative degree is a vector $\{r_1, \ldots, r_m\}$ wherein each r_i is the number of times one has to differentiate the ith output to have at least one of the m inputs appear explicitly. The conditions for the existence of this relative degree, defined about some point x^0, are stated in [21] and are not repeated here. The important point is that the state space exact linearization problem for (4.1) is solvable (about x^0) if and only if there exists some vector relative degree $\{r_1, \ldots, r_m\}$ at x^0 and $r_1 + r_2 + \cdots + r_m = n$.

If this relative degree condition is not satisfied and one has freedom to choose new output functions (say $y_i = \lambda_i(x)$) then there exist necessary and sufficient conditions to find these $\lambda_i(x)$ such that the relative degree condition is satisfied (see [21] for details). If none of these conditions are satisfied then the best that one can do is to linearize the input-output response provided that some relative degree does exist at a certain point. In this case the state space response cannot be completely linearized resulting in zero dynamics [27, 21]. We are primarily interested in full state space linearization whenever possible.

To explore the feasibility of decentralized feedback linearization of (4.1), we consider the following 2-input, 2-output, second-order nonlinear system

$$\begin{aligned} \begin{bmatrix} \dot{x}_1 \\ \dot{x}_2 \end{bmatrix} &= \begin{bmatrix} f_1(x) \\ f_2(x) \end{bmatrix} + \begin{bmatrix} g_{11}(x) \\ g_{12}(x) \end{bmatrix} u_1 + \begin{bmatrix} g_{21}(x) \\ g_{22}(x) \end{bmatrix} u_2 \\ y_1 &= h_1(x) \\ y_2 &= h_2(x). \end{aligned} \tag{4.3}$$

Our strategy here is to close the loop of u_1/y_1 with output feedback to enable the second input-output channel to perform the linearization. That is, we let $u_1 = K_1(y_1)$ thus obtaining

$$\begin{aligned} \begin{bmatrix} \dot{x}_1 \\ \dot{x}_2 \end{bmatrix} &= \begin{bmatrix} f_1(x) + g_{11}(x)K_1(y_1) \\ f_2(x) + g_{12}(x)K_1(y_1) \end{bmatrix} + \begin{bmatrix} g_{21}(x) \\ g_{22}(x) \end{bmatrix} u_2 \\ y_2 &= h_2(x) \end{aligned} \tag{4.4}$$

which is effectively a SISO nonlinear system. Note that this strategy of closing the loop at all but one of the I/O channels is a known tactic in the theory of linear decentralized control [109].

A SISO system has a relative degree r at a point x^0 if [21]

$$L_g L_f^k h(x) = 0 \tag{4.5}$$

for all x in a neighborhood of x^0 and all $k < r - 1$ and

$$L_g L_f^{r-1} h(x^0) \neq 0 \tag{4.6}$$

where $L_g h(x)$ is the Lie or directional derivative of $h(x)$ along $g(x)$ and is written as

$$L_g h(x) = \frac{\partial h}{\partial x} g(x) \tag{4.7}$$

and the iterated Lie derivative $L_g^k h(x)$ is written as

$$L_g^k h(x) = \frac{\partial (L_g^{k-1} h)}{\partial x} h(x) \tag{4.8}$$

with $L_g^0 h(x) = h(x)$.

From (4.4) we have

$$L_{g_2} h_2(x) = \frac{\partial h_2}{\partial x_1} g_{21}(x) + \frac{\partial h_2}{\partial x_2} g_{22}(x) \tag{4.9}$$

which will be nonzero for most systems. This implies a relative degree of $r = 1$ indicating that for most systems of the class (4.3) exact state space linearization will not be possible. If one desires to do input-output linearization the state feedback [19, 110]

$$u_2 = \frac{1}{L_{g_2} L_{\tilde{f}}^{r-1} h_2(x)} (-L_{\tilde{f}}^r h_2(x) + v_2) \tag{4.10}$$

transforms the nonlinear system (4.4) from u_2 to y_2 into the linear system $H(s) = \frac{1}{s^r}$ where $\tilde{f}$ is the vector field in (4.4) containing the feedback term $K_1(y_1)$ and v_2 is an external input to the u_2/y_2 port. For most general systems of the form (4.3), the linearizing u_2 above will depend on the full state x. In fact, for all but the most special cases of (4.3), there is no choice of feedback $K_1(y_1)$ that can allow the linearizing feedback u_2 to depend on y_2 only or even on x_2 only. This means that the nonlinear interconnections cannot be linearized via local feedback.

However, there are several approaches that can yield satisfactory results. One relies on estimating the state x for at least one input-output channel to allow the use of the above linearizing feedback. Furthermore, interconnected systems can be stabilized using feedback linearization and local state feedback. These approaches are detailed in this section as well as several other strategies to designing decentralized control laws for nonlinear systems.

4.1.2 Decentralized Nonlinear Observers

Consider the nonlinear multichannel system as given in (4.1). The *Decentralized Observer Problem* is to be able to generate the full system state at a minimum of one input-output channel (say j) using only local output measurements (y_j) and knowledge of the local input (u_j).

Consider the linear differential operator $\Psi_{\tilde{f},j}$ for channel j, defined as

$$\Psi_{\tilde{f},j}\frac{\partial h_j}{\partial x} = \frac{\partial h_j}{\partial x}\frac{\partial \tilde{f}}{\partial x} + \tilde{f}^T\frac{\partial}{\partial x}\left(\frac{\partial h_j}{\partial x}\right)^T + \dot{\bar{u}}_j{}^T\frac{\partial}{\partial \bar{u}_j}\left(\frac{\partial h_j}{\partial x}\right)^T \tag{4.11}$$

with $\Psi^0_{\tilde{f}}\frac{\partial h_j}{\partial x} = \frac{\partial h_j}{\partial x}$ and $\bar{u}_j = [u_j, \dot{u}_j, \ldots, u_j^{(n-1)}]^T$, is repeatedly applied to the gradient $\frac{\partial h_j}{\partial x}$. The vector $\tilde{f}$ denotes the right hand side of (4.1), that is, $\tilde{f} = f(x) + \sum_{i=1}^m g_i(x)u_i$. Now define the jth channel observability matrix

$$Q_j(x, \bar{u}_j) = \begin{bmatrix} \Psi^0_{\tilde{f},j} \\ \Psi_{\tilde{f},j} \\ \vdots \\ \Psi^{n-1}_{\tilde{f},j} \end{bmatrix} \frac{\partial h_j}{\partial x}. \tag{4.12}$$

The following statement is proposed as a basis for solving the Decentralized Observer Problem and is illustrated in Fig. 15.

Proposition 4.1 *The Decentralized Observer Problem can be solved for channel j if there exists an index set $\Gamma \subset \{1, \ldots, m\}$ and a channel $j \notin \Gamma$ and a set of output feedback functions, $\{K_i(y_i)\}$, $i \in \Gamma$ such that $Q_j(\tilde{x}, \bar{u}_j)$ is of full rank. The state $\tilde{x}$ is defined by the system*

$$\begin{aligned} \dot{\tilde{x}} &= f(\tilde{x}) + \sum_{i\in\Gamma} g_i(\tilde{x})K_i(y_i) + g_j(\tilde{x})u_j \\ y_j &= h_j(\tilde{x}). \end{aligned} \tag{4.13}$$

The proof of Proposition 4.1 is a direct extension of the following lemma found in [38].

Lemma 4.1 *The SISO observer linearization problem for $\dot{x} = f(x, u)$, $y = h(x, u)$ with output injection is solvable in a neighborhood of the point x^0 if and only if the $n \times n$ matrix*

$$Q(x, \bar{u}) = \begin{bmatrix} \Psi^0_f \\ \Psi_f \\ \vdots \\ \Psi^{n-1}_f \end{bmatrix} \frac{\partial h}{\partial x} \tag{4.14}$$

has full rank in a neighborhood of x^0.

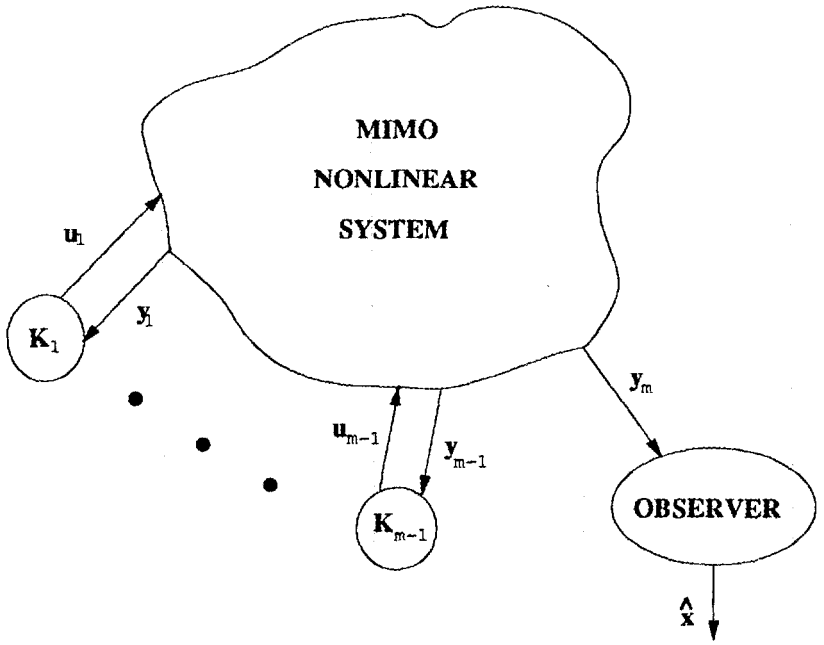

Fig. 15: Decentralized strategy to observer design.

To see how Proposition 4.1 is applied, consider the two-input, two-output, nth order nonlinear system

$$\begin{aligned} \dot{x} &= f(x) + g_1(x)u_1 + g_2(x)u_2 \\ y_1 &= h_1(x) \\ y_2 &= h_2(x). \end{aligned} \tag{4.15}$$

To solve the Decentralized Observer Problem, let $u_1 = K_1(y_1)$ (note that either I/O channel can be used for feedback) and obtain

$$\begin{aligned} \dot{\tilde{x}} &= f(\tilde{x}) + g_1(\tilde{x})K_1(y_1) + g_2(\tilde{x})u_2 \\ y_2 &= h_2(\tilde{x}) \,. \end{aligned} \tag{4.16}$$

Finding the solvability conditions for (4.16) utilizing Proposition 4.1 and Lemma 4.1 simply involves substituting $h_2(\tilde{x})$ for $h(x,u)$ and $f(\tilde{x}) + g_1(\tilde{x})K_1(y_1) + g_2(\tilde{x})u_2$ for $f(x,u)$ respectively into the matrix $Q(x,\bar{u})$.

Remark 4.1 If the SISO observer problem is solvable at one or both input-output channels without any input-output feedback (i.e., $K_i(y_i) = 0$) then one does not need to close the loop at the remaining input-output channel. Thus, we are interested in problems that are not *a priori* solvable.

Remark 4.2 In the linear case, if the centralized observability rank condition is satisfied before linear output feedback is applied then almost any output feedback gain will suffice provided that it does not cancel a pole of the A matrix.

Remark 4.3 The actual construction of the observer utilized in Ref. [38] is omitted here since the same steps can be followed for the above. The approach utilized in Ref. [38] relies on the concept of extended linearization to linearize the transformed system about the reconstructed state. The observer has the features of being dimensioned by an eigenvalue assignment without solving partial differential equations (as in Refs. [36, 37]), and it does take into account the input term of the original system.

Once the observer is constructed, the estimated state can then be utilized in whatever capacity the control designer wishes. In particular, we are interested in the possibility of feedback linearization at this chosen input-output channel. Since the observer is constructed strictly by decentralized means, then this would constitute a method of decentralized feedback linearization. The following theorem states the conditions under which this is possible.

Theorem 4.1 *The nonlinear system (4.1) can be rendered linear via decentralized feedback at some channel j if*

1. *the Decentralized Observer Problem can be solved for channel j and*
2. *the system (4.13) is state space linearizable.*

Proof: The solution of the Decentralized Observer Problem makes the full system state available at channel j by the use of purely local signals. The observer construction of Ref. [38] involves a transformation into observer canonical form which is a one-to-one mapping and thus preserves the linearizability properties of the original system. Therefore, if (4.13) is feedback linearizable then the transformed system after observer construction will also be feedback linearizable. Then, (4.13) can be feedback linearized with the observer state. □

Example 4.1 Consider the following third-order, two-input, two-output system

$$\begin{aligned} \dot{x} &= \begin{bmatrix} x_1^2 + x_2 \\ e^{-x_2} \\ x_2^2 \end{bmatrix} + \begin{bmatrix} 0 \\ x_2 \\ 0 \end{bmatrix} u_1 + \begin{bmatrix} x_1 \\ 0 \\ 0 \end{bmatrix} u_2 \\ y_1 &= \begin{bmatrix} 1 & 0 & 0 \end{bmatrix} x\,, \quad y_2 = \begin{bmatrix} 0 & 0 & 1 \end{bmatrix} x\,. \end{aligned} \tag{4.17}$$

Now we let $u_1 = K_1(y_1)$ which results in the new SISO system

$$\begin{aligned} \dot{\tilde{x}} &= \begin{bmatrix} x_1^2 + x_2 \\ e^{-x_2} + x_2 K_1(y_1) \\ x_2^2 \end{bmatrix} + \begin{bmatrix} x_1 \\ 0 \\ 0 \end{bmatrix} u_2 \\ y_2 &= \begin{bmatrix} 0 & 0 & 1 \end{bmatrix} \tilde{x}\,. \end{aligned} \tag{4.18}$$

Applying the definition of $Q_2(x, \bar{u}_2)$ in (4.12), we obtain

$$Q_2(\tilde{x}, \bar{u}_2) = \begin{bmatrix} 0 & 0 & 1 \\ 0 & 2x_2 & 0 \\ 2x_2^2 \frac{\partial K_1}{\partial y_1} & -2x_2 e^{-x_2} + K_1(y_1) & 0 \end{bmatrix} \tag{4.19}$$

which has full rank if and only if

$$2x_2^3 \frac{\partial K_1}{\partial y_1} \neq 0 \,. \tag{4.20}$$

Thus, the extended Luenberger observer of [38] can be constructed for (4.18) about any point x^0 such that $x_2^0 \neq 0$ and $\frac{\partial K_1}{\partial y_1} \neq 0$. Of the infinitely many possible solutions for $K_1(y_1)$, the simplest is $u_1 = K_1(y_1) = y_1$. With this choice of output feedback at the u_1/y_1 pair, the full state x is observable at the u_2/y_2 pair via the observer construction of Ref. [38]. It is also easily shown that for the above choice of $K_1(y_1)$, the relative degree of the u_2/y_2 pair is $r = n = 3$. Hence, from Theorem 4.1, the system (4.18) is state space linearizable via decentralized feedback. That is, the input u_1 depends only on y_1, and the observer constructed at the u_2/y_2 pair will depend only on the output y_2.

4.1.3 Decentralized Control of the Linearized System

We will assume in this subsection that a centralized or decentralized control strategy has succeeded in linearizing the system and focus on a decentralized control strategy for the linearized system. We assume that the vector relative degree of (4.1), (4.2) is such that $r_1 + r_2 + \cdots + r_m = n$ or that output functions can be found to achieve this.

The linearized system is linear with respect to a nonlinear change in coordinates $z = \Phi(x)$. This coordinate transformation consists of the set of functions [19]

$$\phi_j^i(x) = L_f^{j-1} h_i(x) \,, \quad 1 \leq j \leq r_i \,, \quad 1 \leq i \leq m \tag{4.21}$$

where

$$\Phi(x) = \left[\phi_1^1(x), \cdots, \phi_{r_1}^1(x), \cdots, \phi_1^m(x), \cdots, \phi_{r_m}^m(x)\right]^T \,. \tag{4.22}$$

The state feedback required to perform the linearization (though it may consist of the observed state) will always have the form

$$u = \alpha(x) + \beta(x) v \tag{4.23}$$

where u and v are the control and external input vectors respectively. The linearized system is such that

$$\left[\frac{\partial \Phi}{\partial x}(f(x)+g(x)\alpha(x))\right]_{x=\Phi^{-1}(z)} = Az \tag{4.24}$$

$$\left[\frac{\partial \Phi}{\partial x}(g(x)\beta(x)v)\right]_{x=\Phi^{-1}(z)} = Bv \tag{4.25}$$

where (A, B) are in the Brunovsky canonical form [32, 19, 21]. In these new coordinates the linearized system has the form

$$\begin{bmatrix} \dot{z}^1 \\ \dot{z}^2 \\ \vdots \\ \dot{z}^m \end{bmatrix} = \begin{bmatrix} A_1 & 0 & \cdots & 0 \\ 0 & A_2 & \cdots & 0 \\ \vdots & \vdots & \ddots & \vdots \\ 0 & 0 & \cdots & A_m \end{bmatrix} \begin{bmatrix} \dot{z}^1 \\ \dot{z}^2 \\ \vdots \\ \dot{z}^m \end{bmatrix} + \begin{bmatrix} b_1 & 0 & \cdots & 0 \\ 0 & b_2 & \cdots & 0 \\ \vdots & \vdots & \ddots & \vdots \\ 0 & 0 & \cdots & b_m \end{bmatrix} \begin{bmatrix} v_1 \\ v_2 \\ \vdots \\ v_m \end{bmatrix} \tag{4.26}$$

$$\begin{bmatrix} y_1 \\ y_2 \\ \vdots \\ y_m \end{bmatrix} = \begin{bmatrix} c_1 & 0 & \cdots & 0 \\ 0 & c_2 & \cdots & 0 \\ \vdots & \vdots & \ddots & \vdots \\ 0 & 0 & \cdots & c_m \end{bmatrix} \begin{bmatrix} z^1 \\ z^2 \\ \vdots \\ z^m \end{bmatrix} \tag{4.27}$$

where A_i is the r_ixr_i matrix

$$A_i = \begin{bmatrix} 0 & 1 & 0 & \cdots & 0 \\ 0 & 0 & 1 & \cdots & 0 \\ \vdots & \vdots & \vdots & \ddots & \vdots \\ 0 & 0 & 0 & \cdots & 1 \\ 0 & 0 & 0 & \cdots & 0 \end{bmatrix} \tag{4.28}$$

b_i, c_i, and z^i are the r_ix1 vectors

$$b_i = \begin{bmatrix} 0 \\ 0 \\ \vdots \\ 1 \end{bmatrix}, \quad c_i = \begin{bmatrix} 1 & 0 & \cdots & 0 \end{bmatrix}, \quad z^i = \begin{bmatrix} z_1^i \\ z_2^i \\ \vdots \\ z_{r_i}^i \end{bmatrix} \tag{4.29}$$

and v_i, $i = 1, \ldots, m$, are the m inputs to the linearized system.

The above linear system is decoupled in the sense that the ith output depends only on the ith input. We can see this more clearly by viewing the transfer matrix of the system

$$Y_i(s) = \frac{1}{s^{r_i}} V_i(s), \quad i = 1, \ldots, m \tag{4.30}$$

which is just m chains of r_i integrators each. In fact, the linearizing feedback law (4.23) also solves the noninteracting control problem (input-output decoupling) [33]. Our goal is to control this system via m decentralized control laws. The primary issue of concern in such a control strategy is that of decentralized fixed modes. A decentralized fixed mode [82, 83, 68] is an eigenvalue of the open loop system that is invariant under static output feedback. To determine the existence of fixed modes in the above system, we consider the following decentralized control laws

$$v_i = K_i y_i \ , \quad i = 1, \ldots, m \tag{4.31}$$

where K_i is a scalar real number. We now state the following theorem.

Theorem 4.2 *The linearized system (4.26),(4.27) has no decentralized fixed modes and can be asymptotically stabilized via the following decentralized dynamic output feedback*

$$\begin{aligned} v_i &= H_i \tilde{x}_i + K_i y_i \\ \dot{\tilde{x}}_i &= F_i \tilde{x}_i + S_i y_i \ , \quad i = 1, \ldots, m. \end{aligned} \tag{4.32}$$

Proof: The eigenvalues of the closed loop matrix $A + BKC$ are the n solutions to the equation

$$\lambda^{r_i} - K_i = 0 \ , \quad i = 1, \ldots, m \tag{4.33}$$

which implies that all the eigenvalues lie on a circle in the complex plane. Thus, there are no decentralized fixed modes. It is also true that the above system cannot be stabilized through static decentralized output feedback since at least some eigenvalues will always be in the right half plane or on the $j\omega$ axis. The exception is if all $r_i = 1$ then the eigenvalues can be placed in the left half plane via static or dynamic decentralized output feedback. A theorem in Ref. [68] states that if all fixed modes lie in the open left half plane then dynamic decentralized output feedback will asymptotically stabilize the system. Hence, for the above linear system the control law (4.32) will achieve the desired result. □

The feedback law (4.32) consists of m local output feedback laws each with its own dynamic compensator, and $\tilde{x}$ is the state of the dynamic compensator. With (4.32) as the control law, one obtains an augmented closed loop matrix which we can asymptotically stabilize. The specific design of this dynamic feedback is omitted, and the reader is referred to Ref. [68] for more details. The important point here is that the linearization can be relegated to one controller, and the decentralized stabilization of the resulting linearized system can be relegated to a different set of controllers. Figure 16 demonstrates this approach.

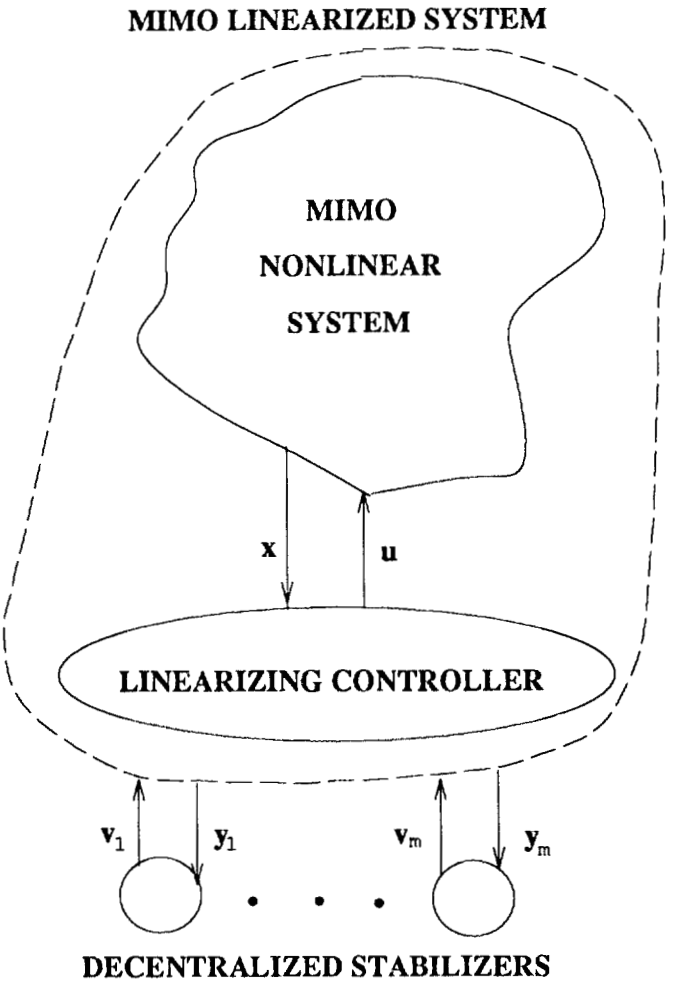

Fig. 16: Multi-level approach to linearization and stabilization.

4.1.4 Stabilization of Interconnected Subsystems

In this subsection, we consider nonlinear interconnected subsystems of the form (4.2) where $x_i \in R^{n_i}$ and u_i and y_i are scalars. Each subsystem has its own input and output (i.e., SISO subsystems) with the outputs depending on the local state only. Our strategy is to linearize each subsystem (ignoring the coupling terms) using only the local state for feedback. Then each subsystem will employ local state feedback (in the linearizing coordinates) to achieve a prescribed degree of exponential stability γ for the full system. The coupling terms must satisfy a norm-bounding inequality for the strategy to succeed. This is a decentralized control strategy because each input requires only the state available at its own subsystem. Earlier work on stabilizing linear large-scale systems appears in Refs. [69, 111]. To achieve this control strategy, we make the following assumption.

Assumption 4.1 The relative degree of the ith subsystem (ignoring the coupling terms) is n_i with respect to the output $y_i = h_i(x_i)$.

Theorem 4.3 *The interconnected system model (4.2), under Assumption 4.1, can be exponentially stabilized to prescribed degree γ in the linearizing coordinates provided the coupling terms*

$$e_i(x) = \left[\frac{\partial \Phi_i}{\partial x_i} \sum_{j=1, j\neq i}^{m} f_{ij}(x_j) \right] \tag{4.34}$$

satisfy the inequality

$$\| e_i(x) \| \leq \sum_{j=1}^{m} \sigma_{ij} \| \Phi_i(x_i) \| , \quad i = 1, \ldots, m \tag{4.35}$$

for all $x_i \in R^{n_i}$, for some nonnegative σ_{ij}, where $\Phi_i(x_i)$ is the linearizing coordinate transformation of the ith subsystem.

Proof: We begin by employing the SISO linearizing feedback. That is,

$$\begin{aligned} u_i &= \frac{-L_{f_{ii}}^{n_i} h_i(x_i)}{L_{g_i} L_{f_{ii}}^{n_i-1} h_i(x_i)} + \frac{1}{L_{g_i} L_{f_{ii}}^{n_i-1} h_i(x_i)} v_i \\ &= \alpha_i(x_i) + \beta_i(x_i) v_i , \quad i = 1, \ldots, m \end{aligned} \tag{4.36}$$

where v_i is our new input. Next, we construct the linearizing coordinates

$$z_i = \Phi_i(x_i) = \begin{bmatrix} h_i(x_i) \\ L_{f_{ii}} h_i(x_i) \\ \vdots \\ L_{f_{ii}}^{n_i-1} h_i(x_i) \end{bmatrix} , \tag{4.37}$$

$i = 1, \ldots, m$. Utilizing Assumption 4.1, we obtain [21]

$$\left[\frac{\partial \Phi_i}{\partial x_i}(f_{ii}(x_i) + g_i(x_i)\alpha_i(x_i))\right] = A_{ii}z_i \tag{4.38}$$

$$\left[\frac{\partial \Phi_i}{\partial x_i}(g_i(x_i)\beta_i(x_i)v_i)\right] = B_i v_i \tag{4.39}$$

with $x_i = \Phi_i^{-1}(z_i)$. This gives us in the new coordinates

$$\begin{aligned} \dot{z}_i &= A_{ii}z_i + B_i v_i + \left[\frac{\partial \Phi_i}{\partial x_i} \sum_{j=1, j\neq i}^{m} f_{ij}(x_j)\right]_{x_i = \Phi_i^{-1}(z_i)} \\ y_i &= C_i z_i\,, \quad i = 1, \ldots, m \end{aligned} \tag{4.40}$$

where A_{ii}, B_i, and C_i are in the Brunovsky canonical form [32], and the above system is completely controllable and completely observable. For convenience we shall refer to the nonlinear interaction term as $e_i(z)$ where z is the full system state vector.

Consider now the system (4.40) with no interaction term (i.e., $e_i(z) = 0$). It is well known [95] that this linear subsystem can be exponentially stabilized by a prescribed degree γ (that is, $z_i(t)\exp(-\gamma t) \to 0$ as $t \to \infty$) by the feedback

$$v_i = -B_i^T K_i z_i \tag{4.41}$$

where K_i is the $n_i \times n_i$ symmetric positive-definite solution of the algebraic Riccati equation (ARE)

$$(A_{ii} + \gamma I_i)^T K_i + K_i(A_{ii} + \gamma I_i) - K_i S_i K_i + Q_i = 0 \tag{4.42}$$

where $S_i = B_i B_i^T$, $Q_i = C_i^T C_i$, and I_i is the $n_i \times n_i$ identity matrix. Then the closed loop subsystem

$$\dot{z}_i = (A_i - S_i K_i)z_i\,, \quad i = 1, \ldots, m \tag{4.43}$$

is exponentially stable with prescribed degree γ. The following result found in Refs. [69, 111] will help us in our proof.

Lemma 4.2 *If the coupling terms $e_i(z)$ satisfy the inequality*

$$\| e_i(z) \| \leq \sum_{j=1}^{m} \sigma_{ij} \| z_i \|\,, \quad i = 1, \ldots, m \tag{4.44}$$

for all $z_i \in R^{n_i}$, where $\sigma_{ij} \geq 0$ and if $\sigma = \sum_{i=1}^{m}\sum_{j=1}^{m} \sigma_{ij}$ satisfy

$$\min_i\,(\lambda_{min}(P_i)) \geq 2\sigma \max_i\,(\lambda_{max}(K_i)) \tag{4.45}$$

where $P_i = Q_i + K_i S_i K_i$ *for* $i = 1, \ldots, m$ *and* $\|\cdot\|$ *is the usual Euclidean vector norm then each subsystem*

$$\dot{z}_i = (A_i - S_i K_i) z_i + e_i(z) \tag{4.46}$$

is exponentially stable with degree γ.

The result in Theorem 4.3 follows by setting $z_i = \Phi_i(x_i)$ in the above lemma. Lemma 4.2 also provides a means for determining the σ_{ij}. □

Remark 4.4 Theorem 4.3 provides a composite control strategy for nonlinear interconnected subsystems. This strategy combines feedback linearization with linear quadratic control to partially linearize and exponentially stabilize the system subject to the stated assumptions. It should be noted that the interconnection nonlinearity $e_i(z)$ can depend explicitly on time t with the above result still valid. Also note that even if the coupling terms in (4.2) were linear, the interaction effects in $e_i(z)$ will still be nonlinear due to the change in coordinates.

Remark 4.5 If one assumes weak interactions (i.e., ϵ-coupling) and a shortcoming in relative degree ($r_i < n_i$) then one can get perturbations in the zero dynamics for sufficiently small ϵ. That is, for $\epsilon = 0$, the only zero dynamics obtained are related to the insufficient relative degree. The zero dynamics that disappear for $\epsilon = 0$ are related to the coupling terms. The next subsection contains a derivation of these zero dynamics and shows under what zeroing inputs and initial conditions they can be obtained. Similar results already exist (see Ref. [112]) in which it is shown that the zero dynamics of a regularly perturbed SISO nonlinear system is singularly perturbed.

Remark 4.6 This result differs from most other decentralized stabilization schemes in that others assume either linear interactions or linear subsystems or both. The primary issues of concern in this result are the ability to satisfy the relative degree assumption and the interaction inequality assumption. The next subsection deals with the issue of insufficient relative degree. The norm bounding assumption on the coupling terms will be easy to satisfy for weakly-coupled systems but more difficult to satisfy for strongly-coupled systems. Thus, applications involving weak coupling (e.g., chemical processes, space structures, power systems) may be more amenable to the methodology of this subsection than strongly-coupled systems.

4.1.5 Weakly Coupled Systems

In this subsection, we derive the zero dynamics equations and the conditions governing their existence for weakly-coupled nonlinear systems. For ease in notation, we consider the two-channel weakly-coupled nonlinear system

$$\begin{aligned} \dot{x}_1 &= f_1(x_1) + g_1(x_1)u_1 + \epsilon f_{12}(x_2),\ y_1 = h_1(x_1) \\ \dot{x}_2 &= f_2(x_2) + g_2(x_2)u_2 + \epsilon f_{21}(x_1),\ y_2 = h_2(x_2) \end{aligned} \tag{4.47}$$

where ϵ is a small positive constant representing strength of coupling between the subsystems. To derive the system's zero dynamics, we first put the system into normal form using the local coordinates transformation utilized in the proof of Theorem 4.3. We also relax the relative degree requirements and let $r_i < n_i$. The new coordinates are

$$z_i = \begin{bmatrix} h_i(x_i) \\ L_{f_i}h_i(x_i) \\ \vdots \\ L_{f_i}^{r_i-1}h_i(x_i) \\ \phi_{r_i+1}(x_i) \\ \vdots \\ \phi_{n_i}(x_i) \end{bmatrix} = \Phi_i(x_i) \tag{4.48}$$

where $\phi_i(x_i)$ are chosen such that $L_{g_i}\phi_i(x_i) = 0$.

From these new coordinates, we get the following normal form

$$\begin{aligned}
\dot{z}_{i1} &= z_{i2} + \epsilon\frac{\partial h_i}{\partial x_i}f_{ij}(x_j) \\
\dot{z}_{i2} &= z_{i3} + \epsilon\frac{\partial L_{f_i}h_i(x_i)}{\partial x_i}f_{ij}(x_j) \\
&\vdots \\
\dot{z}_{i,r_i-1} &= z_{i,r_i} + \epsilon\frac{\partial L_{f_i}^{r_i-2}h_i(x_i)}{\partial x_i}f_{ij}(x_j) \\
\dot{z}_{i,r_i} &= L_{f_i}^{r_i}h_i(x_i) + L_{g_i}L_{f_i}^{r_i-1}h_i(x_i)u_i + \\
&\quad \epsilon\frac{\partial L_{f_i}^{r_i-1}h_i(x_i)}{\partial x_i}f_{ij}(x_j) \\
\dot{z}_{i,r_i+1} &= L_{f_i}\phi_{r_i+1}(x_i) + \epsilon\frac{\partial \phi_{r_i+1}}{\partial x_i}f_{ij}(x_j) \\
&\vdots \\
\dot{z}_{i,n_i} &= L_{f_i}\phi_{n_i}(x_i) + \epsilon\frac{\partial \phi_{n_i}}{\partial x_i}f_{ij}(x_j) \\
y_i &= z_{i1}\,.
\end{aligned} \tag{4.49}$$

To determine the system's zero dynamics, we require $y_i(t) = 0$ for all time. This implies the following constraint equations

$$z_{i1} = 0 \Rightarrow \dot{z}_{i1} = 0 \Rightarrow z_{12} + \epsilon\frac{\partial h_i}{\partial x_i}f_{ij}(x_j) = 0\,. \tag{4.50}$$

At this point we make the assumption that the output functions are linear in x_i. This is reasonable since one often assumes the local state is measurable in complex systems

such as (4.47). Now we differentiate further to get a condition on the input functions to zero the output. The inputs must satisfy

$$u_i^0 = \frac{1}{\frac{\partial h_j}{\partial x_j}\frac{\partial f_{ji}}{\partial x_i} g_i(x_i)}[-\frac{\partial h_j}{\partial x_j}\frac{\partial f_{ji}}{\partial x_i} f_i(x_i) - \tag{4.51}$$

$$\epsilon\frac{\partial h_j}{\partial x_j}\frac{\partial f_{ji}}{\partial x_i} f_{ij}(x_j)], \quad i,j = 1,2, \ i \neq j \tag{4.52}$$

for all time. The initial conditions must satisfy

$$z_{i1}^0 = 0 \tag{4.53}$$

$$z_{i2}^0 = -\epsilon\frac{\partial h_i(x_i)}{\partial x_i} f_{ij}(x_j) \tag{4.54}$$

with the rest of the initial conditions chosen arbitrarily. The zero dynamics are then

$$\begin{aligned}
\dot{z}_{i2} &= z_{i3} + \epsilon\frac{\partial L_{f_i} h_i(x_i)}{\partial x_i} f_{ij}(x_j) \\
&\vdots \\
\dot{z}_{i,r_i-1} &= z_{i,r_i} + \epsilon\frac{\partial L_{f_i}^{r_i-2} h_i(x_i)}{\partial x_i} f_{ij}(x_j) \\
\dot{z}_{i,r_i} &= a_i(z_i) + b_i(z_i)u_i^0 + \epsilon\frac{\partial L_{f_i}^{r_i-1} h_i(x_i)}{\partial x_i} f_{ij}(x_j) \\
\dot{z}_{i,r_i+1} &= p_{i1}(z_i) + \epsilon q_{i1}(z_i) \\
&\vdots \\
\dot{z}_{i,n_i} &= p_{i,n_i-r_i}(z_i) + \epsilon q_{i,n_i-r_i}(z_i)
\end{aligned} \tag{4.55}$$

subject to the above initial conditions and zeroing input.

Remark 4.7 The dimension of the zero dynamics is $n_i - 1$ for each subsystem. However if $\epsilon = 0$, the dimension reduces to $n_i - r_i$. Thus, the order of the zero dynamics is perturbed by the coupling parameter ϵ. Each subsystem has its own zero dynamics, thus this represents a limitation in feedback linearization using decentralized control. That is, even if $r_i = n_i$ one still cannot exactly linearize the subsystems for nonzero ϵ using local state feedback.

4.1.6 Relative Degree Enhancement of Multichannel Systems

The MIMO linearization problem requires the system's vector relative degree (sometimes called characteristic numbers) to be satisfied such that $r_1 + \cdots + r_m = n$. Then

the standard MIMO linearizing feedback (see Ref. [21] for details) can be chosen to exactly linearize the state space as well as the input-output relationship in appropriately chosen coordinates. In this section, we're interested in systems of the form (4.1) that do not satisfy this relative degree condition. It has been shown [21] that this vector relative degree condition is necessary and sufficient for exact state space linearization. Our approach, however, is to transform the MIMO system to a SISO system via state feedback at all but one of the input-output pairs. The feedback functions are chosen to satisfy the necessary conditions to achieve the proper relative degree for the SISO linearization problem.

We present two examples of multi-input systems that are not feedback linearizable in a MIMO sense, but with our method they can be linearized in a SISO sense. It should be noted that the idea of feedback to all but one input/output channel to enhance some property (e.g., controllability, observability, etc.) from the standpoint of the remaining input/output channel is well known in decentralized control for linear subsystems (see Ref. [109]).

The method takes systems of the form (4.1) for which linearization is desired and transforms them to SISO systems via state feedback. The principle is as follows. Choose feedback functions $u_i = K_i(x)$, $i = 1, \ldots, m-1$ such that the SISO relative degree of the mth output channel is equal to n. We formally state this as follows.

Definition 4.1 The *Feedback Linearization Enhancement Problem* for (4.1) is to find feedback functions $u_i = K_i(x)$, Γ is the index set of all such i, $\Gamma \subset \{1, \ldots, m\}$, such that the SISO system

$$\dot{x} = f(x) + \sum_{i \in \Gamma} g_i(x) K_i(x) + g_j(x) u_j \,, \quad y_j = h_j(x) \tag{4.56}$$

has relative degree $r = n$ about some point x^0 for at least one $j \notin \Gamma$.

Remark 4.8 The above problem seeks to linearize the input-state response and the input-output response with respect to the jth input-output pair in a neighborhood of x^0. Thus, the input-output responses at the other $m-1$ input-output pairs will remain nonlinear in the linearizing coordinates. Presumably one would choose the jth input-output pair to be the channel of most interest to the designer. That is, one may wish for one particular input-output response to be linearized while the others are employing state feedback to enable this linearization. This structure is illustrated in Fig. 17.

The main idea behind the solution of the problem is to choose the feedback functions $K_i(x)$ to solve the partial differential equations (4.5), (4.6). One normally would only attempt to solve this problem if the MIMO exact linearization problem is not solvable. If the vector relative degree condition for state space linearization is met then one can obtain linearization of all input-output pairs via the MIMO linearizing

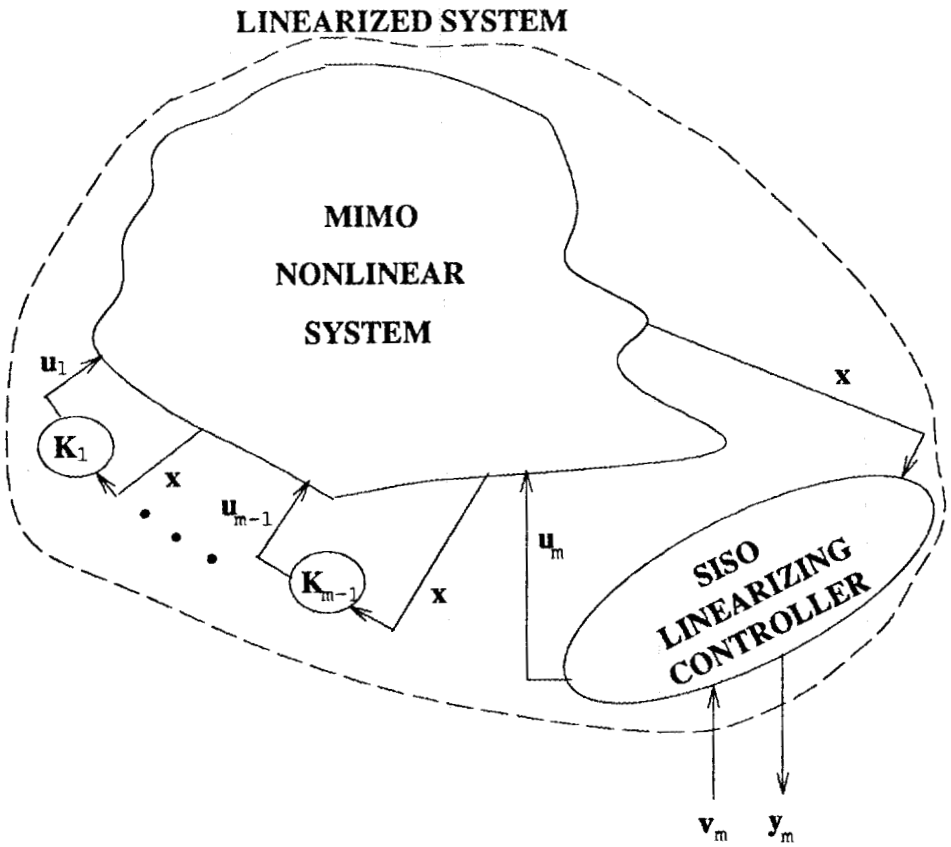

Fig. 17: Illustration of the feedback method for linearization.

feedback (see [21]). The following theorem states the conditions for solvability of the feedback linearization enhancement problem.

Theorem 4.4 *Necessary conditions for the solvability of the Feedback Linearization Enhancement Problem for (4.1) ($n > 1$) are:*
i.) there must exist at least one $i \in \{1, \ldots, m\}$ such that $L_{g_i} h_i = 0$.
ii.) for at least one of these i, there must exist at least one $j \in \{1, \ldots, m\}, j \neq i$ such that $L_{g_j} h_i \neq 0$.

Proof: Consider the system (4.1). Without loss of generality, choose $i = m$ as the open input-output channel. We then obtain the equivalent SISO system

$$\dot{x} = f(x) + \sum_{j=1}^{m-1} g_j(x) K_j(x) + g_m(x) u_m \,, \quad y_m = h_m(x) \,. \tag{4.57}$$

Unless the system is first order (which is unrealistic for a MIMO system), the relative degree conditions for state space linearization require $L_{g_m} h_m = 0$. This would have to be the case for any $i \in \{1, \ldots, m\}$ one would wish to choose as the open input-output channel. If not the case, then no feedback functions, $K_i(x)$, can enhance the relative degree since $r = 1$ in this case. This proves condition i.) is necessary.

Assuming condition i.) is true (with $i = m$), we continue to the function $L_{\tilde{f}} h_m$ where

$$\tilde{f}(x) = f(x) + g_1(x)K_1(x) + \cdots + g_{m-1}(x)K_{m-1}(x)\,. \tag{4.58}$$

Again, assuming that the relative degree of the mth input-output channel is insufficient, we require that at least one $K_i(x)$ be able to satisfy the relative degree conditions. That is, we require $L_{\tilde{f}} h_m \neq 0$. This implies $L_f h_m + \sum_{j=1}^{m-1} (L_{g_j} h_m) K_j \neq 0$. From this it can be seen that at least one $j \in \{1, \ldots, m-1\}$ must exist such that $L_{g_j} h_m \neq 0$ otherwise no K_j will be available to enhance the relative degree. This shows that condition ii.) is necessary. □

Remark 4.9 The necessary conditions in the above theorem are easy to check on most systems, however they are not sufficient. The above theorem is meant to eliminate classes of systems for which the method would prove fruitless. The problem of relative degree enhancement is most effectively demonstrated by example.

Example 4.2 Consider the following third-order nonlinear system

$$\dot{x} = \begin{bmatrix} \sin x_1 + x_2^3 \\ x_2^2 + e^{-x_3} \\ x_1^2 + x_3 \end{bmatrix} + \begin{bmatrix} x_1 \\ 0 \\ 1 \end{bmatrix} u_1 + \begin{bmatrix} 1 \\ 0 \\ 0 \end{bmatrix} u_2\,, \quad y_1 = x_1\,, \quad y_2 = x_3\,. \tag{4.59}$$

A check of this system's relative degree yields $r_1 = 1$ and $r_2 = 1$ which is not sufficient for the MIMO feedback linearization problem to be solvable. However, $L_{g_2} h_2 = 0$, thus let $u_1 = K_1(x)$. This results in the new SISO system

$$\dot{x} = \begin{bmatrix} \sin x_1 + x_2^3 + x_1 K_1(x) \\ x_1^2 + e^{-x^3} \\ x_1^2 + x_3 + K_1(x) \end{bmatrix} + \begin{bmatrix} 1 \\ 0 \\ 0 \end{bmatrix} u_2\,, \quad y_2 = x_3 \tag{4.60}$$

where $\tilde{g} = \begin{bmatrix} 1 & 0 & 0 \end{bmatrix}^T$ and $\tilde{h} = x_3$.

Since $L_{\tilde{g}} \tilde{h} = 0$, we proceed to the next step of the SISO relative degree definition which requires

$$L_{\tilde{g}} L_{\tilde{f}} \tilde{h} = 2x_1 + \frac{\partial K_1}{\partial x_1} = 0\,. \tag{4.61}$$

This can be satisfied by letting $K_1(x) = -x_1^2 + K_1'(x_2, x_3)$. Finally, we require

$$L_{\tilde{g}} L_{\tilde{f}}^2 \tilde{h} = 2x_1 \frac{\partial K_1'}{\partial x_2} \neq 0 \tag{4.62}$$

which can be solved with (among infinitely many solutions) $K_1'(x_2, x_3) = e^{-x_2}$. This results in the feedback function

$$K_1(x) = -x_1^2 + e^{-x_2} \,. \tag{4.63}$$

Substituting (4.63) into (4.60) does indeed yield $r = n = 3$ as required. Furthermore, the point x^0 about which this result holds is any (x_1^0, x_2^0, x_3^0) such that $x_1^0 \neq 0$.

Remark 4.10 The above example shows that the feedback function $K_i(x)$ that solves the problem (if one exists) is far from unique. One may have a great deal of freedom to choose feedback functions that are easier to compute or require only readily available states. For instance, in the above example, one could have chosen $K_1' = x_2$ which is less expensive to compute than an exponential in a real-time control situation. However, one would then have to impose $x_2^0 \neq 0$ as an additional requirement on the operating point x^0.

Example 4.3 Next, consider the fourth-order system

$$\dot{x} = \begin{bmatrix} x_1^3 + x_2 \\ x_2 x_3 + x_4^2 \\ x_1 + x_2 + x_1 x_4 \\ x_1^2 + x_3 x_4 \end{bmatrix} + \begin{bmatrix} 0 \\ x_2 \\ 1 \\ 0 \end{bmatrix} u_1 + \begin{bmatrix} 0 \\ 0 \\ 0 \\ 1 \end{bmatrix} u_2 \,, \quad y_1 = x_1 \,, \quad y_2 = x_3 \,. \tag{4.64}$$

Determination of the system's vector relative degree yields $r_1 = 2$ and $r_2 = 1$, but the input-output decoupling matrix as defined in Ref. [21] is singular. Thus, this system has no relative degree, and the state space response cannot be exactly linearized. However, $L_{g_i} h_i = 0$ for $i = 1, 2$. We choose to let $u_1 = K_1(x)$ which results in the SISO system

$$\dot{x} = \begin{bmatrix} x_1^3 + x_2 \\ x_2 x_3 + x_4^2 + x_2 K_1(x) \\ x_1 + x_2 + x_1 x_4 + K_1(x) \\ x_1^2 + x_3 x_4 \end{bmatrix} + \begin{bmatrix} 0 \\ 0 \\ 0 \\ 1 \end{bmatrix} u_2 \,, \quad y_2 = x_3 \tag{4.65}$$

where $\tilde{g} = \begin{bmatrix} 0 & 0 & 0 & 1 \end{bmatrix}^T$ and $\tilde{h} = x_3$.

Again, we have $L_{\tilde{g}} \tilde{h} = 0$. Proceeding as before, we require

$$L_{\tilde{g}} L_{\tilde{f}} \tilde{h} = x_1 + \frac{\partial K_1}{\partial x_4} = 0 \tag{4.66}$$

which has the solution $K_1(x) = -x_1x_4 + K_1'(x_1, x_2, x_3)$. Continuing the calculations, we get

$$L_{\tilde{g}}L_{\tilde{f}}^2\tilde{h} = (1 + \frac{\partial K_1'}{\partial x_2})(2x_4 - x_1x_2) = 0 \tag{4.67}$$

which results in $K_1' = -x_2 + K_1''(x_1, x_3)$. Finally, we have the condition

$$L_{\tilde{g}}L_{\tilde{f}}^3\tilde{h} = 2x_4 - x_1x_2 \neq 0 \tag{4.68}$$

which does not place a condition on $K_1(x)$. The simplest feedback then that we can apply is

$$K_1(x) = -x_1x_4 - x_2\,. \tag{4.69}$$

This yields $r = n = 4$ as we require, and the operating point x^0 can be any $(x_1^0, \ldots, x_4^0)$ such that

$$2x_4^0 - x_1^0x_2^0 \neq 0. \tag{4.70}$$

Remark 4.11 In both examples it is important to note that the state space and input-output responses have been linearized for the u_2/y_2 input-output pair only. To realize this linearization, one must carry out the coordinates transformation and linearizing feedback for the SISO system (u_2/y_2) as detailed in Ref. [21]. The u_1/y_1 response will remain nonlinear in general.

Remark 4.12 We assume that each input-output pair has the full state x available for feedback. Thus, this is not strictly a decentralized technique, however the observer result of Section 4.1.2 could be combined with this result to produce local control laws. This can be done in the following way. Suppose we are interested in SISO state space linearization at the ℓth input-output channel for the system (4.1) with the conditions of Theorem 4.4 satisfied. Let Γ be the index set of input-output channels utilizing output feedback to allow observer construction at certain channels. Let Ω be the index set of these certain channels. Then the input-output channels in Ω will apply full state feedback (from the observed state constructed at these channels) to enhance the relative degree of the ℓth channel. This system is written as

$$\begin{aligned} \dot{x} &= f(x) + \sum_{i\in\Gamma} g_i(x)K_i^o(y_i) + \sum_{j\in\Omega} g_i(x)K_i^e(x) + g_\ell(x)u_\ell \\ y_\ell &= h_\ell(x) \end{aligned} \tag{4.71}$$

where $K_i^o(y_i)$ is the output feedback necessary to allow observer construction at all $j \in \Omega$, and $K_i^e(x)$ is the state feedback that enhances the relative degree at the ℓth input-output channel. Since the observer construction at all $j \in \Omega$ requires only signals at those channels, the result is completely decentralized.

4.1.7 Concluding Remarks

We have presented several methods for carrying out decentralized control strategies for nonlinear systems. Our goal has been to show that there exist classes of nonlinear systems for which local feedback laws will be able to achieve stabilization of the overall system. For most large systems with nonlinear coupling terms, a decentralized feedback law cannot completely linearize the system. However, via observers or a combination of linearization and local state feedback, the nonlinear system can be asymptotically stabilized.

We have developed a method to design decentralized observers for nonlinear systems. Once this observer problem is solved, one obtains a linear MIMO system in Brunovsky canonical form. This form was shown to contain no decentralized fixed modes thus assuring that decentralized dynamic output feedback will asymptotically stabilize the system. Next, a large system with nonlinear subsystems coupled with nonlinear interconnections was shown to be partially linearizable with local state feedback. Then the system with the nonlinear interconnection terms in the new coordinates can be exponentially stabilized with appropriately chosen linear local state feedback assuming norm bounds on the nonlinear interconnections.

Finally, a new method has been presented for linearizing a nonlinear MIMO system by utilizing feedback at all but one of the input-output channels such that the SISO linearization problem is solvable at the remaining input-output channel. The method has been shown to work via example for systems that are not feedback linearizable in a MIMO sense. Thus, the feedback functions at these input-output channels can be viewed as enhancing the solvability of the SISO feedback linearization problem. The examples show that it is not computationally difficult to find these feedback functions for low-order systems, but becomes more difficult as the system order and the number of input-output pairs rise.

Applications for these strategies would include large-scale nonlinear systems such as flexible structures undergoing slewing maneuvers, power systems, aircraft, automotive systems, and space structures.

4.2 SENSITIVITY MODELS FOR INTERCONNECTED SYSTEMS

The use of sensitivity functions in control theory to make the closed loop system less susceptible to changes in plant parameters has been studied for several decades (see survey by Kokotović and Rutman for an early history [67]). In particular, methods of generating sensitivity functions such that they can be utilized on-line in a control system have been extensively researched. Sensitivity models are a means of generating these sensitivity functions from the nominal plant model. However, very little effort has been spent in generating sensitivity models for coupled subsystems in a

decentralized manner.

But, as an additional tool for decentralized control, it is of interest to determine the feasibility of generating these models using only local signals for interconnected systems. That is, we wish to investigate the possibility that the ith subsystem's output sensitivity function can be generated using only plant signals from the ith subsystem. This is important if one wants to use sensitivity functions in a decentralized control environment. For instance, one could use decentralized sensitivity functions for self-tuning control (tuning the gains of a control law when some of the plant parameters are unknown) as is done in the work of Hung [113].

In this work, decentralized sensitivity models are suggested for certain classes of linear systems. It is the intent of this section to show that decentralized sensitivity models are possible for nonlinear systems as well under some assumptions. Ultimately, the importance of this section is to show that any control law that utilizes sensitivity functions (e.g. adaptive or optimal control laws) can be done in a decentralized framework even for nonlinear systems. Thus, the results of this section could be very practical provided one wishes to employ control laws that make use of sensitivity functions.

4.2.1 Decentralized Sensitivity Models

Consider Fig. 18 which depicts two interconnected MIMO linear systems. The outputs, Y_i, are of dimension p_i, $i = 1, 2$. The inputs, U_i, are of dimension m_i. The unknown parameter vectors, α_i, β_i, γ_i, are of dimensions n_i, r_i, and q_i, respectively. The transfer matrices, Q_i, W_i, W_{ij}, are of compatible dimensions. All vectors and matrices are functions of the Laplace Transform complex variable, s. The transfer matrices, Q_i, represent dynamic feedback from the outputs to the inputs. The transfer matrices, W_{ij}, represent coupling terms between the subsystems. The transfer matrices, W_i, represent the primary dynamics between plant inputs U_i and plant outputs Y_i.

The block transfer matrix of the entire system can be obtained by writing input-output relationships as follows

$$Y_1 = W_1(U_1 - Q_1Y_1) + W_{21}(U_2 - Q_2Y_2) \tag{4.72}$$

$$Y_2 = W_2(U_2 - Q_2Y_2) + W_{12}(U_1 - Q_1Y_1)\,. \tag{4.73}$$

Letting

$$\Delta_1 = I + W_1Q_1 - W_{21}Q_2[I + W_2Q_2]^{-1}W_{12}Q_1 \tag{4.74}$$

$$\Delta_2 = I + W_2Q_2 - W_{12}Q_1[I + W_1Q_1]^{-1}W_{21}Q_2 \tag{4.75}$$

where I is the identity matrix, we obtain the input-output description of the system

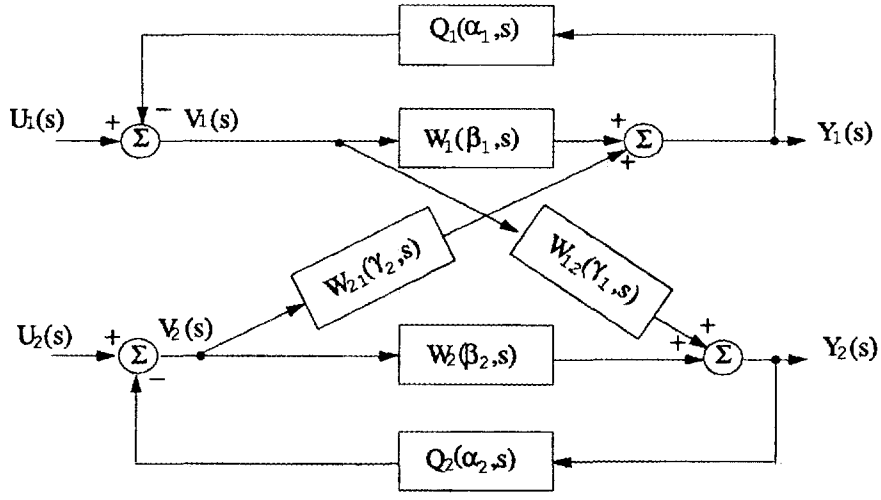

Fig. 18: MIMO system with coupled linear subsystems.

(after some algebraic manipulation)

$$\begin{bmatrix} Y_1 \\ Y_2 \end{bmatrix} = \begin{bmatrix} F_{11} & F_{12} \\ F_{21} & F_{22} \end{bmatrix} \begin{bmatrix} U_1 \\ U_2 \end{bmatrix} \tag{4.76}$$

with

$$\begin{aligned} F_{11} &= \Delta_1^{-1}[W_1 - W_{21}Q_2(I + W_2Q_2)^{-1}W_{12}] && (4.77) \\ F_{12} &= \Delta_1^{-1}[W_{21} - W_{21}Q_2(I + W_2Q_2)^{-1}W_2] && (4.78) \\ F_{21} &= \Delta_2^{-1}[W_{12} - W_{12}Q_1(I + W_1Q_1)^{-1}W_1] && (4.79) \\ F_{22} &= \Delta_2^{-1}[W_2 - W_{12}Q_1(I + W_1Q_1)^{-1}W_{21}]. && (4.80) \end{aligned}$$

We are interested in output sensitivity vectors of the system with respect to the unknown parameter vectors, α_i, β_i, and γ_i. It is sufficient to study sensitivity vectors of the first subsystem since the two subsystems are symmetric as is easily observed.

We proceed with the sensitivity of Y_1 with respect to α_1 which begins by utilizing (4.72)

$$\frac{\partial Y_1}{\partial \alpha_{1i}} = \frac{\partial F_{11}}{\partial \alpha_{1i}} U_1 + \frac{\partial F_{12}}{\partial \alpha_{1i}} U_2 \tag{4.81}$$

where α_{1i} is the ith component of the unknown parameter vector. It is important to note here that the commutativity of SISO systems that yielded the Wilkie-Perkins result [58] of just one sensitivity model (plus the plant itself) to simultaneously generate all the sensitivity functions does not apply. This means that the process of

applying $Y_1(s)$ as an input to a sensitivity filter-sensitivity model pair must be executed n_1 times (for the α_1 parameter vector). Thus, the output sensitivity vectors of this section will be with respect to the ith parameter of the vector in question. This in no way affects the versatility of the decentralized models in this subsection since it would apply to SISO systems as well.

Continuing with the analysis, the sensitivity of F_{11} with respect to the parameter α_{1i} is

$$\frac{\partial F_{11}}{\partial \alpha_{1i}} = -\Delta_1^{-1}\frac{\partial \Delta_1}{\partial \alpha_{1i}}\Delta_1^{-1}[W_1 - W_{21}Q_2(I + W_2Q_2)^{-1}W_{12}] \tag{4.82}$$

where

$$\frac{\partial \Delta_1}{\partial \alpha_{1i}} = [W_1 - W_{21}Q_2(I + W_2Q_2)^{-1}W_{12}]\frac{\partial Q_1}{\partial \alpha_{1i}} . \tag{4.83}$$

With this equation, we can rewrite $\frac{\partial F_{11}}{\partial \alpha_{1i}}$ as (after some algebraic manipulation)

$$\frac{\partial F_{11}}{\partial \alpha_{1i}} = -F_{11}\frac{\partial Q_1}{\partial \alpha_{1i}}F_{11} . \tag{4.84}$$

Likewise, via similar steps, one can obtain

$$\frac{\partial F_{12}}{\partial \alpha_{1i}} = -F_{11}\frac{\partial Q_1}{\partial \alpha_{1i}}F_{12} . \tag{4.85}$$

This leads to

$$\frac{\partial Y_1}{\partial \alpha_{1i}} = -F_{11}\frac{\partial Q_1}{\partial \alpha_{1i}}(F_{11}U_1 + F_{12}U_2) . \tag{4.86}$$

Noting that the term in parentheses is merely (4.72), we have the result

$$\frac{\partial Y_1}{\partial \alpha_{1i}} = -F_{11}\frac{\partial Q_1}{\partial \alpha_{1i}}Y_1 \tag{4.87}$$

which is a completely decentralized result. The output sensitivity vector depends only on the output signal itself plus some transfer matrices.

Several comments are in order at this juncture. First, one would normally be interested in the sensitivity functions evaluated about some known nominal parameter values. In this case, the above partial derivatives are all evaluated about these nominal values. This dependence on the nominal values is suppressed in the analysis to make notation simpler, but it should be assumed. Second, the above result and the ones to follow are decentralized in the sense that only local (i.e., within the given subsystem) signals are needed to compute the sensitivity functions. This is generally what one means by decentralized. The fact that transfer matrices from other subsystems are needed to compute these sensitivity functions does not detract from the decentralized

nature of these results. It is generally assumed in the decentralized control literature that models can be exchanged across subsystems even though signals are not. This is because in a real-time environment, the nominal models will have been known for some time whereas the signals are being generated at the moment (though there are some results that do use only local models).

Proceeding in a likewise manner for the output sensitivity vector with respect to β_1,

$$\frac{\partial Y_1}{\partial \beta_{1i}} = \frac{\partial F_{11}}{\partial \beta_{1i}} U_1 + \frac{\partial F_{12}}{\partial \beta_{1i}} U_2 \tag{4.88}$$

where (after some manipulation)

$$\frac{\partial F_{11}}{\partial \beta_{1i}} = \Delta_1^{-1} \frac{\partial W_1}{\partial \beta_{1i}} [-Q_1 F_{11} + I] \tag{4.89}$$

$$\frac{\partial F_{12}}{\partial \beta_{1i}} = \Delta_1^{-1} \frac{\partial W_1}{\partial \beta_{1i}} Q_1 F_{12} \,. \tag{4.90}$$

Finally, we obtain

$$\frac{\partial Y_1}{\partial \beta_{1i}} = \Delta_1^{-1} \frac{\partial W_1}{\partial \beta_{1i}} V_1 \tag{4.91}$$

where

$$V_1 = U_1 - Q_1 Y_1 \tag{4.92}$$

and represents the error signal between the reference inputs and the feedback signal. Thus, this sensitivity vector can also be generated via a local sensitivity model.

The sensitivity of Y_1 with respect to γ_{1i} is also of interest since one might want to know how the output of the first subsystem is affected by parametric uncertainty in the cross-coupling from subsystem 1 to subsystem 2. We start as before with

$$\frac{\partial Y_1}{\partial \gamma_{1i}} = \frac{\partial F_{11}}{\partial \gamma_{1i}} U_1 + \frac{\partial F_{12}}{\partial \gamma_{1i}} U_2 \tag{4.93}$$

where

$$\frac{\partial F_{11}}{\partial \gamma_{1i}} = \Delta_1^{-1} W_{21} Q_2 (I + W_2 Q_2)^{-1} \frac{\partial W_{12}}{\partial \gamma_{1i}} [Q_1 F_{12} - I] \tag{4.94}$$

$$\frac{\partial F_{12}}{\partial \gamma_{1i}} = \Delta_1^{-1} W_{21} Q_2 (I + W_2 Q_2)^{-1} \frac{\partial W_{12}}{\partial \gamma_{1i}} Q_1 F_{12} \,. \tag{4.95}$$

Combining these equations with (4.93) yields

$$\frac{\partial Y_1}{\partial \gamma_{1i}} = \Delta_1^{-1} W_{21} Q_2 (I + W_2 Q_2)^{-1} \frac{\partial W_{12}}{\partial \gamma_{1i}} [Q_1 (F_{12} - F_{11}) U_1 - V_1] \tag{4.96}$$

which again shows that it can be generated in a decentralized manner.

The three remaining output sensitivity vectors of the first subsystem do not possess the same decentralized features as the above sensitivity vectors. However, they are of interest to us since they still maintain some elements of a decentralized structure. Since the procedure for generating these sensitivity vectors has been established, the results are simply stated as follows

$$\frac{\partial Y_1}{\partial \alpha_{2i}} = -F_{12}\frac{\partial Q_2}{\partial \alpha_{2i}}Y_2 \tag{4.97}$$

$$\frac{\partial Y_1}{\partial \beta_{2i}} = -\Delta_1^{-1}W_{21}Q_2(I + W_2Q_2)^{-1}\frac{\partial W_2}{\partial \beta_{2i}}V_2 \tag{4.98}$$

$$\frac{\partial Y_1}{\partial \gamma_{2i}} = \Delta_1^{-1}\frac{\partial W_{21}}{\partial \gamma_{2i}}V_2 \,. \tag{4.99}$$

From above, one can see that each of these sensitivity vectors requires signals from only the second subsystem. In this sense, they can be generated by decentralized sensitivity models, but they would only be available at the second subsystem. Presumably, one would want these sensitivity vectors at the first subsystem since they do reflect Y_1's dependence on unknown parameters in the second subsystem. However, in some cases one may be able to use this information at the second subsystem where it can be generated via local sensitivity models. This might be the case in adaptive control where the sensitivity of the other subsystem's output to local parameters is needed to update a decentralized control law.

Figure 19 shows the configuration for generating the sensitivities of the first subsystem for the plant model in Fig. 18. Some of the sensitivity models can serve for two different sensitivity vectors, but each of the sensitivity vectors requires a different sensitivity filter. One drawback of decentralized sensitivity models over the centralized case is that the sensitivity models are no longer just a copy of the plant model. As is apparent in Fig. 19, the sensitivity models cannot be written as just a plant model, but some do have physical meaning. For instance, the sensitivity models for $\frac{\partial Y_1}{\partial \alpha_{1i}}$ and $\frac{\partial Y_1}{\partial \alpha_{2i}}$ which are F_{11} and F_{12}, respectively, represent the plant evaluated at the nominal parameter values with $U_2 = 0$ and $U_1 = 0$, respectively, and the other input coming from its respective sensitivity filter. The other sensitivity models are more complicated and are not able to be generated from a copy of the plant model in any obvious way.

As mentioned earlier, the sensitivities of Y_2 with respect to all of the unknown parameter vectors can be generated by exactly the dual of the above sensitivity models. With this figure one can utilize sensitivity-based control designs in a decentralized framework. Thus, well-known sensitivity control schemes (see Ref. [65] for examples) can be utilized at each subsystem. In particular, gradient adaptive control techniques utilizing sensitivity functions would enable one to update subsystem parameters in a completely decentralized setting.

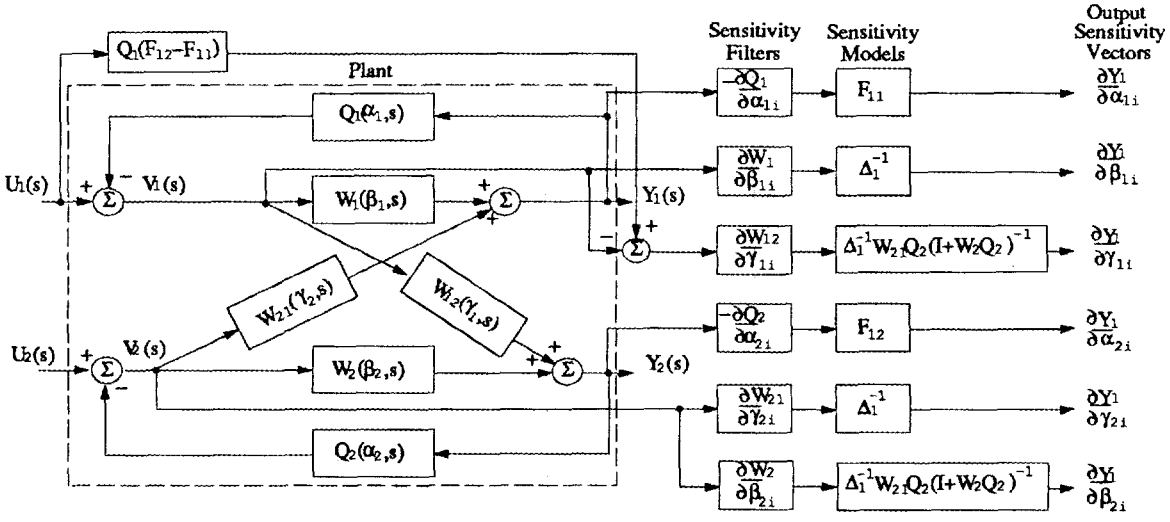

Fig. 19: Sensitivity model configurations for linear coupled subsystems.

The next logical step in generating decentralized sensitivity models is to look at the nonlinear case. It is much more difficult to produce local sensitivity models for coupled nonlinear systems because first-order partials of vector fields will still depend on the state. This implies that partials of coupling terms will require the use of the state vector from another subsystem which cannot be measured or generated locally. This motivates the analysis of less general nonlinear systems where perhaps only one subsystem needs access to a sensitivity model. Consider the following two-channel system depicted in Fig. 20

$$\begin{aligned} \dot{x}_1 &= f_1(x_1,\alpha_1) + B_1u_1 + A_{12}x_2\,, \;\; y_1 = h_1(x_1,\alpha_1) \\ \dot{x}_2 &= A_2(\alpha_2)x_2 + B_2u_2 + A_{21}x_1\,, \;\; y_2 = C_2(\alpha_2)x_2 \end{aligned} \tag{4.100}$$

where only f_1 and h_1 are assumed to be nonlinear. These functions are also assumed to be smooth in their arguments, x_1 and α_1. The second subsystem is completely linear and the coupling terms are linear as well. The terms B_i and A_{ij} are assumed to be independent of α_i.

To generate the sensitivity model for y_1 with respect to α_1, we need the sensitivity models for both x_1 and x_2 with respect to α_1 due to the cross-coupling. Differentiating, we obtain

$$\begin{aligned} \frac{\partial \dot{x}_1}{\partial \alpha_1} &= \frac{\partial f_1}{\partial x_1}\frac{\partial x_1}{\partial \alpha_1} + A_{12}\frac{\partial x_2}{\partial \alpha_1} + \frac{\partial f_1}{\partial \alpha_1} \\ \frac{\partial y_1}{\partial \alpha_1} &= \frac{\partial h_1}{\partial x_1}\frac{\partial x_1}{\partial \alpha_1} + \frac{\partial h_1}{\partial \alpha_1} \end{aligned} \tag{4.101}$$

$$\begin{aligned}\frac{\partial \dot{x}_2}{\partial \alpha_1} &= A_2(\alpha_2)\frac{\partial x_2}{\partial \alpha_1} + A_{21}\frac{\partial x_1}{\partial \alpha_1} \\ \frac{\partial y_2}{\partial \alpha_1} &= C_2(\alpha_2)\frac{\partial x_2}{\partial \alpha_1}\end{aligned}$$

where it is noted that u_i is assumed independent of α_i.

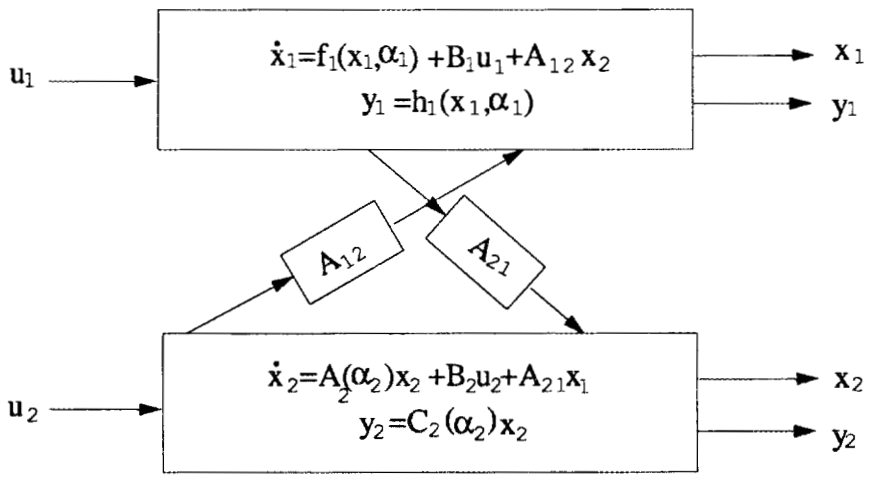

Fig. 20: Two-channel coupled nonlinear system.

From the model (4.101), it can be seen that the output and state sensitivities can all be generated in a decentralized framework. This is because state/output sensitivities form a system with a model requiring only matrices and signals that can be computed locally. The cross sensitivity $\frac{\partial x_2}{\partial \alpha_1}$ can be calculated at subsystem 1 since the above model shows that it too does not require any signals from subsystem 2. The same will not hold true for the sensitivities with respect to α_2 at the second subsystem since they will depend on $\frac{\partial f_1}{\partial x_1}$ which in general is a nonlinear function of x_1. Thus, the state x_1 would be needed at subsystem 2 to compute the sensitivities with respect to α_2 violating the decentralization constraint. Figure 21 illustrates the manner in which the sensitivity functions of the system in (4.100) are computed.

If the control vector fields B_i are not constant (e.g., $g_i(x_i)$ or $g_i(x_i, \alpha_i)$) then the terms $\frac{\partial g_i}{\partial \alpha_i}$ will be multiplying u_i making it impossible for the cross sensitivities to be generated locally (i.e., u_j would be needed in the ith subsystem's sensitivity model). Note also that the sensitivity model (4.101) is a linear system dependent on Jacobians of the $f_{i(j)}$ vectors with respect to α_i. The model is, however, time-varying since the Jacobians will depend on x_i in general. But the model will not depend on the unknown parameters since all parameters will be evaluated at their nominal values.

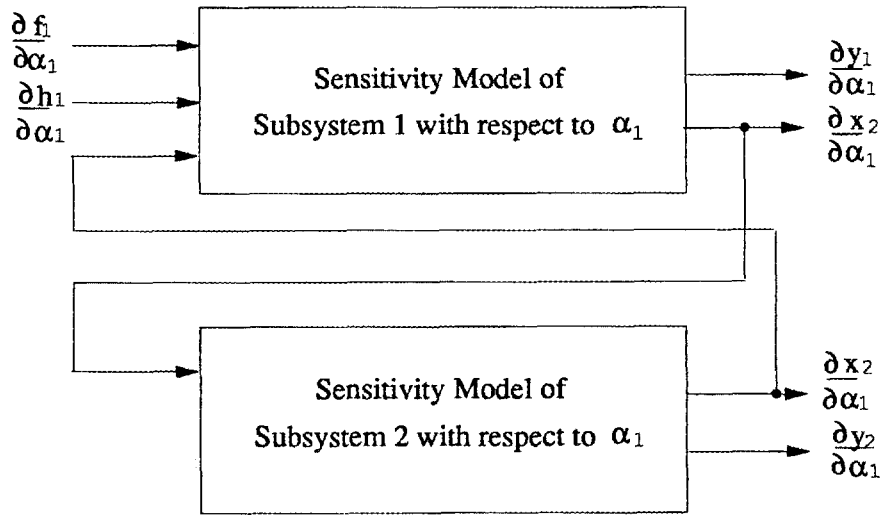

Fig. 21: Sensitivity models for coupled nonlinear systems.

4.2.2 Decentralized Optimal Control via Sensitivity Functions

It is now of interest to apply the above decentralized sensitivity models to performance issues associated with decentralized control. In particular, we concern ourselves with locally optimal control laws which include sensitivity functions in the feedback loop as a means of desensitizing the system from parameter variations. The framework pursued here is that of linear subsystems with linear couplings similar to that of Ref. [80] but utilizing sensitivity functions to address parametric uncertainty in an optimal manner. A version of the centralized case appears in Ref. [65]. The performance index consists of a sum of N local cost criterions where N is the number of subsystems.

Formally, we have

$$\dot{x}_i = A_i(\alpha_i)x_i + \sum_{\substack{j=1 \\ j\neq i}}^{N} A_{ij}x_j + B_i u_i\,, \quad i = 1, \ldots, N \tag{4.102}$$

with $x_i \in R^{n_i}$, $u_i \in R^{m_i}$, and $\alpha_i \in R_{p_i}$ where α_i are the vectors of unknown parameters. It is desired to minimize the quadratic cost criterion

$$J = \sum_{i=1}^{N} \int_0^\infty \left(x_i^T Q_i x_i + u_i^T R_i u_i + \sum_{j=1}^{N} \lambda_{ij}^T S_{ij} \lambda_{ij} \right) dt \tag{4.103}$$

via local state feedback where Q_i,S_{ij} are positive semidefinite matrices, R_i are positive definite matrices, and $\lambda_{ij} = \frac{\partial x_j}{\partial \alpha_i} |_{\alpha_i = \alpha_i^n}$ are the sensitivity vectors associated with the

ith subsystem with α_i^n the nominal parameter values. As was demonstrated in the previous section, the cross-sensitivity functions $\lambda_{ij}, j \neq i$ can be generated at the ith subsystem with only local information needed.

The sensitivity models are described by the following linear time-invariant differential equations

$$\dot{\lambda}_{ii} = \frac{\partial A_i}{\partial \alpha_i} x_i + A_i \lambda_{ii} + \sum_{\substack{j=1 \\ j \neq i}}^{N} A_{ij} \lambda_{ij} \tag{4.104}$$

$$\dot{\lambda}_{ij} = A_j \lambda_{ij} + \sum_{\substack{k=1 \\ k \neq j}} A_{jk} \lambda_{ik} \tag{4.105}$$

which again demonstrate the decentralized nature of sensitivity models for the system (4.102). Define the augmented state vector

$$\tilde{x}_i = \left[x_i^T \; \lambda_{ii}^T \; \lambda_{ij}^T \right]^T , \tag{4.106}$$

and one obtains the following linear time-invariant system

$$\begin{bmatrix} \dot{x}_i \\ \dot{\lambda}_{ii} \\ \dot{\lambda}_{ij} \end{bmatrix} = \begin{bmatrix} A_i \mid_{\alpha_i^n} & 0 & 0 \\ \frac{\partial A_i}{\partial \alpha_i} \mid_{\alpha_i^n} & A_i \mid_{\alpha_i^n} & \sum_{j=1}^{N} A_{ij} \\ 0 & A_{ji} & A_j \mid_{\alpha_j^n} + \sum_{\substack{k=1 \\ k \neq i,j}}^{N} A_{jk} \end{bmatrix} \begin{bmatrix} x_i \\ \lambda_{ii} \\ \lambda_{ij} \end{bmatrix} + \sum_{\substack{j=1 \\ j \neq i}}^{N} \begin{bmatrix} A_{ij} & 0 & 0 \\ 0 & 0 & 0 \\ 0 & 0 & 0 \end{bmatrix} \begin{bmatrix} x_j \\ \lambda_{jj} \\ \lambda_{ji} \end{bmatrix} + \begin{bmatrix} B_i \\ 0 \\ 0 \end{bmatrix} u_i \tag{4.107}$$

where the outputs are defined accordingly but not needed in this analysis. The compact form

$$\dot{\tilde{x}}_i = \tilde{A}_i \tilde{x}_i + \sum_{\substack{j=1 \\ j \neq i}}^{N} \tilde{A}_{ij} \tilde{x}_j + \tilde{B}_i u_i \tag{4.108}$$

which immediately follows from (4.107) leads to the full augmented state space description

$$\dot{\tilde{x}} = \tilde{A} \tilde{x} + \tilde{A}_c \tilde{x} + \tilde{B} u \tag{4.109}$$

where $\tilde{x} = \left[\tilde{x}_1^T \cdots \tilde{x}_N^T \right]^T$, $\tilde{A} = \text{block-diag} \left[\tilde{A}_1 \cdots \tilde{A}_N \right]$, $\tilde{A}_c = \left[\tilde{A}_{ij} \right]$, $j \neq i$, $\tilde{B} = \text{block-diag} \left[\tilde{B}_1 \cdots \tilde{B}_N \right]$, and $u = \left[u_1^T \cdots u_N^T \right]$.

The performance criterion (4.103) can be re-expressed in these new coordinates as

$$J = \sum_{i=1}^{N} \int_0^\infty \left(\tilde{x}_i^T \tilde{Q}_i \tilde{x}_i + u_i^T R_i u_i \right) dt \tag{4.110}$$

where $\tilde{Q}_i = \text{block-diag}\,[Q_i \; S_{ii} \; S_{ij}]$. This is written in the full state space as

$$J = \int_0^\infty \left(\tilde{x}^T \tilde{Q} \tilde{x} + u^T R u \right) dt \tag{4.111}$$

where $\tilde{Q} = \text{block-diag}\left[\tilde{Q}_1 \cdots \tilde{Q}_N\right]$ and $R = \text{block-diag}\,[R_1 \cdots R_N]$. Note that $\tilde{Q}$ and R will be positive semidefinite and positive definite, respectively, if Q_i,S_{ij} and R_i are positive semidefinite and positive definite, respectively.

It is assumed that the decoupled subsystems

$$\dot{\tilde{x}} = \tilde{A}\tilde{x} + \tilde{B}u \tag{4.112}$$

are controllable, i.e., $(\tilde{A}, \tilde{B})$ are a controllable pair. Thus, the cost criterion (4.111) can be minimized by solving the linear quadratic regulator separately for each subsystem. That is, let

$$u = -K\tilde{x} \tag{4.113}$$

where $K = \text{block-diag}\,[K_1 \cdots K_N]$. These K_i are computed by solving the algebraic Riccati equation

$$\tilde{A}^T P + P\tilde{A} - P\tilde{B}R^{-1}\tilde{B}^T P + \tilde{Q} = 0 \tag{4.114}$$

for the unique positive definite matrix $P = \text{block-diag}\,[P_1 \cdots P_N]$. Because of the structure of $\tilde{A}, \tilde{B}, \tilde{Q}, R$, the solution P will automatically be in this block-diagonal form. The feedback K is given as

$$K = R^{-1}\tilde{B}^T P \tag{4.115}$$

which produces the optimal cost

$$J^* = \tilde{x}^T(0) P \tilde{x}(0) \tag{4.116}$$

where it is noted that the initial conditions on the sensitivity vectors are always zero.

The control law (4.113) is completely decentralized, $u = -K_i\tilde{x}_i$, which means that each subsystem can be regulated with only locally available information even in the presence of parametric uncertainty. Indeed, it is the use of locally generated sensitivity functions that sets this strategy apart from others. Figure 22 illustrates this method. Of course, since the interconnections are ignored in the Riccati equation (4.114), the control law (4.113) will generally be suboptimal. However, because each

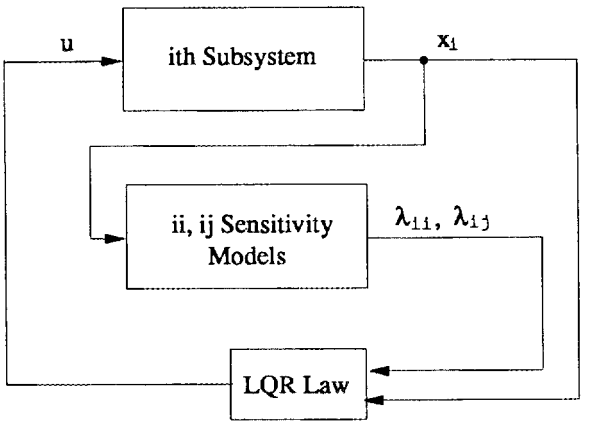

Fig. 22: Decentralized optimal control with sensitivity models.

subsystem is autonomously driven, this strategy will be robust to a wide range of uncertainties in the interconnections. Since the closed loop system is given by

$$\dot{\tilde{x}} = (\tilde{A} - \tilde{B}K + \tilde{A}_c)\tilde{x}\,, \tag{4.117}$$

the interconnections will behave as regular (as opposed to singular) perturbations. In the event of weak coupling, their impact will be small making this suboptimal strategy quite effective. The coupling matrix $\tilde{A}_c$ can be taken into account by applying functional minimization schemes (e.g., see Refs. [74, 84]) that involve coupled Lyapunov equations and iterative procedures. All the necessary terms and definitions for including the interconnections are present in this analysis. This is a straightforward extension of the above method but is omitted here. Finally, if the subsystems are nonlinear then the sensitivity models can be decentralized under the structure in the last section. However, the optimal control strategy pursued would have to involve solving the Hamilton-Jacobi equation unless some linearization procedure were implemented.

4.2.3 Example

We consider a system consisting of two inverted penduli coupled by a spring subject to two independent torque inputs as shown in Fig. 23. Physically, this system is analogous to two one-link manipulators joined together by a string, cable, or other spring-like medium. The deflections from vertical are assumed to be small enough such that the gravity term can be linearized. The equations of motion are [80]

$$\begin{aligned} m\ell_1^2\ddot{\theta}_1 &= mg\ell_1\theta_1 - ka^2(\theta_1 - \theta_2) + u_1 \\ m\ell_2^2\ddot{\theta}_2 &= mg\ell_2\theta_2 - ka^2(\theta_2 - \theta_1) + u_2 \end{aligned} \tag{4.118}$$

where all parameters are defined in Fig. 23 except for g which is the gravitational constant. The state vector is chosen as $x_1 = (\theta_1, \dot{\theta}_1)^T$, the input vector is $u = (u_1, u_2)^T$, and the uncertain parameters are $\alpha_i = \frac{g}{\ell_i}$. These parameters physically represent the squares of the natural frequencies of oscillation of the decoupled penduli. We assume some uncertainty from their nominal values. With this notation the system

$$\dot{x} = \begin{bmatrix} 0 & 1 & \vdots & 0 & 0 \\ \alpha_1 - \frac{ka^2}{m\ell_1^2} & 0 & \vdots & \frac{ka^2}{m\ell_1^2} & 0 \\ \cdots & \cdots & \cdots & \cdots & \cdots \\ 0 & 0 & \vdots & 0 & 1 \\ \frac{ka^2}{m\ell_2^2} & 0 & \vdots & \alpha_2 - \frac{ka^2}{m\ell_2^2} & 0 \end{bmatrix} x + \begin{bmatrix} 0 & \vdots & 0 \\ \frac{1}{m\ell_1^2} & \vdots & 0 \\ \cdots & \cdots & \cdots \\ 0 & \vdots & 0 \\ 0 & \vdots & \frac{1}{m\ell_2^2} \end{bmatrix} u \tag{4.119}$$

is written which falls into the format of (4.102).

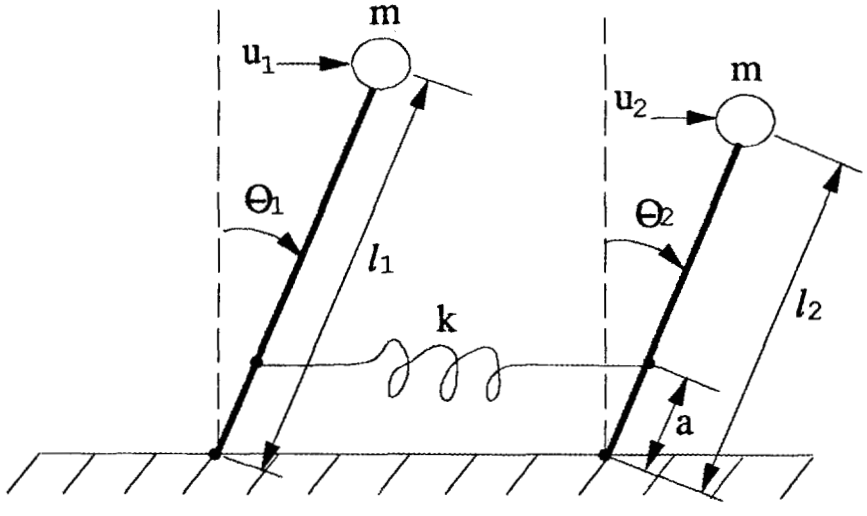

Fig. 23: Inverted penduli coupled by a spring.

The next task is to generate the sensitivity models of the system (4.119). Utilizing (4.104)-(4.105), the sensitivity vectors

$$\begin{aligned} \dot{\lambda}_{11} &= \begin{bmatrix} 0 & 0 \\ 1 & 0 \end{bmatrix} x_1 + \begin{bmatrix} 0 & 1 \\ \alpha_1^n - \frac{ka^2}{m\ell_1^2} & 0 \end{bmatrix} \lambda_{11} + \begin{bmatrix} 0 & 0 \\ \frac{ka^2}{m\ell_1^2} & 0 \end{bmatrix} \lambda_{12} \\ \dot{\lambda}_{12} &= \begin{bmatrix} 0 & 1 \\ \alpha_2^n - \frac{ka^2}{m\ell_2^2} & 0 \end{bmatrix} \lambda_{12} + \begin{bmatrix} 0 & 0 \\ \frac{ka^2}{m\ell_2^2} & 0 \end{bmatrix} \lambda_{11} \end{aligned} \tag{4.120}$$

$$
\begin{aligned}
\dot{\lambda}_{21} &= \begin{bmatrix} 0 & 1 \\ \alpha_1^n - \frac{ka^2}{m\ell_1^2} & 0 \end{bmatrix} \lambda_{21} + \begin{bmatrix} 0 & 0 \\ \frac{ka^2}{m\ell_1^2} & 0 \end{bmatrix} \lambda_{22} \\
\dot{\lambda}_{22} &= \begin{bmatrix} 0 & 0 \\ 1 & 0 \end{bmatrix} x_2 + \begin{bmatrix} 0 & 1 \\ \alpha_2^n - \frac{ka^2}{m\ell_2^2} & 0 \end{bmatrix} \lambda_{22} + \begin{bmatrix} 0 & 0 \\ \frac{ka^2}{m\ell_2^2} & 0 \end{bmatrix} \lambda_{21}
\end{aligned}
$$

are generated. The augmented state vector $\tilde{x}$ is formed as follows

$$
\tilde{x} = \left[x_1^T \, \lambda_{11}^T \, \lambda_{12}^T \, x_2^T \, \lambda_{22}^T \, \lambda_{21}^T \right]^T \tag{4.121}
$$

which is 12th order. Choosing $ka^2 = 1\text{N}\cdot\text{m}$, $m\ell_1^2 = 1\text{kg}\cdot\text{m}^2$, $m\ell_2^2 = 0.5\text{kg}\cdot\text{m}^2$, $\alpha_1^n = \frac{g}{\ell_1} = 1\frac{1}{\text{s}^2}$, and $\alpha_2^n = \frac{g}{\ell_2} = 2\frac{1}{\text{s}^2}$. This leads to the nominal augmented state space description in the form of (4.109)

$$
\begin{aligned}
\dot{\tilde{x}} &= \begin{bmatrix}
0 & 1 & 0 & 0 & 0 & 0 & 0 & 0 & 0 & 0 & 0 & 0 \\
0 & 0 & 0 & 0 & 0 & 0 & 0 & 0 & 0 & 0 & 0 & 0 \\
0 & 0 & 0 & 1 & 0 & 0 & 0 & 0 & 0 & 0 & 0 & 0 \\
1 & 0 & 0 & 0 & 1 & 0 & 0 & 0 & 0 & 0 & 0 & 0 \\
0 & 0 & 0 & 0 & 0 & 1 & 0 & 0 & 0 & 0 & 0 & 0 \\
0 & 0 & 2 & 0 & 0 & 0 & 0 & 0 & 0 & 0 & 0 & 0 \\
0 & 0 & 0 & 0 & 0 & 0 & 0 & 1 & 0 & 0 & 0 & 0 \\
0 & 0 & 0 & 0 & 0 & 0 & 0 & 0 & 0 & 0 & 0 & 0 \\
0 & 0 & 0 & 0 & 0 & 0 & 0 & 0 & 0 & 1 & 0 & 0 \\
0 & 0 & 0 & 0 & 0 & 0 & 1 & 0 & 0 & 0 & 2 & 0 \\
0 & 0 & 0 & 0 & 0 & 0 & 0 & 0 & 0 & 0 & 0 & 1 \\
0 & 0 & 0 & 0 & 0 & 0 & 0 & 0 & 1 & 0 & 0 & 0
\end{bmatrix} \tilde{x} \\
&+ \begin{bmatrix}
0 & 0 & 0 & 0 & 0 & 0 & 0 & 0 & 0 & 0 & 0 & 0 \\
0 & 0 & 0 & 0 & 0 & 0 & 1 & 0 & 0 & 0 & 0 & 0 \\
0 & 0 & 0 & 0 & 0 & 0 & 0 & 0 & 0 & 0 & 0 & 0 \\
0 & 0 & 0 & 0 & 0 & 0 & 0 & 0 & 0 & 0 & 0 & 0 \\
0 & 0 & 0 & 0 & 0 & 0 & 0 & 0 & 0 & 0 & 0 & 0 \\
0 & 0 & 0 & 0 & 0 & 0 & 0 & 0 & 0 & 0 & 0 & 0 \\
0 & 0 & 0 & 0 & 0 & 0 & 0 & 0 & 0 & 0 & 0 & 0 \\
2 & 0 & 0 & 0 & 0 & 0 & 0 & 0 & 0 & 0 & 0 & 0 \\
0 & 0 & 0 & 0 & 0 & 0 & 0 & 0 & 0 & 0 & 0 & 0 \\
0 & 0 & 0 & 0 & 0 & 0 & 0 & 0 & 0 & 0 & 0 & 0 \\
0 & 0 & 0 & 0 & 0 & 0 & 0 & 0 & 0 & 0 & 0 & 0 \\
0 & 0 & 0 & 0 & 0 & 0 & 0 & 0 & 0 & 0 & 0 & 0
\end{bmatrix} \tilde{x} + \begin{bmatrix}
0 & 0 \\ 1 & 0 \\ 0 & 0 \\ 0 & 0 \\ 0 & 0 \\ 0 & 0 \\ 0 & 0 \\ 0 & 2 \\ 0 & 0 \\ 0 & 0 \\ 0 & 0 \\ 0 & 0
\end{bmatrix} u
\end{aligned} \tag{4.122}
$$

which has been evaluated at the nominal values of the uncertain parameters.

The quadratic cost criterion is chosen such that all states and sensitivity functions are weighted equally, i.e., $\tilde{Q}$ is a 12×12 identity matrix. Likewise, R is selected to

be a 2×2 identity matrix. Analysis simulated on MATLAB (trade name of The MathWorks, Inc.) solves the Riccati equation (4.114) and implements the decentralized control strategy of the last section. For comparison purposes, a decentralized design is carried out on the same system without using sensitivity models. That is, the nominal parameter values were taken as exact in the control design. The uncertainties tested were 10% and 20%, respectively, i.e., the true values were $\alpha_1 = 1.1$, $\alpha_2 = 2.2$, and $\alpha_1 = 1.2$, $\alpha_2 = 2.4$ for the two simulation runs. For both designs, the controllability assumption is satisfied.

Table 2: Closed loop poles with no uncertainty

	No sensitivity model	Sensitivity model
		-0.233±j1.255
	-0.866±j0.5	-0.924±j0.582
No interconnections	-1.414	-1.376, -1.058
	-1.414	-0.23±j1.206
		-1.196±j0.41
		-1.79, -1.036
		-2.957±j1.52
	-1.116±j1.207	-0.53±j1.724
Interconnections	-2.329	-0.136±j1.259
	0.0	-0.182±j1.04
		-0.22±j0.301
		-1.189±j0.003

The results are summarized in Tables 2 to 4. The first column of numbers of each table represent the closed loop poles for the 4th order decentralized design without sensitivity models. The second column of numbers of each table represent the closed loop poles for the 12th order decentralized design with sensitivity models. The first row of each table corresponds to the case of ignoring the interconnection terms whereas the second row includes these terms in the closed loop analysis. The results show that the lower order design without sensitivity models fails to stabilize the closed loop system once inaccuracies in the parameters are introduced. In fact, even with no uncertainty in the parameters, one of the closed loop poles is at the origin once the coupling matrix is included. As the uncertainty is increased this pole moves further into the right half plane. But for all three cases of uncertainty (0, 10%, 20%), the higher order design with sensitivity models maintains closed loop stability. The price paid is a higher order system, but the gain is a significant amount of stability robustness with respect to parametric uncertainty. Of course, it must be noted that

Table 3: Closed loop poles with 10% uncertainty

	No sensitivity model	Sensitivity model
		-0.249±j1.445
	0.056	-0.193±j0.836
No interconnections	-1.788	-2.678, -3.629
	0.069	-0.301±j1.542
	-2.898	-0.131±j0.904
		-1.186, -1.187
		-3.405±j0.995
	-1.03±j0.31	-0.205±j1.78
Interconnections	-3.059	-0.168±j1.332
	0.559	-0.072±j0.978
		-0.177±j0.648
		-1.188±j0.001

the true optimal cost J^* will be infinite for all three cases for the lower order design whereas it remains finite for the higher order design.

4.2.4 Concluding Remarks

In this section, we have shown that sensitivity models of linear interconnected systems can be generated at each subsystem using only local signals. This has even been shown for special cases of nonlinear systems. The utility of this result is that any control algorithm that calls for the use of sensitivity functions to alleviate the problems of parametric uncertainty can be implemented in a decentralized setting. Thus, adaptive control, optimal control, system identification, etc., that call for the use of sensitivity functions can be done on interconnected systems using only the local state or output.

In particular, a decentralized optimal control strategy was presented that incorporates sensitivity functions in an augmented state vector. A cost criterion that penalizes these sensitivity functions is utilized which makes the closed loop optimal control law less sensitive to parameter deviations at each subsystem. Moreover, the control is completely decentralized requiring only the solution of algebraic Riccati equations for the feedback gain matrices.

This scheme is applied to a system consisting of two inverted penduli coupled by a spring. It is compared to the same decentralized control law without the use of sensitivity models. When the true natural frequencies of oscillation are allowed to deviate

Table 4: Closed loop poles with 20% uncertainty

	No sensitivity model	Sensitivity model
		-0.24±j1.459
	0.109	-0.173±j0.841
No interconnections	-1.84	-2.736, -3.707
	0.135	-0.281±j1.563
	-2.963	-0.113±j0.908
		-1.186, -1.187
		-3.45±j0.959
	-3.114	-0.183±j1.784
Interconnections	0.601	-0.168±j1.341
	-0.871	-0.063±j0.979
	-1.177	-0.163±j0.669
		-1.188±j0.001

from their known nominal values, the scheme with sensitivity models maintains closed loop stability even up to 20% variation in parameters. The strategy without sensitivity models fails to stabilize the true system when the parameters are varied. The price paid is a higher order system, but the robustness to closed loop stability with sensitivity models makes it very useful for uncertain systems under decentralization constraints.

CHAPTER 5

APPLICATIONS OF NONLINEAR CONTROL

5.1 FLEXIBLE MANIPULATOR CONTROL VIA SINGULAR PERTURBATIONS

This section is concerned primarily with the application of singular perturbations and distributed vibration damping to a two-link flexible manipulator. This result is an example of decentralized nonlinear control with the feedback linearization done by integral manifold methods. Each link only requires its own local measurements for feedback at its joint. In addition, the result takes advantage of new "smart" materials such as piezoelectrics that can significantly dampen vibrations without adding much weight to the structure. The result begins by developing the integral manifold equations of the two-link structure which are needed to determine the linearizing control laws. The appendix contains the dynamical equations of the model as well as the structural data.

5.1.1 Control via the Integral Manifold Approach

According to Sobolev [114], a manifold M_ϵ defined by the equations

$$z = h(\theta, \dot{\theta}, \hat{u}, \ell, \epsilon) \tag{5.1}$$

$$\dot{z} = \dot{h}(\theta, \dot{\theta}, \hat{u}, \ell, \epsilon) \tag{5.2}$$

is an integral manifold for the system (A.1)-(A.4) if it is invariant under solutions of (A.1)-(A.4). That is, if the system lies on the manifold M_ϵ at some time t_0 then the solution trajectory remains on the manifold M_ϵ for all $t > t_0$. If in addition, the flexible dynamics as represented by the flexural vibration equations, (A.3)-(A.4), are asymptotically stable then the solution of the full system, (A.1)-(A.4), will rapidly converge to the integral or slow manifold M_ϵ on a fast manifold and remain on this slow manifold for all time. In addition, the stability of the overall system for small enough ϵ is determined by the stability of the slow subsystem, i.e., the system obtained with $\epsilon = 0$ if the fast dynamics are asymptotically stable (see Refs. [2] and [3]).

In order to apply integral manifold theory, the system model (A.1)-(A.4) must be in singularly perturbed form. This model has been shown to be singularly perturbed in Khorrami and Ozguner [50] for the one-link case and Khorrami [115] for the two-link case. Thus, we concentrate on deriving the slow and fast manifold equations describing the two-link manipulator's behavior. These equations have not been developed previously. To do this, a normalized model of the system is derived.

First, we normalize the link deviations and spatial variables with respect to link lengths. That is

$$x_1 = \frac{\ell_1}{L_1}, \quad x_2 = \frac{\ell_2}{L_2}, \quad y_1 = \frac{\alpha_1}{L_1}, \quad y_2 = \frac{\alpha_2}{L_2}. \tag{5.3}$$

To make use of these normalized variables we divide both sides of (A.1) by $L_1^3 L_2^3$, and we divide both sides of (A.2) by $L_1 L_2^3$. then we divide both sides of (A.3) by $\rho_1 L_1$, and we divide both sides of (A.4) by $\rho_2 L_1 L_2$. Next we define several variables for convenience in notation. Our new control variables become

$$u_1 = \frac{\hat{u}_1}{L_1^3 L_2^3} \quad \text{and} \quad u_2 = \frac{\hat{u}_2}{L_1 L_2^3}, \tag{5.4}$$

and we define

$$J = \frac{I_h}{L_1^3 L_2^3} + \frac{\rho_1}{3L_2^3} + \frac{M_2}{L_1 L_2^3} + \frac{\rho_2}{L_1 L_2^2}. \tag{5.5}$$

The small parameter ϵ is introduced in the following manner: Since ϵ must be related to the stiffness properties of the links, a natural choice (Khorrami and Özgüner [50], Khorrami [115], and Siciliano et al. [116, 117]) is to let ϵ be inversely proportional to the square of the lowest frequency of oscillation due to flexure of the links. Because there are two links, there are two such parameters, ϵ_1 and ϵ_2:

$$\epsilon_i = \frac{\rho_i L_i^4}{E_i I_i}, \quad i = 1, 2. \tag{5.6}$$

This choice of ϵ shows that as the bending stiffness $E_i I_i$ becomes larger ϵ_i becomes smaller which implies that the links behave more like rigid links. Since the y_i terms represent the flexure effects, it can be shown that (Khorrami and Özgüner [50] and Khorrami [115]) y_i is of order ϵ_i. Thus, we let

$$y_i = \epsilon_i z_i, \quad i = 1, 2 \tag{5.7}$$

where z_i is our new variable for flexure effects. It can also be verified (Khorrami and Özgüner [50] and Khorrami [115]) that as ϵ_i vanishes, the dynamics of the rigid body motion are recovered. Working with two different small parameters greatly increases the complexity of the integral manifold equations. Thus, we make the following assumption.

Assumption 5.1 $O(\epsilon_1) = O(\epsilon_2) = O(\epsilon)$.

This allows us to deal with just one small parameter representing the flexibility of the two links. It is important to note that this does not mean that $\epsilon_1 = \epsilon_2$. Indeed, these two parameters can differ significantly provided they are of the same order for approximation purposes. Physically, this assumption means that both links have roughly the same order of magnitude in elasticity properties. As long as one link is not a great deal more flexible than the other, Assumption 5.1 will hold. This assumption does not force any requirements on the relation of the length of one link to the other. If it turns out that one of the links is stiff, say link 1, then $\epsilon_1 = 0$ and in fact the dynamics are even simpler since all terms containing α_1 disappear (see Khorrami [118]). If Assumption 5.1 does not hold and neither link is rigid then one obtains a multi-parameter singular perturbation problem. This corresponds to a three time-scale system which would require additional subsystems to describe (see Kokotović et al. [46], p. 34).

With the terms from above, we can now define the integral manifold:

$$\begin{aligned} M_\epsilon &= \{(\theta_1, \theta_2, \dot{\theta}_1, \dot{\theta}_2, z_1, z_2, \dot{z}_1, \dot{z}_2) | z_i = h_i(\theta_i, \dot{\theta}_i, u_i, x_i, \epsilon), \\ \dot{z}_i &= \dot{h}_i(\theta_i, \dot{\theta}_i, u_i, x_i, \epsilon)\} \end{aligned} \tag{5.8}$$

for $i = 1, 2$ where h_i represents the effects of flexure on the rigid body motion. The h_i variables are obtained by solving a manifold condition which is simply the substitution of $z_i = h_i$ into the transverse motion equation for link i. However, these equations are very difficult to solve so the manifold terms h_i and the torque control terms u_i are expanded in the parameter ϵ as follows:

$$u_i = u_{i0} + \epsilon u_{i1} + O(\epsilon^2) \tag{5.9}$$

$$h_i = h_{i0} + \epsilon h_{i1} + O(\epsilon^2) \tag{5.10}$$

where $h_{ij} = h_{ij}(\theta_i, \dot{\theta}_i, u_i, x_i)$. It should be noted that in the equations to follow, we simplify notation by writing $h_{ij} = h_{ij}(x_i, t)$ to reflect h_{ij}'s dependence on length (x_i) and time (θ_i, $\dot{\theta}_i$, u_i). The h_{ij} terms do not depend on ϵ since this is now assumed in the power series.

Substituting (5.3), (5.4), (5.6)-(5.10) into (A.3) and (A.4), and equating like powers of ϵ, we obtain the following manifold conditions:

Manifold equations for link 1:

$$\begin{aligned} O(1): &\quad x_1\ddot{\theta}_1 = -h_{10,x_1x_1x_1x_1} \\ O(\epsilon): &\quad \ddot{h}_{10} = -h_{11,x_1x_1x_1x_1} + h_{10}\dot{\theta}_1^2 \end{aligned} \tag{5.11}$$

Manifold equations for link 2:

$$
\begin{aligned}
O(1): \quad & \tfrac{1}{L_1}\, x_2(\ddot{\theta}_1 + \ddot{\theta}_2) + \tfrac{1}{L_2}\, \ddot{\theta}_1 \cos\theta_2 = \\
& -\tfrac{1}{L_1}\, h_{20,x_2x_2x_2x_2} - \tfrac{1}{L_2}\, \dot{\theta}_1^2 \sin\theta_2 \\
O(\epsilon): \quad & \tfrac{1}{L_1}\, \ddot{h}_{20} + \tfrac{1}{L_2}\, h_{10}(1,t)\ddot{\theta}_1 \sin\theta_2 = \\
& -\tfrac{1}{L_1}\, h_{21,x_2x_2x_2x_2} + \tfrac{1}{L_1} h_{20}(\dot{\theta}_1 + \dot{\theta}_2)^2 \\
& -\tfrac{1}{L_2}\, \ddot{h}_{10}(1,t)\cos\theta_2 + \tfrac{1}{L_2} h_{10}(1,t)\dot{\theta}_1^2 \cos\theta_2 \\
& -\tfrac{2}{L_2} \dot{h}_{10}(1,t)\dot{\theta}_2 sin\theta_2
\end{aligned}
\tag{5.12}
$$

where $O(\epsilon^2)$ terms have been ignored.

Substituting (5.3)-(5.10) into (A.1) and (A.2), and again equating like powers of ϵ, we obtain the following corrected slow manifold equations representing the rigid body motion on the slow manifold. These equations are corrected in the sense that the flexibility effects from the manifold equations are included to increasingly higher powers in ϵ.

Corrected slow manifold equations for link 1:

$$
\begin{aligned}
O(1): \quad & \left[J + \tfrac{\rho_2}{2L_1^2 L_2} \cos\theta_2\right] \ddot{\theta}_1 + \\
& \left[\tfrac{\rho_2}{3L_1^3} + \tfrac{\rho_2}{2L_1^2 L_2}\, \cos\theta_2\right] (\ddot{\theta}_1 + \ddot{\theta}_2) \\
& = \tfrac{\rho_2}{2L_1^2 L_2}\, (2\dot{\theta}_1 + \dot{\theta}_2)\dot{\theta}_2 \sin\theta_2 + u_{10} \\
O(\epsilon): \quad & \left[\tfrac{\rho_2}{2L_1^2 L_2}\, h_{10}(1,t)\sin\theta_2 - \tfrac{\rho_2}{L_1^2 L_2} \sin\theta_2 \int_0^1 h_{20} dx_2\right] \ddot{\theta}_1 + \\
& [\tfrac{\rho_2}{2L_1^2 L_2}\, h_{10}(1,t)\sin\theta_2 - \\
& \tfrac{\rho_2}{L_1^2 L_2}\, \sin\theta_2 \int_0^1 h_{20} dx_2](\ddot{\theta}_1 + \ddot{\theta}_2) + \\
& \left(\tfrac{M_2}{L_1 L_2^3} + \tfrac{\rho_2}{L_1 L_2^2}\right) \ddot{h}_{10}(1,t) + \tfrac{\rho_2}{2L_1^2 L_2}\, \ddot{h}_{10}(1,t)\cos\theta_2 + \\
& \tfrac{\rho_1}{L_2^3} \int_0^1 x_1 \ddot{h}_{10} dx_1 + \tfrac{\rho_2}{L_1^2} \int_0^1 \left[\tfrac{x_2}{L_1} + \tfrac{\cos\theta_2}{L_2}\right] \ddot{h}_{20} dx_2 \\
& = -\tfrac{\rho_2}{2L_1^2 L_2}(2\dot{\theta}_1 + \dot{\theta}_2) h_{10}(1,t)\dot{\theta}_2 \cos\theta_2 - \\
& \tfrac{\rho_2}{L_1^2 L_2} \dot{\theta}_2 \dot{h}_{10}(1,t)\sin\theta_2 + \\
& \tfrac{2\rho_2}{L_1^2 L_2}(\dot{\theta}_1 + \dot{\theta}_2)\sin\theta_2 \int_0^1 \dot{h}_{20} dx_2 + \\
& \tfrac{\rho_2}{L_1^2 L_2} \dot{\theta}_2 \left[2\dot{\theta}_1 + \dot{\theta}_2\right] \cos\theta_2 \int_0^1 h_{20} dx_2 + u_{11}
\end{aligned}
\tag{5.13}
$$

Corrected slow manifold equations for link 2:

$$
\begin{aligned}
O(1): \quad & \left(\tfrac{\rho_2}{2L_2}\cos\theta_2 + \tfrac{\rho_2}{3L_1}\right)\ddot{\theta}_1 + \tfrac{\rho_2}{3L_1}\ddot{\theta}_2 \\
& = -\tfrac{\rho_2}{2L_2}\dot{\theta}_1^2 \sin\theta_2 + u_{20} \\
O(\epsilon): \quad & \left[-\tfrac{\rho_2}{L_2}\sin\theta_2 \int_0^1 h_{20}dx_2 + \tfrac{\rho_2}{2L_2} h_{10}(1,t)\sin\theta_2\right]\ddot{\theta}_1 + \\
& \tfrac{\rho_2}{L_1}\int_0^1 x_2\ddot{h}_{20}dx_2 + \tfrac{\rho_2}{2L_2}\ddot{h}_{10}(1,t)\cos\theta_2 \\
& = -\tfrac{\rho_2}{L_2}\dot{\theta}_1^2\cos\theta_2 \int_0^1 h_{20}dx_2 + \\
& \tfrac{\rho_2}{2L_2}\dot{\theta}_1^2 h_{10}(1,t)\cos\theta_2 - \\
& \tfrac{\rho_2}{L_2}\dot{h}_{10}(1,t)\dot{\theta}_1\sin\theta_1 + u_{21}
\end{aligned}
\tag{5.14}
$$

where again the $O(\epsilon^2)$ terms have been ignored. It should be noted that the $O(1)$ equations of the slow manifold represent the equations of a two-link rigid manipulator as expected. These equations are the slow subsystem of the flexible manipulator, and in Sect. 5.1.3 we explain the strategy for asymptotically stabilizing the slow subsystem. This terminology is important since it is the slow subsystem that must be stabilized to ensure stability for the full system for small enough ϵ.

Also of interest are the fast manifold equations. To derive this, we introduce the fast or stretched time scale $\tau = t/\sqrt{\epsilon}$. We also define the deviation of the flexure variables from the integral manifold as

$$\eta_i = z_i - h_i. \tag{5.15}$$

Substituting (5.15) and the fast time scale into the flexible dynamics (A.3)-(A.4) and letting $\epsilon \to 0$ (see Kokotović et al. [46], pp. 17-20) we get the boundary layer system

$$\frac{d^2\eta_1}{d\tau^2} = -\eta_{1,x_1x_1x_1x_1} - h_{1,x_1x_1x_1x_1} - x_1(\ddot{\theta}_1)^0 \tag{5.16}$$

$$
\begin{aligned}
\frac{d^2\eta_2}{d\tau^2} &= -\eta_{2,x_2x_2x_2x_2} - h_{2,x_2x_2x_2x_2} - x_2((\ddot{\theta}_1)^0 + (\ddot{\theta}_2)^0) \\
&- \frac{L_1}{L_2}(\ddot{\theta}_1)^0\cos\theta_2^0 - \frac{L_1}{L_2}(\dot{\theta}_1^2)^0\sin\theta_2^0
\end{aligned}
\tag{5.17}
$$

with initial conditions

$$\eta_1^0 = z_1^0 - h_1(\theta_1^0, (\dot{\theta}_1)^0, u_1^0, x_1, 0) \tag{5.18}$$

$$\eta_2^0 = z_2^0 - h_2(\theta_2^0, (\dot{\theta}_2)^0, u_2^0, x_2, 0)\,. \tag{5.19}$$

The above system describes the trajectories (θ_i, η_i), which, for every given initial condition $(\theta_i^0, \dot{\theta}_i^0, \ddot{\theta}_i^0)$, lie on a fast manifold defined by $\theta_i = \theta_i^0$ =const, and rapidly descend to the slow manifold M_0 (i.e., M_ϵ with $\epsilon = 0$).

The above model does not include any viscous damping in the links. If one desires to include this in the model, one will obtain an additional equation of $O(\epsilon^{\frac{1}{2}})$ which results from the fact that the damping coefficient is proportional to the square root of the stiffness term EI. The important point of this is that the $O(\epsilon^{\frac{1}{2}})$ equation will be linear and thus does not need a torque control term for feedback linearization. Of course, without damping, the system equations will never converge to the integral manifold since the fast subsystem (the vibrational dynamics) are not asymptotically stable. But at least some viscous damping will always be present, thus the above slow manifold will exist. The important point here is that the presence or absence of damping does not alter our control strategy.

5.1.2 Distributed Actuator Control

Though flexible manipulators have advantages in terms of speed, mobility, and reduced energy consumption, their vibrational characteristics make control more difficult. Passive damping of flexible robot arms is not adequate due to its additional mass and its inability to adjust to changing flexibility effects. Hence, some kind of active damping is desirable to control the vibrations. In Spong et al. [2] and Siciliano et al. [116], only torque control is used to cancel the vibrational motion. But because of the dynamical complexity of flexible links versus flexible joints, it would appear additional control effort is needed. Current design practice in general flexible structures is to use discrete or point actuators to actively dampen vibrations. However, these flexible systems have an infinite number of degrees of freedom forcing most designs to truncate the system model to a finite number of discrete modes. Choosing which modes to represent the system and where to put the actuators is a difficult problem. In Chassiakos and Bekey [119], an optimal scheme for locating ideal point actuators on a vibrating beam is proposed, and in Barbieri [120], the dynamics of a particular proof mass actuator are incorporated into the system model.

But in Bailey and Hubbard [8], Burke and Hubbard [9, 10], and Crawley and de Luis [11], a distributed actuator which has the possibility of controlling an infinite number of vibrational modes and adds a minimum of dynamical complexity to the system model is proposed. The actuator is spatially distributed and makes use of a polymer film. When a voltage is applied spatially across the faces of the film, it results in a longitudinal strain over the entire plated area of the film, making it a distributed parameter actuator. If this voltage is varied spatially, the strain will also vary spatially and in Bailey and Hubbard [8] candidate voltage functions are revealed as able to control all the vibrational modes of flexible beams with many different boundary conditions. There are other distributed actuators. In Edberg [121], a thermal actuator when applied with a voltage acts as a heat pump producing a temperature gradient that induces a deflection in the beam. Results in Edberg [121] show that if the voltage is chosen properly it can significantly dampen the first

vibrational mode of a cantilever beam.

The dynamics and hardware details of various film actuators are explained in Bailey and Hubbard [8], Burke and Hubbard [9, 10] and Crawley and de Luis [11] and will not be repeated here. Instead, the new equations of the two-link structure with distributed actuator control are derived by adding the polymer actuator to the manifold equations which are essentially Euler-Bernoulli beam models with slewing effects (Schoenwald et al. [51] and Schoenwald and Özgüner [122]). The film type distributed actuator will effect the manifold equations as well as the boundary conditions. This actuator will also impact the corrected slow manifold via the solution of the manifold equations (i.e., the h_{ij} terms). But it will not affect the rigid link motion (i.e., the O(1) corrected slow manifold equations). The primary difference in this section from Bailey and Hubbard [8], Burke and Hubbard [9, 10], and Crawley and de Luis [11] in implementation of the film is that the flexible links are slewing (rigid body motion) as well as vibrating. The new system equations can be stated as follows:

O(1) manifold equation for link 1:

$$x_1\ddot{\theta}_1 = -h_{10,x_1x_1x_1x_1} + \frac{m_1}{\rho_1 L_1^3}\hat{V}_{1,x_1x_1} \tag{5.20}$$

O(1) manifold equation for link 2:

$$\begin{aligned}&\tfrac{1}{L_1}x_2(\ddot{\theta}_1+\ddot{\theta}_2)+\tfrac{1}{L_2}\ddot{\theta}_1\cos\theta_2\\&=-\tfrac{1}{L_1}h_{20,x_2x_2x_2x_2}-\tfrac{1}{L_2}\dot{\theta}_1^2\sin\theta_2+\tfrac{m_2}{\rho_2 L_1 L_2^3}\hat{V}_{2,x_2x_2}\end{aligned} \tag{5.21}$$

where $\hat{V}_i(x_i,t)$ is the voltage applied to the film on the ith link which can vary in both space and time and m_i is a physical constant representing stiffness and other parameters of the film.

The boundary conditions for the system will change with the application of the film voltage $\hat{V}_i(x_i,t)$ and can be stated as follows:

Boundary conditions for link 1:

$$\begin{aligned}&h_{10}(0,t)=h_{10,x_1}(0,t)=0\\&h_{10,x_1x_1}(1,t)=-\tfrac{L_2^3}{\rho_1 L_1^6}u_{20}+\tfrac{m_1}{\rho_1 L_1^3}\hat{V}_1(1,t)\\&h_{10,x_1x_1x_1}(1,t)=\left(\tfrac{M_2}{\rho_1 L_1}+\tfrac{\rho_2}{\rho_1 L_1 L_2}\right)\ddot{\theta}_1+\\&\tfrac{\rho_2 L_2^2}{2\rho_1 L_1^2}(\ddot{\theta}_1+\ddot{\theta}_2)\cos\theta_2-\\&\tfrac{\rho_2 L_2^2}{2\rho_1 L_1^2}(\dot{\theta}_1^2-\dot{\theta}_2^2)\sin\theta_2+\tfrac{m_1}{\rho_1 L_1^3}\hat{V}_{1,x_1}(1,t)\end{aligned} \tag{5.22}$$

Boundary conditions for link 2:

$$
\begin{aligned}
&h_{20}(0,t) = h_{20,x_2}(0,t) = 0 \\
&h_{20,x_2x_2}(1,t) = \tfrac{m_2}{\rho_2 L_2^3}\hat{V}_2(1,t) \\
&h_{20,x_2x_2x_2}(1,t) = \tfrac{m_2}{\rho_2 L_2^3}\hat{V}_{2,x_2}(1,t)\,.
\end{aligned}
\tag{5.23}
$$

In Bailey and Hubbard [8], it is shown that a uniformly spatially varying voltage distribution fails to control even-numbered modes of many types of vibrating beams. But in this section, we propose a uniform distribution for the film since our assumed geometric boundary conditions are clamped-free which are controllable via this distribution (Burke and Hubbard [10]). The shape of the actuator's spatial component is obtained by cutting the film into the desired shape and adhering it to the longitudinal faces of the beams. This implies that only the temporal component of the film voltage can be varied since the shape of the film must be determined *a priori*. Thus, our control strategy focuses on the type of control that would be most effective for the temporal component of the film distribution.

It is proposed here that feedback for this time-varying voltage will enhance the damping properties of the actuator. There are two primary types of feedback currently being considered: (a.) feedback of position error obtained from hub angle measurements and (b.) feedback of endpoint acceleration as is done in Kotnik et al. [123] for a one-link flexible manipulator. Strategy (a.) showed the most encouraging results of the two, however, both methods proved feasible. Results of these simulations appear in a later section.

5.1.3 Approximate Feedback Linearization

From (5.13) and (5.14), we choose the control terms u_{i0} to linearize the O(1) slow subsystem dynamics. This is simply the linearization of the rigid manipulator dynamics and can be done via the well-known computed torque method as is suggested by Spong et al. [2] and Siciliano and Book [3]. Because of the reliance on the rigid link angles and their derivatives in the calculations, the following assumption is made.

Assumption 5.2 θ_i, $\dot{\theta}_i$ are assumed to be measurable.

Assumption 5.2 is quite reasonable since fairly inexpensive hardware is available for such purposes, e.g., shaft encoders and tachometers. The computed torque method will not require the measurement or estimation of joint acceleration, $\ddot{\theta}_i$, thus negating the need for differentiation of measured signals. With the rigid linearizing control law, the O(1) equations for the corrected slow manifold (i.e., the slow subsystem) are as follows:

O(1) rigid body motion equation for link 1:

$$\left(J + \frac{\rho_2}{3L_1^3}\right)\ddot{\theta}_1 + \frac{\rho_2}{3L_1^3}\,\ddot{\theta}_2 = v_1 \tag{5.24}$$

O(1) rigid body motion equation for link 2:

$$\frac{\rho_2}{3L_1}\,\ddot{\theta}_1 + \frac{\rho_2}{3L_1}\,\ddot{\theta}_2 = v_2 \tag{5.25}$$

where v_i are the external inputs needed to implement the desired slewing behavior.

The above equations imply that the $O(1)$ feedback linearization strategy results in two double integrators which are well known to be controllable through PD feedback (i.e., joint angle and velocity feedback). We now briefly discuss how the PD control gains can be chosen from the linearized model. First, we put the linearized model into state space form by defining the following states

$$\begin{aligned} \xi_1 &= \theta_1 - \theta_1^*\,, \quad \xi_2 = \dot{\theta}_1 \\ \xi_3 &= \theta_2 - \theta_2^*\,, \quad \xi_4 = \dot{\theta}_2 \end{aligned} \tag{5.26}$$

where θ_i^* is the desired slewing angle for the ith link. Next, we define two physical constants

$$m_1 = I_h + \frac{1}{3}\rho_1 L_1^3 + \frac{1}{3}\rho_2 L_2^3 + M_2 L_1^2 + \rho_2 L_1^2 L_2 \tag{5.27}$$

$$m_2 = \frac{1}{3}\rho_2 L_2^3 \tag{5.28}$$

which allows us to express the linearized model as

$$\begin{bmatrix} \dot{\xi}_1 \\ \dot{\xi}_2 \\ \dot{\xi}_3 \\ \dot{\xi}_4 \end{bmatrix} = \begin{bmatrix} 0 & 1 & 0 & 0 \\ 0 & 0 & 0 & 0 \\ 0 & 0 & 0 & 1 \\ 0 & 0 & 0 & 0 \end{bmatrix} \begin{bmatrix} \xi_1 \\ \xi_2 \\ \xi_3 \\ \xi_4 \end{bmatrix} + \begin{bmatrix} 0 & 0 \\ \frac{1}{m_1 - m_2} & \frac{-1}{m_1 - m_2} \\ 0 & 0 \\ \frac{-1}{m_1 - m_2} & \frac{m_1}{m_2(m_1 - m_2)} \end{bmatrix} \begin{bmatrix} v_1 \\ v_2 \end{bmatrix}. \tag{5.29}$$

This system has four poles at the origin and its controllability matrix has full rank. Now we define the decentralized feedback laws

$$v_1 = g_{11}\xi_1 + g_{12}\xi_2\,, \quad v_2 = g_{21}\xi_3 + g_{22}\xi_4 \tag{5.30}$$

where the goal is to choose the gains to obtain moderately damped poles without choosing the gains too high so as to excite vibrational modes through the effect of higher order nonlinearities.

Following standard pole placement design techniques, it was decided to place the poles such that two of them are a complex conjugate pair with approximately 3% damping with the other two on the negative real axis. With physical constants of $m_1 = 2.02$ kg-m^2 and $m_2 = 0.0046$ kg-m^2, the gains obtained were $g_{11} = g_{12} = -10$, $g_{21} = -0.5$, and $g_{22} = -0.02$. Other pole placements were analyzed, however as damping increases so do the gains which results in the excitation of higher order nonlinearities. The oscillations in the joint trajectories were particularly sensitive to the velocity gains g_{i2}. Smaller gains resulted in longer settling times. Thus, to achieve greater damping without exciting higher order nonlinearities, the corrective ($O(\epsilon)$) control is needed.

The remainder of the feedback linearization strategy is to choose the control terms u_{ij} to cancel nonlinearities in the $O(\epsilon^j)$ equations. This can be done to an arbitrary power of ϵ. In the appendix, a detailed description of the $O(\epsilon)$ linearizing controller is presented. This control law represents a higher order correction to the rigid linearizing controller. The decision as to when to incorporate the higher order control law will depend upon the particular structure involved. Generally, flexible structures with principal vibratory modes under 10 Hz will benefit from higher order control laws. But, only very flexible structures (ϵ's greater than 0.1) would require anything more than the $O(\epsilon)$ control law. The addition of the distributed actuator will alleviate much of the elasticity problem, but the higher order control law may reduce the amount of energy the distributed actuator is required to add to the system.

5.1.4 Simulation Results

In this subsection, results of our computer simulations on a two-link flexible manipulator are presented with plots of the system's performance appearing at the end of the section. The computer program which handles the simulations implements a finite-dimensional model of the system using the assumed modes method. This method and the derivation of the model are illustrated in the appendix. Also included in the appendix are the structural dimensions of the OSU two-link flexible manipulator upon which this model is based. Gravity effects are not incorporated in the model, but viscous damping is present in the model. The simulated sampling time was 10 milliseconds and a 5th order Runge-Kutta differential equation solver with adaptive stepsize was utilized for solving the system differential equations.

The program simulates a one-mode expansion for each link as derived in the appendix. The first link is modeled as clamped at one end with a mass and moment of inertia at the other end representing the second joint/link assembly. The second link is modeled as clamped-free. These assumed mode shapes represent our effort to accurately include the analytical boundary conditions (5.22),(5.23). The details of these mode shapes are discussed in the appendix. The experimental results in Yurkovich et al. [13] indicate only one mode is apparent in each link, thus a one-

mode approximation is justified. The modal frequencies obtained from FFT plots of tip position are 1.6 Hz for the first link and 1.5 Hz for the second link. From (5.6), $\epsilon_1 = 0.0282$ and $\epsilon_2 = 0.0315$ using data from the appendix. Since $\epsilon_i \propto \frac{1}{\omega_i^2}$, the ratio predicted by the ϵ values is $\frac{\omega_2}{\omega_1} = 0.946$ which is very close to the simulation results of $\frac{\omega_2}{\omega_1} = 0.938$.

The torque control consisted of a PD component plus the O(1) linearizing control described in the last section. The PD controller consists of constant feedback of the shaft velocities and constant feedback of the position error of the rigid link angles. The procedure for choosing the gains for the PD control was explained in Sect. 5.1.3. The distributed actuator control consists of a spatially uniform component and a temporal component consisting of constant position error feedback as described in Sect. 5.1.2. Several other types of feedback were implemented including tip acceleration and tip deflection, however the position error feedback achieved the most encouraging results and in a physical system it would be easy to measure. The boundary conditions (5.22),(5.23) are incorporated in the distributed control law via distribution theory since the uniform spatial distribution must be differentiated twice at the boundaries (which involves taking derivatives of delta distributions).

In all plots the first link is initially displaced 45 degrees above a reference line and the second link is initially displaced yet another 45 degrees from the first link. All angular velocities and accelerations are initially zero and so is the initial tip deflection, velocity, and acceleration. The desired final position is for the two links to be on a straight line with each other at the reference line, i.e., $\theta_1 = \theta_2 = 0$ and both links at rest. That is, both links are slewed through an angle of 45 degrees. The film actuator simulated here is a normalized model of the one described in Bailey and Hubbard [8] and Burke and Hubbard [9, 10]. This implies that the film physical constants are simply embedded in the applied voltage. Thus, the results obtained are applicable to many types of film actuators.

Figures 24 and 25 show the joint angles and velocities vs. time for the above described torque control and slewing maneuvers but without the film actuator. It can be seen that the links achieved their desired positions in about 3 s. The joint angle and velocity responses of link 2 oscillate as is seen in Figs. 24 and 25 but this is not the case for link 1. The first link has a much heavier mass than the second link (about 10 times as heavy as link 2) making it more difficult to oscillate. Also, nonlinearities of $O(\epsilon)$ (which are not cancelled by the torque law) create a more overdamped response at the joint of link 1. Figure 24 shows the hub angle responses with PD control and the O(1) linearizing control. Plots not shown here indicate that PD control by itself has a very similar response to Fig. 24, but the responses take approx. 0.5 s longer to settle down. Thus, the linearization helps but not substantially. The addition of the distributed actuator has little effect on the hub angle profiles.

Figures 26 and 27 illustrate the tip deflections with and without the film actuator. The torque control applied is exactly the same as in Figs. 24 and 25. As can be seen,

the maximum absolute deflection has been reduced in the first link from 3.9 cm to 2.4 cm, and in the second link from 8.7 cm to 3.7 cm. The improvement is most noticeable in the second link (approx. 60% reduction) which would normally be the payload-carrying link. The distributed actuator force for link 1 is overdamped, thus the reason for the reduction of deflection in link 1 on the positive side but not on the negative side as is apparent in Fig. 26. The small phase shift evident in the tip deflections of the second link is due to the position error feedback of the film actuator. The film feeds back the position error in a decentralized fashion, i.e., the ith link's film feeds back the ith link's joint angle error. Because of the nonlinearities in the flexure equations (which are of $O(\epsilon)$ and are not linearized by the torque controller here), there is a small phase shift between the joint angles and tip deflection.

Also important in vibrational dampening is the reduction of tip velocity. One can imagine a payload on the tip of the second link and the importance of keeping the endpoint speed at a minimum. The plots in Figs. 28 and 29 indicate that the tip velocities are reduced particularly in the second link whose maximum endpoint velocity has been reduced by a factor of 6. The tip velocities also settle faster with the film actuator than without it. The final plots illustrated in Figs. 30 and 31 show the applied control energy at the hubs as well as the applied film actuator force. As expected, the torque applied at the first joint is more than that applied at the second joint due to the heavier mass of the the first link. The film actuator force applied to the links is similar in shape to the joint controls (due to the position error feedback) but on a different scale.

5.1.5 Conclusions

In this section we have proposed a design methodology for the control of a two-link flexible robot. Our approach differs from others in that we combine an approximate feedback linearization strategy via hub actuation with distributed vibration control. The distributed actuator consists of a thin film that can theoretically dampen an infinite number of vibrational modes of flexible beams if a properly chosen spatial distribution is applied to the polymer. The time-varying component of the actuator voltage may incorporate feedback of the position error or possibly the tip acceleration of each link in a decentralized fashion. The film actuator acts as a kind of fast control which speeds convergence to an approximate slow manifold and thus, allows more accurate rigid body control. We also consider the distributed parameter model of the dynamics of the flexible links to design the approximate linearizing control laws. The simulation results show that the film actuator does reduce flexural vibrations as compared to joint control alone. Further research should be focused on improvements in feedback schemes for the distributed actuator as well as incorporating other strategies for the rigid body motion control such as sliding mode control and pointwise optimal control (see Young and Özgüner [124] and Tadikonda and Baruh [125]).

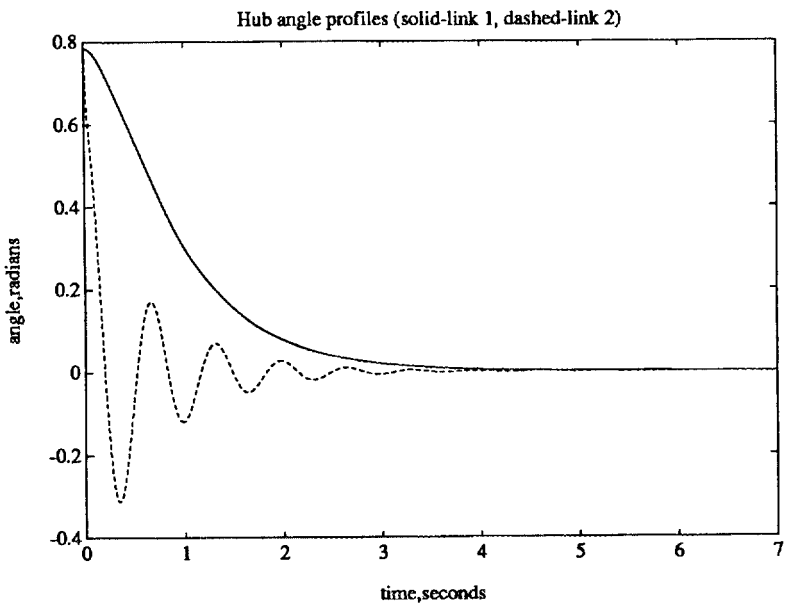

Fig. 24: Joint angle plots with PD feedback and O(1) linearizing control.

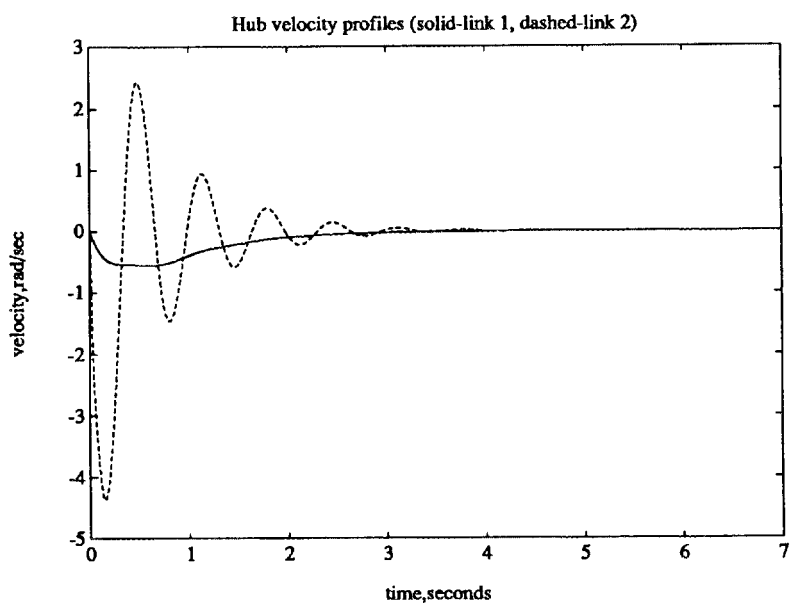

Fig. 25: Joint velocity plots with PD feedback and O(1) linearizing control.

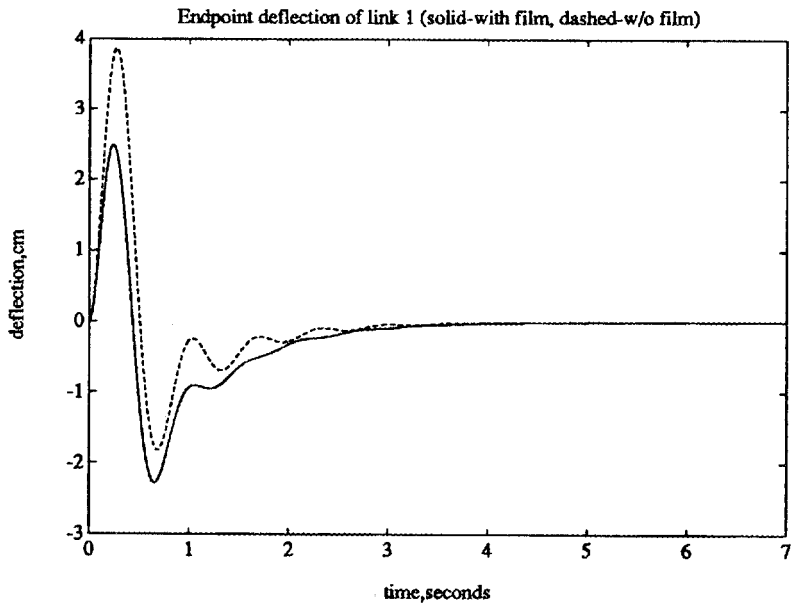

Fig. 26: Tip deflections of link 1 with and without distributed actuator.

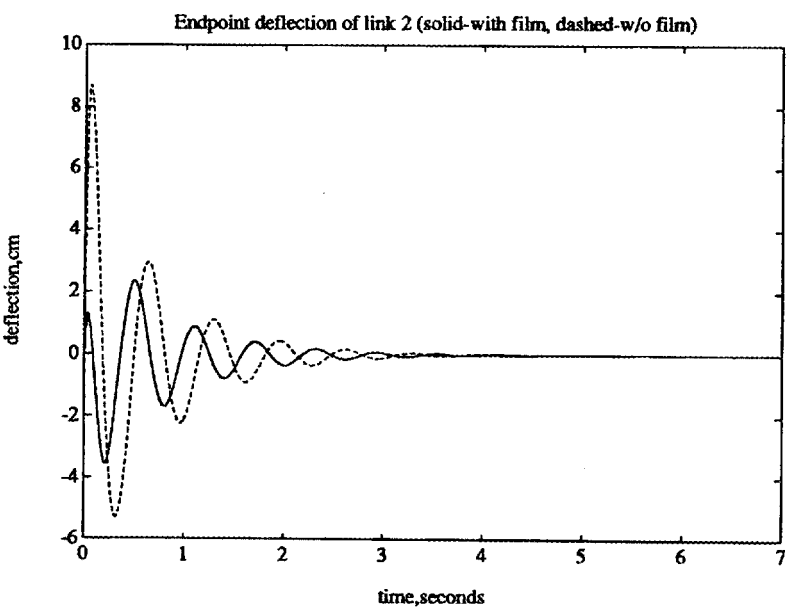

Fig. 27: Tip deflections of link 2 with and without distributed actuator.

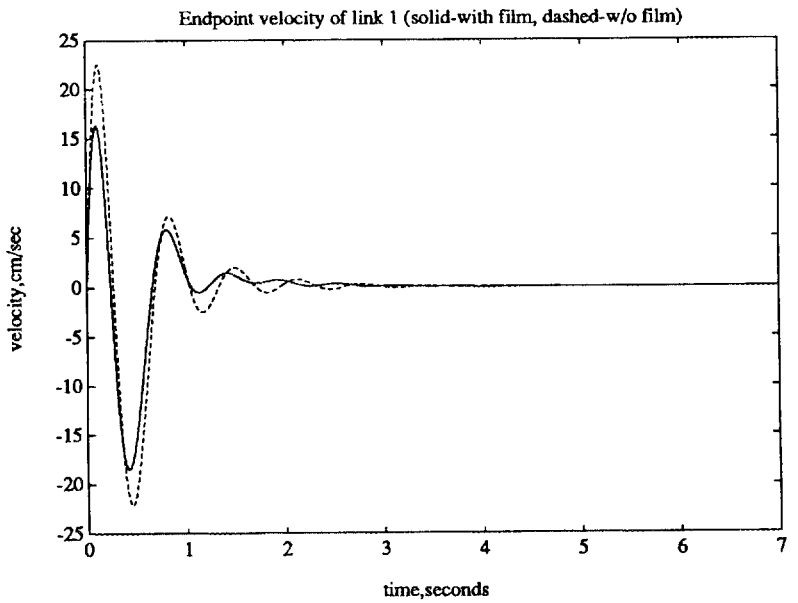

Fig. 28: Tip velocities of link 1 with and without distributed actuator.

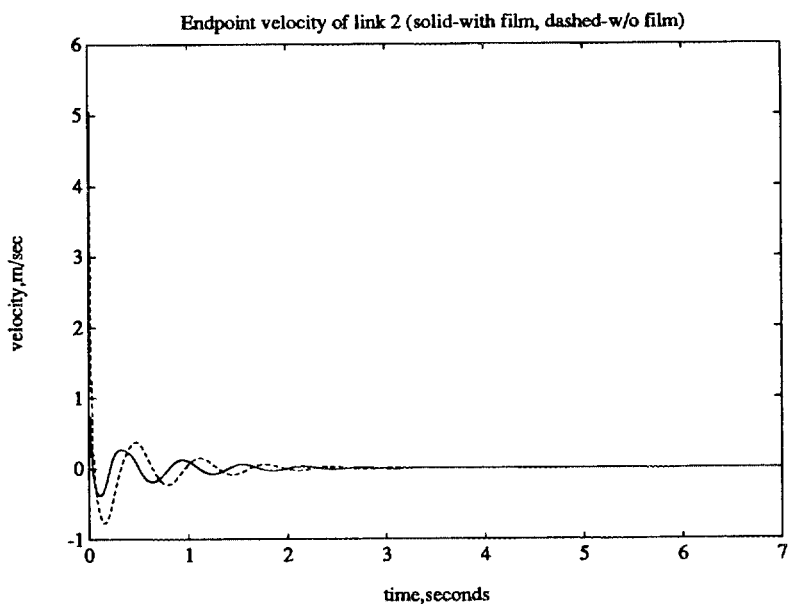

Fig. 29: Tip velocities of link 2 with and without distributed actuator.

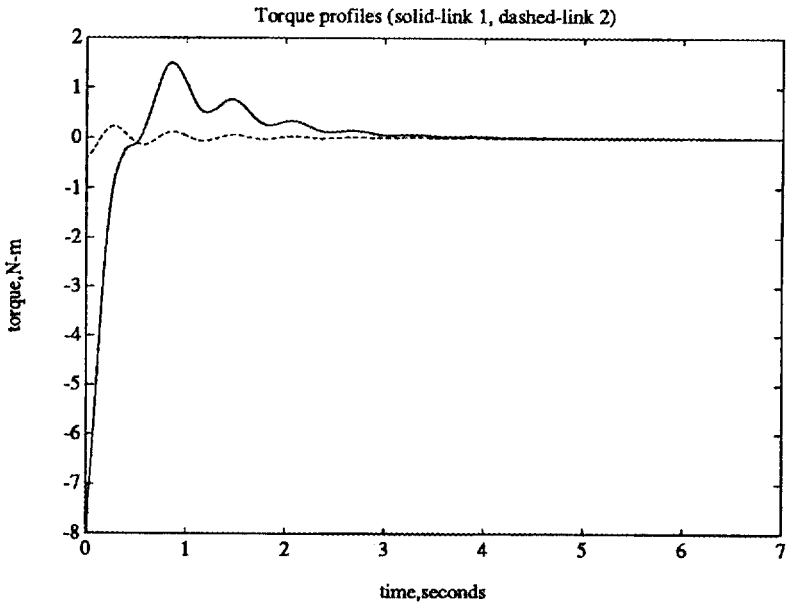

Fig. 30: Profiles of hub actuator energy.

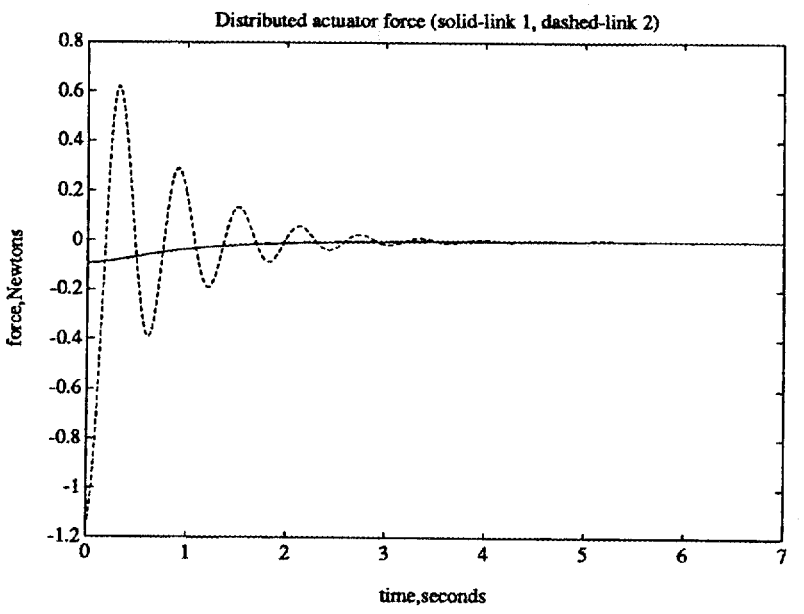

Fig. 31: Profiles of distributed actuator force.

5.2 APPLICATIONS OF SENSITIVITY MODELS TO THE SPACE STATION

Space Station Freedom is one of the largest collaborative space projects ever undertaken by NASA. It involves not only NASA but several large aerospace corporations as well as other countries including the European Community and Japan. The goal of this structure, when complete, is to orbit the earth as a permanently manned station for space experimentation and exploration of man-space interaction issues. It will also serve as a docking station for the space shuttle. Since it will have to supply its own power generation, the issue of self-sustaining power systems in space will be dealt with as well. Figure 32 shows a diagram of the space station with many of its most important components labeled.

The primary attitudinal control element of the station is the control moment gyro (CMG) near the center. Also located at the center is the guidance, navigation, and control (GNC) unit. This will determine the location of the sun and provide information to each solar array panel as to its correct orientation to track the sun. The control elements that position the array panels are the alpha and beta gimbals. Each of these gimbals is a large brushless, direct drive dc motor that turns about a single axis. The combination of these gimbals enable the array panels to track virtually any sun trajectory. The center of the station will also house the astronaut's quarters and experimentation areas as well as the shuttle docking port. The primary focus of this section, however, is on the beta gimbals which are attached to the solar array panels. The control of this gimbal is hampered by many factors such as station vibrations, array panel flexibility, plume impingement from shuttle dockings, and friction to name just a few. It is this last factor that motivates the work of this section. In particular, the uncertainty surrounding the magnitudes and types of motor friction at the beta gimbals make the area of sensitivity analysis a natural one for consideration.

The problem of motor control in the presence of friction has been a subject of considerable interest for many years. Most large systems require some kind of actuation, and these actuators are often plagued by friction. A principal issue in pointing control is the modeling of friction in the motors and bearings (for a survey on friction see Ref. [126]). In a report by Rocketdyne [127], the dynamics of the beta gimbals are described with the inclusion of three types of friction: Coulomb, Dahl, and viscous. Both Coulomb and Dahl friction are nonlinear which necessitates the use of linearization in obtaining linear models for control designs. It is desired to control the beta gimbals optimally with respect to a quadratic cost criterion that penalizes tracking deviations as well as energy output from the motor.

Since friction models are difficult to experimentally derive, it is useful to include a term in the cost criterion which will take into account uncertainty in the friction parameters. This is done by including a sensitivity model in the feedback loop. The

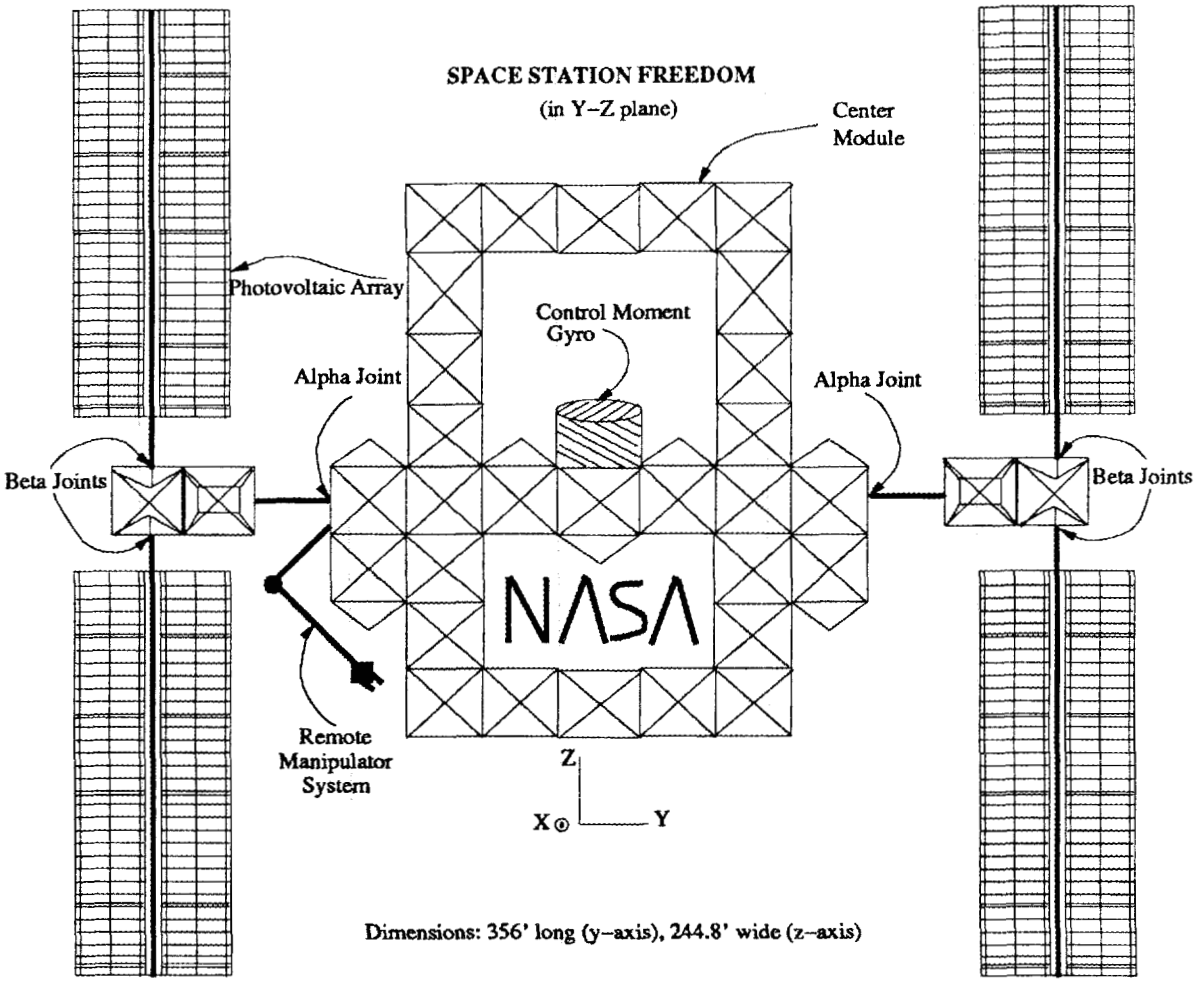

Fig. 32: Illustration of Space Station Freedom.

sensitivity model derives the partial derivative of the state with respect to uncertain friction parameters. These functions provide a measure of how the system state will change if the uncertain parameters deviate from their nominal values. We include a quadratic penalty on these functions which will induce control laws that are less sensitive to deviations from nominal friction parameters. While pursuing sensitivity analysis with respect to these parameters, the small deviations are for these parameters only. The overall model continues to be nonlinear.

The friction models incorporated in the beta gimbal dynamics are based upon theoretical and experimental analysis done at both the NASA Lewis Research Center and the Rocketdyne division of Rockwell International. Coulomb and viscous friction

are present in the motor itself whereas Dahl friction is primarily in the bearings. Viscous friction is a form of linear damping and is simple to model, but Coulomb friction is a function of the sign of the relative angular velocity between the array panel and the station inertial frame. The Dahl model [128] is a first order dynamic model that depends on not only the sign of the relative velocity but also the square of a more complicated expression. Thus, it will be highly nonlinear. Nonetheless, the tools of sensitivity analysis are still applicable. Furthermore, a fourth type of friction, namely static friction, is also included in this model. This is the amount of torque required to overcome the inertia in the motor and its load to get the rotor moving. It does not enter the dynamics directly but rather as an inequality, and thus no sensitivity function for static friction is computed.

The procedure outlined in this section is as follows. First, the beta gimbal dynamics are utilized to derive a sensitivity model for each of the uncertain friction parameters. Second, an optimal control law is designed via linear quadratic regulator theory with the incorporation of a term penalizing the sensitivity functions. This control law is based upon a linearized model of the beta gimbal dynamics. Finally, some discussion of future analysis and simulations is presented.

5.2.1 Generation of Sensitivity Models

The beta gimbal dynamics as detailed in Ref. [127] are arranged in block diagram form in Fig. 33. From this diagram, the equations governing the beta gimbal/solar array panel assembly can be obtained.

If $T_S > \mid K_T I_M + J_T \ddot{\theta}_R \mid$, then

$$\begin{aligned} \dot{I}_M &= -\frac{K_{BEMF}}{L_M}\dot{\theta}_R - \frac{R_M}{L_M} I_M + \frac{1}{L_M} V_M \\ \ddot{\theta}_R &= 0 \\ \dot{T}_D &= 0 \end{aligned} \tag{5.31}$$

else

$$\begin{aligned} \dot{I}_M &= -\frac{K_{BEMF}}{L_M}\dot{\theta}_R - \frac{R_M}{L_M} I_M + \frac{1}{L_M} V_M \\ \ddot{\theta}_R &= \frac{K_T}{J_T} I_M - \frac{K_{VS}}{J_T}\dot{\theta}_R - \frac{T_C}{J_T}\mathrm{sgn}(\dot{\theta}_R) - \frac{1}{J_T} T_D - \ddot{\theta}_S \\ \dot{T}_D &= \{\sigma \mid 1 - \frac{T_D}{T_{DL}}\mathrm{sgn}(\dot{\theta}_R) \mid^2 \mathrm{sgn}(1 - \frac{T_D}{T_{DL}}\mathrm{sgn}(\dot{\theta}_R))\}\dot{\theta}_R \end{aligned} \tag{5.32}$$

where the terms are defined in Table 5. The sign function is defined as

$$\mathrm{sgn}(x) = \begin{cases} 1 & x > 0 \\ 0 & x = 0 \\ -1 & x < 0 \end{cases} . \tag{5.33}$$

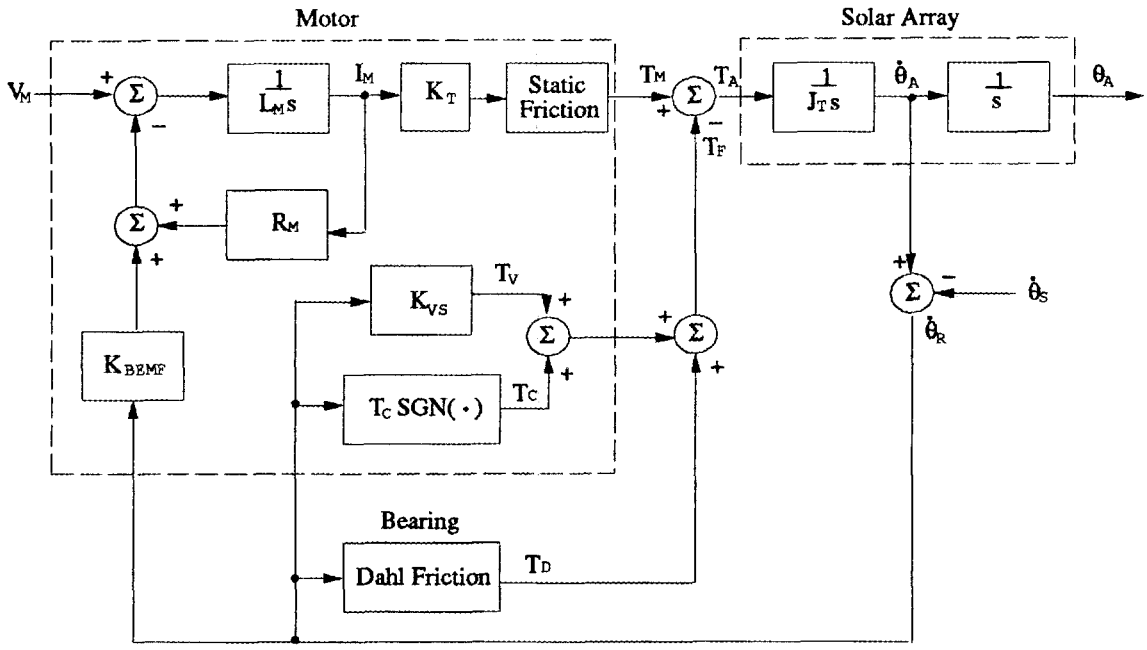

Fig. 33: Dynamics of beta gimbal and solar array panel.

The Dahl friction term T_D represents bearing friction in the beta gimbals and is hysteretic in nature. In the paper by Dahl [128], several models of solid friction damping in mechanical vibrations are proposed to explain bearing friction. The above first order nonlinear differential equation for T_D is one such model which has achieved wide use in simulation studies involving ball bearing friction. Other simpler (i.e., nondynamic) models of bearing friction exist, but currently we pursue the more rigorous model above.

The state space description is obtained by letting $x_1 = I_M$, $x_2 = \theta_R - \theta_R^*$, $x_3 = \dot{\theta}_R$, and $x_4 = T_D$ where θ_R^* is a constant setpoint that represents the desired tracking angle. The unknown parameters are defined as $\alpha_1 = K_{VS}$, $\alpha_2 = T_C$, and $\alpha_3 = T_{DL}$ which are the friction parameters. Concentrating on the case when the gimbal joint is moving (thus ignoring static friction), results in the state space equations

$$\begin{bmatrix} \dot{x}_1 \\ \dot{x}_2 \\ \dot{x}_3 \\ \dot{x}_4 \end{bmatrix} = \begin{bmatrix} -\frac{R_M}{L_M}x_1 - \frac{K_{BEMF}}{L_M}x_3 \\ x_3 \\ \frac{K_T}{J_T}x_1 - \frac{\alpha_1}{J_T}x_3 - \frac{\alpha_2}{J_T}\mathrm{sgn}(x_3) - \frac{1}{J_T}x_4 - \ddot{\theta}_S \\ \{\sigma \left|1 - \frac{x_4}{\alpha_3}\mathrm{sgn}(x_3)\right|^2 \mathrm{sgn}(1 - \frac{x_4}{\alpha_3}\mathrm{sgn}(x_3))\}x_3 \end{bmatrix} + \begin{bmatrix} \frac{1}{L_M} \\ 0 \\ 0 \\ 0 \end{bmatrix} V_M \quad (5.34)$$

with the compact form

$$\dot{x} = f(x, \alpha, \ddot{\theta}_S) + g(x)u \quad (5.35)$$

Table 5: Terms used in gimbal and array panel dynamics

$\theta_A, \dot{\theta}_A$	Solar array inertial angle and rate
$\theta_R, \dot{\theta}_R$	Relative solar array angle and rate
$\theta_S, \dot{\theta}_S$	Station inertial angle and rate
I_M	Current applied to motor
J_T	Solar array mass moment of inertia
L_M, R_M	Motor armature inductance and resistance
K_{BEMF}	Back EMF constant
K_T	Motor torque to current constant
K_{VS}	Motor viscous friction constant
T_A	Torque applied to base of array
T_C	Motor Coulomb friction
T_D	Dahl bearing friction
σ	Dahl friction slope
T_{DL}	Dahl friction limit
T_S	Static friction torque
T_F	Total friction torque
T_M	Drive motor torque
T_V	Motor viscous friction torque
V_M	Input motor voltage

where $u = V_M$ is our control and $\alpha = [\alpha_1\ \alpha_2\ \alpha_3]^T$.

The state trajectory sensitivity functions are defined as the partial derivative of the state with respect to the parameter of interest (see Sect. 2.3 for a survey on sensitivity analysis). These sensitivity functions can be generated by simulating the following linear differential equation

$$\frac{\partial \dot{x}}{\partial \alpha_i} = \frac{\partial f}{\partial x}\frac{\partial x}{\partial \alpha_i} + \frac{\partial f}{\partial \alpha_i}, \quad i = 1, 2, 3 \tag{5.36}$$

where

$$\frac{\partial f}{\partial x} = \begin{bmatrix} -\frac{R_M}{L_M} & 0 & -\frac{K_{BEMF}}{L_M} & 0 \\ 0 & 0 & 1 & 0 \\ \frac{K_T}{J_T} & 0 & -\frac{\alpha_1}{J_T} & -\frac{1}{J_T} \\ 0 & 0 & \tau_1(x,\alpha) & \tau_2(x,\alpha) \end{bmatrix} \tag{5.37}$$

$$\tau_1(x,\alpha) = \sigma(1-\frac{x_4}{\alpha_3}\mathrm{sgn}(x_3))^2\mathrm{sgn}(1-\frac{x_4}{\alpha_3}\mathrm{sgn}(x_3)) \tag{5.38}$$

$$\tau_2(x,\alpha) = -2\sigma(1-\frac{x_4}{\alpha_3}\mathrm{sgn}(x_3))\frac{\mathrm{sgn}(x_3)}{\alpha_3}\mathrm{sgn}(1-\frac{x_4}{\alpha_3}\mathrm{sgn}(x_3))x_3 \tag{5.39}$$

$$\frac{\partial f}{\partial \alpha_1} = \begin{bmatrix} 0 \\ 0 \\ -x_3 \\ 0 \end{bmatrix} \tag{5.40}$$

$$\frac{\partial f}{\partial \alpha_2} = \begin{bmatrix} 0 \\ 0 \\ -\mathrm{sgn}(x_3) \\ 0 \end{bmatrix} \tag{5.41}$$

$$\frac{\partial f}{\partial \alpha_3} = \begin{bmatrix} 0 \\ 0 \\ 0 \\ 2\sigma\left(1-\frac{x_4}{\alpha_3}\mathrm{sgn}(x_3)\right)\frac{x_4\mathrm{sgn}(x_3)}{\alpha_3^2}\mathrm{sgn}\left(1-\frac{x_4}{\alpha_3}\mathrm{sgn}(x_3)\right)x_3 \end{bmatrix} \tag{5.42}$$

which is obtained by differentiating (5.35) with respect to α_i. This model is linear in the sensitivity functions even though the right hand side of (5.36) is nonlinear in x. In this case, (5.36) is a linear time-varying differential equation. The above equation also assumes that u and $\ddot{\theta}_S$ are independent of α_i.

Ordinarily, one is interested in the behavior of the state trajectory sensitivity functions in a neighborhood about some nominal parameter values. This implies that one would evaluate all instances of α_i with their known nominal values on the right hand sides (5.36)-(5.42). Thus, all parameters of the sensitivity model would be known. The above model is most useful for rather small deviations in the friction parameters from their nominal values. Relative parameter deviations of more than 20% probably require the inclusion of second order sensitivity functions (see [65]) which are a straightforward extension to the above model.

5.2.2 Optimal Control Design

It is desired to control the positioning of the solar array panels via optimal control. The standard linear quadratic regulator is a useful tool to achieve this goal, but the model described by (5.34) possesses uncertainty in its parameters due to unknown friction models. It is of interest here to include an additional term in the cost criterion that penalizes nonzero sensitivity functions. This would have the effect of inducing control laws that minimize the influence on the system state by uncertainty in friction

model parameters. This motivates the following performance criterion

$$J = \int_0^\infty [x^T Q x + u^T R u + \sum_{i=1}^{3} \lambda_i^T S_i \lambda_i] dt \tag{5.43}$$

where $\lambda_i = \frac{\partial x}{\partial \alpha_i}$, R is positive definite, and Q, S_i are positive semi-definite matrices.

To find the control law that minimizes J will require an augmented state vector

$$\tilde{x} = \left[x^T \ \lambda_1^T \ \lambda_2^T \ \lambda_3^T\right]^T \tag{5.44}$$

which has the following dynamical description

$$\dot{\tilde{x}} = \begin{bmatrix} f(x, \alpha, \ddot{\theta}_S) \\ \frac{\partial f}{\partial \alpha_1} + \frac{\partial f}{\partial x}\lambda_1 \\ \vdots \\ \frac{\partial f}{\partial \alpha_4} + \frac{\partial f}{\partial x}\lambda_4 \end{bmatrix} + \begin{bmatrix} g(x) \\ 0 \\ \vdots \\ 0 \end{bmatrix} u \tag{5.45}$$

or more compactly

$$\dot{\tilde{x}} = \tilde{f}(\tilde{x}) + \tilde{g}(\tilde{x}) u \ . \tag{5.46}$$

The above transforms (5.43) to

$$J = \int_0^\infty (\tilde{x}^T \tilde{Q} \tilde{x} + u^T R u) dt \tag{5.47}$$

where $\tilde{Q} = \text{block-diag}\,[Q \ S_1 \ \cdots \ S_3]$.

Now all that remains to be done is to linearize the system in (5.45). Once linearization is accomplished, the quadratic regulator can be set up to solve for the control gains. The approach utilized is that of Jacobian or Taylor series linearization which is done about an operating point. The linear quadratic regulator is then solved with this linearized system and the $\tilde{Q}$ and R matrices from above. A Riccati equation [95] will then be solved to obtain the gains for the optimal control law. Figure 34 illustrates this approach.

A linearized model can be obtained about the point $\tilde{x}^0$ as follows (if $\tilde{x}^0$ is not an equilibrium point of (5.45) then minor modifications must be made)

$$A = \frac{\partial \tilde{f}}{\partial \tilde{x}} \mid_{\tilde{x}=\tilde{x}^0} \ , \quad B = \tilde{g}(\tilde{x}) \mid_{\tilde{x}=\tilde{x}^0} \ . \tag{5.48}$$

The optimal control analysis is carried out by combining the cost criterion (5.47) with the above model. A Riccati equation utilizing the A and B matrices from (5.48) will yield the optimal control gains for the full system (5.45).

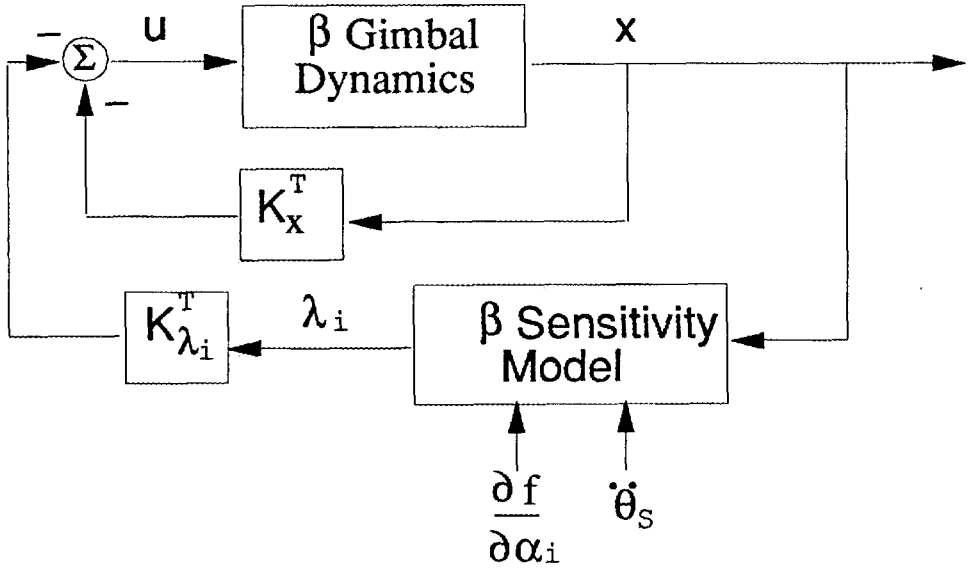

Fig. 34: Block diagram for optimal control with sensitivity functions.

Remark 5.1 The only reason for the linearization is to obtain a set of feedback gains for the control strategy. If one desires to utilize the nonlinear model to obtain gains the implementation of the control law is still the same. In addition, a PID control law can be realized with the PID gains obtained from the linear quadratic regulator. All that is needed is the addition of $x_5 = \int_0^\infty (\theta_R - \theta_R^*)dt$, $\dot{x}_5 = x_2$ to the state space dynamics (5.34).

Remark 5.2 Once physical parameters are included in the sensitivity model as well as the gimbal dynamics, computer simulations can be carried out to determine the choice of Q, R, and S_i matrices in the cost criterion. The simulation results may suggest further refinements to the control design depicted in Fig. 34, but the concept of sensitivity functions is a useful means to alleviate uncertainty in model parameters.

Remark 5.3 A reduction in model order can be achieved by utilizing singular perturbation theory. If the motor inductance L_M is small relative to the motor resistance R_M the first state can be eliminated by setting $L_M \dot{x}_1 = 0$. This will result in an algebraic equation for x_1 which can be substituted into the equation for $\dot{x}_3$. This reduction in model order not only saves on feedback terms but also improves simulation studies by eliminating the numerical stiffness of the dynamics (5.34) for small L_M.

CHAPTER 6

SUMMARY AND FUTURE RESEARCH

In this report, new results combining decentralized and nonlinear control techniques are developed. Performance issues such as optimality and robustness to parametric uncertainty are investigated as well. The goal of this work was to develop effective control schemes that could be utilized for the multi-body dynamical systems one often encounters on space structures, robotics, automotive systems, and automation devices. Since these systems often have multiple input-output ports and nonlinear dynamic behavior, decentralized nonlinear control was a natural field of endeavor. But often ignored in the study of nonlinear systems are the subjects of optimization and robustness. In Chap. 3, we introduced new methods for optimizing nonlinear systems and reducing parameter uncertainty effects in nonlinear systems. Both methods utilized feedback linearization which was a major theme of this dissertation.

Further research on optimization of nonlinear systems may involve investigation of more general nonlinear systems including those with zero dynamics, discontinuities, and partial differential equations. This may require the use of different methodologies including that of sliding mode theory and distributed parameter systems. Optimizing general nonlinear systems is a very computationally intense procedure, and any additional work on this subject should involve some numerical analysis of developed techniques. Parametric uncertainty is only one type of uncertainty encountered in dynamical systems. Unstructured uncertainty or unmodeled dynamics would be a next step of investigation. Very little has been done in this area. The standard tool for linear unstructured uncertainty is that of H^∞ methods. These methods have not been extended to nonlinear systems in any substantial way, but preliminary work by van der Schaft [88] has attacked the problem by applying H^∞ methods to the *linearized* system.

In Chap. 4, large-scale nonlinear systems are studied. The strategy was to convert these systems into linear ones and apply standard decentralized control techniques. But decentralized feedback linearization proved impossible to solve due to the absence of the full state for feedback. This led to the decentralized nonlinear observer problem as outlined in Chap. 4. It also motivated decentralized stabilization schemes in which the full system is not linearized, but instead a nominal linear system plus nonlinear perturbations is shown to be exponentially stabilizable. Further results on

enhancing the linearizability of multichannel nonlinear systems via partial feedback were presented.

A possible extension of these results could be achieved with sliding mode theory. In particular, the theory of nonlinear sliding observers could be extended to decentralized systems by applying the equivalent control method [87]. Another possibility looked into but not included in this report is that of decentralized nonlinear invertibility to allow reconstruction of the full state at each input-output channel. This idea would involve combining the concepts of decentralized linear observers and inversion of nonlinear systems. Mathematically, this would be difficult to implement but it may be possible to arrive at approximate methods.

The rest of Chap. 4 focused on sensitivity-based methods of handling parametric uncertainty in large-scale systems. Both linear and nonlinear systems were analyzed, but primary attention was paid to linear systems due to the difficulty in generating local sensitivity models for general nonlinear systems. An easily obtained extension to the decentralized optimal control result in that chapter is to take into account the interconnection terms by solving coupled Lyapunov equations [74]. Additional work on this topic might involve more thorough investigations of generating sensitivity models for nonlinear systems perhaps by using feedback linearization. Applications of this work could involve automotive systems where it may be desirable to handle robustness issues in a decentralized framework due to the expense in exchanging information over the whole car.

Chapter 5 focused on two applications of theory developed in this report with some modifications due to the nature of applied control. First, a two-link flexible manipulator is controlled via decentralized feedback linearization and decentralized distributed control. The feedback linearization is based on a singular perturbation approach. An asymptotic expansion of the manipulator dynamics as a power series in a small parameter representing stiffness of the links is carried out to determine the approximate feedback linearizing control laws. Each torque controller has its own feedback law requiring the use of only locally measurable signals. The distributed vibration control is carried out by a polymer actuator and also depends on signals available at its own link. This control strategy required extensive modeling effort to obtain equations solvable on a computer. This is detailed in the appendix. Though this control strategy is not an explicit application of the theory in Chap. 4, it does show how decentralized nonlinear control can be applied on a real system via approximate techniques and theoretical tools such as singular perturbations. Indeed, for most real-world applications, combinations of well-known control methods and approximate means will be needed to obtain satisfactory results.

Finally, Chap. 5 closed with a look at sensitivity analysis of the gimbal motors on Space Station Freedom. It was proposed that an optimal control law include feedback of the sensitivity functions to reduce the effects of friction parameter uncertainty on closed-loop performance. Much work remains to be done on this approach. As of

now, each gimbal motor will have a control law designed as though the gimbals are decoupled from each other. This strategy has been necessitated by the absence of simple control methods that would take into account interconnections between subsystems. This is as much a modeling problem as it is a control problem. Perhaps decentralized control can alleviate these interaction issues. Indeed, future work could apply the decentralized sensitivity results of Chap. 4 to larger parts of the space station.

REFERENCES

[1] M. Fliess and M. Hazewinkel, *Algebraic and Geometric Methods in Nonlinear Control Theory.* Dordrecht, Holland: D. Reidel, 1986.

[2] M. W. Spong, K. Khorasani, and P. V. Kokotović, "An integral manifold approach to the feedback control of flexible joint robots," *IEEE Journal of Robotics and Automation*, vol. RA–3, pp. 291–300, 1987.

[3] B. Siciliano and W. J. Book, "A singular perturbation approach to control of lightweight flexible manipulators," *International Journal of Robotics Research*, vol. 7, no. 4, pp. 79–90, 1988.

[4] S. Nicosia, P. Tomei, and A. Tornambè, "Nonlinear control and observation algorithms for a single–link flexible robot arm," *International Journal of Control*, vol. 49, pp. 827–840, 1989.

[5] A. De Luca and B. Siciliano, "Trajectory control of a non–linear one–link flexible arm," *International Journal of Control*, vol. 50, no. 5, pp. 1699–1715, 1989.

[6] X. Ding, T. J. Tarn, and A. K. Bejczy, "A novel approach to the modelling and control of flexible robot arms," in *Proceedings of the IEEE Conference on Decision and Control*, (Austin, TX), pp. 52–57, Dec. 1988.

[7] F. Khorrami and S. Zheng, "Vibration control of flexible–link manipulators," in *Proceedings of the American Control Conference*, (San Diego, CA), pp. 175–180, 1990.

[8] T. Bailey and J. E. Hubbard, Jr., "Distributed piezoelectric–polymer active vibration control of a cantilever beam," *Journal of Guidance and Control*, vol. 8, no. 5, pp. 605–611, 1985.

[9] S. E. Burke and J. E. Hubbard, Jr., "Active vibration control of a simply supported beam using a spatially distributed actuator," *IEEE Control Systems Magazine*, vol. 7, no. 4, pp. 25–30, 1987.

[10] S. E. Burke and J. E. Hubbard, Jr., "Distributed actuator control design for flexible beams," *Automatica*, vol. 24, no. 5, pp. 619–627, 1988.

[11] E. F. Crawley and J. de Luis, "Use of piezoelectric actuators as elements of intelligent structures," *AIAA Journal*, vol. 25, no. 10, pp. 1373–1385, 1987.

[12] S. A. Collins, R. J. Notestine, C. E. Padilla, M. Ramey, E. Schmitz, and A. H. von Flotow, "Design, manufacture, and application to space robotics of distributed piezoelectric film sensors," in *Proc. AIAA Conf. Guid. Nav. Contr.*, pp. 1899–1906, 1990.

[13] S. Yurkovich, A. P. Tzes, and K. L. Hillsley, "Controlling coupled flexible links rotating in the horizontal plane," in *Proceedings of the American Control Conference*, (San Diego, CA), pp. 362–367, 1990.

[14] K. J. Astrom and B. Wittenmark, *Adaptive Control.* Reading, MA: Addison–Wesley, 1989.

[15] D. P. Atherton, *Nonlinear Control Engineering.* New York: Van Nostrand Reinhold, 1982.

[16] J. J. E. Slotine and W. Li, *Applied Nonlinear Control.* Englewood Cliffs, NJ: Prentice–Hall, 1991.

[17] M. Vidyasagar, *Nonlinear Systems Analysis.* Englewood Cliffs, NJ: Prentice–Hall, 1978.

[18] R. W. Brockett, "Feedback invariants for nonlinear systems," in *Proceedings of the IFAC World Congress*, (Helsinki, Finland), pp. 1115–1120, 1978.

[19] D. Cheng, A. Isidori, W. Respondek, and T. J. Tarn, "Exact linearization of nonlinear systems with outputs," *Mathematical Systems Theory*, vol. 21, pp. 63–83, 1988.

[20] L. R. Hunt, R. Su, and G. Meyer, "Global transformations of nonlinear systems," *IEEE Transactions on Automatic Control*, vol. AC-28, no. 1, pp. 24–31, 1983.

[21] A. Isidori, *Nonlinear Control Systems.* Berlin: Springer–Verlag, second ed., 1989.

[22] B. Jacubczyk and W. Respondek, "On linearization of control systems," *Bulletin de L'Acadèmie Polonaise des Sciences, Série des Sciences Mathématiques*, vol. 28, no. 9–10, pp. 517–522, 1980.

[23] M. Spivak, *A Comprehensive Introduction to Differential Geometry.* Houston, TX: Publish or Perish, 1979.

[24] A. J. Krener, "On the equivalence of control systems and the linearization of nonlinear systems," *SIAM J. Control and Optimization*, vol. 11, no. 4, pp. 670–676, 1973.

[25] L. R. Hunt, R. Su, and G. Meyer, "Design for multi-input nonlinear systems," in *Differential Geometric Control Theory* (R. W. Brockett, R. S. Millman, and H. J. Sussmann, eds.), pp. 268–298, Boston, MA: Birkhäuser, 1983.

[26] R. Su, "On the linear equivalents of nonlinear systems," *Systems and Control Letters*, vol. 2, no. 1, pp. 48–52, 1982.

[27] C. I. Byrnes and A. Isidori, "A frequency domain philosophy for nonlinear systems," in *Proceedings of the IEEE Conference on Decision and Control*, (Las Vegas, NV), pp. 1569–1573, Dec. 1984.

[28] W. T. Baumann and W. J. Rugh, "Feedback control of nonlinear systems by extended linearization," *IEEE Transactions on Automatic Control*, vol. AC–31, pp. 40–46, 1986.

[29] C. Réboulet, P. Mouyon, and C. Champetier, "About the local linearization of nonlinear systems," in *Algebraic and Geometric Methods in Nonlinear Control Theory* (M. Fliess and M. Hazewinkel, eds.), pp. 311–322, Dordrecht, Holland: D. Reidel, 1986.

[30] B. Charlet, J. Levine, and R. Marino, "On dynamic feedback linearization," *Systems and Control Letters*, vol. 13, pp. 143–151, 1989.

[31] H. Nijmeijer and A. J. van der Schaft, *Nonlinear Dynamical Control Systems.* Berlin: Springer–Verlag, 1990.

[32] P. Brunovsky, "A classification of linear controllable systems," *Kybernetika*, vol. 6, no. 3, pp. 173–188, 1970.

[33] A. Isidori, A. J. Krener, C. Gori–Giorgi, and S. Monaco, "Nonlinear decoupling via feedback: A differential geometric approach," *IEEE Transactions on Automatic Control*, vol. AC-26, no. 2, pp. 331–345, 1981.

[34] E. A. Misawa and J. K. Hedrick, "Nonlinear observers–A state–of–the–art survey," *ASME Transactions on Dynamic Systems, Measurement and Control*, vol. 111, pp. 344–352, 1989.

[35] D. Bestle and M. Zeitz, "Canonical form observer design for nonlinear time-variable systems," *International Journal of Control*, vol. 38, pp. 419–431, 1983.

[36] A. J. Krener and A. Isidori, "Linearization by output injection and nonlinear observers," *Systems and Control Letters*, vol. 3, pp. 47–52, 1983.

[37] A. J. Krener and W. Respondek, "Nonlinear observers with linearizable error dynamics," *SIAM J. Control and Optimization*, vol. 23, no. 2, pp. 197–216, 1985.

[38] M. Zeitz, "The extended Luenberger observer for nonlinear systems," *Systems and Control Letters*, vol. 9, pp. 149–156, 1987.

[39] A. N. Tikhonov, "On the dependence of solutions of differential equations on a small parameter," *Matematicheskii Sbornik*, vol. 22, pp. 193–204, 1948. (in Russian).

[40] A. B. Vasil'eva, "Asymptotic behavior of solutions to certain problems involving nonlinear differential equations containing a small parameter multiplying the highest derivatives," *Russian Math. Surveys*, vol. 18, pp. 13–81, 1963.

[41] F. Hoppensteadt, "Stability in systems with parameters," *Journal of Mathematical Analysis and Applications*, vol. 18, pp. 129–134, 1967.

[42] J. D. Cole, *Perturbation Methods in Applied Mathematics.* Waltham, MA: Blaisdell, 1968.

[43] A. Nayfeh, *Perturbation Methods.* New York: John Wiley and Sons, 1973.

[44] J. H. Chow and P. V. Kokotović, "A decomposition of near–optimum regulators for systems with slow and fast modes," *IEEE Transactions on Automatic Control*, vol. AC–21, pp. 701–705, 1976.

[45] H. K. Khalil and P. V. Kokotović, "Control strategies for decision makers using different models of the same system," *IEEE Transactions on Automatic Control*, vol. AC–23, pp. 289–298, 1978.

[46] P. V. Kokotović, H. K. Khalil, and J. O'Reilly, *Singular Perturbation Methods in Control: Analysis and Design.* London: Academic Press, 1986.

[47] P. Sannuti and P. V. Kokotović, "Near optimum design of linear systems by a singular perturbation method," *IEEE Transactions on Automatic Control*, vol. AC–14, pp. 15–22, 1969.

[48] K. K. D. Young, P. V. Kokotović, and V. I. Utkin, "A singular perturbation analysis of high-gain feedback systems," *IEEE Transactions on Automatic Control*, vol. AC–22, no. 6, pp. 931–938, 1977.

[49] B. D. Riedle and P. V. Kokotović, "Integral manifolds of slow adaptation," *IEEE Transactions on Automatic Control*, vol. AC-31, pp. 316–324, 1986.

[50] F. Khorrami and Ü. Özgüner, "Singular perturbation analysis of a distributed parameter model of flexible manipulators," in *Proceedings of the American Control Conference*, (Atlanta, GA), pp. 1704–1709, 1988.

[51] D. Schoenwald, Ü. Özgüner, and H. Chan, "An analysis of distributed vibration control of flexible manipulators using integral manifolds," in *Proceedings of the IEEE Conference on Decision and Control*, (Tampa, FL), pp. 2095–2100, Dec. 1989.

[52] Ü. Özgüner, "Near–optimal control of composite systems: The multi time–scale approach," *IEEE Transactions on Automatic Control*, vol. AC-24, no. 4, pp. 652–655, 1979.

[53] H. W. Bode, *Network Analysis and Feedback Amplifier Design.* Princeton, NJ: Van Nostrand Reinhold, 1945.

[54] I. M. Horowitz, *Synthesis of Feedback Systems.* New York: Academic Press, 1963.

[55] J. B. Cruz and W. R. Perkins, "A new approach to the sensitivity problem in multivariable feedback system design," *IEEE Transactions on Automatic Control*, vol. AC–9, pp. 216–223, 1964.

[56] P. V. Kokotović, "Method of sensitivity points in the investigation and optimization of linear control systems," *Automation and Remote Control*, vol. 25, pp. 1512–1518, 1964.

[57] D. F. Wilkie and W. R. Perkins, "Essential parameters in sensitivity analysis," *Automatica*, vol. 5, pp. 191–197, 1969.

[58] D. F. Wilkie and W. R. Perkins, "Generation of sensitivity functions for linear systems using low–order models," *IEEE Transactions on Automatic Control*, vol. AC–14, pp. 123–129, 1969.

[59] P. V. Osburn, H. P. Whitaker, and A. Kezer, "New developments in the design of model reference adaptive control systems," in *ISA 29th Annual Meeting*, (New York), 1961. Paper No. 61-39.

[60] P. Dorato, "On sensitivity in optimal control systems," *IEEE Transactions on Automatic Control*, vol. AC–8, pp. 256–257, 1963.

[61] S. Bingulac, J. H. Chow, and J. R. Winkelman, "Simultaneous generation of sensitivity functions–transfer function matrix approach," *Automatica*, vol. 24, no. 2, pp. 239–242, 1988.

[62] D. D. Šiljak, *Nonlinear Systems.* New York: Wiley, 1969.

[63] J. B. Cruz, *Feedback Systems.* New York: McGraw–Hill, 1972.

[64] J. B. Cruz, *System Sensitivity Analysis.* Stroudsburg, PA: Dowden, Hutchinson & Ross, 1973.

[65] P. M. Frank, *Introduction to System Sensitivity Theory.* New York: Academic Press, 1978.

[66] R. Tomović, *Sensitivity Analysis of Dynamic Systems.* New York: McGraw–Hill, 1963.

[67] P. V. Kokotović and R. S. Rutman, "Sensitivity of automatic control systems (survey)," *Automation and Remote Control*, vol. 26, pp. 727–749, 1965.

[68] S. H. Wang and E. J. Davison, "On the stabilization of decentralized control systems," *IEEE Transactions on Automatic Control*, vol. AC–18, pp. 473–478, 1973.

[69] D. D. Šiljak and M. Vukčević, "Decentralization, stabilization, and estimation of large–scale systems," *IEEE Transactions on Automatic Control*, vol. AC-21, pp. 363–366, 1976.

[70] E. J. Davison, "Multivariable tuning regulators: The feed–forward and robust control of a general servomechanism problem," *IEEE Transactions on Automatic Control*, vol. AC–21, pp. 35–47, 1976.

[71] E. J. Davison, "The robust control of a servomechanism problem for linear time–invariant multivariable systems," *IEEE Transactions on Automatic Control*, vol. AC–21, pp. 25–34, 1976.

[72] E. J. Davison, "The robust decentralized control of a general servomechanism problem," *IEEE Transactions on Automatic Control*, vol. AC–21, pp. 14–24, 1976.

[73] J. C. Geromel and J. Bernussou, "An algorithm for optimal decentralized regulation of linear quadratic interconnected systems," *Automatica*, vol. 15, pp. 489–491, 1979.

[74] J. C. Geromel and J. Bernussou, "Optimal decentralized control of dynamic systems," *Automatica*, vol. 18, pp. 545–557, 1982.

[75] M. K. Sundareshan, "Generation of multilevel control and estimation schemes," *IEEE Transactions on Systems, Man, and Cybernetics*, vol. SMC-7, pp. 144–152, 1977.

[76] E. F. Mageriou and Y. C. Ho, "Decentralized stabilization *via* game theoretic methods," *Automatica*, vol. 13, pp. 393–399, 1977.

[77] M. E. Sezer and D. D. Šiljak, "On decentralized stabilization and structure of linear large scale systems," *Automatica*, vol. 17, pp. 641–644, 1981.

[78] N. R. Sandell, Jr., P. Varaiya, M. Athans, and M. G. Safonov, "Survey of decentralized control methods for large–scale systems," *IEEE Transactions on Automatic Control*, vol. AC–23, pp. 108–128, 1978.

[79] M. Jamshidi, *Large–Scale Systems: Modeling and Control.* New York: North–Holland, 1983.

[80] D. D. Šiljak, *Decentralized Control of Complex Systems.* New York: Academic Press, 1991.

[81] M. S. Mahmoud, "Multilevel systems control and applications: A survey," *IEEE Transactions on Systems, Man, and Cybernetics*, vol. SMC-7, pp. 125–143, 1977.

[82] B. D. O. Anderson and D. J. Clements, "Algebraic characterization of fixed modes in decentralized control," *Automatica*, vol. 17, pp. 703–712, 1981.

[83] E. J. Davison and Ü. Özgüner, "Characterizations of decentralized fixed modes for interconnected systems," *Automatica*, vol. 19, pp. 169–182, 1983.

[84] F. Khorrami, S. Tien, and Ü. Özgüner, "DOLORES: A software package for analysis and design of optimal decentralized control," in *Proceedings of the 40th IEEE National Aerospace & Electronics Conference*, (Dayton, OH), pp. 1704–1709, 1988.

[85] A. Iftar and Ü. Özgüner, "Contractible controller design and optimal control with state and input inclusion," *Automatica*, vol. 25, 1989.

[86] W. S. Levine, T. L. Johnson, and M. Athans, "Optimal limited state variable feedback controllers for linear systems," *IEEE Transactions on Automatic Control*, vol. AC-16, no. 6, pp. 785–793, 1971.

[87] V. I. Utkin, "Variable structure systems with sliding mode: A survey," *IEEE Transactions on Automatic Control*, vol. AC–22, no. 2, pp. 212–222, 1977.

[88] A. J. van der Schaft, "On a state space approach to nonlinear H^∞ control," *Systems and Control Letters*, vol. 16, pp. 1–8, 1991.

[89] O. Akhrif and G. L. Blankenship, "Robust stabilization of feedback linearizable systems," in *Proceedings of the IEEE Conference on Decision and Control*, (Austin, TX), pp. 1714–1719, Dec. 1988.

[90] D. A. Schoenwald and Ü. Özgüner, "Robust feedback linearization of uncertain nonlinear systems," in *Proceedings of the American Control Conference*, (Chicago, IL), June 1992.

[91] M. W. Spong and H. Sira–Ramirez, "Robust control design techniques for a class of nonlinear systems," in *Proceedings of the American Control Conference*, (Seattle, WA), pp. 1515–1522, 1986.

[92] D. G. Taylor, P. V. Kokotović, R. Marino, and I. Kanellakopoulos, "Adaptive regulation of nonlinear systems with unmodeled dynamics," *IEEE Transactions on Automatic Control*, vol. AC–34, no. 4, pp. 405–412, 1989.

[93] A. E. Bryson and Y. C. Ho, *Applied Optimal Control.* New York: Blaisdell, 1969.

[94] F. L. Lewis, *Optimal Control.* New York: John Wiley & Sons, 1986.

[95] B. D. O. Anderson and J. B. Moore, *Optimal Control: Linear Quadratic Methods.* Englewood Cliffs, NJ: Prentice–Hall, 1990.

[96] M. W. Spong and M. Vidyasagar, *Robot Dynamics and Control.* New York: John Wiley & Sons, 1989.

[97] K. Nam and A. Arapostathis, "A model–reference adaptive control scheme for pure–feedback nonlinear systems," *IEEE Transactions on Automatic Control*, vol. AC–33, no. 9, pp. 803–811, 1988.

[98] S. S. Sastry and A. Isidori, "Adaptive control of linearizable systems," *IEEE Transactions on Automatic Control*, vol. AC–34, no. 11, pp. 1123–1131, 1989.

[99] I. Kanellakopoulos, P. V. Kokotović, and R. Marino, "Adaptive control design for a class of nonlinear systems," in *Proceedings of the American Control Conference*, (San Diego, CA), pp. 1713–1717, 1990.

[100] G. Leitmann, "On the efficacy of nonlinear control in uncertain linear systems," *ASME Transactions on Dynamic Systems, Measurement and Control*, vol. 102, pp. 95–102, 1981.

[101] R. K. Miller and A. N. Michel, *Ordinary Differential Equations.* New York: Academic Press, 1982.

[102] B. R. Barmish, I. R. Petersen, and A. Feuer, "Linear ultimate boundedness control of uncertain dynamical systems," *Automatica*, vol. 19, pp. 523–532, 1983.

[103] J. S. Thorp and B. R. Barmish, "On guaranteed stability of uncertain linear systems via linear control," *Journal of Optimization Theory and Applications*, vol. 35, no. 4, pp. 559–579, 1981.

[104] G. P. Matthews and R. A. DeCarlo, "Decentralized variable structure control of interconnected multi–input multi–output nonlinear systems," *Circuits, Systems, and Signal Processing*, vol. 6, no. 3, pp. 363–387, 1987.

[105] R. G. Morgan and Ü. Özgüner, "A decentralized variable structure control algorithm for robotic manipulators," *IEEE Transactions on Robotics and Automation*, vol. RA-1, no. 1, pp. 57–65, 1985.

[106] Ü. Özgüner, S. Yurkovich, and F. Al–Abbass, "Decentralized variable structure control of a two–arm robotic system," *Journal of Robotic Systems*, vol. 4, no. 3, pp. 377–395, 1987.

[107] A. S. Hauksdottir and R. E. Fenton, "State observers and state–feedback controllers for a class of non–linear systems," *International Journal of Control*, vol. 48, no. 3, pp. 833–855, 1988.

[108] D. Schoenwald and Ü. Özgüner, "Some issues in decentralized control of nonlinear systems," in *Proceedings of the IEEE Conference on Decision and Control*, (Brighton, UK), Dec. 1991.

[109] J. P. Corfmat and A. S. Morse, "Decentralized control of linear multi–variable systems," *Automatica*, vol. 12, no. 2, pp. 169–182, 1976.

[110] A. Isidori and A. Ruberti, "On the synthesis of linear input–output responses for nonlinear systems," *Systems and Control Letters*, vol. 4, pp. 17–22, 1984.

[111] M. K. Sundareshan, "Exponential stabilization of large-scale systems: Decentralized and multilevel schemes," *IEEE Transactions on Systems, Man, and Cybernetics*, vol. SMC-7, pp. 478–483, 1977.

[112] S. S. Sastry, J. Hauser, and P. V. Kokotović, "Zero dynamics of regularly perturbed systems may be singularly perturbed," *Systems and Control Letters*, vol. 13, pp. 299–314, 1989.

[113] S. T. Hung, "Multi-input/multi-output sensitivity points tuning," Master's thesis, University of Illinois, Urbana-Champaign, May 1985.

[114] V. A. Sobolev, "Integral manifolds and decomposition of singularly perturbed systems," *Systems and Control Letters*, vol. 5, pp. 1169–1179, 1984.

[115] F. Khorrami, *Asymptotic perturbation and Lyapunov stability based approaches for control of flexible and rigid robot manipulators.* PhD thesis, The Ohio State University, Aug. 1988.

[116] B. Siciliano, W. J. Book, and G. De Maria, "An integral manifold approach to control of a one link flexible arm," in *Proceedings of the IEEE Conference on Decision and Control*, (Athens, Greece), pp. 1131–1134, 1986.

[117] B. Siciliano, A. J. Calise, and V. R. P. Jonnalagadda, "Optimal output fast feedback in two-time scale control of flexible arms," in *Proceedings of the IEEE Conference on Decision and Control*, (Athens, Greece), pp. 1400–1403, 1986.

[118] F. Khorrami, "Analysis of multi-link flexible manipulators via asymptotic expansions," in *Proceedings of the IEEE Conference on Decision and Control*, (Tampa, FL), pp. 2089–2094, 1989.

[119] A. G. Chassiakos and G. A. Bekey, "On the modelling and control of a flexible manipulator arm by point actuators," in *Proceedings of the IEEE Conference on Decision and Control*, (Athens, Greece), pp. 1145–1150, 1986.

[120] E. Barbieri, *Modelling and Control of Planar Flexible Structures with Application to an Optical-Tracking System.* PhD thesis, The Ohio State University, Sept. 1988.

[121] D. L. Edberg, "Control of flexible structures by applied thermal gradients," *AIAA Journal*, vol. 25, no. 6, pp. 877–883, 1987.

[122] D. Schoenwald and Ü. Özgüner, "On combining slewing and vibration control in flexible manipulators via singular perturbations," in *Proceedings of the IEEE Conference on Decision and Control*, (Honolulu, HI), Dec. 1990.

[123] P. T. Kotnik, S. Yurkovich, and Ü. Özgüner, "Acceleration feedback for control of a flexible manipulator arm," *Journal of Robotic Systems*, vol. 5, no. 3, pp. 181–196, 1988.

[124] K. K. D. Young and Ü. Özgüner, "Frequency shaped sliding mode synthesis," in *Proceedings of the American Control Conference*, (San Diego, CA), May 1990.

[125] S. Tadikonda and H. Baruh, "Pointwise-optimal control of robotic manipulators," *ASME Transactions on Dynamic Systems, Measurement and Control*, vol. 110, pp. 210–213, 1988.

[126] D. A. Haessig, Jr. and B. Friedland, "On the modeling and simulation of friction," *ASME Transactions on Dynamic Systems, Measurement and Control*, vol. 113, pp. 354–362, 1991.

[127] J. K. Cheng, "Solar array beta gimbal digital control analysis," Engineering Information Document EID–00988, Rocketdyne Division, Rockwell International, Jan. 1992.

[128] P. R. Dahl, "Solid friction damping of mechanical systems," *AIAA Journal*, vol. 14, no. 12, pp. 1675–1682, 1976.

Appendix A

THE TWO-LINK FLEXIBLE STRUCTURE MODEL

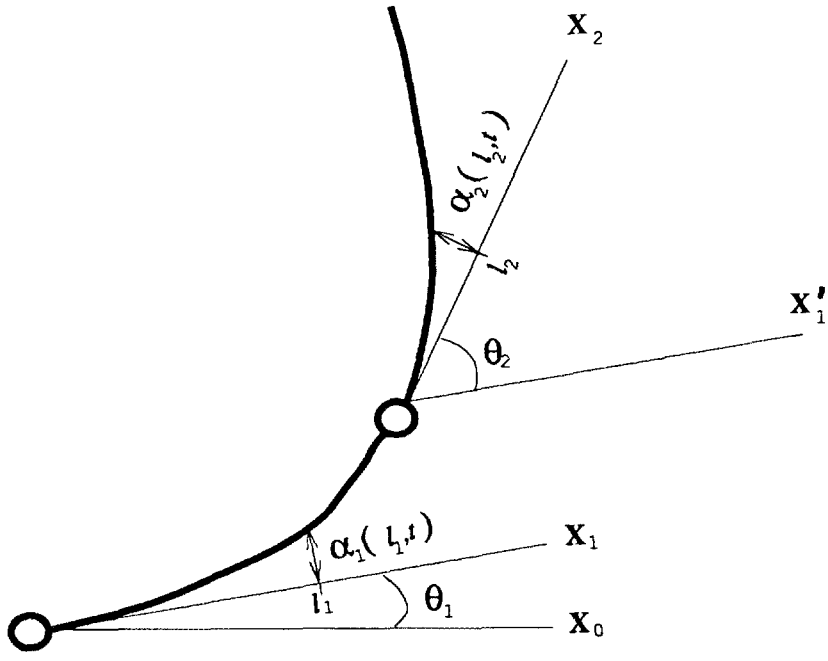

Fig. 35: Geometry of two-link flexible manipulator.

Table 6: Two-link dynamics terms

I_h	hub inertia
L_i	length of link i
E_iI_i	stiffness term for link i
ρ_i	mass density of link i
M_i	mass of hub i
ℓ_i	spatial variable for link i
$\alpha_i(\ell_i, t)$	flexure of link i at location ℓ_i
θ_i	rigid link angle of link i
$\hat{u}_i$	input torque at joint i

A.1 DYNAMICAL EQUATIONS

The first link rigid body motion (θ_1):

$$
\begin{aligned}
&[I_h + \tfrac{1}{3}\rho_1 L_1^3 + M_2 L_1^2 + \rho_2 L_1^2 L_2 + \tfrac{1}{2}\rho_2 L_1 L_2^2 \cos\theta_2 + \\
&(M_2 + \rho_2 L_2)\alpha_1^2(L_1,t) - \rho_2 \cos\theta_2 \alpha_1(L_1,t) \textstyle\int_0^{L_2} \alpha_2 dl_2 + \\
&\tfrac{1}{2}\rho_2 L_2^2 \alpha_1(L_1,t)\sin\theta_2 + \rho_1 \textstyle\int_0^{L_1} \alpha_1^2 dl_1 - \\
&\rho_2 L_1 \sin\theta_2 \textstyle\int_0^{L_2} \alpha_2 dl_2]\ddot{\theta}_1 + \\
&[\tfrac{1}{3}\rho_2 L_2^3 + \tfrac{1}{2}\rho_2 L_1 L_2^2 \cos\theta_2 + \\
&\tfrac{1}{2}\rho_2 L_2^2 \alpha_1(L_1,t)\sin\theta_2 + \rho_2 \textstyle\int_0^{L_2} \alpha_2^2 dl_2 + \\
&\rho_2 \alpha_1(L_1,t)\cos\theta_2 \textstyle\int_0^{L_2} \alpha_2 dl_2 - \rho_2 L_1 \sin\theta_2 \textstyle\int_0^{L_2} \alpha_2 dl_2](\ddot{\theta}_1 + \ddot{\theta}_2) + \\
&(M_2 + \rho_2 L_2) L_1 \ddot{\alpha}_1(L_1,t) + \tfrac{1}{2}\rho_2 L_2^2 \ddot{\alpha}_1(L_1,t)\cos\theta_2 - \\
&\rho_2 \ddot{\alpha}_1(L_1,t)\sin\theta_2 \textstyle\int_0^{L_2} \alpha_2 dl_2 + \\
&\rho_1 \textstyle\int_0^{L_1} l_1 \ddot{\alpha}_1 dl_1 + \rho_2 \textstyle\int_0^{L_2} [l_2 + L_1\cos\theta_2 + \alpha_1(L_1,t)\sin\theta_2]\ddot{\alpha}_2 dl_2 \\
&= -2\rho_1 \dot{\theta}_1 \textstyle\int_0^{L_1} \alpha_1 \dot{\alpha}_1 dl_1 - 2\rho_2(\dot{\theta}_1 + \dot{\theta}_2) \textstyle\int_0^{L_2} \alpha_2 \dot{\alpha}_2 dl_2 - \\
&2M_2 \dot{\theta}_1 \alpha_1(L_1,t)\dot{\alpha}_1(L_1,t) - 2\rho_2 L_2 \dot{\theta}_1 \alpha_1(L_1,t)\dot{\alpha}_1(L_1,t) + \\
&\tfrac{1}{2}\rho_2 L_2^2 [2\dot{\theta}_1 + \dot{\theta}_2][L_1 \dot{\theta}_2 \sin\theta_2 - \alpha_1(L_1,t)\dot{\theta}_2\cos\theta_2] - \\
&\rho_2 L_2^2 \dot{\theta}_1 \dot{\alpha}_1(L_1,t)\sin\theta_2 + 2\rho_2 L_1(\dot{\theta}_1 + \dot{\theta}_2)\sin\theta_2 \textstyle\int_0^{L_2} \dot{\alpha}_2 dl_2 - \\
&2\rho_2(\dot{\theta}_1 + \dot{\theta}_2)\alpha_1(L_1,t)\cos\theta_2 \textstyle\int_0^{L_2} \dot{\alpha}_2 dl_2 - \\
&2\rho_2 \dot{\theta}_1 \dot{\alpha}_1(L_1,t)\cos\theta_2 \textstyle\int_0^{L_2} \alpha_2 dl_2 + \\
&\rho_2 \dot{\theta}_2 [2\dot{\theta}_1 + \dot{\theta}_2][L_1\cos\theta_2 + \alpha_1(L_1,t)\sin\theta_2] \textstyle\int_0^{L_2} \alpha_2 dl_2 + \hat{u}_1
\end{aligned}
\tag{A.1}
$$

The second link rigid body motion (θ_2):

$$
\begin{aligned}
&[\tfrac{1}{2}\rho_2 L_1 L_2^2 \cos\theta_2 + \rho_2\alpha_1(L_1,t)\cos\theta_2 \textstyle\int_0^{L_2} \alpha_2 dl_2 - \\
&\rho_2 L_1 \sin\theta_2 \textstyle\int_0^{L_2} \alpha_2 dl_2 + \\
&\tfrac{1}{2}\rho_2 L_2^2 \alpha_1(L_1,t)\sin\theta_2]\ddot{\theta}_1 + [\tfrac{1}{3}\rho_2 L_2^3 + \rho_2 \textstyle\int_0^{L_2} \alpha_2^2 dl_2](\ddot{\theta}_1 + \ddot{\theta}_2) + \\
&\rho_2 \textstyle\int_0^{L_2} l_2 \ddot{\alpha}_2 dl_2 + \tfrac{1}{2}\rho_2 L_2^2 \ddot{\alpha}_1(L_1,t)\cos\theta_2 - \\
&\rho_2 \ddot{\alpha}_1(L_1,t)\sin\theta_2 \textstyle\int_0^{L_2} \alpha_2 dl_2 \\
&= -2\rho_2(\dot{\theta}_1 + \dot{\theta}_2)\textstyle\int_0^{L_2} \alpha_2\dot{\alpha}_2 dl_2 - \rho_2\alpha_1(L_1,t)\dot{\theta}_1^2 \sin\theta_2 \textstyle\int_0^{L_2} \alpha_2 dl_2 - \\
&2\rho_2\dot{\alpha}_1(L_1,t)\dot{\theta}_1\cos\theta_2 \textstyle\int_0^{L_2} \alpha_2 dl_2 - \rho_2 L_1 \dot{\theta}_1^2 \cos\theta_2 \textstyle\int_0^{L_2} \alpha_2 dl_2 - \\
&\tfrac{1}{2}\rho_2 L_1 L_2^2 \dot{\theta}_1^2 \sin\theta_2 + \tfrac{1}{2}\rho_2 L_2^2 \dot{\theta}_1^2 \alpha_1(L_1,t)\cos\theta_2 - \\
&\rho_2 L_2^2 \dot{\alpha}_1(L_1,t)\dot{\theta}_1 \sin\theta_2 + \hat{u}_2
\end{aligned}
\tag{A.2}
$$

The flexure of the first link (α_1):

$$
\rho_1 l_1 \ddot{\theta}_1 + \rho_1 \ddot{\alpha}_1 = -E_1 I_1 \alpha_{1,l_1 l_1 l_1 l_1} + \rho_1 \alpha_1 \dot{\theta}_1^2 \tag{A.3}
$$

The flexure of the second link (α_2):

$$
\begin{aligned}
&\rho_2 l_2(\ddot{\theta}_1 + \ddot{\theta}_2) + \rho_2\ddot{\alpha}_2 = -E_2 I_2 \alpha_{2,l_2 l_2 l_2 l_2} + \rho_2\alpha_2(\dot{\theta}_1 + \dot{\theta}_2)^2 - \\
&\rho_2 L_1 \ddot{\theta}_1 \cos\theta_2 - \rho_2\ddot{\alpha}_1(L_1,t)\cos\theta_2 + \rho_2\alpha_1(L_1,t)\dot{\theta}_1^2\cos\theta_2 - \\
&\rho_2 L_1 \dot{\theta}_1^2 \sin\theta_2 - 2\rho_2\dot{\alpha}_1(L_1,t)\dot{\theta}_2\sin\theta_2 - \rho_2\alpha_1(L_1,t)\ddot{\theta}_1\sin\theta_2
\end{aligned}
\tag{A.4}
$$

The boundary conditions are:

First link:

$$
\begin{aligned}
&\alpha_1(0,t) = \alpha_{1,l_1}(0,t) = 0 \\
&E_1 I_1 \alpha_{1,l_1 l_1 l_1}(L_1,t) = -\hat{u}_2 \\
&(M_2 + \rho_2 L_2)[L_1\ddot{\theta}_1 + \ddot{\alpha}_1(L_1,t)] - \\
&\rho_2 L_2 \alpha_1(L_1,t)\dot{\theta}_1^2 + \tfrac{1}{2}\rho_2 L_2^2(\ddot{\theta}_1 + \ddot{\theta}_2)\cos\theta_2 - \\
&\tfrac{1}{2}\rho_2 L_2^2 \dot{\theta}_1(\dot{\theta}_1^2 - \dot{\theta}_2^2)\sin\theta_2 + \rho_2 \textstyle\int_0^{L_2} \ddot{\alpha}_2 \cos\theta_2 dl_2 - \\
&\rho_2 \textstyle\int_0^{L_2} [2(\dot{\theta}_1 + \dot{\theta}_2)\dot{\alpha}_2 \sin\theta_2 + \\
&\alpha_2(\ddot{\theta}_1 + \ddot{\theta}_2)\sin\theta_2 - \alpha_2(\dot{\theta}_1^2 - \dot{\theta}_2^2)\cos\theta_2] dl_2 - \\
&M_2 \dot{\theta}_1^2 \alpha_1(L_1,t) = E_1 I_1 \alpha_{1,l_1 l_1 l_1}(L_1,t)
\end{aligned}
$$

Second link:

$$\alpha_2(0,t) = \alpha_{2,l_2}(0,t) = 0$$

$$\alpha_{2,l_2l_2}(L_2,t) = \alpha_{2,l_2l_2l_2}(L_2,t) = 0$$

A.2 CORRECTIVE CONTROL DESIGN

To determine the $O(\epsilon)$ control law, the h_{i0} terms must be computed from the $O(1)$ manifold equations (5.11)-(5.12) along with the boundary conditions. These terms are then plugged into the $O(\epsilon)$ slow subsystem equations which will then yield the linearizing control law. The $O(\epsilon)$ control law will not depend on x_1 or x_2 since all the h_{i0} terms will either be integrated with respect to x_i or evaluated at the endpoints. Integrating (5.11) four times with respect to x_1 and using boundary conditions from Sect. A.1 to solve for constants of integration, one obtains the following power series in x_1 for h_{10}

$$\begin{aligned} h_{10} &= -\frac{1}{120}\ddot{\theta}_1 x_1^5 + [(\frac{1}{4} + \frac{\rho_2 L_2}{6\rho_1 L_1})\ddot{\theta}_1 \\ &+ \frac{\rho_2 L_2^2}{12\rho_1 L_1^2}(\ddot{\theta}_1 + \ddot{\theta}_2)\cos\theta_2 - \frac{\rho_2 L_2^2}{12\rho_1 L_1^2}(\dot{\theta}_1^2 - \dot{\theta}_2^2)\sin\theta_2]x_1^3 \\ &+ [-(\frac{2}{3} + \frac{\rho_2 L_2}{2\rho_1 L_1})\ddot{\theta}_1 - \frac{\rho_2 L_2^2}{4\rho_1 L_1^2}(\ddot{\theta}_1 + \ddot{\theta}_2)\cos\theta_2 \\ &+ \frac{\rho_2 L_2^2}{4\rho_1 L_1^2}(\dot{\theta}_1^2 - \dot{\theta}_2^2)\sin\theta_2]x_1^2 \end{aligned} \tag{A.5}$$

where the $O(1)$ linearizing control law has been plugged into the boundary condition that contains u_2. Likewise, the same procedure can be followed to obtain h_{20}

$$\begin{aligned} h_{20} &= -\frac{1}{120}(\ddot{\theta}_1 + \ddot{\theta}_2)x_2^5 + [-\frac{L_1}{24L_2}\ddot{\theta}_1\cos\theta_2 - \frac{L_1}{24L_2}\dot{\theta}_1^2\sin\theta_2]x_2^4 \\ &+ [\frac{1}{12}(\ddot{\theta}_1 + \ddot{\theta}_2) + \frac{L_1}{6L_2}\ddot{\theta}_1\cos\theta_2 + \frac{L_1}{6L_2}\dot{\theta}_1^2\sin\theta_2]x_2^3 \\ &+ [-\frac{1}{6}(\ddot{\theta}_1 + \ddot{\theta}_2) - \frac{L_1}{4L_2}\ddot{\theta}_1\cos\theta_2 - \frac{L_1}{4L_2}\dot{\theta}_1^2\sin\theta_2]x_2^2 . \end{aligned} \tag{A.6}$$

Since all terms in the $O(\epsilon)$ slow manifold equations are nonlinear in θ_i, the u_{i1} control terms will need to cancel everything. This will result in a linear system to $O(\epsilon^2)$. The specific control laws are as follows

$$\hat{u}_{11} = [\frac{1}{2}\rho_2 L_1 L_2^2 h_{10}(1,t)\sin\theta_2 - \rho_2 L_1 L_2^2 \sin\theta_2 \int_0^1 h_{20}dx_2]\ddot{\theta}_1$$

Appendix A

THE TWO-LINK FLEXIBLE STRUCTURE MODEL

As stated in Chap. 1, most derived dynamical models of flexible structures are based upon a finite-dimensional approximation of the exact model. In this appendix, the model dynamics are derived as in Khorrami and Özgüner [1] and Khorrami [2] via the Hamiltonian formulation. Due to the brevity of this work, the reader is referred to Khorrami [2] for a more thorough treatment of the derivation of the dynamics. The following assumptions are made in the development of this model.

Assumption 1.1 All motion is restricted to the horizontal plane. Thus, gravity effects are ignored.

Assumption 1.2 In the formulation of the potential energy term, shear, torsion, and axial displacement have been neglected.

Assumption 1.3 It is assumed that there is no payload at the tip of the second link.

Figure 35 illustrates the geometry of the two-link manipulator. It should be noted that θ_i represents the angle between the line tangent to the ith hub (X_i) and the line tangent to the $i-1$th hub (X_{i-1}). The quantity α_i is the deflection between X_i and the link itself as a function of the position along the ith link (ℓ_i). The following terms are defined in Table 6 to obtain the dynamical equations which follow.

$$
\begin{aligned}
&+ \quad [\frac{1}{2}\rho_2 L_1 L_2^2 h_{10}(1,t)\sin\theta_2 - \rho_2 L_1 L_2^2 \sin\theta_2 \int_1^0 h_{20} dx_2](\ddot{\theta}_1 + \ddot{\theta}_2) \\
&+ \quad \frac{1}{2}\rho_2 L_1 L_2^2 \ddot{h}_{10}(1,t)\cos\theta_2 + \rho_2 L_1 L_2^2 \cos\theta_2 \int_0^1 \ddot{h}_{20} dx_2 \\
&+ \quad \frac{1}{2}\rho_2 L_1 L_2^2 (2\dot{\theta}_1 + \dot{\theta}_2) h_{10}(1,t)\dot{\theta}_2 \cos\theta_2 + \rho_2 L_1 L_2^2 \dot{\theta}_2 \dot{h}_{10}(1,t)\sin\theta_2 \\
&- \quad 2\rho_2 L_1 L_2^2 (\dot{\theta}_1 + \dot{\theta}_2)\sin\theta_2 \int_0^1 \dot{h}_{20} dx_2 - \rho_2 L_1 L_2^2 \dot{\theta}_2 (2\dot{\theta} + \dot{\theta}_2)\cos\theta_2 \int_0^1 h_{20} dx_2 \\
&+ \quad (\rho_1 L_1^3 + \rho_2 L_1^2 L_2)\ddot{h}_{10}(1,t) + \rho_1 L_1^3 \int_0^1 x_1 \ddot{h}_{10} dx_1 + \rho_2 L_2^3 \int_0^1 x_2 \ddot{h}_{20} dx_2
\end{aligned}
\tag{A.7}
$$

$$
\begin{aligned}
\hat{u}_{21} \quad = \quad & [-\rho_2 L_1 L_2^2 \sin\theta_2 \int_0^1 h_{20} dx_2 + \frac{1}{2}\rho_2 L_1 L_2^2 h_{10}(1,t)\sin\theta_2]\ddot{\theta}_1 \\
&+ \quad \frac{1}{2}\rho_2 L_1 L_2^2 \ddot{h}_{10}(1,t)\cos\theta_2 + \rho_2 L_1 L_2^2 \dot{\theta}_1^2 \cos\theta_2 \int_0^1 h_{20} dx_2 \\
&- \quad \frac{1}{2}\rho_2 L_1 L_2^2 \dot{\theta}_1^2 h_{10}(1,t)\cos\theta_2 + \rho_2 L_1 L_2^2 \dot{h}_{10}(1,t)\dot{\theta}_1 \sin\theta_1 + \rho_2 L_2^3 \int_0^1 x_2 \ddot{h}_{20} dx_2
\end{aligned}
\tag{A.8}
$$

where u_{11} and u_{21} are obtained via (5.4).

A.3 FINITE-DIMENSIONAL REPRESENTATION

In this section, an assumed modes representation of the flexure variables α_i is chosen and a one mode expansion of α_i is inserted into the system equations to obtain a finite-dimensional representation of the dynamics. The resulting equations are programmed on computer to model the two-link structure. As in many studies of one link cases, a "good choice" of trial functions for the solution is required. This is further complicated due to the moving boundary condition at the tip of the first link. One choice may be the eigenfunctions used in the single link case. Another choice may be to treat the first link as clamped-pinned and the second one as pinned-free. But here, the first link is modeled as clamped at the hub and carrying a mass with an inertia at the free end. Hereafter, these mode shapes will be referred to as CLTI mode shapes (cantilever with tip inertia). The second link is modeled as clamped-free. The assumed modes method requires that the flexure be expanded as

$$
\alpha_i = \sum_{j=1}^{N_i} \phi_{ij}(\ell_i) q_{ij} \tag{A.9}
$$

where i is the link number, j is the mode number, ϕ is the mode shape, and q is the modal displacement.

The usual clamped-free mode shapes fail to account for the loading effects the second link has on the first link. This was deemed to be a significant problem in

determining modal frequencies for the first link based on comparisons between experimental and simulation results. CLTI mode shapes have been used in flexible robotics before to model links with a payload (see, for instance, Oakley and Cannon [3]). But, here they are used to model a link with another attached link as the payload. The assumed modes boundary conditions for the two links are

$$\begin{aligned}
\alpha_1(0,t) &= 0\,, \quad \alpha_{1,\ell_1}(0,t) = 0 && \text{(A.10)}\\
E_1 I_1 \alpha_{1,\ell_1\ell_1}(L_1,t) &= -(M_{p_1} O_{p_1}^2 + I_{p_1})\ddot{\alpha}_{1,\ell_1}(L_1,t) - M_{p_1} O_{p_1} \ddot{\alpha}_1(L_1,t) && \text{(A.11)}\\
E_1 I_1 \alpha_{1,\ell_1\ell_1\ell_1}(L_1,t) &= M_{p_1} \ddot{\alpha}_1(L_1,t) + M_{p_1} O_{p_1} \ddot{\alpha}_{1,\ell_1}(L_1,t) && \text{(A.12)}\\
\alpha_2(0,t) &= 0\,, \quad \alpha_{2,\ell_2}(0,t) = 0 && \text{(A.13)}\\
\alpha_{2,\ell_2\ell_2}(L_2,t) &= 0\,, \quad \alpha_{2,\ell_2\ell_2\ell_2}(L_2,t) = 0 && \text{(A.14)}
\end{aligned}$$

where M_{p_1} is the mass of the attached joint and link, I_{p_1} is the mass moment of inertia of the joint plus link, and O_{p_1} is the distance from the endpoint of link 1 to the center of mass of the joint plus link 2 attachment. The first equation represents the clamped boundary condition at joint 1. The next two equations correspond to the mass plus inertia attached to the endpoint of the first link. The fourth and fifth equations model the clamped-free boundary conditions of the second link.

The clamped-free mode shapes for the second link can be found in many books such as Blevins [4] and are written as

$$\begin{aligned}
\phi_{2i}(\ell_2) &= \cosh\left(\frac{\hat{\lambda}_{2i}\ell_2}{L_2}\right) - \cos\left(\frac{\hat{\lambda}_{2i}\ell_2}{L_2}\right) && \text{(A.15)}\\
&- \left(\frac{\cosh\hat{\lambda}_{2i} + \cos\hat{\lambda}_{2i}}{\sinh\hat{\lambda}_{2i} + \sin\hat{\lambda}_{2i}}\right)\left(\sinh\left(\frac{\hat{\lambda}_{2i}\ell_2}{L_2}\right) - \sin\left(\frac{\hat{\lambda}_{2i}\ell_2}{L_2}\right)\right)
\end{aligned}$$

where $\hat{\lambda}_{2i}$ is the eigenvalue obtained from the characteristic equation

$$\cosh\hat{\lambda}_{2i}\cos\hat{\lambda}_{2i} + 1 = 0\,, \quad i = 1, 2, \ldots\,. \qquad \text{(A.16)}$$

The CLTI mode shapes for link 1 can be expressed as (Bhat and Wagner [5])

$$\begin{aligned}
\phi_{1i}(\ell_1) &= \cosh\left(\frac{\hat{\lambda}_{1i}\ell_1}{L_1}\right) - \cos\left(\frac{\hat{\lambda}_{1i}\ell_1}{L_1}\right) && \text{(A.17)}\\
&- \frac{C_{\text{num}_i}}{C_{\text{den}_i}}\left(\sinh\left(\frac{\hat{\lambda}_{1i}\ell_1}{L_1}\right) - \sin\left(\frac{\hat{\lambda}_{1i}\ell_1}{L_1}\right)\right)
\end{aligned}$$

where

$$C_{\text{num}_i} = \cosh\hat{\lambda}_{1i} + \cos\hat{\lambda}_{1i} - \frac{M_{p_1} O_{p_1}^2 + I_{p_1}}{\rho_1}\left(\frac{\hat{\lambda}_{1i}}{L_1}\right)^3 (\sinh\hat{\lambda}_{1i} + \sin\hat{\lambda}_{1i}) \qquad \text{(A.18)}$$

$$
\begin{aligned}
& - \frac{M_{p_1} O_{p_1}}{\rho_1} \left(\frac{\hat{\lambda}_{1i}}{L_1}\right)^2 (\cosh \hat{\lambda}_{1i} - \cos \hat{\lambda}_{1i}) \\
C_{\mathrm{den}_i} &= \sinh \hat{\lambda}_{1i} + \sin \hat{\lambda}_{1i} - \frac{M_{p_1} O_{p_1}^2 + I_{p_1}}{\rho_1} \left(\frac{\hat{\lambda}_{1i}}{L_1}\right)^3 (\cosh \hat{\lambda}_{1i} - \cos \hat{\lambda}_{1i}) \quad \text{(A.19)} \\
& - \frac{M_{p_1} O_{p_1}}{\rho_1} \left(\frac{\hat{\lambda}_{1i}}{L_1}\right)^2 (\sinh \hat{\lambda}_{1i} - \sin \hat{\lambda}_{1i})
\end{aligned}
$$

and $\hat{\lambda}_{1i}$ is the solution of the characteristic equation

$$
\begin{aligned}
& \left[\frac{M_{p_1}(M_{p_1} O_{p_1}^2 + I_{p_1})\hat{\lambda}_{1i}^4}{\rho_1^2 L_1^4} - \left(\frac{M_{p_1} O_{p_1} \hat{\lambda}_{1i}^2}{\rho_1 L_1^2}\right)^2 - 1\right] \cosh \hat{\lambda}_{1i} \cos \hat{\lambda}_{1i} \\
+ & \left[\frac{(M_{p_1} O_{p_1}^2 + I_{p_1})\hat{\lambda}_{1i}^3}{\rho_1 L_1^3} + \frac{M_{p_1} \hat{\lambda}_{1i}}{\rho_1 L_1}\right] \cosh \hat{\lambda}_{1i} \sin \hat{\lambda}_{1i} \\
+ & \left[\frac{(M_{p_1} O_{p_1}^2 + I_{p_1})\hat{\lambda}_{1i}^3}{\rho_1 L_1^3} - \frac{M_{p_1} \hat{\lambda}_{1i}}{\rho_1 L_1}\right] \sinh \hat{\lambda}_{1i} \cos \hat{\lambda}_{1i} \qquad \text{(A.20)} \\
+ & \; 2\frac{M_{p_1} O_{p_1} \hat{\lambda}_{1i}^2}{\rho_1 L_1^2} \sinh \hat{\lambda}_{1i} \sin \hat{\lambda}_{1i} + \left(\frac{M_{p_1} O_{p_1} \hat{\lambda}_{1i}^2}{\rho_1 L_1^2}\right)^2 \\
- & \; \frac{M_{p_1}(M_{p_1} O_{p_1}^2 + I_{p_1})\hat{\lambda}_{1i}^4}{\rho_1^2 L_1^4} - 1 = 0\,, \quad i = 1, 2, \ldots .
\end{aligned}
$$

From the OSU manipulator structural data, it was determined that M_{p_1} = mass of joint 2 + mass of link 2 = 0.721 kg, O_{p_1} = distance from point of attachment to center of mass of second joint/link = 4.64 cm, and I_{p_1} = mass moment of inertia of cylindrical hub and rectangular link = 0.0016 kg-m^2. Solving the characteristic equation, we obtained $\hat{\lambda}_{11} = 1.153$ and from the tables in Blevins [4] $\hat{\lambda}_{21} = 1.8751$.

The resulting model will be of the following form:

$$
\mathcal{M}(X)\ddot{X} + KX + F(X, \dot{X}) = U \qquad \text{(A.21)}
$$

where $X = [\theta_1 \; \theta_2 \mid q_{1,1} \; q_{1,2} \; \cdots q_{1,N_1} \; q_{2,1} \; q_{2,2} \; \cdots \; q_{2,N_2}]$, N_1 and N_2 are the number of modes retained in the model from flexural effects of each link respectively. The following expressions can be defined in terms of the variables of the above approximation:

$$
A_{ij} \triangleq \int_0^{L_i} \rho_i \ell_i \phi_{ij}(\ell_i) d\ell_i \qquad \text{(A.22)}
$$

$$
B_{ij} \triangleq \int_0^{L_i} \rho_i \phi_{ij}^2(\ell_i) d\ell_i \qquad \text{(A.23)}
$$

$$C_{1j} \triangleq \phi_{1j}(L_1) \tag{A.24}$$

$$C_{2j} \triangleq \int_0^{L_2} \rho_2 \phi_{2j}(\ell_2) d\ell_2 \tag{A.25}$$

$$\lambda_{ij}\phi_{ij} \triangleq \frac{\partial^4 \phi_{ij}}{\partial \ell_i^4}. \tag{A.26}$$

This will allow one to calculate the following terms:

$$\int_0^{L_i} \alpha_i d\ell_i, \quad \int_0^{L_i} \ell_i \alpha_i d\ell_i, \quad \text{and} \quad \int_0^{L_i} \alpha_i^2 d\ell_i. \tag{A.27}$$

The one-mode approximation results in the following dynamic equations:

$$M \begin{pmatrix} \ddot{\theta}_1 \\ \ddot{\theta}_2 \\ \ddot{q}_1 \\ \ddot{q}_2 \end{pmatrix} + F_r \begin{pmatrix} \dot{\theta}_1^2 \\ \dot{\theta}_2^2 \\ \dot{\theta}_1\dot{\theta}_2 \end{pmatrix} + F_{r_f} \begin{pmatrix} \dot{\theta}_1\dot{q}_1 \\ \dot{\theta}_1\dot{q}_2 \\ \dot{\theta}_2\dot{q}_1 \\ \dot{\theta}_2\dot{q}_2 \end{pmatrix} + \begin{pmatrix} 0 \\ 0 \\ \mu_1\dot{q}_1 + k_1 q_1 \\ \mu_2\dot{q}_2 + k_2 q_2 \end{pmatrix} = \begin{pmatrix} u_1 \\ u_2 \\ V_1 \\ V_2 \end{pmatrix} \tag{A.28}$$

where the first term on the left hand side is the inertia term, the second and third terms are the Coriolis and centrifugal force vectors, the fourth term is the viscous damping plus stiffness elements, and the vector on the right hand side is the control term. The first two elements of the control vector are the torque controls, and the second two elements are the film actuation forces (physical constants embedded within these two terms). The elements for these matrices are obtained from the following spatially discretized equations of motion (with $N_1 = N_2 = 1$).

The first link rigid body motion (θ_1):

$$
\begin{aligned}
&[I_h + \tfrac{1}{3}\rho_1 L_1^3 + \tfrac{1}{3}\rho_2 L_2^3 + M_2 L_1^2 + \rho_2 L_1^2 L_2 + \rho_2 L_1 L_2^2 \cos\theta_2 + \\
&(M_2 + \rho_2 L_2) \textstyle\sum_{i=1}^{N_1} \sum_{j=1}^{N_1} C_{1i} C_{1j} q_{1i} q_{1j} + \rho_2 L_2^2 \sin\theta_2 \sum_{i=1}^{N_1} C_{1i} q_{1i} + \\
&\textstyle\sum_{i=1}^{N_2} B_{2i} q_{2i} - 2L_1 \sin\theta_2 \sum_{i=1}^{N_2} C_{2i} q_{2i} + \\
&\textstyle\sum_{i=1}^{N_1} B_{1i} q_{1i}^2]\ddot{\theta}_1 + [\tfrac{1}{3}\rho_2 L_2^3 + \tfrac{1}{2}\rho_2 L_1 L_2^2 \cos\theta_2 + \\
&\tfrac{1}{2}\rho_2 L_2^2 \sin\theta_2 \textstyle\sum_{i=1}^{N_1} C_{1i} q_{1i} + \\
&\textstyle\sum_{i=1}^{N_2} B_{2i} q_{2i}^2 + \cos\theta_2 \sum_{i=1}^{N_1} C_{1i} q_{1i} \sum_{i=1}^{N_2} C_{2i} q_{2i} - \\
&L_1 \sin\theta_2 \textstyle\sum_{i=1}^{N_2} C_{2i} q_{2i}]\ddot{\theta}_2 + \\
&(M_2 + \rho_2 L_2) L_1 \textstyle\sum_{i=1}^{N_1} C_{1i} \ddot{q}_{1i} + \tfrac{1}{2}\rho_2 L_2^2 \cos\theta_2 \sum_{i=1}^{N_1} C_{1i} \ddot{q}_{1i} - \\
&\sin\theta_2 \textstyle\sum_{i=1}^{N_1} C_{1i} \ddot{q}_{1i} \sum_{i=1}^{N_2} C_{2i} q_{2i} + \\
&\textstyle\sum_{i=1}^{N_1} A_{1i} \ddot{q}_{1i} + \sum_{i=1}^{N_2} A_{2i} \ddot{q}_{2i} + L_1 \cos\theta_2 \sum_{i=1}^{N_2} C_{2i} \ddot{q}_{2i} + \\
&\sin\theta_2 \textstyle\sum_{i=1}^{N_1} C_{1i} q_{1i} \sum_{i=1}^{N_2} C_{2i} \ddot{q}_{2i} + \\
&2\dot{\theta}_1 \textstyle\sum_{i=1}^{N_1} B_{1i} q_{1i} \dot{q}_{1i} + 2\dot{\theta}_1 \sum_{i=1}^{N_2} B_{2i} q_{2i} \dot{q}_{2i} + 2\dot{\theta}_2 \sum_{i=1}^{N_2} B_{2i} q_{2i} \dot{q}_{2i} + \\
&2M_2 \dot{\theta}_1 \textstyle\sum_{i=1}^{N_1} \sum_{j=1}^{N_2} C_{1i} C_{1j} q_{1i} \dot{q}_{1j} + 2\rho_2 L_2 \dot{\theta}_1 \sum_{i=1}^{N_1} \sum_{j=1}^{N_2} C_{1i} C_{1j} q_{1i} \dot{q}_{1j} - \\
&\rho_2 L_1 L_2^2 \dot{\theta}_1 \dot{\theta}_2 \sin\theta_2 - \\
&\tfrac{1}{2}\rho_2 L_1 L_2^2 \dot{\theta}_2^2 \sin\theta_2 + \rho_2 L_2^2 \dot{\theta}_1 \dot{\theta}_2 \cos\theta_2 \textstyle\sum_{i=1}^{N_1} C_{1i} q_{1i} + \\
&\tfrac{1}{2}\rho_2 L_2^2 \dot{\theta}_2^2 \cos\theta_2 \textstyle\sum_{i=1}^{N_1} C_{1i} q_{1i} + \rho_2 L_2^2 \dot{\theta}_1 \sin\theta_2 \sum_{i=1}^{N_1} C_{1i} \dot{q}_{1i} - \\
&2L_1 \dot{\theta}_1 \sin\theta_2 \textstyle\sum_{i=1}^{N_2} C_{2i} \dot{q}_{2i} - 2L_1 \dot{\theta}_2 \sin\theta_2 \sum_{i=1}^{N_2} C_{2i} \dot{q}_{2i} + \\
&2\dot{\theta}_1 \cos\theta_2 \textstyle\sum_{i=1}^{N_1} C_{1i} q_{1i} \sum_{i=1}^{N_2} C_{2i} \dot{q}_{2i} + \\
&2\dot{\theta}_2 \cos\theta_2 \textstyle\sum_{i=1}^{N_1} C_{1i} q_{1i} \sum_{i=1}^{N_2} C_{2i} \dot{q}_{2i} + \\
&2\dot{\theta}_1 \cos\theta_2 \textstyle\sum_{i=1}^{N_1} C_{1i} \dot{q}_{1i} \sum_{i=1}^{N_2} C_{2i} q_{2i} - 2L_1 \dot{\theta}_1 \dot{\theta}_2 \cos\theta_2 \sum_{i=1}^{N_2} C_{2i} q_{2i} - \\
&2\dot{\theta}_1 \dot{\theta}_2 \sin\theta_2 \textstyle\sum_{i=1}^{N_1} C_{1i} q_{1i} \sum_{i=1}^{N_2} C_{2i} q_{2i} - \\
&L_1 \dot{\theta}_2^2 \cos\theta_2 \textstyle\sum_{i=1}^{N_2} C_{2i} q_{2i} - \dot{\theta}_2^2 \sin\theta_2 \sum_{i=1}^{N_1} C_{1i} q_{1i} \sum_{i=1}^{N_2} C_{2i} q_{2i} = \hat{u}_1
\end{aligned}
\tag{A.29}
$$

The second link rigid body motion (θ_2):

$$
\begin{aligned}
&[\tfrac{1}{3}\rho_2 L_2^3 + \tfrac{1}{2}\rho_2 L_1 L_2^2 \cos\theta_2 + \\
&\cos\theta_2 \textstyle\sum_{i=1}^{N_1} C_{1i} q_{1i} \sum_{i=1}^{N_2} C_{2i} q_{2i} - L_1 \sin\theta_2 \sum_{i=1}^{N_2} C_{2i} q_{2i} + \\
&\tfrac{1}{2}\rho_2 L_2^2 \sin\theta_2 \textstyle\sum_{i=1}^{N_1} C_{1i} q_{1i} + \sum_{i=1}^{N_2} B_{2i} q_{2i}^2]\ddot{\theta}_1 + \\
&[\tfrac{1}{3}\rho_2 L_2^3 + \textstyle\sum_{i=1}^{N_2} B_{2i} q_{2i}^2]\ddot{\theta}_2 + \\
&\textstyle\sum_{i=1}^{N_2} A_{2i}\ddot{q}_{2i} + \tfrac{1}{2}\rho_2 L_2^2 \cos\theta_2 \sum_{i=1}^{N_1} C_{1i}\ddot{q}_{1i} - \\
&\sin\theta_2 \textstyle\sum_{i=1}^{N_1} C_{1i}\ddot{q}_{1i} \sum_{i=1}^{N_2} C_{2i} q_{2i} + \\
&2\dot{\theta}_1 \textstyle\sum_{i=1}^{N_2} B_{2i} q_{2i}\dot{q}_{2i} + 2\dot{\theta}_2 \sum_{i=1}^{N_2} B_{2i} q_{2i}\dot{q}_{2i} + \\
&\dot{\theta}_1^2 \sin\theta_2 \textstyle\sum_{i=1}^{N_1} C_{1i} q_{1i} \sum_{i=1}^{N_2} C_{2i} q_{2i} + \\
&2\dot{\theta}_1 \cos\theta_2 \textstyle\sum_{i=1}^{N_1} C_{1i}\dot{q}_{1i} \sum_{i=1}^{N_2} C_{2i} q_{2i} + \\
&L_1\dot{\theta}_1^2 \cos\theta_2 \textstyle\sum_{i=1}^{N_2} C_{2i} q_{2i} + \tfrac{1}{2}\rho_2 L_1 L_2^2 \dot{\theta}_1^2 \sin\theta_2 - \\
&\tfrac{1}{2}\rho_2 L_2^2 \dot{\theta}_1^2 \cos\theta_2 \textstyle\sum_{i=1}^{N_1} C_{1i} q_{1i} - \rho_2 L_2^2 \dot{\theta}_1 \sin\theta_2 \sum_{i=1}^{N_1} C_{1i}\dot{q}_{1i} = \hat{u}_2
\end{aligned}
\tag{A.30}
$$

The flexure of the first link (α_1):

$$
\rho_1\ddot{\theta}_1 l_1 + \rho_1 \sum_{i=1}^{N_1} \phi_{1i}\ddot{q}_{1i} + E_1 I_1 \sum_{i=1}^{N_1} \phi_{1i}^{(4)} q_{1i} - \rho_1 \dot{\theta}_1^2 \sum_{i=1}^{N_1} \phi_{1i} q_{1i} = 0 \tag{A.31}
$$

The flexure of the second link (α_2):

$$
\begin{aligned}
&\rho_2\ddot{\theta}_1 l_2 + \rho_2\ddot{\theta}_2 l_2 + \rho_2 \textstyle\sum_{i=1}^{N_2} \phi_{2i}\ddot{q}_{2i} + \\
&E_2 I_2 \textstyle\sum_{i=1}^{N_2} \phi_{2i}^{(4)} q_{2i} - \rho_2\dot{\theta}_1^2 \sum_{i=1}^{N_2} \phi_{2i} q_{2i} - \\
&2\rho_2\dot{\theta}_1\dot{\theta}_2 \textstyle\sum_{i=1}^{N_2} \phi_{2i} q_{2i} - \rho_2\dot{\theta}_2^2 \sum_{i=1}^{N_2} \phi_{2i} q_{2i} + \\
&\rho_2 L_1\ddot{\theta}_1 \cos\theta_2 + \rho_2 \cos\theta_2 \textstyle\sum_{i=1}^{N_1} C_{1i}\ddot{q}_{1i} - \\
&\rho_2\dot{\theta}_1^2 \cos\theta_2 \textstyle\sum_{i=1}^{N_1} C_{1i} q_{1i} + \rho_2 L_1\dot{\theta}_1^2 \sin\theta_2 + \\
&2\rho_2\dot{\theta}_2 \sin\theta_2 \textstyle\sum_{i=1}^{N_1} C_{1i}\dot{q}_{1i} + \\
&\rho_2\ddot{\theta}_1 \sin\theta_2 \textstyle\sum_{i=1}^{N_1} C_{1i} q_{1i} = 0
\end{aligned}
\tag{A.32}
$$

The last two equations are partial differential equations, i.e., these equations are not only valid for all $t \geq 0$ but for all $0 \leq l_i \leq L_i$, whereas the first two equations are just ordinary differential equations since the mode shapes are evaluated inside known integrals. To convert the last two equations into ordinary differential equations, multiply through by ϕ_{ik}, $i = 1, 2$ and integrate from 0 to L_i. Since the ϕ_{ik}'s are orthogonal (the integral from 0 to L_i is an inner product, *i.e.*, the ϕ_{ik}'s belong to the space $\mathcal{L}_2[0, L_i]$), all the terms drop out except the $\phi_{ik}\phi_{ik}$ integral, thus one is left with N_i ordinary differential equations, one for each mode for each link.

The flexure of the first link (α_1):

$$A_{1k}\ddot{\theta}_1 + B_{1k}\ddot{q}_{1k} + E_1 I_1 \frac{\lambda_{1k}}{\rho_1} B_{1k} q_{1k} - B_{1k} q_{1k} \dot{\theta}_1^2 = 0, \; k = 1, 2, \ldots, N_1 \tag{A.33}$$

The flexure of the second link (α_2):

$$\begin{aligned} & A_{2k}\ddot{\theta}_1 + A_{2k}\ddot{\theta}_2 + B_{2k}\ddot{q}_{2k} + E_2 I_2 \tfrac{\lambda_{2k}}{\rho_2} B_{2k} q_{2k} - B_{2k} q_{2k} \dot{\theta}_1^2 - \\ & 2B_{2k} q_{2k} \dot{\theta}_1 \dot{\theta}_2 - B_{2k} q_{2k} \dot{\theta}_2^2 + L_1 \cos\theta_2 C_{2k} \ddot{\theta}_1 + \cos\theta_2 C_{2k} \textstyle\sum_{i=1}^{N_1} C_{1i} \ddot{q}_{1i} - \\ & \cos\theta_2 C_{2k} \textstyle\sum_{i=1}^{N_1} C_{1i} q_{1i} \dot{\theta}_1^2 + L_1 \sin\theta_2 C_{2k} \dot{\theta}_1^2 + 2\sin\theta_2 C_{2k} \textstyle\sum_{i=1}^{N_1} C_{1i} \dot{q}_{1i} \dot{\theta}_2 + \\ & \sin\theta_2 C_{2k} \textstyle\sum_{i=1}^{N_1} C_{1i} q_{1i} \ddot{\theta}_1 = 0, \; k = 1, 2, \ldots, N_2. \end{aligned} \tag{A.34}$$

The following parameters were assumed for the simulation:
$L_1 = 0.75$ m, $L_2 = 0.5$ m;
$\rho_1 = 0.792$ kg/m, $\rho_2 = 0.11$ kg/m;
$M_1 = 2.84$ kg, $M_2 = 0.666$ kg;
$I_h = 1.5$ kg - m^2;
$\mu_1 = 0.373 \frac{\text{N·s}}{\text{m}}$, $\mu_2 = 0.373 \frac{\text{N·s}}{\text{m}}$;
$E_1 I_1 = 8.8778$ N-m^2, $E_2 I_2 = 0.2183$ N-m^2.

A.4 REFERENCES

[1] F. Khorrami and Ü. Özgüner, "Singular perturbation analysis of a distributed parameter model of flexible manipulators," in *Proceedings of the American Control Conference,* (Atlanta, GA), pp. 1704-1709, 1988.

[2] F. Khorrami, *Asymptotic perturbation and Lyapunov stability based approaches for control of flexible and rigid robot manipulators.* PhD thesis, The Ohio State University, August 1988.

[3] C. M. Oakley and R. H. Cannon, Jr., "End-point control of a two-link manipulator with a very flexible forearm: Issues and experiments," in *Proceedings of the American Control Conference,* (Pittsburgh, PA), pp. 1381-1388, 1989.

[4] R. D. Blevins, *Formulas for Natural Frequency and Mode Shape.* New York: Van Nostrand Reinhold, 1979.

[5] B. R. Bhat and H. Wagner, "Natural frequencies of a uniform cantilever with a tip slender in the axial direction," *Journal of Sound and Vibration*, vol. 45, no. 2, pp. 304-307, 1976.

INTERNAL DISTRIBUTION

1. R. L. Anderson
2. S. M. Babcock
3. H. R. Brashear
4. C. R. Brittain
5. C. L. Carnal
6. N. E. Clapp
7. R. A. Dory
8. B. G. Eads
9. D. N. Fry
10. J. M. Googe
11. W. R. Hamel
12. J. E. Hardy
13. J. H. Harris
14. R. A. Hess
15. J. O. Hylton
16. J. M. Jansen
17. S. W. Kercel
18. R. L. Kress
19. R. F. Lind
20. D. W. McDonald
21. J. A. McEvers
22. A. C. Miller
23. G. N. Miller

24–33. D. A. Schoenwald

34. J. O. Stiegler
35. P. A. Tapp
36. K. W. Tobin
37. R. E. Uhrig
38. G. R. Wetherington
39. J. D. White
40. D. F. Craig

41–42. Central Research Library

43. Y-12 Technical Reference Library

44–45. Laboratory Records

46. Laboratory Records–Record Copy
47. ORNL Patent Section
48. I&C Division Publications Office

EXTERNAL DISTRIBUTION

49. Professor Dr.-Ing. Michael Zeitz, Institut fuer Systemdynamik und Regelungstechnik, Universitaet Stuttgart, Pfaffenwaldring 9, D-7000 Stuttgart 80, Germany
50. Professor Gonzalo Arce, Department of Electrical Engineering, University of Delaware, Newark, DE 19716
51. Professor T. W. Wang, Department of Chemical Engineering, University of Tennessee, Knoxville, TN 37996-2200
52. Professor J. D. Birdwell, Department of Electrical Engineering, University of Tennessee, Knoxville, TN 36996-2100
53. B. Chexal, Electric power Research Institute, 3412 Hillview Avenue, Palo Alto, CA 94303
54. V. Radeka, Brookhaven National Laboratory, Instrumentation Division, 535-B, Upton, NY 11973
55. M. M. Sevik, Carderock Division, Naval Surface Warfare Center, Code 1900, Bethesda, MD 20084-5000
56. R. M. Taylor, Leeds and Northup, Sunneytown Pike, North Wales, PA 19454
57. Assistant Manager for Energy Research and Development, U.S. Department of Energy, DOE-OR, P.O. Box 2001, Oak Ridge, TN 37831-8600

58–59. Office of Scientific and Technical Information, U.S. Department of Energy, P.O. Box 62, Oak Ridge, TN 37831